

Novel Macromolecular Architectures via a Combination of Cyclodextrin Host/Guest Complexation and RAFT Polymerization

Zur Erlangung des akademischen Grades eines
DOKTORS DER NATURWISSENSCHAFTEN
(Dr. rer. nat.)
Fakultät für Chemie und Biowissenschaften
Karlsruher Institut für Technologie (KIT) - Universitätsbereich

genehmigte

DISSERTATION

von

Bernhard Volkmar Konrad Jakob Schmidt

aus

Hanau, Deutschland

Dekan: Prof. Dr. Martin Bastmeyer
Referent: Prof. Dr. Christopher Barner-Kowollik
Korreferent: Prof. Dr. Michael A. R. Meier
Tag der mündlichen Prüfung: 19.07.2013

Die vorliegende Arbeit wurde von Juni 2010 bis Mai 2013 unter Anleitung von Prof. Dr. Christopher Barner-Kowollik am Karlsruher Institut für Technologie (KIT) - Universitätsbereich angefertigt.

The true measure of a man is how he treats someone who can do him absolutely no good.
Samuel Johnson

Publications arising from the present thesis

1. Cyclodextrin-Complexed RAFT Agents for the Ambient Temperature Aqueous Living/Controlled Radical Polymerization of Acrylamido-Monomers
Schmidt, B. V. K. J.; Hetzer, M.; Ritter, H.; Barner-Kowollik, C. *Macromolecules* **2011**, *44* (18), 7220-7232.
2. Miktoarm Star Polymers via Cyclodextrin-Driven Supramolecular Self-Assembly
Schmidt, B. V. K. J.; Hetzer, M.; Ritter, H.; Barner-Kowollik, C. *Polym. Chem.* **2012**, *3*, 3064-3067.
3. Supramolecular Three-Armed Star Polymers via Cyclodextrin Host/Guest Self-Assembly
Schmidt, B. V. K. J.; Rudolph, T.; Hetzer, M.; Ritter, H.; Schacher, F. H.; Barner-Kowollik, C. *Polym. Chem.* **2012**, *3*, 3139-3154.
4. UV-Light and Temperature Supramolecular ABA Triblock Copolymers via Reversible Cyclodextrin Complexation
Schmidt, B. V. K. J.; Hetzer, M.; Ritter, H.; Barner-Kowollik, C. *Macromolecules* **2013**, *46* (3), 1054-1065.
5. Complex Macromolecular Architecture Design via Cyclodextrin Host/Guest Complexes
Schmidt, B. V. K. J.; Hetzer, M.; Ritter, H.; Barner-Kowollik, C. *Prog. Polym. Sci* **2013**, *accepted*.
6. Modulation of the Thermoresponsive Behavior of Poly(*N,N*-diethylacrylamide) via Cyclodextrin Host/Guest Interactions
Schmidt, B. V. K. J.; Hetzer, M.; Ritter, H.; Barner-Kowollik, C. *Macromol. Rapid Commun.* **2013**, *34* (16), 1306-1311.

Abstract

The design of complex macromolecular architectures constitutes an important field in modern polymer chemistry and provides the opportunity to generate a broad range of materials with tuneable properties. The introduction of supramolecular chemistry had a significant impact on the synthesis of macromolecular architectures with a wide range of useful material properties ranging from self-healing to stimuli-response. In particular, cyclodextrins (CDs) have proven to be very versatile building blocks due to their ability to act as hosts in supramolecular inclusion complexes with hydrophobic molecules. In the course of the current thesis the possibilities of the combination of CD based supramolecular chemistry and reversible addition-fragmentation chain transfer (RAFT) polymerization with regard to the preparation of new macromolecular architectures were investigated. With the synthesis of variable macromolecular building blocks a broad range of macromolecular architectures are accessible *via* CD host/guest chemistry.

A new method was developed to solubilize hydrophobic RAFT reagents in water and to utilize them in aqueous RAFT polymerizations of several acrylamides, *i.e.* *N,N*-dimethylacrylamide (DMAAm), *N,N*-diethylacrylamide (DEAAm) and *N*-isopropylacrylamide (NIPAAm). The polymerization kinetics were investigated showing control similar to fully water soluble systems. Furthermore, high endgroup fidelities were found and efficient chain extensions were performed. Thus, for the first time, water soluble polymers with hydrophobic endgroups were prepared in aqueous solution in one step with good control over molecular weight and molar mass dispersity (D_m). After the preparation of endfunctionalized polymers, the complexity of the architectures was increased *via* the utilization of several building blocks. Supramolecular three arm star polymers were accessible *via* a three fold CD-functional core molecule and guest functionalized polymers. The formation of supramolecular three armed star polymers was shown to be temperature responsive leading to the disassembly of the star polymers after heating. This process is proceeding in a reversible fashion as

the supramolecular star polymers re-formed after cooling to ambient temperature. A further increase in complexity was achieved in the synthesis of AB₂ miktoarm star polymers. In this case, a mid-chain guest functionalized PDMAAm was synthesized as well as a β -CD-endfunctionalized PDEAAm. Complexation in water lead to the formation of the desired miktoarm star polymers. The PDEAAm block was utilized to investigate the temperature induced aggregation behavior. Significant differences between supramolecular miktoarm stars and non star-shaped polymers were found that can be attributed to different architectures in solution.

Furthermore, supramolecular bound ABA block copolymers were prepared *via* the combination of CD endfunctionalized poly(hydroxypropyl methacrylamide) (PHP-MA) and doubly guest functionalized PDMAAm or PDEAAm. Adamantyl- and azobenzene-guests were utilized allowing the disassembly of the block copolymers at elevated temperature (in the case of adamantyl- and azobenzene-guests) or *via* irradiation of UV-light (in the case of azobenzene-guests). The utilization of thermoresponsive PDEAAm, which loses water solubility at elevated temperatures, and PHP-MA, which is water soluble in the complete temperature range, enables the study of temperature-induced aggregation of the system.

In addition, the thermoresponsive behavior of PDEAAm was modulated *via* the formation of supramolecular host/guest complexes with hydrophobic polymer end-groups and CD. This effect could be reversed *via* the addition of competing guest molecules or *via* enzymatic degradation of the CD moieties.

Zusammenfassung

Im Rahmen dieser Doktorarbeit wurden die Möglichkeiten der Kombination von Cyclodextrin (CD)-basierter supramolekularer Chemie und reversibler Additions-Fragmentierungs Kettentransfer (RAFT) Polymerisation untersucht. Dabei wurden neuartige makromolekulare Architekturen aufgebaut, sowie eine Methode entwickelt wasserlösliche Polymere mit wasserunlöslichen Endgruppen in Wasser in einem Schritt herzustellen. In dieser Arbeit wurde die RAFT Polymerisation verwendet um wasserlösliche CD- und Gast-funktionalisierte Polymere herzustellen und durch die systematische Kombination unterschiedlicher Bausteine eine Vielzahl von makromolekularen Architekturen mittels supramolekularer Wechselwirkungen zu erzeugen, wobei als analytische Methoden 2D Kernmagnetische Resonanz Spektroskopie (NMR) und dynamische Lichtstreuung (DLS) verwendet wurden.

Eine neue Methode um wasserunlösliche RAFT Reagenzien mittels CD in Wasser aufzulösen und für die Kontrolle der Polymerisation von verschiedenen Acrylamiden in Wasser bei Raumtemperatur zu verwenden wurde entwickelt, die sich die Eigenschaft der CDs zu Nutze macht, hydrophobe Moleküle in wässriger Phase zu homogenisieren. Die Untersuchung der Kinetik der Polymerisationen zeigte sehr gute Ergebnisse, die vergleichbar mit den voll wasserlöslichen Systemen sind. Es konnte eine sehr hohe Endgruppen Funktionalität und effektive Kettenverlängerung erreicht werden. Diese Methode ermöglicht es zum ersten Mal wasserlösliche Polymere mit hydrophober Endgruppe in Wasser in einem Schritt mit hohem Endfunktionalisierungsgrad und guter Kontrolle über Polydispersität und molekularer Masse zu gewinnen.

Nachdem gezielt Endgruppen mittels CDs in Polymere eingebracht wurden, konnte die Komplexität der erzeugten Polymere durch die Verwendung mehrerer Bausteine für die Synthese von Sternpolymeren erhöht werden. Supramolekulare dreiarmlige Sternpolymere konnten mittels dreifach CD-substituiertem Kernmolekül und Gast-endfunktionalisierten Polymeren hergestellt werden. Die Bildung des supramolekularen dreiarmligen Sterns ist temperaturabhängig. So konnten die supramolekularen Stern-Polymere durch die Einwirkung von Hitze aufgebrochen werden, wobei sich nach Abkühlung die supramolekularen Bindungen wieder ausbildeten. Eine Erhöhung der Komplexität der erzeugten Architekturen wurde in einem supramolekularem AB_2 Mikroarm Stern realisiert, d.h. ein Sternpolymer bei dem die Arme mindestens aus zwei unterschiedlichen Polymertypen gebildet werden. In diesem Fall wurde ein Polymer mittels RAFT Polymerisation hergestellt, das in der Mitte der Kette eine Gast-Gruppe trägt. Durch die Zugabe eines CD-endfunktionalisierten Polymers konnte eine Mikroarm Stern-Struktur in Wasser gebildet werden. Einer der Blöcke wurde bewusst thermoresponsiv gewählt, um die Temperatur-induzierte Bildung von Ag-

gregaten zu untersuchen. Dabei wurden signifikante Unterschiede zwischen supramolekularen Stern-Proben und Nicht-Stern Blindproben gefunden, die auf unterschiedliche Architekturen in Lösung zurückzuführen sind.

Als weitere komplexe makromolekulare Architektur konnten erstmals supramolekular gebundene ABA Blockcopolymere durch die Kombination von CD-endfunktionalisiertem Poly(hydroxypropyl methacrylamid) (PHPMA) mit zweifach Gast-substituierten Poly(dimethylacrylamid) (PDMAAm) oder Poly(diethylacrylamid) (PDEAAm) gebildet werden. Hierbei wurden Adamantyl- und Azobenzol-Gäste verwendet, die die außerordentliche Eigenschaft mit sich bringen die Verbindung der Blöcke durch erhöhte Temperatur (im Fall von Adamantyl- und Azobenzol-Gästen) und Einstrahlung von UV-Licht (im Fall von Azobenzol-Gästen) zu brechen. Die Bildung, Zerlegung durch äußere Einwirkung und Rückbildung der supramolekularen Blockcopolymere in wässriger Lösung konnte mittels 2D NMR und DLS verfolgt werden. Die Verwendung von thermoresponsivem PDEAAm, das bei erhöhter Temperatur seine Löslichkeit in Wasser verliert, und des im gesamten Temperaturbereich wasserlöslichen PHPMA-Blocks ermöglichte es weiterhin das Temperatur-induzierte Aggregierungsverhalten der Blockcopolymere in wässriger Lösung zu untersuchen.

Zusätzlich konnte das thermoresponsive Verhalten von Gast-funktionalisiertem PDEAAm durch die Bildung von supramolekularen Wirt/Gast Komplexen moduliert werden. Eine Umkehrung des Effekts konnte durch die Zugabe eines Überschusses von Gast Molekülen oder durch enzymatischen Abbau des CD erreicht werden.

Contents

Contents	i
1 Introduction	1
2 Theoretical Background and Literature Overview	3
2.1 Reversible Addition-Fragmentation Chain Transfer Polymerization . . .	3
2.2 Cyclodextrins and their Complexes	15
2.3 Complex Macromolecular Architectures Governed by CD Complexes .	21
3 CD-Complexed RAFT Agents	33
3.1 Introduction	33
3.2 Results and Discussion	35
3.3 Conclusions	53
3.4 Experimental Part	54
4 Supramolecular ABA Triblock Copolymers	61
4.1 Introduction	61
4.2 Results and Discussion	63
4.3 Conclusions	80
4.4 Experimental Part	81
5 Supramolecular Three Armed Star Polymers	85
5.1 Introduction	85
5.2 Results and Discussion	87
5.3 Conclusions	98
5.4 Experimental Part	98
6 AB₂ Miktoarm Star Polymers	101
6.1 Introduction	101

6.2	Results and Discussion	102
6.3	Conclusions	113
6.4	Experimental Part	114
7	Modulation of the Thermoresponsivity of PDEAAm via CD Addition	119
7.1	Introduction	119
7.2	Results and Discussion	121
7.3	Conclusions	130
7.4	Experimental Part	131
8	Conclusions and Outlook	135
9	Experimental Part	139
9.1	Materials	139
9.2	Additional Experimental Procedures	140
9.3	Characterization and Methods	145
	Bibliography	149
	List of Abbreviations	167
	Appendices	171
	Curriculum Vitae	217
	Publications and Conference Contributions	219
	Acknowledgements	224

Introduction

Polymeric materials play a significant role in contemporary society, *e.g.* as consumables, as high performance materials or in high-tech applications. The progress in these fields depends to a significant amount on the achievements of polymer science. Especially the development of novel complex macromolecular architectures have driven polymer scientists in recent years.¹⁻³ The ability to control macromolecular architectures gives rise to the fabrication of materials with novel or improved properties and thus enables the development of new products in a broad range of applications, *e.g.* microelectronic materials,⁴ drug/gene delivery,⁵ biomedical materials,⁶ supersoft elastomers⁷ or hybrid materials.⁸

The development of reversible-deactivation radical polymerization techniques, *e.g.* nitroxide-mediated radical polymerization (NMP),^{9,10} atom transfer radical polymerization (ATRP),^{11,12} and reversible addition-fragmentation chain transfer (RAFT) polymerization,¹³⁻¹⁵ has provided very suitable and convenient tools for the preparation of complex macromolecular architectures in a controlled fashion. The introduction of *click* chemistry had a further impact on the preparation of complex macromolecular architectures.¹⁶⁻¹⁹ The utilization of complex building blocks with a large diversity, based on the high tolerance of functional groups obtained from reversible-deactivation radical polymerization techniques in highly efficient mild and fast coupling reactions enables the synthesis of complex macromolecular architectures in a modular fashion, *e.g.* via copper(I)-catalyzed azide-alkyne cycloaddition (CuAAC),²⁰ thiol-ene^{21,22} or Diels-Alder reactions.²³

Apart from reversible-deactivation radical polymerization techniques and *click* chemistry, supramolecular chemistry had a significant impact on polymer science. Supramolecular interactions provide a set of new properties that can be utilized in materials design and especially in the formation of complex macromolecular architectures, *e.g.* reversibility or stimuli-response. Several supramolecular systems have been utilized in polymer chemistry, *e.g.* hydrogen bonding,^{24,25} metal complexes²⁶ as well as in-

clusion complexes.^{27–29} One of the frequently utilized inclusion complex systems are cyclodextrins (CDs),^{30,31} as they form host/guest complexes with hydrophobic guest molecules/recognition sites. The combination of CD-based host/guest chemistry and polymer science has been under investigation with regard to a variety of applications, *e.g.* drug delivery,³² nano-structures,²⁸ supramolecular polymers,³³ self-healing materials,³⁴ amphiphiles³⁵ or bioactive materials.³⁶

Considering complex macromolecular architectures, CDs offer the opportunity to generate complex macromolecular architectures via supramolecular interactions. To facilitate the formation of complex macromolecular architectures via CD host/guest chemistry, control over polymer end functionality is necessary. End functionalized building blocks can subsequently be applied for the formation of novel architectures via the combination of suitable host and guest functionalized blocks. As different building blocks are utilized, in principle almost unlimited combinations are conceivable, making the formation of complex macromolecular architectures possible in a modular fashion. CD-based supramolecular interactions usually occur in aqueous solution, which restricts the nature of the polymer building blocks to water-soluble polymers. Especially RAFT polymerization is a perfect tool for the formation of water-soluble polymers in a controlled fashion, *e.g.* with control over end functionality, low molar mass dispersity (D_m) and control over molar mass. One of the major tasks in the present work is the formation of novel complex macromolecular architectures governed by supramolecular CD host/guest complexes via building blocks synthesized with RAFT polymerization. Thus, the RAFT process is utilized to control polymer functionalities, while supramolecular interactions are utilized to control polymer topology and composition.

In the current thesis, RAFT polymerization was utilized to generate polymers with CD- or guest-endgroups. Therefore, a method was developed to synthesize hydrophilic polymers with hydrophobic guest endgroups directly in water via complexation of guest-functionalized RAFT reagents with CD for the first time. Polymers with tailored endfunctionality were subsequently utilized in the formation of supramolecular macromolecular architectures.

Doubly guest functionalized polymers were connected to CD functionalized polymers via supramolecular interactions to form novel ABA block copolymers. Singly guest endfunctionalized polymers were connected to a threefold CD functionalized core to form three-armed star polymers. With mid-chain guest functionalized and a CD endfunctionalized polymer, supramolecular ABA miktoarm star polymers were prepared. Furthermore, CD host/guest interactions were utilized to modulate the thermoresponsive behavior of poly(*N,N*-diethylacrylamide) (PDEAAm).

Theoretical Background and Literature Overview

As stated in the introduction, the present thesis is based on a combination of reversible-deactivation radical polymerization *via* the RAFT process and supramolecular CD host/guest complexes. The RAFT process provides the opportunity to generate polymers with specific endgroups, *e.g.* guest functionalities for CD. These polymers can subsequently be exploited for the formation of novel complex macromolecular architectures, *e.g.* block copolymers, star polymers or miktoarm star polymers. The underlying theoretical background is described in the following sections as well as an overview of CD mediated complex macromolecular architectures that have been published in the literature so far.

2.1 Reversible Addition-Fragmentation Chain Transfer Polymerization

2.1.1 Living Polymerization

A living polymerization is strictly speaking a chain propagation reaction that – after full monomer conversion – is still capable of propagation *via* addition of further monomer.³⁷ In an ideal case this occurs in polymerization reactions without any chain transfer and termination.^{38,39} Furthermore, the rate of initiation should be fast compared to the rate of propagation, which results in the synthesis of polymer chains with an overall similar degree of polymerization (D_p).⁴⁰ Anionic and some cationic polymerizations are treated as classical/truly living polymerization, while the more recent atom transfer radical polymerization (ATRP),^{11,41,42} nitroxide-mediated polymerization (NMP)^{9,39,43,44} and the RAFT polymerization^{13,45–48} are treated as polymeriza-

tion with living characteristics, as controlled radical polymerization⁴⁹ or reversible-deactivation radical polymerization. All living polymerization techniques have in common that D_p increases linearly with monomer conversion, block copolymers can be formed *via* sequential monomer addition and low D_m are achieved.

In the case of ATRP, radical chain ends are generated *via* a transition metal catalyzed one electron redox-process that leads to halide terminated dormant chains or radical bearing active chains.⁴¹ An equilibrium between dormant and active species that is centered on dormant species controls the reaction. In NMP, the persistent radical effect is utilized.³⁹ A nitroxide acts as a radical trap for active chains. As the process of chain termination *via* a nitroxide is reversible, an activation/deactivation equilibrium is formed. In both processes, ATRP and NMP, a small amount of active species leads to the minimization of radical termination events. The RAFT process is an alternative method to control radical polymerizations and achieves living behavior. Macromolecular design *via* the interchange of xanthates (MADIX) has an identical mechanism to RAFT yet uses slightly different controlling agents. Both methods were patented in 1998^{50,51} and are utilized in polymer research very often since then.^{13,46} The RAFT process will be described in detail in the next sections.

RAFT and MADIX differ substantially from the other controlled radical polymerizations, as for the control of the polymerization no persistent radical effect is utilized (refer to Section 2.1.2), leading to an increase in propagation rate compared to the other controlled radical polymerization techniques. The process is tolerant to functional monomers, *e.g.* acrylic acid or vinyl acetate (refer to Section 2.1.3), and is especially useful for the preparation of water-soluble polymers (refer to Section 2.1.4). The RAFT process, as the other living polymerization techniques, is a tool for the synthesis of complex macromolecular architectures, *e.g.* block copolymers or star polymers (refer to Section 2.1.5).

2.1.2 Mechanism and Kinetics

The central element in the RAFT process is the chain transfer agent (CTA) that allows for control on the polymerization:

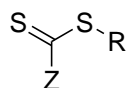


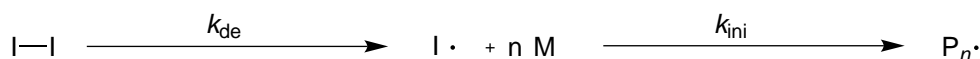
Figure 2.1: General structure of a CTA/RAFT agent.

The CTA is typically a thiocarbonyl thio compound featuring two substituents that are usually abbreviated as R- and Z-group (refer to Figure 2.1). These two substituents

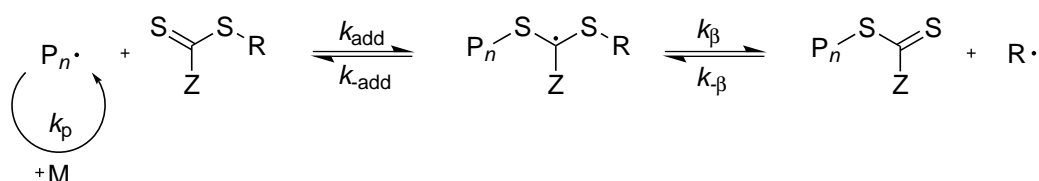
have a profound influence on the reactivity of the CTA and the RAFT process can be varied *via* the modification of these substituents. The R-group is also called the radical leaving group and the Z-group is also called the stabilizing group.^{52,53}

As depicted in Scheme 2.1 the RAFT equilibria do not create or terminate radicals. Except of the termination reactions, every reaction in the RAFT process generates a radical. There are only bimolecular cooperative chain transfer reactions⁵⁴ and – in contrast to ATRP and NMP – no persistent radicals are involved that are endfunction-izing polymers in a monomolecular process. Thus, no decrease in the polymerization rate should ideally occur from the RAFT process itself under the assumption that fragmentation and reinitiation are not rate defining. Nevertheless, often inhibition or slower propagation rates compared to conventional free radical polymerization are observed.^{13,55} The RAFT process can be divided into five distinct reaction sequences: Initiation, pre-equilibrium, reinitiation, main-equilibrium and termination. The mechanism of the RAFT process is depicted in Scheme 2.1:

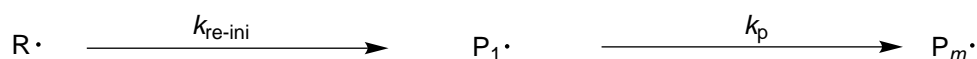
I. Initiation



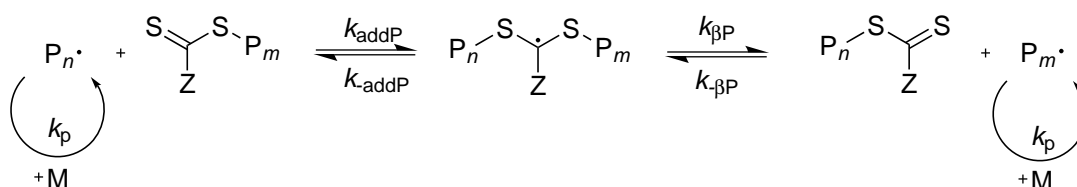
II. Pre-equilibrium



III. Reinitiation



IV. Main-equilibrium



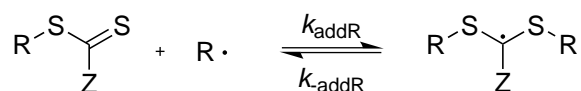
V. Termination



Scheme 2.1: Basic mechanism of the RAFT process.

The initiation occurs *via* the formation of primary radicals $I\bullet$ that form during the decay of a radical initiator I_2 with the rate coefficient k_{de} . The formed radicals react with monomers to short oligomeric chains $P_n\bullet$ with the rate coefficient k_{ini} until a radical reacts with a CTA molecule. The ratio of CTA to initiator should be high, especially when high endgroup functionalization is necessary, *e.g.* for chain extensions or complex macromolecular architecture formation. Furthermore, a high initiator concentration has the drawback of an increased probability of termination reactions due to higher radical concentration.⁵⁴

The initiator derived chain adds to a CTA molecule with the rate constant k_{add} . Subsequently the thiocarbonyl centered radical undergoes β -fragmentation with the rate coefficient k_β , which leads to the formation of a free radical $R\bullet$ and a thiocarbonyl thio capped chain. The reaction of the formed radical $R\bullet$ with the rate coefficients k_{addR} and k_{-addR} with another CTA molecule (refer to Scheme 2.2) is usually negligible due to the short life time of the intermediate. In the case of slow fragmentation and side-reactions of the intermediate the reaction should be taken into account.¹³



Scheme 2.2: Reversible chain transfer in the RAFT process.

For the description of the chain transfer, the chain transfer constants C_{tr} and C_{-tr} are defined:

$$C_{tr} = \frac{k_{tr}}{k_p} = \frac{k_{add}}{k_p} \cdot \frac{k_\beta}{k_{-add} + k_\beta} \quad (2.1)$$

and

$$C_{-tr} = \frac{k_{-tr}}{k_i} = \frac{k_{-add}}{k_i} \cdot \frac{k_{-add}}{k_{-add} + k_\beta} \quad (2.2)$$

The transfer constants depend strongly on the R- and Z-group present in the CTA. The higher the value of C_{tr} , the better is the control of the polymerization.^{13,53} The formed $R\bullet$ radical should reinitiate the polymerization effectively. Furthermore, the R-group has to be a good homolytic leaving group and especially a better leaving group than the radical of the monomer so that fragmentation towards the R-group is preferred. Thus, a balance between reinitiation and leaving group ability has to be found for an effective RAFT process.

The main equilibrium starts when all CTA molecules have reacted. In the equilibrium,

the intermediate fragments with the rate coefficient $k_{-\text{addP}}$ to the macroradical $P_n\bullet$ or $P_m\bullet$ and a thiocarbonyl thio chain end. With the rate coefficient k_{addP} , the thiocarbonyl thio chain end adds a macroradical again. Whenever a fragmentation takes place, the macroradical can add new monomers with the propagation rate constant k_p . The kinetics of the main equilibrium can be described with the chain transfer constant C_{trP} , which can differ slightly from the chain transfer constant of the pre-equilibrium C_{tr} . If the polymer fragments $P_n\bullet$ or $P_m\bullet$ are treated as identical, the following assumption can be made:

$$k_{-\text{addP}} = k_\beta \quad (2.3)$$

which effects the chain transfer constant of the main equilibrium C_{trP} as follows:

$$C_{\text{trP}} = \frac{k_{\text{addP}}}{2 \cdot k_p} \quad (2.4)$$

For optimal control of the polymerization, C_{trP} should be high,^{13,53} *i.e.* the higher C_{trP} the closer is the plot of D_p against conversion to linearity. Furthermore, \mathcal{D}_m is decreasing with higher C_{trP} . In the ideal case, there is the same probability for chain growth for all propagating chains, which leads to narrow molecular weight distributions. Following this mechanism a large quantity of the formed polymers should bear the thiocarbonyl thio Z-group on one end and the R-group on the other end. Furthermore initiator derived chains are formed in minor amounts.

Termination reactions occur intrinsically, as in free radical polymerization, radical recombination with k_{trec} and disproportionation with k_{td} .

As with all living polymerization techniques, D_p and the number average molecular mass M_n can be calculated from the conversion and the concentrations of initiator and monomer. D_p is based on the concentration of monomer $[M]$, the concentration of CTA $[CTA]$, the average number of chains that are formed in a termination reaction d , the initiator efficiency f and the initiator concentration $[I_2]$:

$$D_p = \frac{[M]_0 - [M]_t}{[CTA]_0 + d \cdot f([I_2]_0 - [I_2]_t)} \quad (2.5)$$

With a large excess of CTA compared to initiator follows:

$$D_p \approx \frac{[M]_0 - [M]_t}{[CTA]_0} \quad (2.6)$$

M_n can be calculated analogously with the molar mass of the monomer m_M and the

molar mass of the CTA m_{CTA} :

$$M_n = \left(\frac{[M]_0 - [M]_t}{[\text{CTA}]_0 + d \cdot f([I_2]_0 - [I_2]_t)} \cdot m_M \right) + m_{\text{CTA}} \quad (2.7)$$

A simplification analogous to the calculation of D_p leads to:

$$M_n \approx \left(\frac{[M]_0 - [M]_t}{[\text{CTA}]_0} \cdot m_M \right) + m_{\text{CTA}} \quad (2.8)$$

In this case a linear relation between M_n or D_p and the monomer conversion is evident, which is characteristic for polymerizations with living character. In an ideal RAFT process the formed thiocarbonyl thio functionalized macromolecule can be reinitiated for chain extension. Too high initiator concentrations lead to the formation of unreactive chains, as the degree of initiator functionalized polymers is increasing. As mentioned earlier, CTAs are often sulfur containing thiocarbonyl thio compounds that have to be chosen according to the monomer. For an efficient RAFT polymerization, the choice of the respective R- and Z-group are crucial. The RAFT agent needs a reactive C-S double bond, which results in high k_{add} values. The intermediate radicals should ideally fragment rapidly, based on a weak S-R bond which leads to a large k_{β} value. Furthermore, the intermediate should partition in favor of the products, *i.e.* $k_{\beta} > k_{-\text{add}}$ and $\text{R}\bullet$ should effectively reinitiate the polymerization:

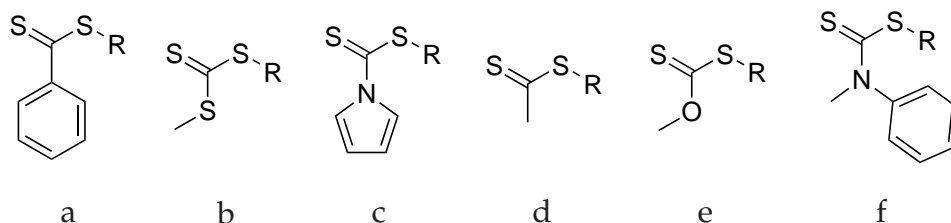


Figure 2.2: Different types of CTAs.¹³

In Figure 2.2 different Z-groups for CTAs are presented, *e.g.* aromatic (a) or aliphatic (d) dithioesters, trithiocarbonates (b), xanthates (e) and dithiocarbamates (c and f). The rate coefficients for addition and the transfer constants decrease from left to right.^{52,54,56} Via the Z-group, the addition and fragmentation rates are modified. The R-group has to be a good radical leaving group that is able to reinitiate the polymerization. Common R-groups include tertiary carbon atoms, *e.g.* in a cyanoisopropyl group, a cumyl group or an *iso*-butyric acid, or secondary carbon atoms, *e.g.* in a benzylic group or a *iso*-propionic acid.

2.1.3 Applicability of the Method and Reaction Conditions

The RAFT process gives the opportunity to perform reversible-deactivation radical polymerizations with a large variety of monomers, *e.g.* styrenic monomers, (meth)acrylates, (meth)acrylamides, vinyl acetate and *N*-vinyl monomers. A tertiary cyanoalkyl dithiobenzoate can act as CTA for styrene (Sty) and methyl methacrylate (MMA) (refer to compound **CPDB** in Figure 2.3).

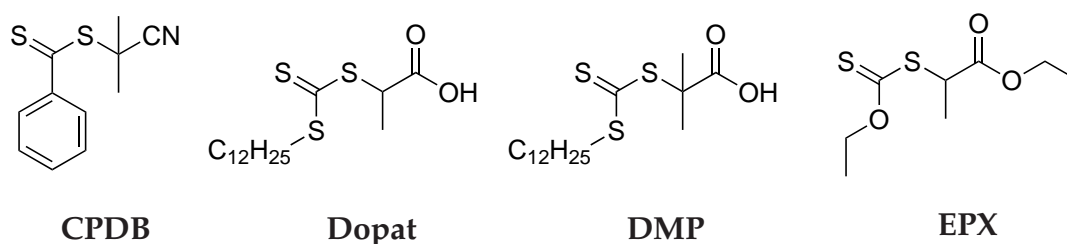


Figure 2.3: Commonly utilized CTAs (**CPDB**: 2-cyano-2-propyl benzodithioate; **Dopat**: 2-((dodecylsulfanyl)carbonothioyl)sulfanyl propionic acid; **DMP**: 2-(dodecylthiocarbonothioylthio)-2-methylpropionic acid ; **EPX**: ethyl 2-((ethoxycarbonothioyl)thio)propanoate).

Another common class of CTAs are trithiocarbonates connected to tertiary or secondary carboxylic acids or esters (refer to the compounds **Dopat** or **DMP** in Figure 2.3) that can be used to polymerize styrenics, acrylates or acrylamides. Xanthates (refer to compound **EPX** in Figure 2.3) or cyanoalkyldithiocarbamates can be utilized in the polymerization of vinyl acetate or *N*-vinyl monomers, *e.g.* *N*-vinylpyrrolidone or *N*-vinylcarbazole.

The reaction conditions can usually be adopted from the corresponding conventional free radical polymerization with a commonly used polymerization temperature ranging from ambient temperature to 140 °C. Usually, organic solvents are utilized, yet protic solvents such as alcohols or water can be utilized as well. Furthermore, bulk or emulsion polymerizations are described in the literature.¹³ For the initiation every radical source is in principle utilizable,⁵⁰ but in most cases thermal initiators are employed, *e.g.* 2,2'-azo-bis-(isobutyronitril) (**AIBN**). Other initiation methods are self-initiation,^{57,58} UV-irradiation,⁵⁹ γ irradiation⁶⁰ or a plasma field.⁶¹

2.1.4 Preparation of Water-Soluble Polymers *via* RAFT Polymerization

RAFT polymerization is arguably the most useful controlled radical polymerization technique for the synthesis of water-soluble polymers.⁶² In principle a polymerization in organic solvents or directly in water is possible. For the polymerization in water several water-soluble CTAs and initiators are available (refer to Figure 2.4). In the case of organic solvents as reaction media a usual RAFT polymerization can be conducted as long as the monomer and polymer are soluble in the respective organic solvent. This is true for some of the mostly used monomers, *e.g.* *N*-isopropylacrylamide (**NIPAAm**), **DEAAm**, *N,N*-dimethylacrylamide (**DMAAm**) or *N,N*-dimethylaminoethyl methacrylate (**DMAEMA**). Nevertheless, problems arise when ionic or very hydrophilic monomers are considered that are only soluble in water or at least their corresponding polymers, *e.g.* styrene sulfonate,⁶³ 2-acrylamido-2-methylpropanesulfonic acid (**AMPS**),⁶⁴ (3-methacryloylamino-propyl)-(2-carboxy-ethyl)-dimethyl-ammonium (carboxybetaine methacrylamide) (**CBMAA-3**)⁶⁵ or acrylamide (**AAm**).⁶⁶ Apart from the monomer choice, water as reaction solvent can have several advantages, when compared to organic solvents. Water is non-toxic, relatively cheap and has a high heat capacity. Some drawbacks are its high boiling point, thus water is not easy to recycle or to remove.

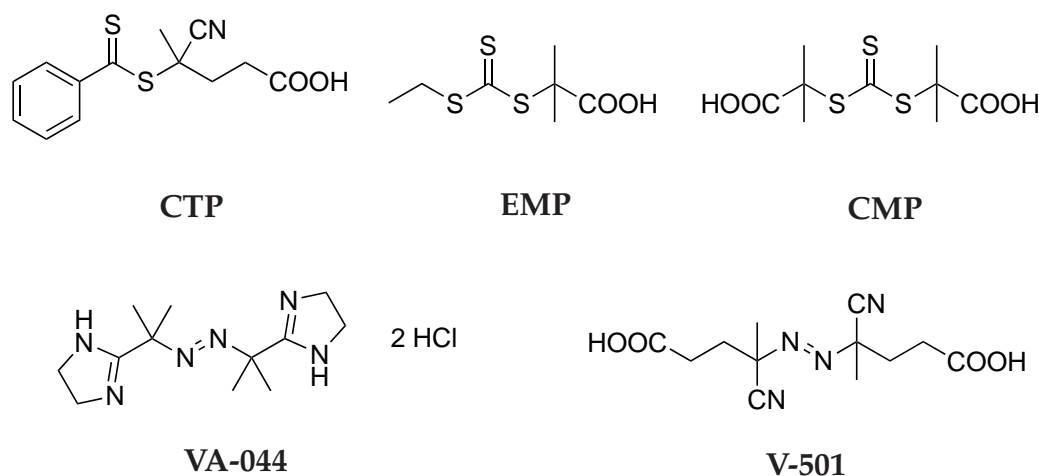


Figure 2.4: Commonly utilized water-soluble CTAs and radical initiators (**CTP**: 4-cyano-4-(phenylcarbonothioylthio)pentanoic acid; **EMP**: 2-(((ethylthio)carbonothioyl)thio)-2-methylpropanoic acid; **CMP**: 2-(1-carboxy-1-methylethylsulfanylthiocarbonylsulfanyl)-2-methylpropanoic acid; **VA-044**: 2,2'-azobis[2-(2-imidazolin-2-yl)propane]dihydrochloride; **V-501**: 4,4'-azobis(4-cyanovaleric acid)).

The CTA should be water-soluble in an aqueous polymerization, *e.g.* 4-cyano-4-(phenylcarbonothioylthio)pentanoic acid (**CTP**), 2-(((ethylthio)carbonothioyl)thio)-2-methylpropanoic acid (**EMP**) or 2-(1-carboxy-1-methylethylsulfanylthiocarbonylsulfanyl)-2-methylpropionic acid (**CMP**). Nevertheless some side reactions are known that lead to less well defined polymers. McCormick and coworkers spent significant effort to study RAFT polymerization in water. At high temperatures and under neutral or basic conditions the CTA can undergo hydrolysis.^{62,67,68} In the case of the polymerization of acrylamides, aminolysis can happen after hydrolysis of the respective monomer.^{62,67} Of course, hydrolysis of an amide is not a preferred process, yet when the equivalents of CTA to monomer are considered, already a small portion of hydrolysis can lead to loss of CTA and thus control of the polymerization. Usually a higher molecular mass than expected and broader molecular mass distributions are observed. A possibility to overcome these issues is to polymerize in slightly acidic media, *e.g.* acetic acid buffer, at low temperatures or at best in acidic media and at low temperatures. In these cases even controlled RAFT polymerizations of acrylamides in water are possible.^{66,69,70}

Several monomer classes for water-soluble polymers are available (refer to Figure 2.5) and can be chosen for the respective application.^{62,71} There are anionic monomers or monomers that can easily be deprotonated, *e.g.* styrene sulfonate,⁶³ **AMPS**⁶⁴ or acrylic acid (**AA**).⁷² Cationic monomers, monomers that can be protonated or quaternized, *e.g.* 2-vinylpyridine (**2VP**),⁷³ 4-vinylpyridine (**4VP**)^{73,74} or **DMAEMA**,^{75,76} are available as well. Furthermore, zwitterionic monomers, *e.g.* **CBMAA-3**⁶⁵ or 3-dimethyl(methacryloyloxyethyl) ammonium propane sulfonate (**DMAPS**),⁷⁷ have been utilized in RAFT polymerizations. A very frequently employed class of monomers are non-ionic monomers, which are mostly acrylamides, *e.g.* **AAm**,⁶⁶ **DMAAm**,⁶⁶ **DEAAm**,⁷⁸ **NIPAAm**⁷⁹ and *N*-(2-hydroxypropyl)methacrylamide (**HPMA**).^{65,80}

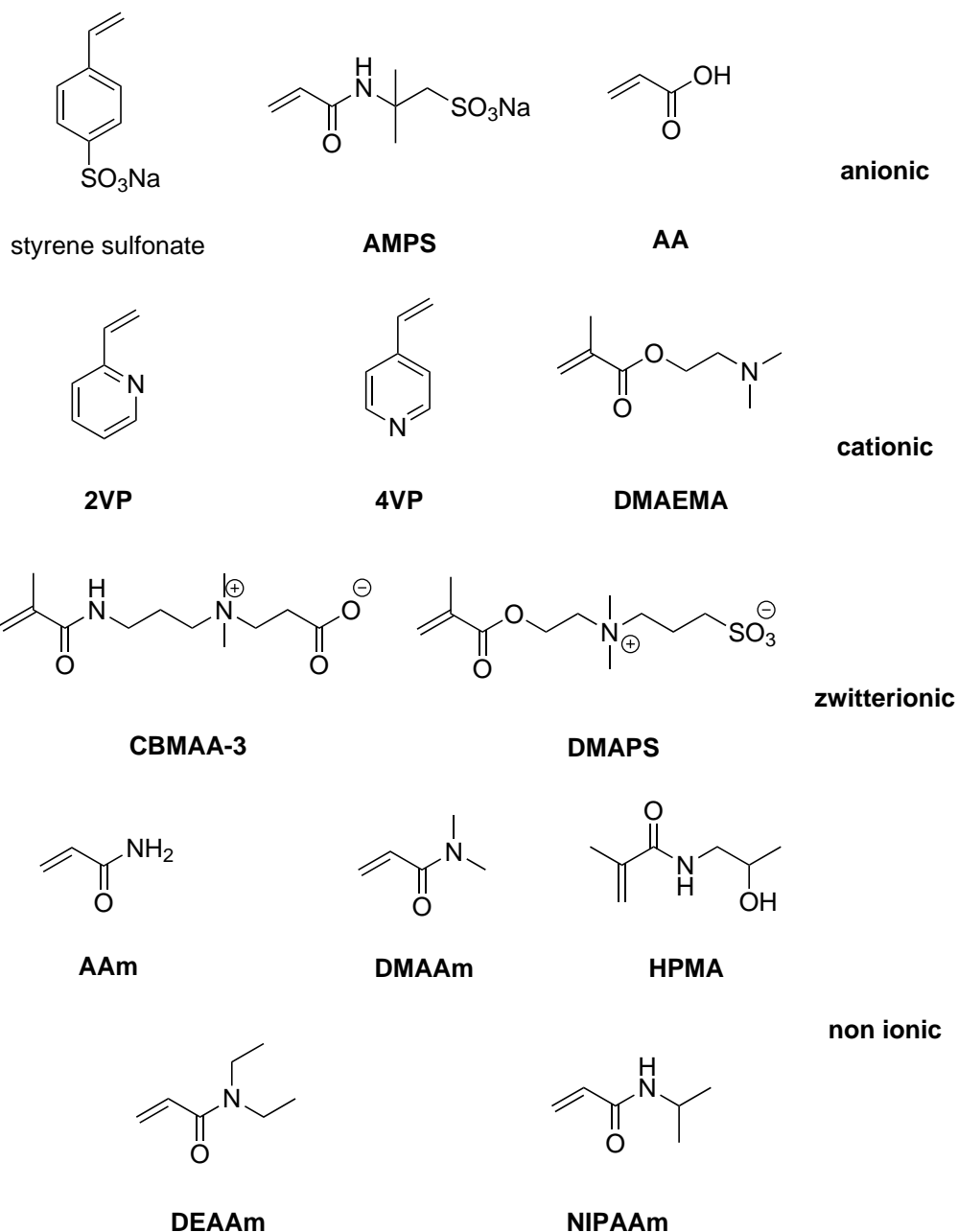


Figure 2.5: Selection of monomers for the preparation of water-soluble polymers (**AMPS**: 2-acrylamido-2-methylpropane sulfonic acid; **2VP**: 2-vinylpyridine; **4VP**: 4-vinylpyridine; **DMAEMA**: *N,N*-dimethylaminoethyl methacrylate; **CBMAA-3**: (3-methacryloylamino-propyl)-(2-carboxy-ethyl)-dimethyl-ammonium (carboxybetaine methacrylamide); **DMAPS**: 3-dimethyl(methacryloyloxyethyl) ammonium propane sulfonate; **AAm**: acrylamide; **DMAAm**: *N,N*-dimethylacrylamide; **HPMA**: *N*-(2-hydroxypropyl)methacrylamide; **DEAAm**: *N,N*-diethylacrylamide; **NIPAAm**: *N*-isopropylacrylamide).

2.1.5 Complex Macromolecular Architectures *via* RAFT Polymerization

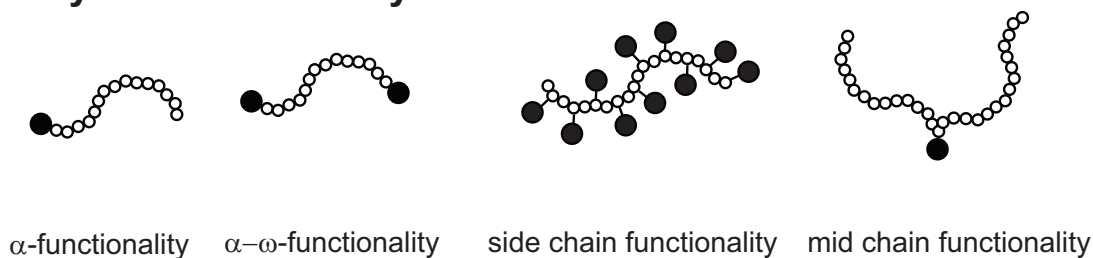
The RAFT process is a tool to generate a broad range of macromolecular architectures (refer to Figure 2.6). As the structure of the CTA is retained in the formed polymer, a modification of the CTA in the R- or Z-part provides the opportunity to incorporate specific endgroups into polymers,⁸¹ e.g. azides,^{82,83} alkynes,⁸² amines,⁸⁴ alcohols⁸⁵ or carboxylic acids.^{86,87} The broad range of possible endgroups leads to a broad range of applications and combinations. Furthermore, several reactive endgroups can be utilized in the formation of complex macromolecular architectures, e.g. in modular ligation reactions.^{17,18,20,88}

An alternative possibility is an endgroup conversion of thiocarbonyl thio endgroups, e.g. thermolysis,⁸⁹ hydrolysis,⁹⁰ aminolysis⁸⁶ or reduction.⁹¹ Furthermore oxidation,⁹² radical-⁸⁹ and irradiation-induced⁹³ endgroup removal have been reported in the literature.

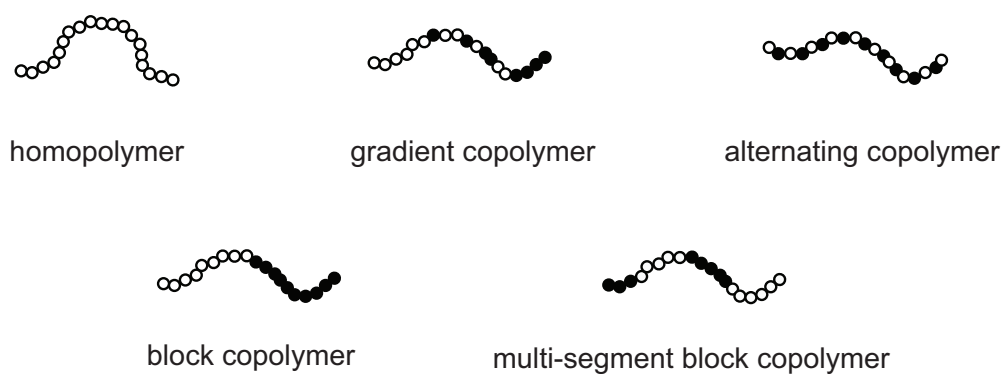
Block copolymers can be generated *via* modular ligation reactions, e.g. CuAAC.^{81,82} Another possibility is the utilization of a macro-CTA, *i.e.* a polymer that contains a thiocarbonyl thio endgroup. These polymers can be reinitiated and chain extended after initiator and monomer addition.⁹⁴ An alternative strategy is the addition of further monomer after high conversion of the first monomer, but in that case gradient block copolymers with tapered transition⁴⁹ are obtained.⁵⁴ These gradient copolymers are usually not very well suited for microphase separations. A drawback of block copolymer generation *via* macro-CTAs is that only monomers with similar reactivity can be utilized.⁸¹ A possibility to connect electron rich monomers with electron deficient monomers is the utilization of *N*-(4-pyridinyl)-*N*-methyldithiocarbamate.⁹⁵ With this CTA, the formation of block copolymers of methyl methacrylate and vinyl acetate is possible *via* protonation of the pyridinyl substituent.

Other complex structures can be formed *via* specially designed CTAs,^{13,96} e.g. star polymers,⁹⁷ polymer brushes,⁹⁸ dendritic structures⁹⁹ or amphiphiles.¹⁰⁰

Polymer Functionality



Polymer Composition



Polymer Topology

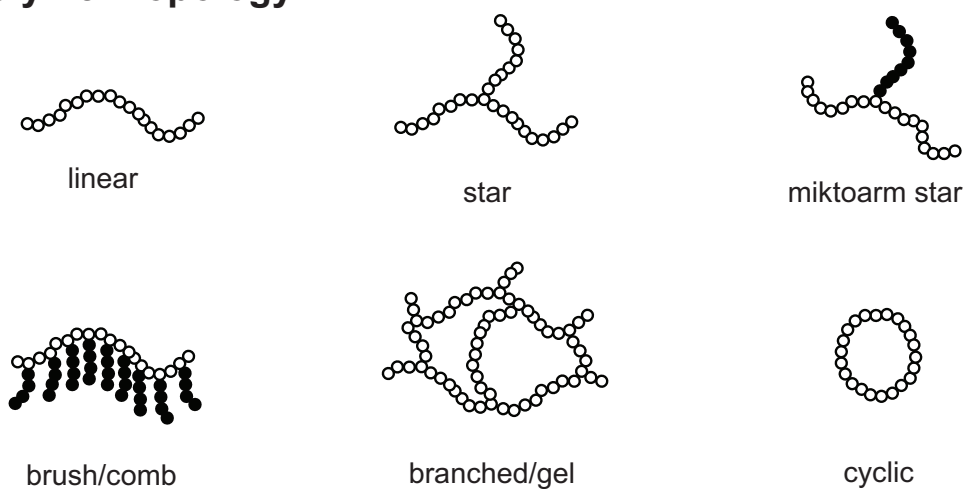


Figure 2.6: Overview of macromolecular architectures that are accessible *via* RAFT polymerization.

2.2 Cyclodextrins and their Complexes

2.2.1 Supramolecular Chemistry

The term of supramolecular chemistry has been defined by Jean-Marie Lehn in 1978. The Nobel laureate of 1987 has defined it as chemistry of non-covalent interactions between host and guest molecules.^{101,102} It can be viewed as chemistry beyond the molecule: While molecular chemistry is based on intramolecular covalent bonds, supramolecular chemistry is based on intermolecular non-covalent bonds.^{103–105} Several non-covalent interactions have proven to be versatile in supramolecular chemistry, *e.g.* hydrogen bonding, metal-ligand interactions or van der Waals interactions.¹⁰⁴ Thus, supramolecular chemistry leads to the formation of supramolecular objects that are defined by the nature of the molecular components and furthermore by the type of interaction between them.¹⁰⁴ In recent years the field of supramolecular chemistry has evolved into areas such as molecular devices and machines or molecular recognition, such as self-assembly and self-organization. One of the frequently utilized host compounds in supramolecular chemistry are CDs that are the focus of the next sections.

2.2.2 Structure and Properties of CDs

CDs are cyclic oligo saccharides of α -D-glucose that are formed through glycosidic α -1,4 bonds.¹⁰⁶ CDs are synthesized in an industrial biochemical process from starch *via* enzymatic pathways with CD glycosyl transferases, *e.g.* from *bacillus macerans*.¹⁰⁷ The commonly utilized CDs, also called native CDs, are the ones with $n = 6, 7$ or 8 repeating units and are called α -CD, β -CD and γ -CD, respectively (refer to Figure 2.7).

The chemical structure of the CDs resolves in a shallow truncated cone shape of the CD which forms a cavity with openings of two sizes. The exterior of the molecule is very polar/hydrophilic due to many hydroxyl groups whereas the interior is quite nonpolar/hydrophobic. The property of different polarity in different parts of the molecule leads to the most important and utilized ability of CDs: They readily form inclusion complexes with hydrophobic molecules that fit into the cavity in polar environments, mainly in aqueous solution. The complex formation results in several changes of the properties of the guest molecule. First of all, the water solubility of hydrophobic molecules rises significantly. Furthermore, the vapour pressure decreases after complexation as well as the stability against oxidation under air or light induced degradation.¹⁰⁸ In several cases CDs activate chemical reactions, *e.g.* the hydrolysis of various phenylesters.^{108,109} As CDs are optically active, they are also utilized in chi-

ral catalysis.¹¹⁰ Other applications include drug delivery,^{32,111,112} catalysis,¹¹² chromatography (also for chiral separation)¹¹³ or as food ingredient to mask odours or protect food ingredients against decomposition.^{112,114}

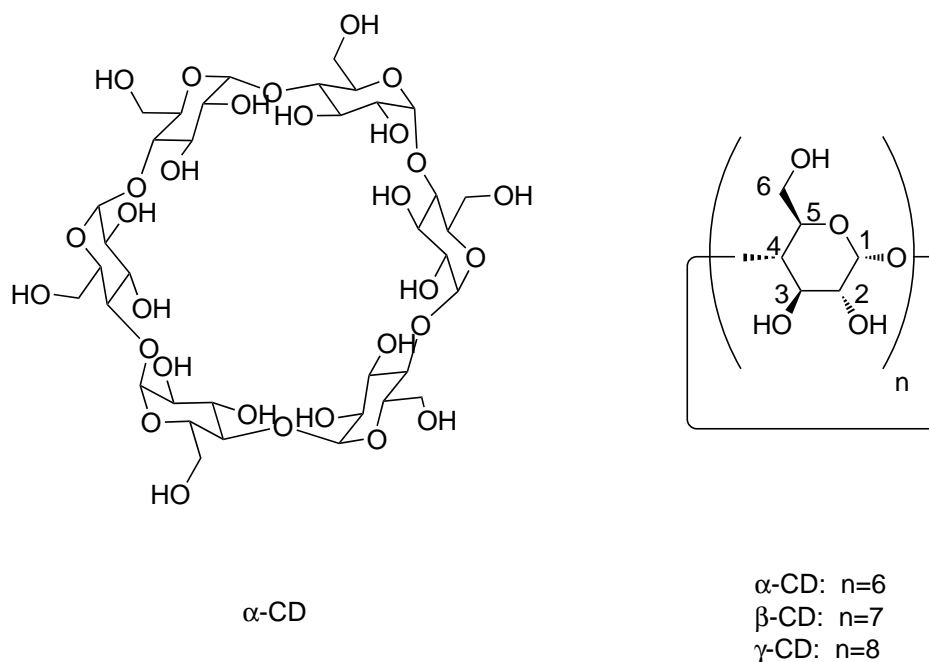


Figure 2.7: Chemical structure of native CDs and common labelling of C-atoms in the glucose units.

Table 2.1: Dimensions and water solubility of native CDs.

Type of CD	α -CD	β -CD	γ -CD
Number of glucose units	6	7	8
Cavity length [\AA]	8	8	8
Approx. cavity diameter [\AA]	5.2	6.6	8.4
Water solubility at 25 °C [mol L^{-1}]	0.121	0.016	0.168

CD host/guest complexes can be prepared in solution,^{115,116} by coprecipitation^{116,117} or in a slurry^{116,117} as well as in the solid state, *e.g.* cogrinding or milling.^{115–117} In the case of complex formation in solution, sometimes a cosolvent has to be added to enhance the accessibility of the guest, which is depending on the water solubility of the guest molecule.

2.2.3 Thermodynamics and Theory of CD Inclusion Complexation

The complexation of CDs with guest (G) molecules can be considered as a bimolecular process:¹⁰⁶



These equilibria summarize the formation of CD:G 1:1, 1:2 or 2:1 complexes with the following association constants:

$$K_{11} = \frac{[GCD]}{[G][CD]} \quad (2.9)$$

$$K_{12} = \frac{[GCD_2]}{[GCD][CD]} \quad (2.10)$$

$$K_{21} = \frac{[G_2CD]}{[G][GCD]} \quad (2.11)$$

In general, the formation of more complicated CD host/guest complexes G_mCD_n can be described by the following equilibrium



and equation for the overall association constant β_{mn} :

$$\beta_{mn} = \frac{[G_m][CD_n]}{[G]^m[CD]^n} \quad (2.12)$$

The driving force for the complex formation is not yet fully understood.^{106,115} Nevertheless, some contributing factors can be identified. The release of water molecules from the cavity leads to an increase in entropy of the system. Furthermore van der Waals interactions and hydrophobic interactions between guest and interior of CD contribute to complex formation. In some cases hydrogen bonding between guest and the rim of CD takes place. From the temperature dependence of the association constant, enthalpy ($\Delta H_{\text{complex}}$) and entropy ($\Delta S_{\text{complex}}$) of complexation are obtainable.¹⁰⁸ In most cases, $\Delta H_{\text{complex}}$ is negative which leads to complex dissociation at

higher temperatures,^{106,116,118,119} whereas $\Delta S_{\text{complex}}$ can have negative or positive values depending on the interactions that take place during complexation. In the complex formation several steps have to be considered:^{108,120}

1. The guest molecule has to approach the CD
2. Enthalpy rich water molecules have to be released from the cavity (results in a rising entropy of the system)
3. The hydration shell of the guest has to be removed at least partly
4. Interactions (mostly weak van der Waals attractions) of the guest molecule with the rim of the CD and the inside (the guest molecule enters the cavity)
5. Possible formation of hydrogen bonds between CD and guest
6. Re-formation of the hydration shell of exposed parts of the guest molecule and around the CD molecule

From the point of complex formation kinetics in steps 1, 4 and 5 the size of the guest molecule plays an important role and no complex formation is observed for guests that extend the cavity size. The assembly of water molecules relies on several factors, *e.g.* pH value or ionic strength, which is independent from the respective guest molecule. Most likely steps 3 and 4 can be considered rate determining.¹²⁰ The size of the guest group is not only a criterion whether it is possible for the guest to enter but also for the stability of the complex. As the interactions between CD and guest are rather weak and of a short range, the complex stability depends strongly on a good fit between CD and guest. In some cases a weak fit between CD and guest can be compensated with the formation of different complex geometries/stoichiometries (refer to Section 2.2.4).

2.2.4 Complex Types, Common Host/Guest Pairs and their Stability

From the geometry of CD two complexation modes are possible. Depending of the dimension of the guest, it can enter the cavity from the primary or the secondary side of CD (refer to Figure 2.8). The primary side is on the face of C6 and OH-6 and has a slightly smaller opening. The secondary side is on the face of C2 and C3 with a slightly larger opening of the cavity. Complexes with different complexation modes can be identified *via* multi dimensional NMR spectroscopy¹²¹ and X-ray crystallography.^{106,122–124} Furthermore, different complex stoichiometries are possible.¹¹² The most common cases are 1:1 CD/guest complexes but 2:1 and 1:2 are described as well, *e.g.* the complex 1-bromoadamantane with 2 α -CD molecules¹²⁵ or the complex of γ -CD with 2 pyrene molecules.^{126,127} The complex stoichiometry can be identified *via* the method of continuous variation, *i.e.* Job's plot.^{121,125,128} In this analysis the product of mole fraction and complexation induced change in the chemical shift in the NMR spectrum is plotted against the mole fraction of guest or CD. The position of the maximum of the obtained curve indicates the complex stoichiometry.

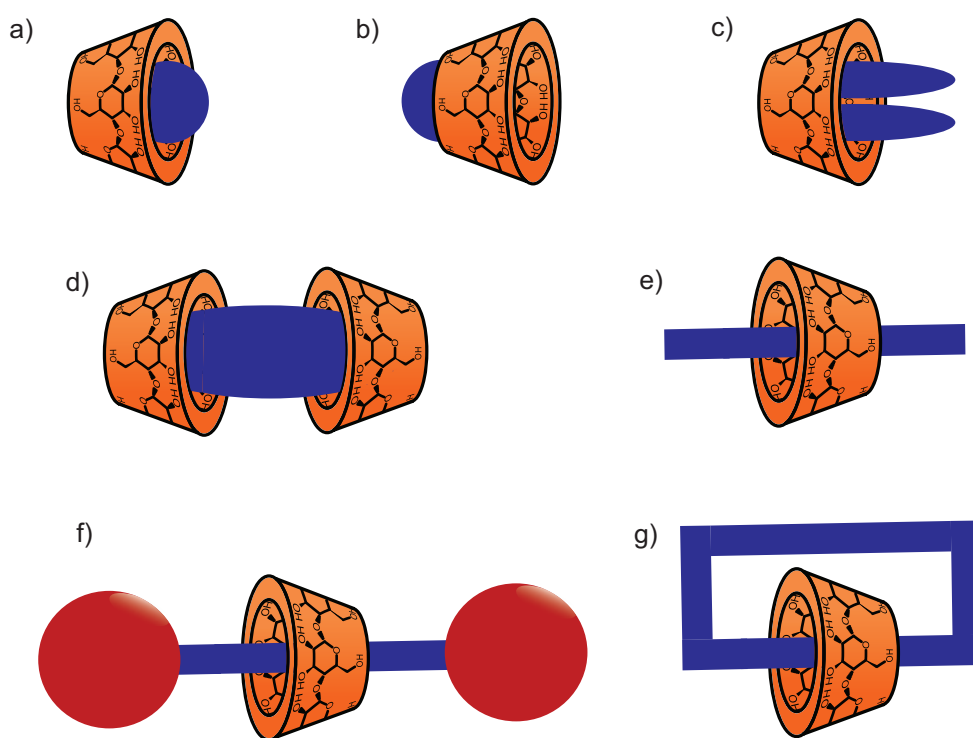


Figure 2.8: Different types of complexation: a) 1:1 CD/guest complex from the secondary side, b) 1:1 CD/guest complex from the primary side, c) 1:2 CD/guest complex, d) 2:1 CD/guest complex, e) pseudo rotaxane, f) rotaxane and g) catenane.

CD complexes with axial shaped guests are called pseudo rotaxanes if they are not fixed *via* stopper groups (refer to Figure 2.8).¹²⁹ After fixation with large stopper

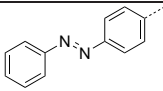
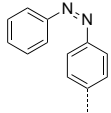
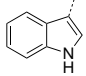
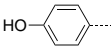
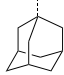
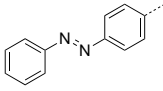
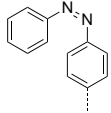
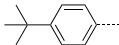
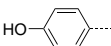
molecules that suppress the dethreading of CD, complexes of CD with axial guests are called rotaxanes.^{129,130} In that case the CD complexation loses its reversibility and the formed bond between host and guest is a mechanical bond. Another class of mechanically interlocked molecules are catenanes, which are the connection of two or more rings *via* intertwining (Figure 2.8).¹³¹

The different complex types can be transferred to polymers as well, *e.g.* in poly pseudo rotaxanes,^{132,133} polyrotaxanes,¹³⁴ side chain pseudo polyrotaxanes,¹³⁵ side chain polyrotaxanes¹³⁶ or pseudo rotaxane star polymers.^{137,138} Rotaxane formation can be utilized, *e.g.* for the formation of supramolecular polymers¹³⁹ or hydrogels.¹⁴⁰ The concept of mechanical bonds was utilized for example in the synthesis of mechanically interlocked block copolymers.^{141,142}

While the complex stoichiometry can be addressed *via* Job's plot, the association constant, and thus an equivalent for the complex stability, is accessible *via* isothermal titration calorimetry¹⁴³ or the Benesi-Hildebrand plot^{144–146} for instance. In isothermal titration calorimetry the evolution of heat is measured during the addition of guest or host to a host or guest solution, respectively. A fit of the plot of molar ratio against enthalpy leads to $\Delta G_{\text{complex}}$ and thus the association constant can be derived, while the surface under the curve gives the complexation enthalpy $\Delta H_{\text{complex}}$. The utilization of the Benesi-Hildebrand plot gives the opportunity to obtain association constants *via* changes of absorption in UV spectra or the chemical shift in NMR spectra.

Table 2.2 shows a selection of different guests with the respective association constant. For, α -CD mono or *para* substituted aromatic structures are commonly utilized, *e.g.* phenyl or azobenzene with association constants up to 10^4 M^{-1} , as well as aliphatic chains or poly(ethyleneglycol) (PEG). One of the strongest associations are reported between α -CD and indole with an association constant of 10^7 M^{-1} probably due to the formation of additional hydrogen bonds. The adamantyl-group is a well-known guest group for β -CD with association constants up to 10^5 M^{-1} . Azobenzene and *tert*-butyl phenyl are also utilized in several examples. In the case of γ -CD, very bulky guests are necessary, *e.g.* two pyrene molecules or cyclododecane.

Table 2.2: Common guests for the native CDs and the respective association constants.

Guest	Structure	Type of CD	$\log \beta$ [$\log \text{M}^{-1}$]
<i>trans</i> -Azobenzene		α	4.0 ¹⁴⁷
<i>cis</i> -Azobenzene		α	0.6 ¹⁴⁸
Indole		α	7.8 ¹⁴⁹
Phenol		α	4.2 ¹⁴⁹
Adamantyl		β	4.6 ¹⁵⁰
<i>trans</i> -Azobenzene		β	2.7 ¹⁵¹
<i>cis</i> -Azobenzene		β	0.4 ¹⁵¹
<i>tert</i> -Butyl phenyl		β	4.4 ¹⁵²
Phenol		β	3.4 ¹⁴⁹

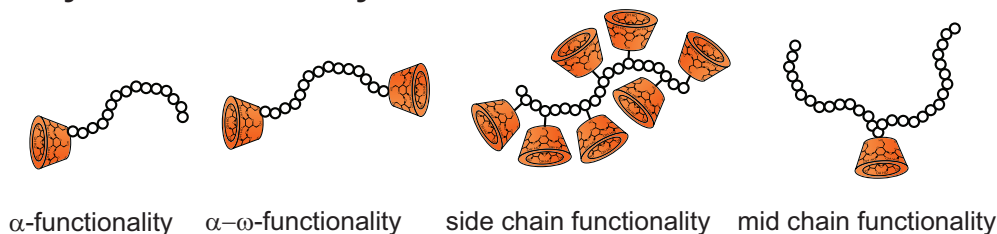
2.3 Complex Macromolecular Architectures Governed by CD Complexes

In recent years CD complexes have proven to be a perfect tool for the generation of complex macromolecular architectures. Almost every conceivable architecture has been described so far. Especially the development of controlled radical polymerization techniques for the synthesis of endfunctionalized polymers had a very significant impact on the research in this area.

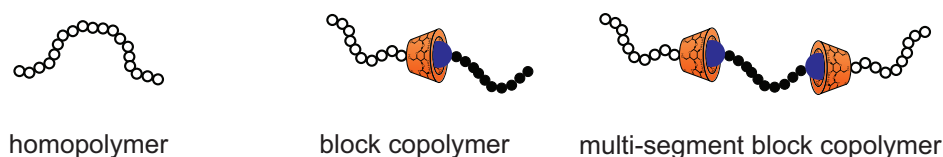
Figure 2.9 shows a compilation of different architectures that were generated *via* CD host/guest complexes so far. CDs have been utilized for the modification of polymer functionality, polymer composition and polymer topology. CD functionalized polymers are rather readily accessible *via* living/controlled radical polymerization giving control of end chain and mid chain functionality. Diverse supramolecular polymer compositions can be obtained *via* incorporation of CD complexes at the interface between different blocks. To achieve more complex topologies, a combination of dif-

ferent functionalized building blocks is necessary, *e.g.* multi CD functionalized polymer strands. In general, the control over polymer functionality gives rise to the formation of complex supramolecular polymer compositions and topologies.

Polymer Functionality



Polymer Composition



Polymer Topology

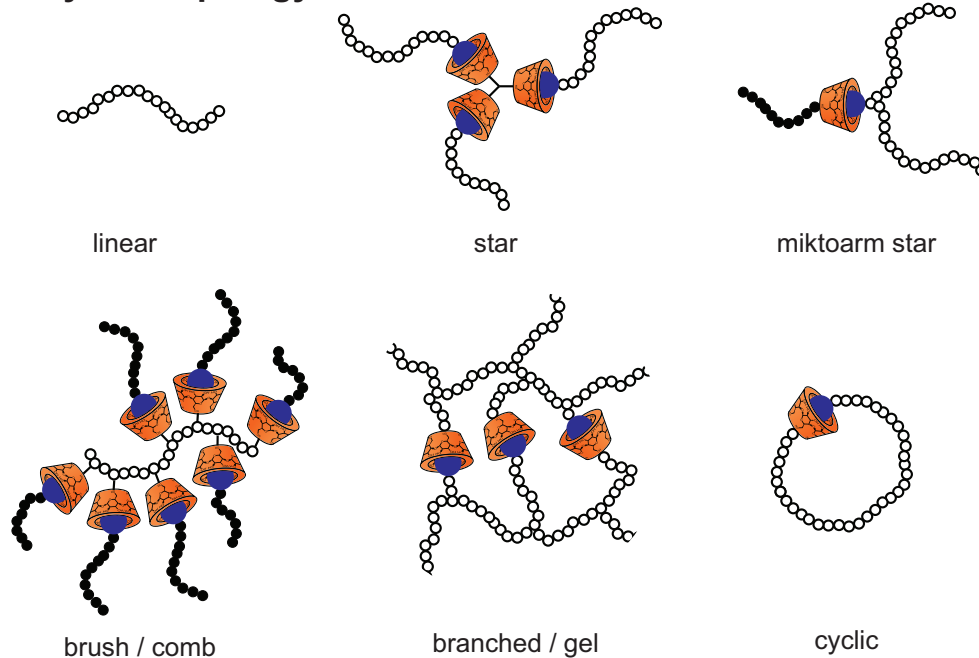


Figure 2.9: Complex macromolecular architectures *via* CD-driven supramolecular complexation and macromolecular building blocks with CD moieties (CD is depicted in orange; guest groups are depicted in blue).

2.3.1 Common CD Containing Building Blocks

Although CDs possess a large number of functional groups, the reactivity of the primary and secondary hydroxyl groups differs significantly, which gives the opportunity to exclude some of the hydroxyl groups in specific reactions.^{153,154} Nevertheless, at least 6 hydroxyl groups with the same reactivity exist in a CD molecule. To obtain mono functionalization, the reaction conditions have to be monitored carefully. The most commonly used intermediate is the mono tosylate at C6, which can be synthesized in pyridine for all native CDs^{155–157} or in aqueous NaOH solution for β -CD and α -CD.^{158,159} The tosylate can be transformed into several useful building blocks, *e.g.* azide,^{156,157} thiol¹⁶⁰ or amine *via* nucleophilic substitution with a diamine.¹⁶¹ The azide is available *via* a nucleophilic substitution of the tosylate with sodium azide,^{156,157,159} whereas the thiol is formed *via* a nucleophilic substitution with thiourea and subsequent hydrolysis.^{160,162} The azide can be further converted into an amine *via* reduction.^{155–157} With these 3 substituents a large variety of modern polymer conjugation reactions can be utilized, *e.g.* CuAAC^{158,163} and thiol-ene reactions.¹⁶⁴ CD-functionalized polymerization mediators, *e.g.* for NMP,¹⁶⁵ ATRP¹⁶⁶ or RAFT¹⁶⁷ have been described in the literature as well as post-polymerization conjugation reactions with CDs.^{166,168} Mono functionalizations at C2 are described in the literature as well,^{169,170} yet C2 or C3 derivatives are not utilized as frequent as the C6 derivatives. Certainly an esterification of the hydroxyl groups is possible as well, yet the selectivities are usually low. Either full conversions are initially targeted or lower substitution grades are targeted and the obtained mixtures have to be purified in inconvenient procedures.

2.3.2 Block Copolymers

The formation of block copolymers *via* CD complexes is mainly restricted to AB diblock copolymers so far. Almost exclusively β -CD has been utilized in that regard. The synthesis of supramolecular diblock copolymers is straight forward as only two components are needed: a CD-functionalized polymer and a guest functionalized polymer. These building blocks are commonly obtained *via* controlled radical polymerization techniques yet in some cases cationic or anionic polymerization have been utilized as well.

One of the first examples is an AB diblock copolymer of PNIPAAm and P4VP synthesized *via* RAFT polymerization by Zhang and coworkers that has proven to be pH- and thermoresponsive.¹⁷¹ This block copolymer was exploited in temperature- and pH-induced micellization and vesicle formation which was observed *via* DLS, SLS, fluorescence measurements and TEM. At a pH value over 4.8 and a temperature of

25 °C vesicles were formed and at a pH value of 2.5 and a temperature of 60 °C micelles were formed. Another example of double stimuli responsive block copolymers, *i.e.* with schizophrenic behavior, has been described by Liu and coworkers.¹⁶⁶ Again pH- and thermoresponsive behaviour was combined but this time *via* PDMAEMA and PNIPAAm blocks synthesized *via* ATRP. Vesicle formation was observed at low pH values and high temperatures (pH 4 and 50 °C), whereas micelles were formed at high pH values and low temperatures (pH 9 and 25 °C), which was proven *via* TEM, DLS and SLS. Voit and coworkers described a supramolecular diblock copolymer consisting of PNIPAAm synthesized *via* ATRP and poly(2-methyl-2-oxazoline) synthesized *via* cationic ring-opening polymerization.¹⁷² The temperature-responsive PNIPAAm block was utilized for temperature-induced aggregation. These examples evidence the impact that CD-based supramolecular chemistry can have in the area of macromolecular architectures.

CD complexes provide another possibility for stimuli response. Not only different polymer types can be utilized in the area of stimuli-responsive materials, yet the supramolecular connection is addressable *via* external stimuli as well. One of the first examples is the utilization of a voltage responsive connection *via* a ferrocene endgroup which was described by Yin and coworkers.¹⁷³ A β -CD functionalized PSty and a ferrocene functionalized PEG were utilized. The connection between the blocks can be disrupted, as ferrocene molecules can be oxidized reversibly and the ferrocene cation does not fit into the β -CD cavity. At first, block copolymer vesicles were obtained that dissociated upon application of an electric current. The rate of dissociation and the release of a test molecule could be adjusted *via* the amount of the voltage. Another example of diblock copolymers with stimuli responsive linkage was described by the same group.¹⁷⁴ Supramolecular based nanotubes were formed (length \sim 220 nm and diameter \sim 90 nm) *via* a supramolecular poly(ϵ -caprolactone-*b*-AA) (PCL-*b*-PAA) diblock copolymer. The supramolecular complex was formed between azobenzene and α -CD that leads to a light responsive linkage between the blocks. Furthermore, the nanotubes were loaded with Rhodamine B that could be released *via* light induced disassembly of the nanotubes. Stenzel and coworkers prepared supramolecular core shell nanoparticles with a PMMA core and poly(hydroxy ethylacrylate) (PHEA) shell.¹⁶⁴ The guest functionalized PHEA building block was obtained directly *via* RAFT polymerization, whereas the CD functionalized PMMA block was obtained *via* RAFT polymerization of MMA, a Chugaev thermolytic end-group conversion and a subsequent thiol-ene reaction with mono thiol functionalized β -CD. Core shell nanoparticles (diameter \sim 150 nm) were obtained after mixing of the building blocks in DMF and subsequent water addition or by the generation of core PMMA nanoparticles in water and addition of the water soluble building blocks. The addition of free β -CD led to the disassembly of the complexes and aggregation of the

water insoluble blocks.

A diblock copolymer with a special linking moiety was described by Zhou and coworkers.¹⁵⁸ In this case a dilinker consisting of α -CD and β -CD connected with a short spacer was utilized to form a diblock copolymer of PNIPAAm and PCL. Furthermore, cell targeting ligands were introduced to enhance cell uptake efficacy. To protect the formed core shell nano-sized assemblies in body fluids, PEG moieties were incorporated as well. The formed assemblies were utilized in drug delivery experiments that showed tumor-triggered release of loaded molecules. This particular example shows how powerful CD complexes are as a tool for the formation of macromolecular architectures with regard to the specific application, e.g. drug delivery¹⁵⁸ or the formation of nano objects.^{173,174} Especially the stimuli-responsive nature of several CD/guest pairs gives the opportunity to disassemble the block copolymer at the junction of the different blocks. Thus, the distinct properties of block copolymers can be utilized but with the additional property of disassembling the blocks. This concept has been utilized recently by Hawker and coworkers in block copolymer lithography with block copolymers that are coupled *via* hydrogen bonds. This example shows that supramolecular bonded block copolymers can indeed mimic the behavior of their covalent analogues.¹⁷⁵

2.3.3 Brush Polymers

The synthesis of supramolecular brush polymers can be conducted *via* two pathways. Either CD molecules are connected to a backbone or surface and a guest endfunctionalized polymer is added or guest molecules are connected to a polymer backbone or surface and CD-endfunctionalized polymers are added. The forming complexes lead to brush-like architectures. Of course the complex formation is governed by equilibria and thus the obtained grafting density strongly depends on the association constants. Furthermore, steric factors play an important role as CDs have a very bulky structure that can suppress high grafting densities.

A supramolecular brush formation in solution has been described by Bernard and coworkers.¹⁶⁸ A CD-containing backbone was synthesized in a two step procedure. Firstly, trimethyl silyl protected propargyl methacrylate was polymerized *via* RAFT, subsequently the terminal alkyne groups were deprotected and conjugated with β -CD- N_3 in a CuAAC reaction. Short PAA chains endfunctionalized with an adamantyl-group were synthesized and brushes were formed in aqueous solution. The brush formation was proven *via* DLS and NOESY (nuclear Overhauser enhancement spectroscopy). Although a dodecyl functional RAFT agent was utilized, no competing complex formation was evident, which was proven *via* comparison of dodecyl-functional chains with chains after RAFT endgroup removal. Jiang and coworkers presented

a supramolecular brush with a copolymer of *N*-vinylpyrrolidone and a CD functional monomer and doubly adamantyl endfunctionalized PCL.¹⁷⁶ Interestingly, micellar aggregates were obtained, as shown by TEM and DLS, and no gel formation was observed, although a doubly guest functional polymer was utilized. Later Zhang and coworkers presented a supramolecular brush consisting of a CD-functionalized polymer backbone and adamantyl functionalized oligo ethylene glycol dendrons. The thermoresponsive behavior was studied as a function of several factors, *e.g.* dendrimer generation or hydrophobicity of the dendrimer endgroups.¹⁷⁷ In that way the LCST could be tuned from 34 °C - 56 °C. It was found that the dehydration and collapse of the oligo ethylene glycol chains leads to disassembly of the host/guest complexes, which was studied *via* NMR and ITC.

Apart from solution studies several reports regarding surface brushes exist in the literature. Li and coworkers studied the grafting of doubly adamantyl endfunctionalized polymers on CD modified cellulose.¹⁷⁸ After the formation of the supramolecular complexes the grafting was proven *via* XPS, ellipsometry, TGA and FT-IR. Thus, a supramolecular grafting on the renewable resource cellulose was achieved. Reinhoudt and Huskens introduced the concept of molecular printboards, *i.e.* mono layers of CD host molecules on a planar surface that are capable of the stable attachment of guest molecules.¹⁷⁹ This concept has been exploited to generate different grafted structures, *e.g.* on gold¹⁷⁹ or SiO₂.¹⁸⁰ Furthermore, patterns on the surface have been generated *via* micro contact printing.¹⁸⁰⁻¹⁸² These molecular printboards have been utilized to immobilize proteins,^{183,184} fluorescent dyes¹⁸² or Eu³⁺ luminescent complexes.¹⁸¹ A similar approach was utilized to graft an azobenzene functionalized cell recognition peptide onto an α -CD functionalized gold surface that showed reversible and photocontrolable cell attachment.¹⁸⁵

2.3.4 Star Polymers

CD-based star polymers can be divided into two categories. Star polymers with CD as a core moiety due to its high concentration of functionality, which is the most frequent utilization of CDs for star polymers. The other possibility is to utilize host/guest complexes to obtain supramolecular star polymers, *e.g.* *via* a core molecule with several CD moieties and guest functionalized polymers.

One of the first reports of CD-centered stars is from the work of Haddleton and coworkers, where a 21 arm star polymer consisting of PMMA or PSty arms was synthesized *via* ATRP with a grafting-from approach.¹⁸⁶ Furthermore, block copolymer stars were formed from the obtained macro initiators. A similar approach was conducted by Stenzel *et al.*, who described a CD-centered 18 arm PSty star synthesized *via* living radical polymerization mediated by a half-metallocene iron carbonyl com-

plex¹⁸⁷ and a CD-centered 7 arm star formed *via* RAFT polymerization of Sty,^{58,188} as well as block copolymers with ethyl acrylate.¹⁸⁸ The range of utilized monomers for the arm-forming polymers was subsequently extended later to *tert*-butyl acrylate,¹⁸⁹ oligo ethyleneimine,¹⁹⁰ azobenzene monomers,¹⁹¹ 2-ethyl-2-oxazoline,¹⁹² glycomonomers,¹⁹³ HEA,¹⁹³ NIPAAm¹⁹⁴ and PNIPAAm-*b*-PDMAAm¹⁹⁵ by several research groups. Kakuchi and coworkers utilized mono amino β -CD to attach a NMP initiator, followed by a living/controlled radical polymerization of Sty.¹⁹⁶ The remaining hydroxyl groups were utilized to attach ATRP initiator *via* esterification and subsequently MAA or *tert*-butyl acrylate was polymerized to form a CD centered miktoarm structure. Recently Haddleton and coworkers introduced 7 thiols on the secondary face of β -CD for subsequent thiol-ene reactions, *e.g.* with oligo ethylene glycol methacrylate (OEGMA), and utilized the remaining 14 hydroxyl functions as initiator for the ring-opening polymerization of CL, which leads to the formation of a CD-centered miktoarm star polymer.¹⁹⁷ These examples are of particular interest because the different reactivities of the β -CD hydroxyl groups were utilized to generate a complex macromolecular architecture. An alternative architecture involving CD-core star polymers has been published recently by Wenz and coworkers which is a combination of rotaxane and star architectures.¹⁹⁸ Here α -CD centered PMMA stars were threaded onto a PEG backbone and fixed *via* large stopper molecules. PMMA chains were grafted from ATRP initiators connected to the threaded α -CD moieties on the rotaxane and were characterized *via* diffusion-ordered NMR spectroscopy (DOSY), SEC and AFM. An interesting feature of the thus formed brushes is their sensitivity to mechanical forces during SEC measurement, which led to the scission of the PEG thread. A similar approach was followed by Yui and coworkers.¹⁹⁹ PEG was threaded with α -CD to form a polyrotaxane. The remaining hydroxyl groups of the α -CD threads were utilized to grow P(lactide) (PLA). Continuous anisotropic phases were formed in the bulk state. The crystallization behavior was studied *via* DSC, X-ray diffraction and polarized optical microscopy. An accelerated stereo complex formation was found that was attributed to the enhanced moveability due to the rotaxane structure. Fewer reports are in the literature on star architectures governed by host/guest complexes. An interesting architecture in that regard is the connection of two CD-centered stars with a doubly guest functional polymer, which leads to a dumbbell shape in solution that has been described in two studies.^{200,201} In the first report β -CD centered PNIPAAm with 4 arms was connected with a doubly adamantyl functionalized PEG, the complex formation was proven *via* NOESY and the change in the LCST was monitored depending on host/guest ratio or the molecular weight of the employed PEG.²⁰⁰ Later, β -CD centered PNIPAAm was connected with a doubly adamantyl functionalized poly(propylene glycol) (PPG).²⁰¹ As this system contains two thermoresponsive polymer types, the aggregation behavior was studied depending on

the temperature *via* DLS, NMR, fluorescence measurements, AFM and TEM. The formation of supramolecular block copolymers was evident in cold water, whereas micelle formation was observed at temperatures over 8 °C and above 22 °C micelle destabilization was observed. The formation of an ABC miktoarm star polymer was published recently by Zhu and coworkers that required several functionalization reaction with β -CD.¹⁶³ In brief, β -CD was mono tosylated, converted into the azide and mono tosylated again. PEG was conjugated *via* CuAAC, the remaining tosylate was converted into the azide and subsequently an ATRP initiator was added *via* CuAAC. DMAEMA was polymerized *via* ATRP to obtain a miktoarm star with two different arms. A third arm consisting of adamantyl functional PMMA was connected *via* supramolecular complex formation. Due to the hydrophobic character of PMMA, micelles were obtained in solution and characterized *via* DLS and TEM. Wu and coworkers utilized a threefold β -CD core to connect three guest functionalized oligo ethylene glycol dendrimer arms.²⁰² The thermoresponsive behavior of the formed dendrimer stars was investigated showing a variation in the LCST from 43 to 72 °C depending on dendrimer generation, dendrimer endgroup (ethyl or methyl) and ratio of different dendrimer types (with ethyl or methyl endgroup). Furthermore, the effect of salt concentration was investigated as well as the thermally induced decomposition of the supramolecular complexes.

Jiang and coworkers utilized host guest complexes to form brush-like star architectures with different spherical cores, *e.g.* SiO₂ nanoparticles,²⁰³ CdS quantum dots^{204,205} or gold.²⁰⁶ In the case of SiO₂ nanoparticles, PEG arms were utilized and subsequently α -CD was added to induce hydrogel formation. In another work quantum dots were utilized as a core for azobenzene or ferrocene endfunctionalized PDMAAm-*b*-PNIPAAm block copolymers.^{204,205} The thermoresponsive nature of the PNIPAAm blocks was utilized to induce hydrogel formation above the LCST. The hydrogels showed a variation of photoluminescence depending on the temperature and thus the gel formation, which can be attributed to the confinement of the quantum dots in the gel. Furthermore, UV-light and electrochemical response was probed. CD-functionalized gold nanoparticles were grafted with azobenzene endfunctionalized PNIPAAm-*b*-PDMAAm, which gave the opportunity to disrupt the supramolecular complex upon UV-irradiation.²⁰⁶ Heating above the LCST of the PNIPAAm block led to the formation of vesicles. A similar approach was described earlier.²⁰⁷ In this case gold nanoparticle cores with α -CD shell were utilized as well. Azobenzene endfunctionalized PNIPAAm homopolymer was supramolecularly attached. Subsequently the photoresponsive behavior and the thermal behavior of the aggregates were studied in detail.

2.3.5 Branched Polymers and Gels

The probably most intensively studied field in CD driven macromolecular architectures is the formation of branched structures and hydrogels. Several reviews based on these materials can be found elsewhere.^{28,30,208–210} Nevertheless, in this section a short overview on polymeric CD-based hydrogels and branched structures that have been synthesized *via* controlled radical polymerization is presented. In general, the formation of branched structures and hydrogels can be conducted *via* different pathways. A large amount of host and/or guest functionalities can be incorporated into the side chain of the polymers or as endgroup to induce supramolecular crosslinking. Furthermore, single CD molecules can be utilized as crosslinkers if the guest group is small and two guests can be included, which leads to single-CD crosslinking points. Alternatively CDs can act as crosslinker *via* aggregation/crystallization.

An example of the latter category utilizes OEGMA based polymers with side chains of POEGMA as a double brush structure that was formed *via* ATRP. The formation of a hydrogel was induced *via* addition of α -CD.¹³⁵ Interestingly, the formation of hexagonal crystals was observed in the hydrogel which is due to the formation of columnar microcrystalline domains of α -CD. Later P(EG-*co*-DMAEMA) brushes were utilized to form thermo- and pH-responsive gels after α -CD addition.²¹¹ The gelation behavior was altered *via* copolymer concentration, pH value, PEG branch density and the chain uniformity of the copolymers. With these gels drug release at different pH values and temperatures was studied. The same crosslinking method was employed with PEG-*b*-PDMAEMA blockcopolymers, which lead to a series of different microgel morphologies depending on pH value or ionic strength, *e.g.* hexagonal, bowl or spherical structures that could be visualized *via* TEM.²¹² A recent utilization of α -CD based crosslinking *via* a poly pseudo rotaxane formation is the supramolecular anchoring of DNA polyplexes in hydrogels formed from PEG-*b*-PCL-*b*-PDMAEMA blockcopolymers and α -CD.²¹³ The polymers were synthesized *via* a combination of ATRP and ring-opening polymerization. Subsequently, DNA polyplexes were formed from blockcopolymer micelles and plasmid DNA. The addition of free PEG chains and α -CD leads to hydrogel formation. The following studies on the release of the incorporated DNA showed sustained release of stable polyplexes with high bioactivity. A β -CD centered star polymer of PDMAEMA was protonated and utilized to form networks with polyanionic PAA-*b*-PEG di- and triblock copolymers.²¹⁴ Depending on the structure of the polyanionic block, fibrillar or spherical microstructured gels were obtained. SEM, TEM, DLS and rheological measurements were carried out to study the obtained materials. Furthermore, the remaining cavity in the β -CD moiety was utilized to include a model drug and study the release behavior. Another example is the temperature induced formation of PNIPAAm hydrogels from a β -CD centered PNIPAAm-*b*-PDMAAm three arm star polymer.¹⁹⁵ Again, the β -CD cavity

was utilized for small molecule release. As described before in Section 2.3.4, quantum dot centered hydrogels formed due to the LCST of PNIPAAm blocks have been generated as well.^{204,205}

Kang and coworkers presented the synthesis of a doubly β -CD functionalized poly(2-(methacryloyloxy)ethyl succinate) *via* RAFT polymerization.¹⁶⁷ This polymer was utilized in the formation of poly pseudo rotaxanes with an acrylate endfunctionalized PEG-*b*-PPG-*b*-PEG. The acrylate functions were subsequently reacted in a thiol-ene reaction with a multifunctional thiol to form permanent crosslinking points. Thus, a sliding hydrogel was obtained evidencing pH response (from the succinate) and thermoresponse (from the PEG and PPG blocks). Swelling ratios and thermal properties could be adjusted *via* different chain lengths of the β -CD functionalized polymer which is rather easy *via* changing the conditions of the RAFT polymerization.

2.3.6 Other Architectures

Jiang and coworkers presented a block copolymer-like structure consisting of Frechét-type benzyl ether dendrons (generations 1, 2, and 3) with an azobenzene at the apex and a β -CD functionalized PNIPAAm.²¹⁵ These supramolecular block copolymer amphiphiles formed vesicles or micelles in aqueous solution depending on dendron generation. Furthermore, UV-irradiation lead to the disassembly and formation of irregular particles which could be reversed *via* irradiation of visible light. Heating above the LCST of the PNIPAAm block leads to reversible aggregation of the particles. Vesicles of a doubly CD endfunctionalized P(ether imide) were prepared by Jiang and coworkers.²¹⁶ β -CD cavities were present on the inner and outer walls of the vesicle that could be addressed *via* guest functionalized PEGs depending on the molecular weight, *e.g.* with 1k and 2k PEG inner and outer surface was modified, whereas with 5k PEG the inner surface was modified only partially. Giacomelli *et al.* formed PSty centered micelles with β -CD surface.¹⁶⁵ The underlying β -CD functionalized PSty was prepared *via* NMP. The formation of a supramolecular cyclic polymer was described by Harada and coworkers.²¹⁷ A PEG with azobenzene and β -CD endgroup was utilized in that regard. The formation of cycles could be performed in high dilution, whereas intermolecular complexes were formed at higher concentration. The azobenzene moiety was exploited for UV-light triggered dethreading of the complex. Between the PEG and β -CD a aromatic unit was incorporated that was competing in complexation with the azobenzene depending on the temperature, which was shown *via* temperature dependent NOESY.

A supramolecular enzyme polymer conjugate was described by Feiters and coworkers.²¹⁸ β -CD functionalized PSty was prepared *via* ATRP that formed vesicles in aqueous solution. These vesicles bear CD-units on the outer and inner surface. The β -CD

moieties were subsequently utilized to conjugate adamantyl-PEG-functionalized horseradish peroxidase that showed catalytical activity although it was connected supramolecularly to the PSty vesicle.

CD-Complexed RAFT Agents

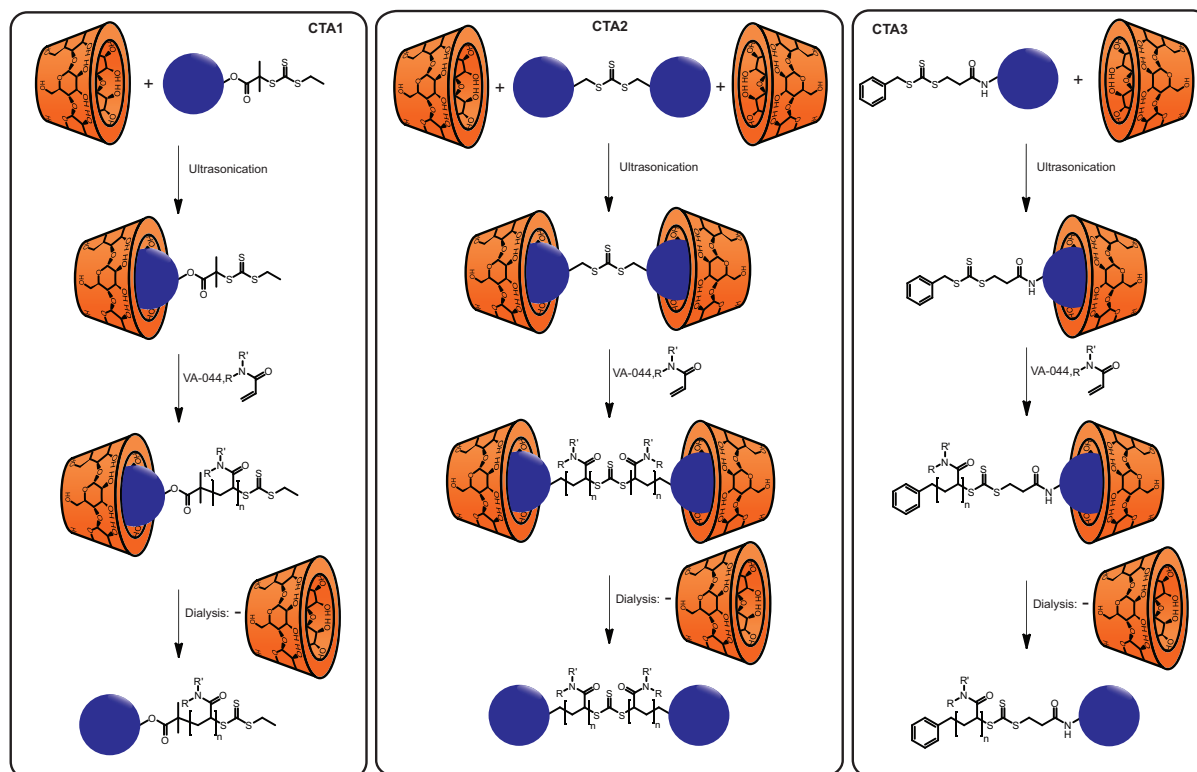
3.1 Introduction

RAFT polymerization has emerged as a very efficient tool for the synthesis of water-soluble polymers due to its high tolerance of functional monomers^{62,72,219,220} (see Section 2.1.4). The polymerization itself can be conducted directly in water with a broad range of water-soluble monomers that include methacrylates,⁷⁶ methacrylamides,⁸⁰ styrenics,⁶³ acrylates²²¹ and acrylamides^{66,69,222} so far. Furthermore, the utilization of water is interesting from an environmental and economic point of view as water is non-toxic, non-flammable and readily available. Thus, it is easy to handle safely and low priced.

The possibility to solubilize hydrophobic molecules in water is an interesting application of CDs. In this context, hydrophobic monomers were solubilized in water with CDs, e.g. in radical polymerization,^{223,224} living radical polymerization,^{225–227} enzymatic polymerization²²⁸ and Rhodium-catalyzed polymerization.²²⁹ To connect the solubilizing effect of CDs with RAFT polymerization, the aqueous RAFT polymerization of three acrylamido monomers, namely DMAAm, DEAAm and NIPAAm in the presence of a hydrophobic CTA that is solubilized via a host/guest complex was investigated. The employed hydrophobic CTAs bear the 4-*tert*-butyl phenyl-group that is well known to form stable host/guest complexes with β -CDs.^{152,230} Three novel CTAs were synthesized, which contain the guest-group in regions of variable reactivity within the molecule. The guest group can be incorporated in the R-, the Z-group or both. As the CTA allows control over the chain-end functionality in RAFT polymer-

ROESY measurements were performed in collaboration with M. Hetzer and Prof. H. Ritter (Heinrich Heine Universität Düsseldorf). Parts of this chapter were reproduced with permission from Schmidt, B. V. K. J.; Hetzer, M.; Ritter, H.; Barner-Kowollik, C. *Macromolecules* **2011**, *44* (18), 7220-7232 (DOI: 10.1021/ma2011969). Copyright 2011 American Chemical Society.

ization, hydrophobic chain ends are obtained directly (as depicted in Scheme 3.1).



Scheme 3.1: Procedure for the RAFT polymerization of acrylamido-monomers with CD-complexed CTAs (DMAAm: $R=R'=Me$; DEAAm: $R=R'=Et$; NIPAAm: $R=i-Pr$, $R'=H$): R-approach (1), combined approach (2) and Z-approach (3). The guest-substituent, *i.e.* 4-*tert*-butyl phenyl, is depicted blue.

The hydrophobic chain ends may have further use as guests in complex self-assemblies with CD-functionalized polymers or surfaces, *e.g.* to construct supramolecular block copolymers^{171,172} or to obtain supramolecular grafting, *e.g.* on cellulose.¹⁷⁸ In the case of thermoresponsive polymers that show T_c behavior such as PNIPAAm or PDEAAm, it is well known that hydrophobic endgroups can induce a change in the observed T_c .^{231–233} Therefore a modulation of the thermoresponsivity of these polymers is possible. Furthermore, most water-soluble CTAs contain carboxylic- or sulfonic-acid groups which lead to acid-functionalized polymers.^{71,100,222} In cases where acid-functionalized water-soluble polymers – *e.g.* because of unspecific interactions in biological systems – are undesirable, a polymer analogous removal/modification is required which can be complicated depending on the reaction type. Therefore, it is interesting to study the polymerization via hydrophobic guest-functionalized CTA/CD complexes in water. The current approach provides the opportunity to generate hydrophilic polymers without acidic endgroups in one step. In the present chapter the first aqueous RAFT mediated polymerization of hydrophilic

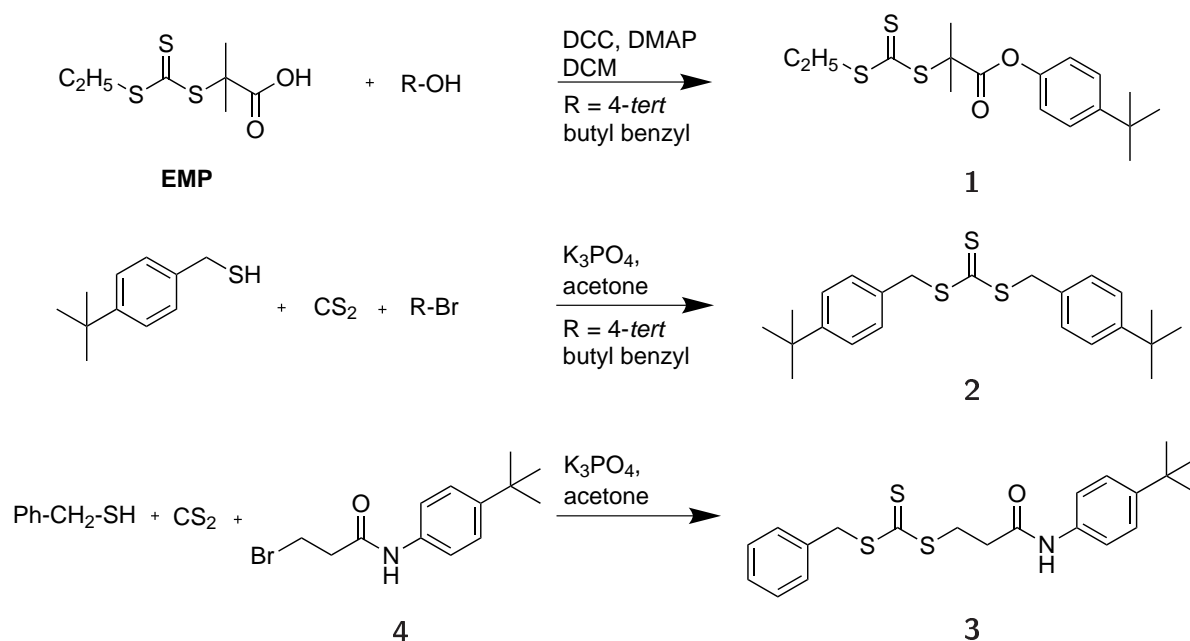
monomers employing a supramolecular CD/CTA host/guest complex utilizing 4-*tert*-butyl phenyl substituted CTAs is described. The presented approach is the first methodology that leads to hydrophilic polymers with hydrophobic endgroups in one step via aqueous RAFT polymerization. High molecular weights and conversions were reached at 25 °C with good control over D_m and molecular weight as determined via *N,N*-dimethylacetamide (DMAc) SEC. Furthermore, the first living radical polymerization of DEAAm in aqueous solution is described. The structure of the synthesized polymers was confirmed via electrospray ionization-mass spectrometry (ESI-MS) and $^1\text{H-NMR}$ spectroscopy. The living character of the polymer chains was proven via chain extension experiments and the recorded evolution of the full molecular weight distribution with conversion. In addition, several methods for the post-polymerization removal of the employed CDs were studied.

3.2 Results and Discussion

The approach for the utilization of hydrophobic CTAs in aqueous RAFT polymerizations via CD inclusion complexes includes the synthesis of novel hydrophobic CTAs that are subjected to complex formation with randomly methylated CD (Me- β -CD) and are subsequently used in the RAFT polymerization of DMAAm, DEAAm and NIPAAm.

3.2.1 Design and Synthesis of the Chain Transfer Agents

Several trithiocarbonate-CTAs for the aqueous RAFT-polymerization of hydrophilic monomers are mentioned in the literature.^{71,79,100,222} As R-group, usually the benzyl- or a tertiary- α -carbonyl-group are employed. The synthesis of trithiocarbonates can be carried out via the deprotonation of thiols, their nucleophilic attack on carbon disulfide and nucleophilic attack of the resulting trithiocarbonate salt on bromo-compounds. O'Reilly and coworkers recently presented an elegant way to synthesize trithiocarbonate-CTAs utilizing potassium phosphate as base in acetone.²³⁴ This synthetic route was employed for all of the CTAs described in the current chapter. As guest group the 4-*tert*-butyl phenyl motif was chosen due to its high complexation-constant with β -CD ($K \sim 18000 - 25000 \text{ L}\cdot\text{mol}^{-1}$).²³⁰ From an earlier publication of Wenz and coworkers¹⁵² a similar association constant of Me- β -CD with the 4-*tert*-butyl phenyl-group can be anticipated from a close analog (heptakis-(2,6-di-O-methyl)- β -CD).



Scheme 3.2: Synthetic routes for the utilized complexable CTAs.

As depicted in Scheme 3.2, the synthesis of the guest-functionalized CTAs was accomplished either directly or in two stages to include guest-groups for β -CD-complexes into the CTAs. The guest group was incorporated in the R-group (**1**), Z-group (**3**) or both (**2**). One possibility was the use of DCC-coupling after the synthesis of a precursor CTA (*e.g.* synthesis of **1**). An alternative route was the synthesis of a guest-functionalized molecule containing a bromine leaving group (*e.g.* **3**). The direct route utilized guest-functionalized thiols and bromides (*e.g.* **2**). The synthesized CTAs were characterized via NMR-spectroscopy and ESI-MS.

3.2.2 Complexation of Chain Transfer Agents with Me- β -CD

For the utilization of the guest-functionalized CTAs in aqueous RAFT polymerizations host/guest complexes have to be formed with CD. Me- β -CD was chosen as host compound due to its increased water solubility compared to β -CD.¹¹¹ The complexation was accomplished via mixing the guest-functionalized CTAs with aqueous 40 wt.% Me- β -CD-solution and ultrasonication until a clear yellow solution was obtained. Depending on the structure of the CTA the suspension had to be ultrasonicated for variable times, as the ultrasonication time depends on the complex stability and the possibility to disperse the CTA in the aqueous solution.

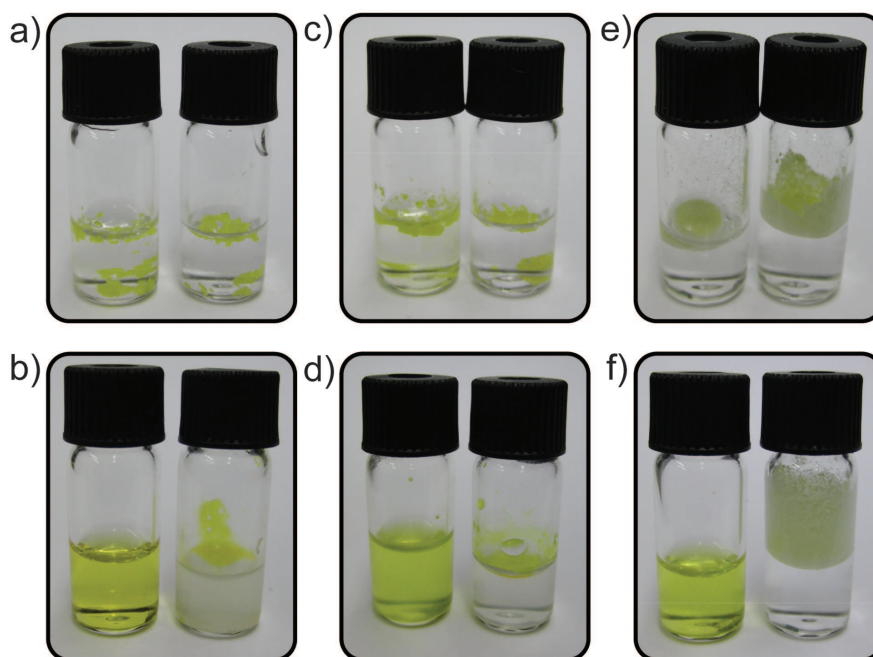


Figure 3.1: Mixtures of **1** (a and b), **2** (c and d) and **3** (e and f) with aqueous 40 wt.% Me- β -CD-solution (left) and deionized water (right). Top: Before ultrasonication, bottom: After ultrasonication.

Figure 3.1 shows CTA/Me- β -CD-solutions and as control CTA/water-solutions before ultrasonication and after ultrasonication at ambient temperature. From the yellow color in the solution after ultrasonication it is obvious that the CTA/Me- β -CD complex was formed. In contrast, the solution in the control experiment shows no yellow color. To ensure complete inclusion, a 5-fold excess was used for all CTAs. For **1** a homogenous solution was obtained after 35 min, for **2** and **3** a homogenous solution was obtained after 100 min of ultrasonication.

A further method to characterize the CTA/Me- β -CD complexes is the two-dimensional ROESY (rotating frame nuclear Overhauser enhancement spectroscopy) NMR-technique.^{172,235} In general there are two modes for the formation of the inclusion complex. The guest can insert into the hydrophobic cavity via the primary, *i.e.* the side with the smaller opening, or the secondary face of the CD, *i.e.* the side with the larger opening. From the resonances in the ROESY spectrum it is in principal possible to assign the formed type of the complex. The complexation of **1** with Me- β -CD could be evidenced via the resonance of the *tert*-butyl-protons at 1.33 ppm with the inner protons of Me- β -CD (signal between 3.27 and 3.87 ppm) in D₂O at 25 °C as depicted in Figure 3.2. Furthermore, the signal of the *tert*-butyl protons is shifted from 1.30 to 1.33 ppm, thus changing place with the signal of the methyl protons from the ethyl-group. Interestingly, the signal for the α -methyl protons of **1** splits into two distinct signals due to chemical inequivalency after complex formation. This signal shows resonance

with the C2-methoxy group which is due to a complex with an insertion from the secondary side as shown in Figure 3.2. Nevertheless, the unspecific resonances between the *tert*-butyl groups with the C2-methoxy- and the C6-methoxy-group suggest a mixture of both inclusion modes.

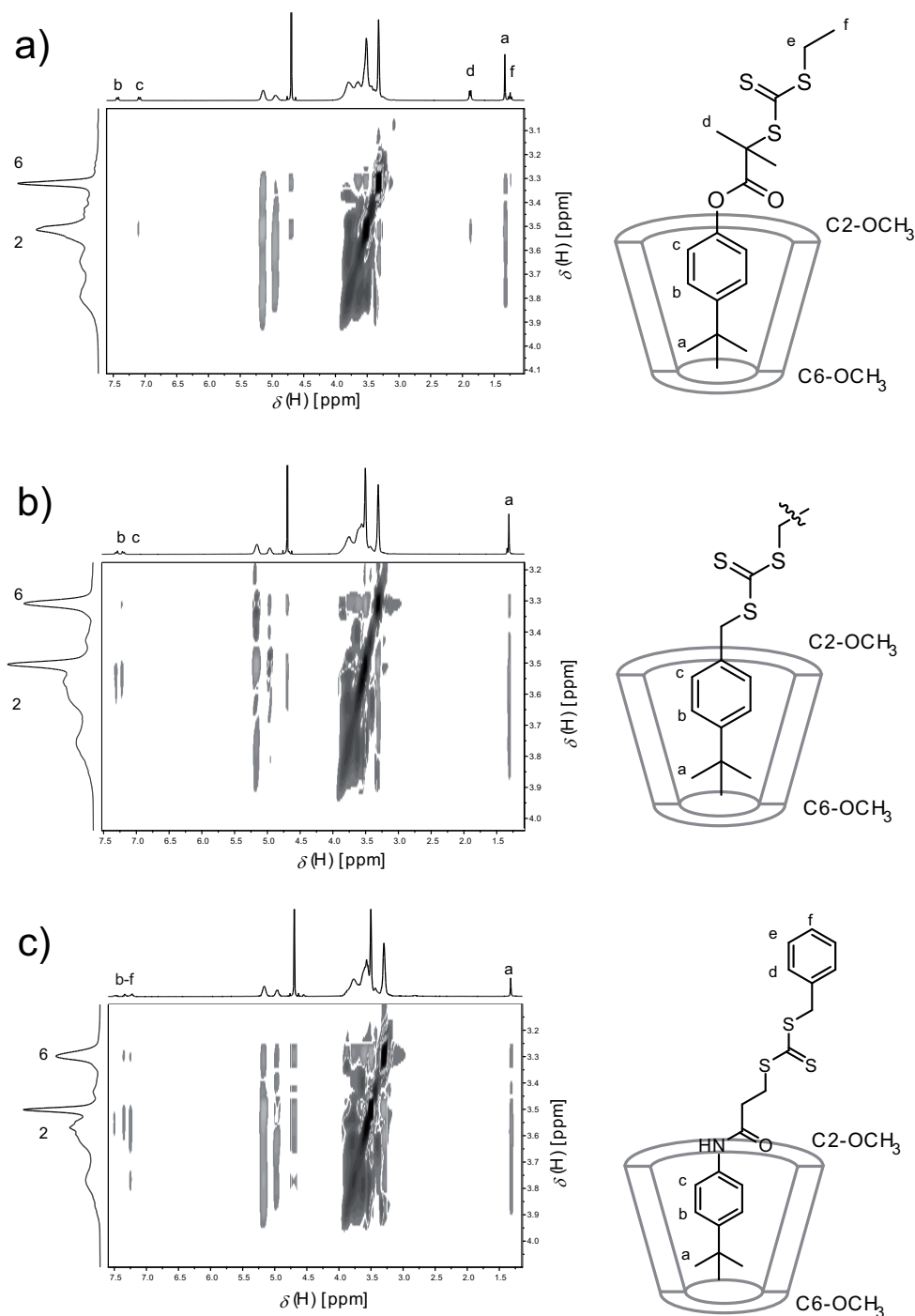


Figure 3.2: 2D ROESY spectrum of a 1:1 molar mixture of a) 1, b) 2 and c) 3 and Me- β -CD in D₂O at 25 °C and a schematic illustration of the corresponding host/guest complexes.

The 2D ROESY spectrum of **2** and **3** show the interaction between the CTA and Me- β -CD. The direction of the inclusion is not clearly assignable, although weak interaction of the aromatic protons with the C2-methoxy group indicate a complexation via the secondary face of Me- β -CD (refer to Figure 3.2). For **3**, the resonances of the aromatic protons with the C6-methoxy- and C2-methoxy-protons indicate a complexation on both ends.

A comparison between the different CTAs shows several effects that have an influence on the complex-stability upon monomer addition. One matter is the nature of the monomer, *e.g.* hydrophobicity and its ability to act as a guest, which is discussed below. An additional point is the hydrophobicity of the CTA with respect to the hydrophobicity of weak guest-groups, *e.g.* dodecyl-, hexyl- or butyl-groups.^{236,237} Although other CTAs exhibit the possibility to form inclusion-complexes with Me- β -CD, *e.g.* the analog of **1** with a dodecyl- instead of an ethyl-group, addition of hydrophilic monomers leads to complete demixing due to the loss of the inclusion complex. Most likely, the hydrophobicity of the dodecyl-group is too weakly masked by a CD. Therefore, the complex is lost as competing guest-molecules, *e.g.* monomers, are added and the single host/guest complex with the 4-*tert*-butyl phenyl group is not strong enough to keep the whole CTA in solution. It is obvious that the stability of the host/guest complex is additionally correlated with the number of guest-groups incorporated into the CTA. The more guest groups are incorporated, the more stable is the complex. As the host/guest complexes are in equilibrium with the free molecules, it is advantageous to have two complexed groups in one CTA molecule. If one of the two host/guest complexes is lost, the remaining one can keep the entire molecule in solution and accessible for the re-formation of the second complex.

3.2.3 Polymerization with Complexed Chain Transfer Agents

For the polymerization of acrylamido monomers with Me- β -CD complexed CTA three steps were carried out as depicted in Scheme 3.1: Firstly, the complex was formed via ultrasonication of the appropriate CTA in aqueous 40 wt.% Me- β -CD-solution. Secondly, monomer, water and initiator were added, the reaction was degassed and the polymerization subsequently commenced. Thirdly, the polymerization mixture was subjected to dialysis to remove residual monomer, initiator and Me- β -CD.

As discussed by McCormick and coworkers a major concern in aqueous RAFT polymerization of acrylamides is the hydrolysis/aminolysis of the CTA during the polymerization.^{62,67,238} A solution for hydrolysis suppression/prevention is the use of acetic acid/acetate buffer as solvent and low temperature initiators, *e.g.* VA-044.^{67,79} Under these conditions McCormick and colleagues evidenced that a controlled polymerization of acrylamide, DMAAm and NIPAAm via the RAFT process in aque-

ous media is possible.^{66,69,79} Furthermore, it is well known that low temperatures favour the stability of β -CD-complexes. For these reasons all polymerizations were conducted at 25 °C. As the CTA/Me- β -CD complexes were not soluble in acetic acid/acetate buffer, a series of DMAAm polymerizations – as a test system – were conducted in variable reaction media with **1** or **EMP** to determine the effect of the reaction media on the polymerization. The results are summarized in Figure 3.3.

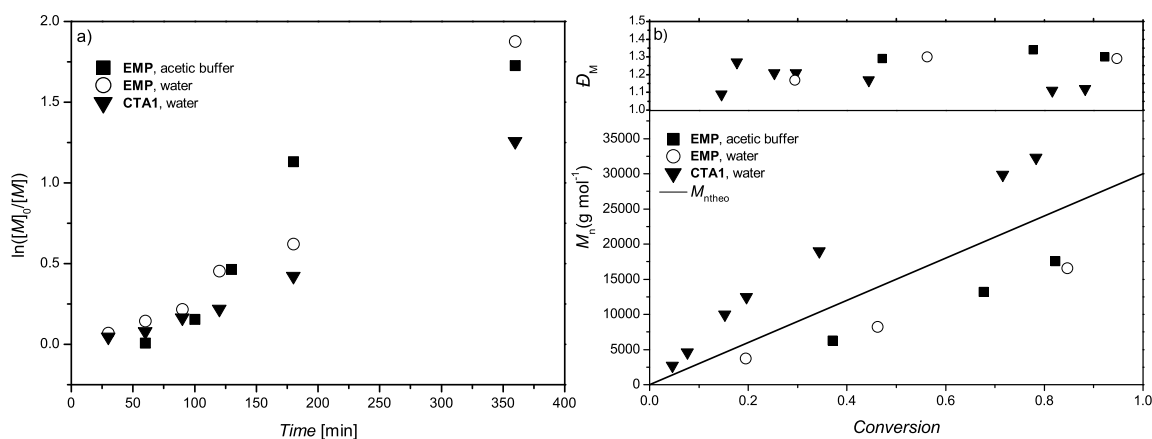


Figure 3.3: a) Comparison between the kinetic plots of **EMP**-mediated polymerization in acetic acid/acetate buffer, **EMP**-mediated polymerization in water or **1**/CD-mediated polymerization at 25 °C with a DMAAm/CTA/I ratio of 300/1/0.2 and a DMAAm concentration of 3.5 mol·L⁻¹ b) Comparison of the obtained molecular weights and \bar{D}_m as a function of monomer conversion.

Figure 3.3 a shows that the polymerization reaction with the complexed **1** (triangles) proceeds slower than the polymerizations with **EMP** in acetic acid/acetate buffer (filled squares) or water (open circles), whereas the **EMP**-mediated polymerizations show comparable reaction rates. Nevertheless, the reaction with **1** leads to a conversion of 70% in 6 h, while the reactions with **EMP** have a conversion of approximately 80% within 6 h. It is proposed that the difference in reaction rate is a result of the increasing steric hindrance associated with the bulky CD-complex. Although a slower reaction is observed, a superior control over the polymerization with the **1**/CD complex can be noted. Lower \bar{D}_m were observed in these polymerizations as summarized in Figure 3.3 b. In the case of **1** (triangles) the observed molecular weight was higher than the theoretical molecular weight whereas the molecular weight is lower than the theoretical molecular weight in the case of **EMP** (squares and open circles). As the polymerization has living/controlled character in both acetic acid/acetate buffer and pure water with **EMP** as CTA at 25 °C, there is no need to carry out the polymerization at acidic pH values in the case of complexed CTAs.

Removal of the Cyclodextrin after the Polymerization

For the removal of the CD several methods were applied. A test-polymerization with DMAAm and **1** was carried out, divided into several samples and purified in different ways. To compare the residual amounts of the CD in the products, the peak area of the eluting CD in the SEC-analysis was calculated relatively to the peak area of the polymer. The Me- β -CD content in the untreated mixture is given in entry 1 of Table 3.1. Dialysis was performed utilizing dialysis tubing with a MWCO of 3500 Da but the treatment of the samples was varied. One purification method was the treatment of the crude polymerization solution with trifluoroacetic acid for 2 h as CDs are hydrolyzed by strong acids and the solution was dialysed for 3 days at ambient temperature afterwards (entry 2 in Table 3.1). For comparison, the crude polymerization mixture was dialysed for 3 days at ambient temperature (entry 3 in Table 3.1). An alternative method was dialysis for 3 days at ambient temperature and subsequently dialysis for 1 day or 2 days at 45 °C (entries 4 and 5 in Table 3.1). Furthermore enzymatic treatment with Taka-Diastase in acetic acid/acetate buffer at 37 °C for 1 day was employed after dialysis for 3 days at ambient temperature and another dialysis for 3 days at ambient temperature after the enzymatic treatment (entry 6 in Table 3.1). The enzymatic treatment with Taka Diastase from *Aspergillus oryzae* should lead to degradation of the CDs as it contains the enzyme α -amylase which is known to hydrolyse the α -1,4-glycosidic bond of the CDs.^{239–241}

Table 3.1: Results for the different purification methods quantified with the residual amount of Me- β -CD according to SEC measurements.

Entry	purification procedure	Me- β -CD [% Area]
1	no purification	29.1
2	CF ₃ COOH 2 h, dialysis 3 d ambient temp.	7.5
3	dialysis 3 d ambient temp.	8.4
4	dialysis 3 d ambient temp., dialysis 1 d 45 °C	5.4
5	dialysis 3 d ambient temp., dialysis 2 d 45 °C	3.3
6	dialysis 3 d ambient temp., Taka-Diastase acetate buffer 1 d 37 °C, dialysis 3 d ambient temp.	4.1

As listed in Table 3.1 dialysis at elevated temperatures, *e.g.* 45 °C, provides the best results with only 3.3% Me- β -CD remaining (entry 5 in Table 3.1). Nevertheless, enzymatic treatment has a very similar performance with 4.1% Me- β -CD remaining (entry 6 in Table 3.1; the corresponding elugrams can be found in Figure 3.4). In the case of PDEAAm and PNIPAAm, dialysis at elevated temperatures leads to the precipitation of the polymers that supports the removal of residual CD. Generally, it should be

noted that dialysis leads to a loss of low molecular weight polymers and oligomers. Especially in the case of low target molecular weights, the molecular weight distributions are thus to some extent affected.

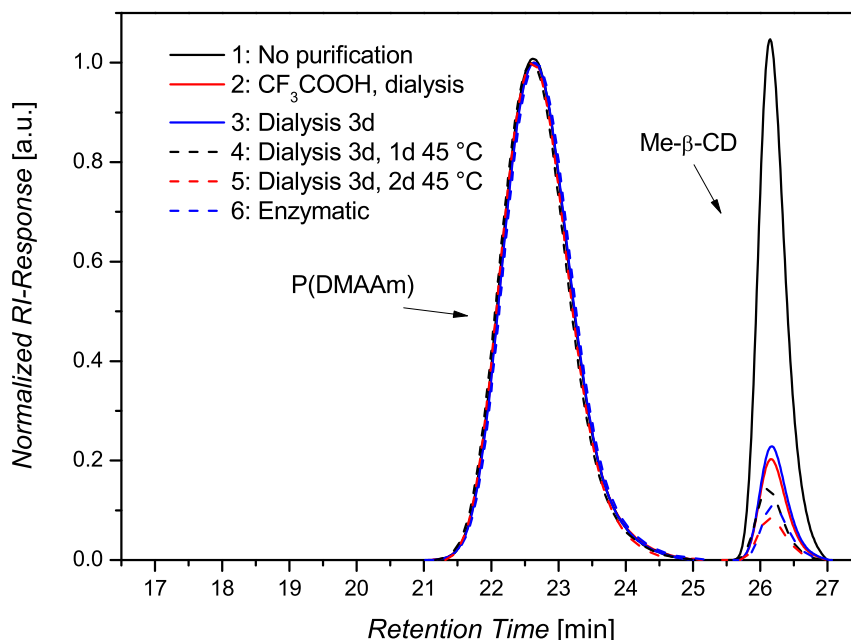


Figure 3.4: Elugrams of the purification methods study depicting the PDMAAm peak and the peaks of the residual Me- β -CD.

Polymerization of *N,N*-Dimethylacrylamide with Complexed Chain Transfer Agents

DMAAm is very frequently employed in polymer chemistry. In the living/controlled radical polymerization with complexed CTAs the best control is obtained with **1** compared to **2** and **3** (see Table 3.2, 3.3 and 3.4). This can be mostly attributed to the complex stability and the tertiary α -ester R-group in **1**. A monomer concentration of $3.0 \text{ mol}\cdot\text{L}^{-1}$ was chosen and the CTA/initiator ratio was held constant at 1/0.2. The complex of **1** with Me- β -CD was stable throughout the reaction time and even at high monomer/CTA ratios up to 1000/1. Therefore molecular weights ranging from 10000 to $94000 \text{ g}\cdot\text{mol}^{-1}$ were obtained in good agreement with theoretical values. High conversion was reached in short reaction times even at the low polymerization temperature of $25 \text{ }^\circ\text{C}$. The resulting D_m lie between 1.06 and 1.17 (see Table 3.2 and Figure 3.5 d). Although the polymers were purified as described in the experimental section a small residue of unremoved CD (approx. 0.4 - 5.5%) remained. Apart from residual CD, the SEC traces are unimodal, show only minor low molecular weight tailing and no high molecular weight coupling products.

Table 3.2: Results for the living/controlled RAFT polymerization of DMAAm at 25 °C in aqueous solution with **1**.

DMAAm/CTA/I	Time / h	Conv.	$M_{n\text{theo}} / \text{g}\cdot\text{mol}^{-1}$	$M_{n\text{SEC}} / \text{g}\cdot\text{mol}^{-1}$	\mathcal{D}_m
107/1/0.2	6	65	7300	10500	1.17
198/1/0.2	6	88	18000	17000	1.09
294/1/0.2	12	> 99	29500	36500	1.08
585/1/0.2	12	94	55000	62000	1.06
1018/1/0.2	12	98	99300	94000	1.06

Time resolved experiments with regard to conversion and molecular weight were carried out to confirm the living character of the polymerization (refer to Appendix A.1 for a collection of NMR-spectra). As depicted in Figure 3.5, the kinetic first order plot shows linearity which confirms a constant radical concentration during the reaction and evidences a short induction period (< 30 min). The molecular weights are increasing linearly with conversion which evidences the living character of the polymerization and the \mathcal{D}_m is decreasing with increasing conversion. Further proof for the living radical polymerization comes from the chain extension of purified macro-CTAs with DMAAm. A quantitative reinitiation was observed that leads to a shift in molecular weight from 10500 to 97500 $\text{g}\cdot\text{mol}^{-1}$ with a final \mathcal{D}_m of 1.08. Nevertheless, small amounts of chain-chain coupling products were observed in the high molecular weight region.

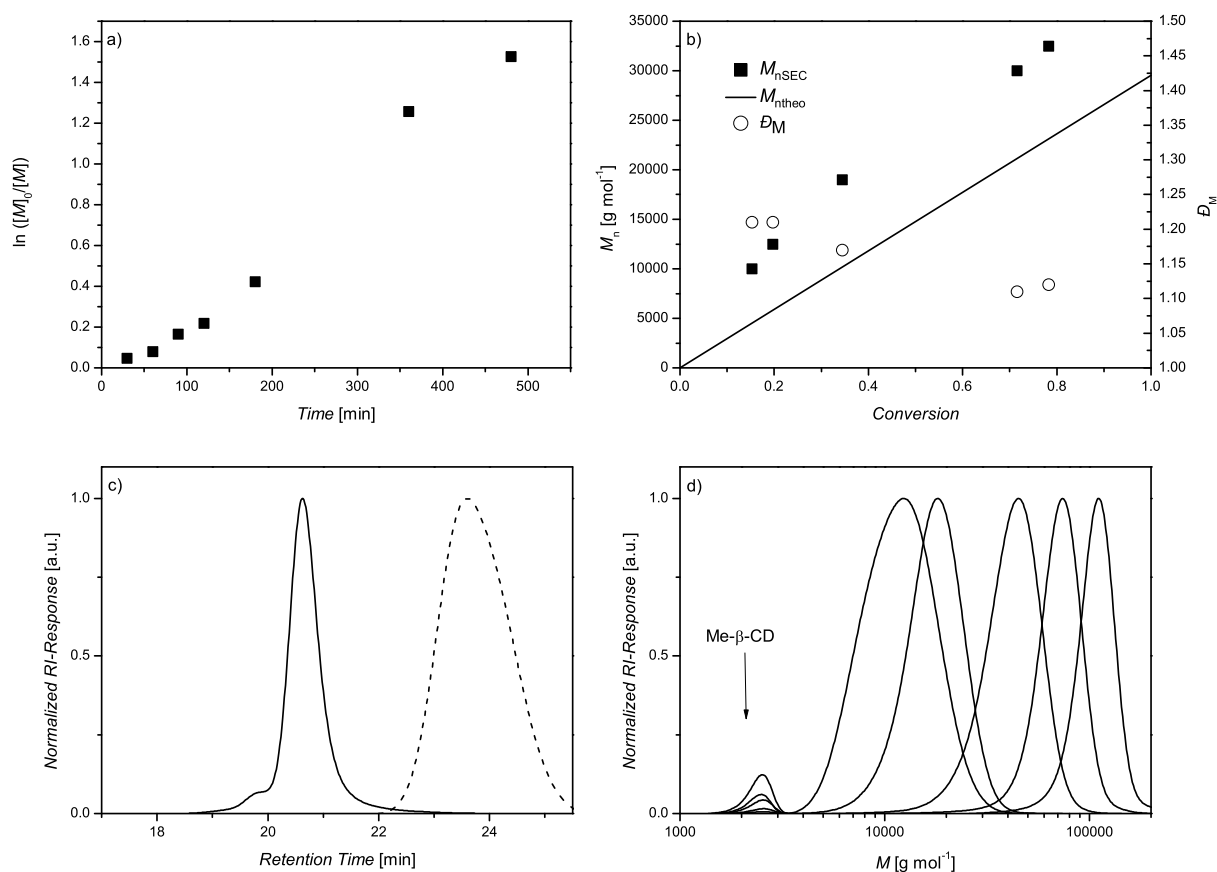


Figure 3.5: a) Kinetic plot for the polymerization of DMAAm at 25 °C with **1**; b) Evolution of M_n with conversion at 25 °C with DMAAm/**1**/I: 297/1/0.2; c) Chain-extension at 25 °C for 24 h; d) Molecular weight distributions for different monomer/CTA ratios (DMAAm/**1** (conversion) from left to right: 107/1 (65%); 198/1 (88%); 294/1 (> 99%); 585/1 (94%); 1018/1 (98%)).

The molecular structure of low molecular weight samples was confirmed via ESI-MS ($M_n = 3000 \text{ g}\cdot\text{mol}^{-1}$) and ¹H-NMR ($M_n = 10500 \text{ g}\cdot\text{mol}^{-1}$) (see Appendix A.2/A.3), evidencing the incorporation of the hydrophobic endgroups into the hydrophilic polymer. The mass spectrometric data shows no signals from initiator terminated polymer which is in accord with highly efficient chain-extension experiments.

With **2** turbidity was observed upon monomer addition that vanished in the beginning of the polymerization. In the polymerizations with **3** turbidity was observed at monomer/CTA ratios exceeding 300/1. Nevertheless, molecular masses of up to $156000 \text{ g}\cdot\text{mol}^{-1}$ were reached with \bar{D}_m ranging from 1.31 to 1.54 (refer to Table 3.3/3.4 and Figure 3.6/3.7) with high conversions in short reaction times. As stated above, less control over the polymerization is observed with **2** and **3**. The less stable complexes of Me-β-CD with **2** and **3** lead to partial demixing on monomer and water addition as observed via a turbidity of the solution. Such a demixing explains the higher disagreement of experimental molecular weights compared to theoretical molecular

weights, as less CTA molecules are accessible in the solution in the case of turbidity, thus leading to higher molecular weights. The broader molar-mass dispersity of the polymers prepared with **2** and **3** can be also attributed to the partial demixing as the undissolved CTA molecules react on a slower time scale. Therefore, low molecular weight tailing is observed which leads to higher \mathcal{D}_m . Nevertheless, chain-extension experiments were conducted that proof the living character of the polymerization based on a high reinitiation efficiency.

Table 3.3: Results for the living/controlled RAFT polymerization of DMAAm at 25 °C in aqueous solution with **2**.

DMAAm/CTA/I	Time / h	Conv.	$M_{n\text{theo}} / \text{g}\cdot\text{mol}^{-1}$	$M_{n\text{SEC}} / \text{g}\cdot\text{mol}^{-1}$	\mathcal{D}_m
56/1/0.2	6	80	4800	13000	1.24
99/1/0.2	6	95	9500	22000	1.35
203/1/0.2	6	87	17400	32000	1.29
340/1/0.2	6	> 99	29100	49500	1.42
603/1/0.2	12	> 99	59800	82500	1.32
1184/1/0.2	12	> 99	117300	141000	1.51

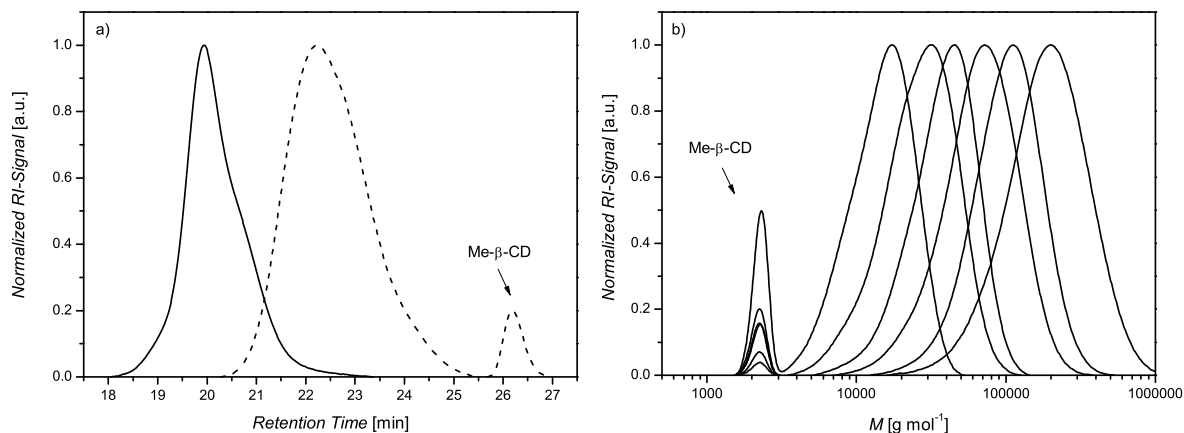
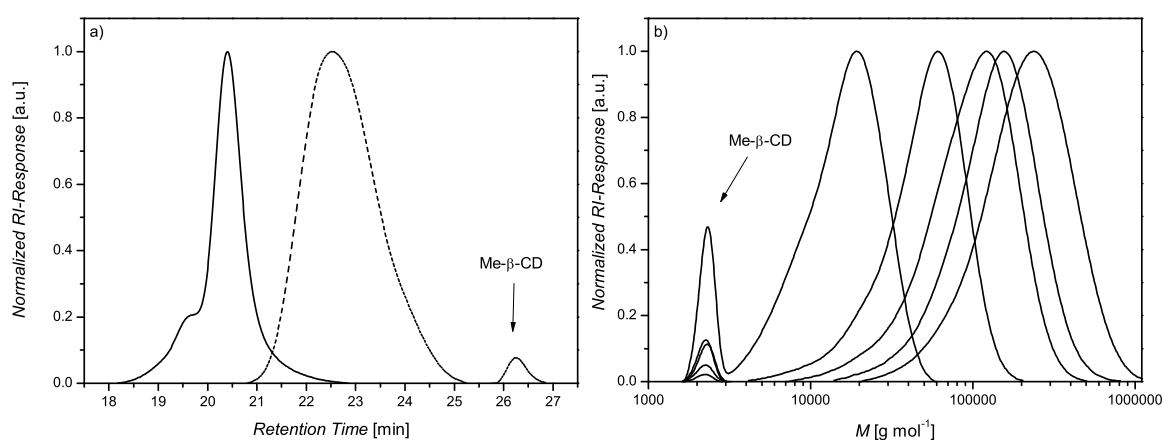


Figure 3.6: a) Chain-extension with DMAAm at 25 °C for 24 h; b) Molecular weight distributions for different monomer/**2** ratios (DMAAm/**2** from left to right (conversion): 56/1 (80%); 99/1 (95%); 203/1 (87%); 340/1 (> 99%); 603/1 (> 99%); 1184/1 (> 99%)).

Table 3.4: Results for the living/controlled RAFT polymerization of DMAAm at 25 °C in aqueous solution with **3**.

DMAAm/CTA/I	Time / h	Conv.	$M_{n\text{theo}} / \text{g}\cdot\text{mol}^{-1}$	$M_{n\text{SEC}} / \text{g}\cdot\text{mol}^{-1}$	D_m
51/1/0.2	6	76	4600	14000	1.31
108/1/0.2	6	70	7700	19500	1.27
203/1/0.2	6	78	15600	38000	1.43
306/1/0.2	12	93	27900	70000	1.53
588/1/0.2	12	> 99	58000	102500	1.46
1002/1/0.2	12	> 99	100000	156500	1.54

**Figure 3.7:** a) Chain-extension with DMAAm at 25 °C for 24 h; b) Molecular weight distributions for different monomer/**3** ratios (DMAAm/**3** from left to right (conversion): 51/1 (76%); 108/1 (70%); 203/1 (78%); 306/1 (93%); 588/1 (> 99%); 1002/1 (> 99%)).

Polymerization of *N,N*-Diethylacrylamide with Complexed Chain Transfer Agents

PDEAAm is a polymer that exhibits a very low T_c of around 30 °C.²⁴² At a reaction temperature of 25 °C it should be possible to polymerize DEAAm in aqueous media via the RAFT process. Although the living radical polymerization in organic media has been described,⁷⁸ a living/controlled radical polymerization of this monomer in aqueous solution has not been accomplished yet. **1**, **2** and **3** were employed for the polymerization of DEAAm. The monomer concentration was held constant at 3.5 mol·L⁻¹, the temperature at 25 °C and the CTA/initiator ratio at 1/0.2. As with DMAAm, **1** shows the best control over the polymerizations. No turbidity or demixing is noticed for monomer/CTA ratios up to 200/1 and only a slight turbidity is observed for higher CTA/monomer ratios in the case of **1**. Molecular weights from 2500 up to 87000 g·mol⁻¹ that were in good agreement with the theoretical values were reached in short reaction times, *e.g.* 12 h or 18 h, with quantitative conversions

and \bar{D}_m ranging from 1.05 to 1.11 (see Table 3.5 and Figure 3.8 d). The resulting molecular weight distributions are unimodal and display no evidence for high molecular weight termination products or low molecular weight tailing, except for the lowest target molecular weight where low molecular weight ($< 1000 \text{ g}\cdot\text{mol}^{-1}$) species are observed.

Table 3.5: Results for the living/controlled RAFT polymerization of DEAAm at 25 °C in aqueous solution with **1**.

DEAAm/CTA/I	Time / h	Conv.	$M_{\text{ntheo}} / \text{g}\cdot\text{mol}^{-1}$	$M_{\text{nSEC}} / \text{g}\cdot\text{mol}^{-1}$	\bar{D}_m
12/1/0.2	12	> 99	1900	2500	1.10
42/1/0.2	12	> 99	5800	5000	1.11
80/1/0.2	12	> 99	10600	10000	1.09
163/1/0.2	12	> 99	21100	18000	1.08
248/1/0.2	12	> 99	32000	29000	1.07
426/1/0.2	18	> 99	54600	55000	1.06
813/1/0.2	18	> 99	103800	87000	1.05

To confirm the living character of the polymerization, time resolved experiments with regard to conversion and molecular mass were carried out (refer to Appendix A.4 for a collection of NMR-spectra) and chain extensions were performed as depicted in Figure 3.8. Besides a constant radical concentration as evidenced by a linear first-order plot with a short induction period below 30 min, the molecular weight grows linearly with conversion as expected for polymerizations with living character. Furthermore, the experimental molecular weights are in good agreement with the theory and the \bar{D}_m are decreasing with increasing conversion. The chain extension affords a very high reinitiation efficiency with a growth in molecular weight from 8500 to 83000 $\text{g}\cdot\text{mol}^{-1}$ and a \bar{D}_m of 1.13 for the resulting polymer with a small amount of chain-chain coupling products.

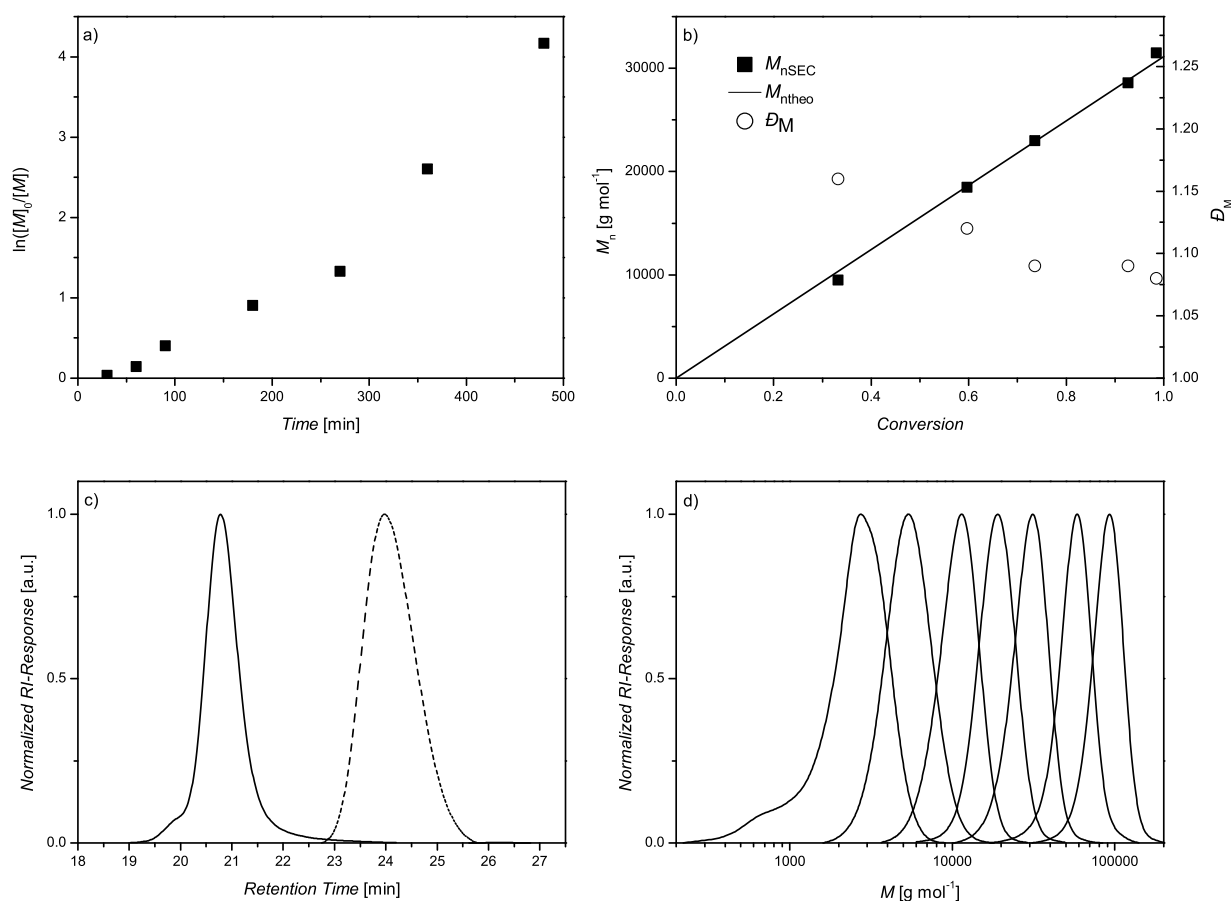


Figure 3.8: a) Kinetic plot for the polymerization of DEAAm at 25 °C with **1**; b) Evolution of M_n with conversion at 25 °C with DEAAm/**1**/I: 241/1/0.2; c) Chain-extension at 25 °C for 24 h; d) Molecular weight distributions for different monomer/CTA ratios (DEAAm/**1** from left to right (conversion > 99%): 12/1; 42/1; 80/1; 163/1; 248/1; 426/1; 813/1).

ESI-MS and ¹H-NMR were recorded of a low molecular weight sample ($M_n = 4000 \text{ g}\cdot\text{mol}^{-1}$) to confirm the structure of the synthesized polymers. The results are in agreement with the expected polymer structure proving the incorporation of the hydrophobic endgroups into the hydrophilic polymer (refer to Appendix A.5/A.6). Furthermore, there is no indication of initiator derived chains in the ESI-MS spectrum which explains the high reinitiation efficiency.

For the other CTAs (**2** and **3**) turbid solutions were observed upon water addition. Nevertheless, high conversions were reached in short reaction times and molecular weights ranging from 4000 to 116000 $\text{g}\cdot\text{mol}^{-1}$ were reached with \bar{D}_m from 1.10 to 1.39 (see also Table 3.6/3.7 and Figure 3.9/3.10). Similar to the polymerizations of DMAAm with **2** and **3** a disagreement of the experimental molecular weights with those theoretically predicted was noted that could be due to the turbid nature of the solution at the beginning of the polymerization process. It is also worth noting that the polymers remained in solution throughout the entire reaction time with all three CTAs

although it is known from literature that hydrophobic endgroups lead to a lower T_c in PDEAAm.²³³

Table 3.6: Results for the living/controlled RAFT polymerization of DEAAm at 25 °C in aqueous solution with 2.

DEAAm/CTA/I	Time / h	Conv.	$M_{n,theo} / g \cdot mol^{-1}$	$M_{n,SEC} / g \cdot mol^{-1}$	\bar{D}_m
13/1/0.2	12	> 99	1700	4000	1.13
51/1/0.2	6	94	5600	10500	1.22
81/1/0.2	6	> 99	10300	13000	1.32
158/1/0.2	12	> 99	20100	28000	1.30
481/1/0.2	12	97	59200	73500	1.23
799/1/0.2	12	> 99	101000	107000	1.23

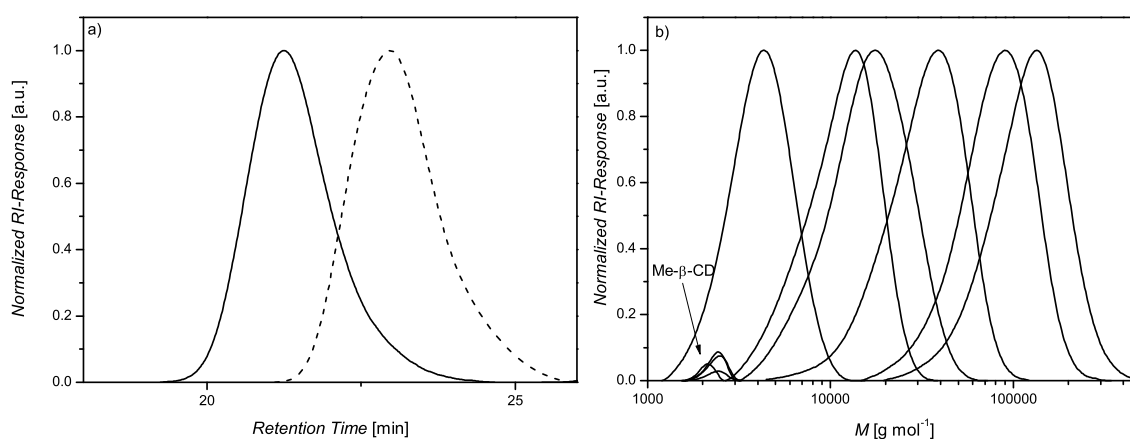


Figure 3.9: a) Chain-extension with DEAAm at 25 °C for 24 h; b) Molecular weight distributions for different monomer/2 ratios (DEAAm/2 from left to right (conversion): 12/1 (> 99%); 51/1 (94%); 81/1 (> 99%); 158/1 (> 99%); 481/1 (97%); 799/1 (> 99%)).

Table 3.7: Results for the living/controlled RAFT polymerization of DEAAm at 25 °C in aqueous solution with 3.

DEAAm/CTA/I	Time / h	Conv.	$M_{n,theo} / g \cdot mol^{-1}$	$M_{n,SEC} / g \cdot mol^{-1}$	\bar{D}_m
13/1/0.2	12	92	1500	4500	1.14
40/1/0.2	12	89	4500	14000	1.36
79/1/0.2	12	97	15300	15500	1.39
160/1/0.2	12	> 99	20300	23500	1.27
243/1/0.2	12	99	30700	41000	1.09
505/1/0.2	12	> 99	62700	59000	1.23
810/1/0.2	12	99	102000	116000	1.10

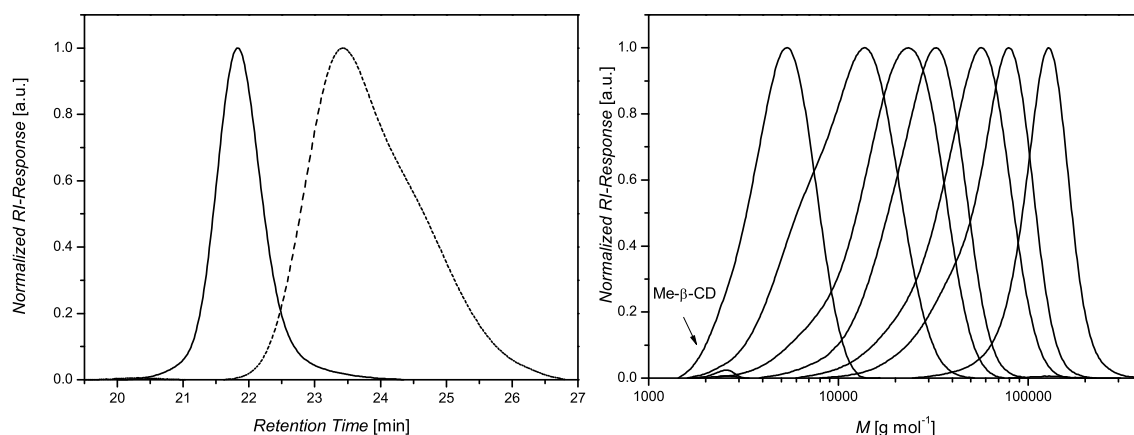


Figure 3.10: a) Chain-extension with DEAAm at 25 °C for 24 h; b) Molecular weight distributions for different monomer/**3** ratios (DEAAm/**3** from left to right (conversion): 13/1 (92%); 40/1 (89%); 79/1 (97%); 160/1 (> 99%); 243/1 (99%); 505/1 (> 99%); 810/1 (99%)).

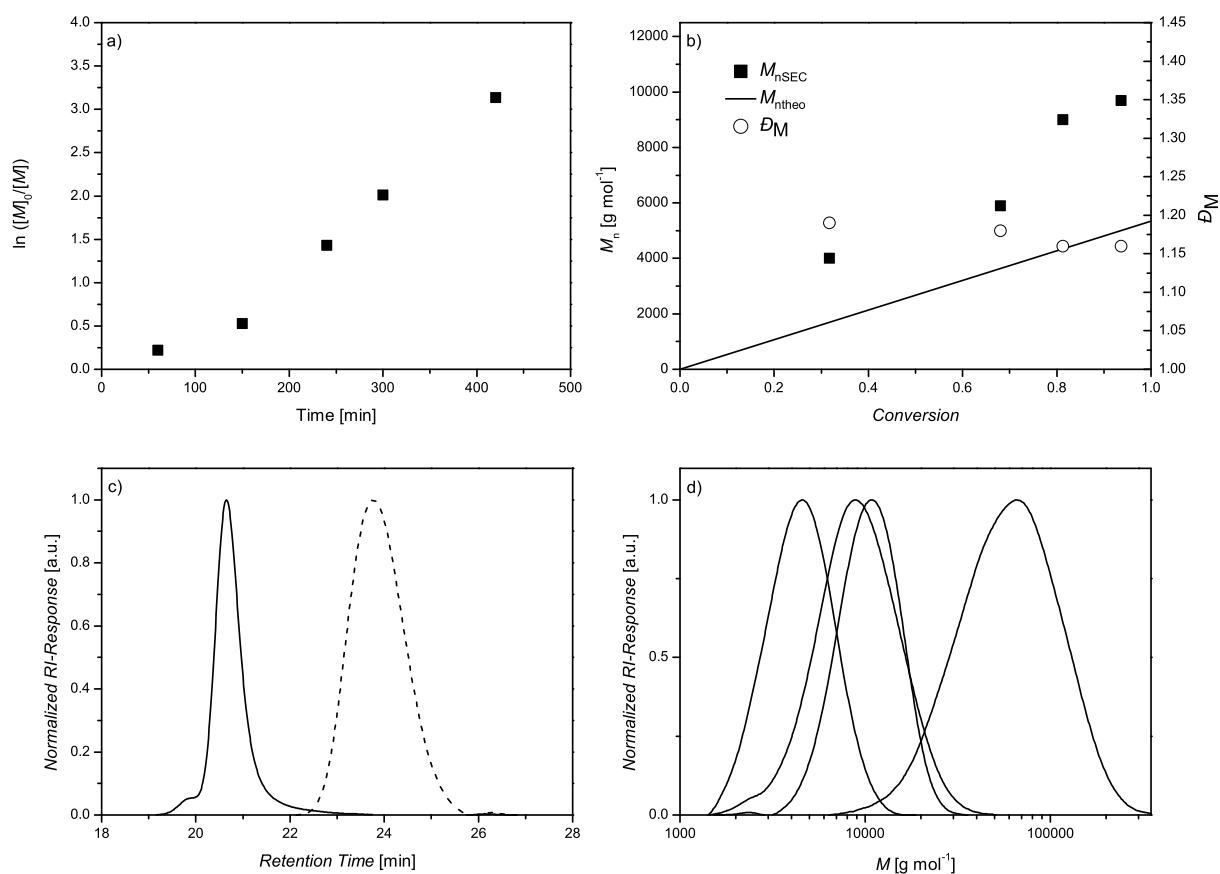
Polymerization of *N*-Isopropylacrylamide with Complexed Chain Transfer Agents

Another important acrylamido monomer is NIPAAm. Due to the T_c of PNIPAAm that is close to human body temperature, many efforts have been made for its synthesis.^{72,79,232} As the T_c of PNIPAAm is close to 31 °C,²⁴³ which is comparable to the T_c of PDEAAm, a controlled polymerization of NIPAAm is feasible at 25 °C in aqueous media.⁷⁹ Therefore it should be possible to polymerize NIPAAm with CD-complexed CTAs at 25 °C in aqueous media as well.

In the case of NIPAAm, a controlled polymerization was only possible with **1**. The other CTAs showed complete demixing upon addition of the monomer and water, which is further discussed in the subsequent section. Nevertheless, with **1** polymers up to 50000 g·mol⁻¹ were synthesized with D_m ranging from 1.15 to 1.46 with quantitative conversions in 18 or 20 h. The monomer concentration was held constant at 2.5 mol·L⁻¹, the polymerization temperature at 25 °C and the CTA/initiator ratio at 1/0.2. The results are summarized in Table 3.8. A significant excess of the experimental molecular weights compared to the theoretically predicted ones by a factor of 1.5 - 2.0 was evidenced that could be due to a partial disassembly of the CTA/CD complex. The obtained polymers show unimodal molecular weight distributions with no significant tailing in the low molecular region. Furthermore, no high molecular weight termination products are visible.

Table 3.8: Results for the living/controlled RAFT polymerization of NIPAAm at 25 °C in aqueous solution with 1.

NIPAAm/CTA/I	Time / h	Conv.	$M_{n\text{theo}} / \text{g}\cdot\text{mol}^{-1}$	$M_{n\text{SEC}} / \text{g}\cdot\text{mol}^{-1}$	D_M
15/1/0.2	18	> 99	2100	4000	1.15
39/1/0.2	18	> 99	4800	7500	1.29
44/1/0.2	18	> 99	5500	9000	1.15
260/1/0.2	20	> 99	30100	50000	1.46

**Figure 3.11:** a) Kinetic plot for the polymerization of NIPAAm at 25 °C with 1; b) Evolution of M_n with conversion at 25 °C with NIPAAm/1/I: 44/1/0.2; c) Chain-extension at 25 °C for 24 h; d) Molecular weight distributions for different monomer/CTA ratios (NIPAAm/1 from left to right (conversion > 99%): 15/1; 39/1; 44/1; 260/1).

A constant radical concentration is supported by a linear first-order plot evidencing a short induction period of approximately 30 min (refer to Appendix Figure A.7 for a collection of NMR-spectra). A confirmation of living radical polymerization was accomplished via a chain-extension experiment and a time resolved experiment that indicated a linear increase of molecular weight with conversion (see Figure 3.11). Higher experimental molecular weights compared to the theoretical molecular weights

are observed, as discussed above. The chain extension shows that the amount of dead chains is negligible as chain-extension from 9000 to 90000 g·mol⁻¹ was performed with very high efficiency leading to a \bar{D}_m of 1.11 showing only minor chain-chain coupling products.

In addition to the kinetic studies, ESI-MS was performed to evidence the structure of the obtained polymers. As depicted in the Appendix (Figure A.8) the results fit very well to the expected values indicating the incorporation of the hydrophobic end-groups into the hydrophilic polymers. Furthermore, there is no indication of initiator derived chains that matches with the observed high reinitiation efficiency. ¹H-NMR was measured (refer to Appendix A.9) indicating the incorporation of the hydrophobic endgroup in the aromatic region of the spectrum.

Effect of the Monomer Structure on the RAFT Polymerization with Complexed Chain Transfer Agents

A comparison of the studied monomers evidences that with increasing guest-character the complexation of the CTAs decreases. With DMAAm no turbidity was observed for **1** and only slight turbidity for **2** and **3**. This effect is also reflected in the control over molecular weights and \bar{D}_m as the best control is achieved with **1**. In the polymerization of DEAAm, only slight turbidity was observed with CTA **1** where DEAAm/**1** ratios exceeded 300/**1**. With **2** and **3** turbidity was observed with DEAAm/CTA ratios from 13/**1** to 813/**1**. In analogy to the polymerization of DMAAm the **1** mediated polymerizations of DEAAm show the best control over molecular weight and \bar{D}_m . The overall trend is continuing in the polymerization with NIPAAm as it could only be conducted with **1** and only short chains up to 50000 g·mol⁻¹ could be synthesized with an increasing \bar{D}_m towards longer chains. It appears that the substituents in the acrylamido monomers have a significant effect on the stability of the CTA/CD complex. DMAAm disturbs the complex only weakly whereas DEAAm leads to a significant expulsion of CTA molecules from the CD cavity. NIPAAm leads to expulsion in all cases with **2** or **3** and complexes with **1** were only stable up to a monomer/CTA ratio of 260/**1**. The complex stability is increasing from NIPAAm over DEAAm to DMAAm which is in contrast to the ability of the substituent in the acrylamido monomer to act as a competing guest in the CD. The more hydrophobic and bulky *iso*-propyl group in NIPAAm has a more pronounced effect on the CTA/CD complex stability than the ethyl group in DEAAm which itself has a larger effect on the CTA/CD complex than the methyl-group in DMAAm. We propose that this effect is due to a shift in the host/guest equilibrium towards disassembly of the complex induced by additional guest molecules. These can be either monomers or additional water molecules. As monomers have to be employed in higher equivalents to synthesize high molecu-

lar weight polymers in living/controlled radical polymerizations the possibility that the monomer leads to expulsion of the CTA from the Me- β -CD rises with increasing target molecular weights. An increasing amount of water may also lead to a loss of the CTA/CD complex.¹¹⁶ The amount of water increases with increasing target chain length as more water is needed to retain a solution-polymerization. Therefore, the decrease in the complexation efficiency in the case of higher targeted molecular weights can be explained by the increasing employed amount of monomer and water molecules in these cases.

3.3 Conclusions

The utilization of CDs provides new opportunities for the synthetic methodology of living/controlled radical polymerization. Based on the concept of supramolecular chemistry, host/guest complexes seem to be attractive as controlling agents in living radical polymerizations. The first aqueous RAFT polymerization of acrylamido monomers, *e.g.* DMAAm, DEAAm and NIPAAm, with a supramolecular complex of CD and hydrophobic CTAs, could be performed. The solubility of three novel guest-functionalized CTAs in water was enhanced drastically via a CD/CTA inclusion complex. These complexes were thereafter utilized in living/controlled radical polymerizations at 25 °C in water leading to hydrophilic polymers with hydrophobic endgroups in one step. The polymerization leads to polymers with high molar masses and low \mathcal{D}_m ($7500 \leq M_n \leq 116000 \text{ g}\cdot\text{mol}^{-1}$; $1.06 \leq \mathcal{D}_m \leq 1.54$ for PDMAAm, $2500 \leq M_n \leq 150000 \text{ g}\cdot\text{mol}^{-1}$; $1.05 \leq \mathcal{D}_m \leq 1.39$ for PDEAAm and $4000 \leq M_n \leq 50000 \text{ g}\cdot\text{mol}^{-1}$; $1.15 \leq \mathcal{D}_m \leq 1.46$ for PNIPAAm). Furthermore, the first living radical polymerization of DEAAm in water was described. The living character of the polymerizations was confirmed by a linear increase of the molecular weight with conversion and chain extensions showed very high reinitiation efficiencies. ESI mass spectra as well as ¹H-NMR-spectra were in good agreement with the expectations evidencing the incorporation of hydrophobic endgroups in the hydrophilic acrylamido polymers. Thus, the first living/controlled polymerization of hydrophilic acrylamido monomers with hydrophobic CTA leading directly to hydrophobic endfunctionalized polymers in aqueous solution is provided.

3.4 Experimental Part

Synthesis of 4-(*tert*-butyl)phenyl 2-(((ethylthio)carbonothioyl)thio)-2-methylpropanoate (1)

In a 50 mL Schlenk-flask EMP (1.02 g, 4.55 mmol, 1.0 eq.), 4-*tert*-butyl phenol (1.71 g, 11.38 mmol, 2.5 eq.) and DMAP (0.22 g, 1.80 mmol, 0.4 eq.) were dissolved in anhydrous DCM (20 mL). At 0 °C a solution of DCC (1.90 g, 9.21 mmol, 2.0 eq.) in anhydrous DCM (12 mL) was added. After one hour the solution was warmed to ambient temperature, stirred overnight, filtered and concentrated under reduced pressure. The residual yellow oil was purified via column chromatography on silica-gel with *n*-hexane:ethyl acetate 20:1 as eluent. The product was obtained as yellow oil which solidified upon cooling (1.54 g, 4.32 mmol, 95%).

$^1\text{H-NMR}$ (400 MHz, CDCl_3): [δ , ppm] = 1.30 (s, 9H, $(\text{CH}_3)_3$), 1.34 (t, 3H, $^3J = 7.4$ Hz, $\text{CH}_2\text{-CH}_3$), 1.83 (s, 6H, $\text{C-(CH}_3)_2$), 3.32 (q, 2H, $^3J = 7.4$ Hz, CH_2), 7.00 (d, 2H, $^3J = 8.8$ Hz, CH-C-O), 7.37 (d, 2H, $^3J = 8.8$ Hz, $\text{CH-C-C(CH}_3)_3$). $^{13}\text{C-NMR}$ (100 MHz, CDCl_3): [δ , ppm] = 12.9 (CH_3), 25.4 ($(\text{CH}_3)_2$), 31.3 ($(\text{CH}_3)_3$), 31.4 (CH_2), 34.5 ($\text{C-(CH}_3)_3$), 55.8 ($\text{C-(CH}_3)_2$), 120.7 (CH-C-O), 126.2 ($\text{CH-C-C-(CH}_3)_3$), 148.7 (CH-C-O ; $\text{C-C(CH}_3)_3$), 171.8 (C=O), 221.1 (C=S). **ESI-MS**: $[\text{M} + \text{Na}^+]_{\text{exp}} = 379.11$ m/z and $[\text{M} + \text{Na}^+]_{\text{calc}} = 379.04$ m/z.

Synthesis of bis(4-*tert*-butyl)benzyl carbonotrithioate (2)

In a 50 mL round-bottom-flask, 4-*tert*-butylbenzyl mercaptan (1.0 mL, 5.36 mmol, 1.0 eq.) was dissolved in a suspension of $\text{K}_3\text{PO}_4 \cdot \text{H}_2\text{O}$ (1.39 g, 6.02 mmol, 1.1 eq.) in acetone (20 mL) at ambient temperature. After stirring for 10 min at ambient temperature carbon disulfide (1.0 mL, 16.56 mmol, 3.1 eq.) was added and the solution turned yellow. 4-*Tert*-butyl benzylbromide (1.0 mL, 5.44 mmol, 1.0 eq.) was added after 10 min and the mixture stirred at ambient temperature overnight. The mixture was filtered and the filtrate concentrated under reduced pressure. The yellow oily residue was purified via column chromatography on silica-gel with *n*-hexane as eluent. A yellow oil was obtained which solidified upon cooling (1.82 g, 4.52 mmol, 84%).

$^1\text{H-NMR}$ (400 MHz, CDCl_3): [δ , ppm] = 1.30 (s, 18H, $\text{C-(CH}_3)_3$), 4.59 (s, 4H, $\text{CH}_2\text{-S}$), 7.25 - 7.29 (m, 4H, CH), 7.31 - 7.36 (m, 4H, CH). $^{13}\text{C-NMR}$ (100 MHz, CDCl_3): [δ , ppm] = 31.3 (CH_3), 34.6 ($\text{C-(CH}_3)_3$), 41.3 (CH_2), 125.7 (CH), 128.97 (CH), 131.8 ($\text{C-C-(CH}_3)_3$), 150.8 (C-CH_2), 223.2 (C=S). **ESI-MS**: $[\text{M} + \text{Na}^+]_{\text{exp}} = 424.99$ m/z and $[\text{M} + \text{Na}^+]_{\text{calc}} = 425.14$ m/z.

Synthesis of 3-bromo-*N*-(4-(*tert*-butyl)phenyl)propanamide (4)

In a 100 mL Schlenk-flask 4-*tert*-butyl-aniline (1.5 mL, 9.42 mmol, 1.0 eq.) and triethylamine (1.9 mL, 13.60 mmol, 1.4 eq.) were dissolved in anhydrous THF (30 mL). At 0 °C 3-bromopropionyl chloride (1.3 mL, 13.14 mmol, 1.4 eq.) in anhydrous THF (15 mL) was added dropwise and stirred at ambient temperature overnight. Sat. NaHCO₃-solution (180 mL) was added and extracted with DCM (2 × 180 mL). The combined organic extracts were washed with deionized H₂O (180 mL) and brine (180 mL), dried over Na₂SO₄, filtered and concentrated under reduced pressure. The solid residue was recrystallized twice from *n*-hexane:ethyl acetate 5:1 to give the product as pale yellow crystals (1.37 g, 4.83 mmol, 51%).

¹H-NMR (400 MHz, CDCl₃): [δ, ppm] = 1.30 (s, 9H, (CH₃)₃), 2.92 (t, 2H, ³J = 6.6 Hz, CH₂-C=O), 3.71 (t, 2H, ³J = 6.6 Hz, CH₂Br), 7.34, (d, 2H, ³J = 8.5 Hz, CH-C-(CH₃)₃), 7.38 (NH), 7.44 (d, 2H, ³J = 8.5 Hz, CH-CN). **¹³C-NMR** (100 MHz, CDCl₃): [δ, ppm] = 27.2 (CH₂-Br), 31.3 (C-(CH₃)₃), 34.4 (C-(CH₃)₃), 40.7 (CH₂-C=O), 119.9 (CH-C-NH), 125.9 (CH-C-C-(CH₃)₃), 134.8 (C-NH), 147.8 (C-C-(CH₃)₃), 167.9 (C=O). **ESI-MS**: [M + Na⁺]_{exp} = 306.12 m/z and [M + Na⁺]_{calc} = 307.18 m/z.

Synthesis of benzyl (3-((4-(*tert*-butyl)phenyl)amino)-3-oxopropyl) carbonotrithioate (3)

In a 50 mL round-bottom-flask benzylmercaptan (498 μL, 4.23 mmol, 1.0 eq.) was dissolved in a suspension of K₃PO₄·H₂O (1.08 g, 4.69 mmol, 1.1 eq.) in 25 mL acetone at ambient temperature. After stirring for 10 min at ambient temperature carbon disulfide (766 μL, 12.69 mmol, 3.0 eq.) was added and the solution turned yellow. 3-Bromo-*N*-(4-(*tert*-butyl)phenyl)propanamide (4) (1.20 g, 4.23 mmol, 1.0 eq.) was added after 10 min and the mixture stirred at ambient temperature overnight. 1M HCl (160 mL) were added and extracted twice with DCM (2 × 160 mL). The combined organic extracts were washed with deionized H₂O (160 mL), brine (160 mL), dried over Na₂SO₄, filtered and concentrated under reduced pressure. The solid residue was recrystallized from *n*-hexane:ethyl acetate 1:1 to give the product as a yellow solid in two fractions (1.21 g, 3.00 mmol, 71%).

¹H-NMR (400 MHz, CDCl₃): [δ, ppm] = 1.30 (s, 9H, (CH₃)₃), 1.60 (s, 1H, NH), 2.79 (t, 2H, ³J = 7.0 Hz, C=O-CH₂), 3.73 (t, 2H, ³J = 7.0 Hz, S-CH₂-CH₂), 4.61 (s, 2H, CH₂), 7.25 - 7.45 (m, 9H, H_{arom}). **¹³C-NMR** (100 MHz, CDCl₃): [δ, ppm] = 31.3 (C-(CH₃)₃), 32.0 (CH₂-C=O), 34.4 (C-(CH₃)₃), 36.1 (CH₂-CH₂-S), 41.5 (CH₂), 119.8 (CH-C-NH), 125.9 (CH-C-C(CH₃)₃), 127.8 (CH), 128.7 (CH-CH-C-CH₂), 129.3 (CH-C-CH₂), 134.8, 134.9 (C-NH, C-CH₂), 147.6 (C-C-(CH₃)₃), 168.5 (C=O), 223.7 (C=S). **ESI-MS**: [M + Na⁺]_{exp}

= 426.27 m/z and $[M + Na^+]_{\text{calc}} = 426.100$ m/z.

Exemplary Procedure for the Polymerization of DMAAm

1 (4.9 mg, 0.014 mmol, 1.0 eq.) and Me- β -CD-solution (40 wt.% in deionized H₂O, 228 mg, 0.070 mmol, 5.0 eq.) were added to a Schlenk-tube. The two-phase mixture was ultrasonicated until a clear yellow solution was obtained. Subsequently, a stirring-bar, DMAAm (274 mg, 2.77 mmol, 198.9 eq.), VA-044 (1.0 mg, 0.003 mmol, 0.2 eq.) and deionized H₂O (0.8 mL) were added. After three freeze-pump-thaw cycles the tube was sealed and placed into an oil bath at 25 °C and removed after 6 h. The tube was subsequently cooled with liquid nitrogen to stop the reaction. A NMR-sample was withdrawn for the determination of conversion, inhibited with a pinch of hydroquinone (approx. 5 mg) and D₂O was added. A conversion of 88% was calculated based on the NMR data (see Chapter 9.3 for details of the calculation). The residue was dialysed with a SpectraPor3 membrane (MWCO = 3500 Da) for 3 days at ambient temperature and for 2 days at 45 °C. The solvent was removed *in vacuo* to yield the polymer as a yellow solid (96 mg, 39%, SEC(DMAc): $M_{\text{nSEC}} = 17000$ g·mol⁻¹, $\mathcal{D}_m = 1.09$).

In the case of short-chain polymers (with targeted M_n below 3500 g·mol⁻¹) the reaction mixture was dialysed with a SpectraPor3 membrane (MWCO = 1000 Da) for three days at ambient temperature. The polymer sample was subsequently diluted with acetic acid/acetate buffer, the α -amylase containing enzyme-mixture Taka-Diastase was added to degrade the residual CDs, the mixture was incubated at 37 °C for 24 h and boiled for 10 min.^{239,241} Finally, the mixture was dialysed against water for 3 days at ambient temperature and the solvent removed *in vacuo*.

For the other polymerizations the Me- β -CD/CTA/initiator ratio was kept constant at 5/1/0.2. The DMAAm/CTA ratio was altered and water was added to keep the concentration constant at 3.0 mol·L⁻¹. The experiments with **2** and **3** were conducted in an analogous fashion.

Exemplary Procedure for the Chain Extension of PDMAAm

PDMAAm ($M_{\text{nSEC}} = 10500$ g·mol⁻¹, $\mathcal{D}_m = 1.17$, 20.0 mg, 0.002 mmol, 1.0 eq.) as macro-CTA, DMAAm (183 mg, 1.85 mmol, 925.0 eq.), VA-044 (0.3 mg, 0.001 mmol, 0.5 eq.) and deionized H₂O (0.6 mL) were added to a Schlenk-tube. After three freeze-pump-thaw cycles the tube was placed into an oil bath at 25 °C and kept there for 24 h. The reaction-mixture was cooled with liquid nitrogen, subjected to air and dialysed for 3 days at ambient temperature. The solvent was removed *in vacuo* to give the polymer

as a yellow solid (197 mg, 97%, **SEC(DMAc)**: $M_{nSEC} = 97500 \text{ g}\cdot\text{mol}^{-1}$, $D_m = 1.08$).

Exemplary Procedure for Kinetic Measurements of DMAAm

1 (12.2 mg, 0.034 mmol, 1.0 eq.) and Me- β -CD-solution (40 wt.% in deionized H₂O, 551 mg, 0.168 mmol, 4.9 eq.) were added to a Schlenk-tube. The two-phase mixture was ultrasonicated until a clear yellow solution was obtained. Subsequently, DMAAm (1.00 g, 10.10 mmol, 297.1 eq.), VA-044 (2.2 mg, 0.007 mmol, 0.2 eq.) and deionized H₂O (2.7 mL) were added. The solution was separated into several tubes with a stirring-bar and three freeze-pump-thaw cycles were applied. Subsequently, the tubes were sealed and placed into an oil bath at 25 °C. After specific time intervals the tubes were cooled with liquid nitrogen. Samples for NMR analysis were withdrawn, a pinch of hydroquinone (approx. 5 mg) was added to inhibit further polymerization and D₂O was added. The conversion was calculated via comparison of the vinyl-proton integrals with the appropriate integrals of the backbone or side chains of the polymers (see Chapter 9.3 for details). The residual sample in each tube was purified by dialysis for 3 days at ambient temperature and 1 day at 45 °C. The solvent was removed *in vacuo* and the polymer subjected to SEC-analysis.

Exemplary Procedure for the Polymerization of DEAAm

1 (5.0 mg, 0.014 mmol, 1.0 eq.) and Me- β -CD-solution (40 wt.% in deionized H₂O, 228 mg, 0.070 mmol, 5.0 eq.) were added to a Schlenk-tube. The two-phase mixture was ultrasonicated until a clear yellow solution was obtained. Subsequently, a stirring bar, DEAAm (142 mg, 1.12 mmol, 80.0 eq.), VA-044 (0.9 mg, 0.003 mmol, 0.2 eq.) and deionized H₂O (0.2 mL) were added. After three freeze-pump-thaw cycles the tube was sealed and placed into an oil bath at 25 °C and removed after 12 h. The tube was subsequently cooled with liquid nitrogen to stop the reaction. A NMR-sample was withdrawn for the determination of conversion, inhibited with a pinch of hydroquinone (approx. 5 mg) and acetone-D₆ was added. A conversion of > 99% was calculated based on the NMR data (see Chapter 9.3 for details). The residue was dialysed with a SpectraPor3 membrane (MWCO = 3500 Da) for 3 days at ambient temperature and for 1 day at 45 °C. The solvent was removed *in vacuo* to yield the polymer as a yellow solid (110 mg, 75%, **SEC(DMAc)**: $M_{nSEC} = 10000 \text{ g}\cdot\text{mol}^{-1}$, $D_m = 1.09$).

In the case of short-chain polymers (with targeted M_n below 3500 g·mol⁻¹) the reaction mixture was dialysed with a SpectraPor3 membrane (MWCO = 1000 Da) for three days at ambient temperature. The polymer sample was subsequently diluted with acetic acid/acetate buffer, the α -amylase containing enzyme-mixture Taka-Diastase was added to degrade the residual CDs, the mixture incubated at 37 °C for 24 h and

boiled for 10 min. Finally, the mixture was dialysed against water for 3 days at ambient temperature and the solvent removed *in vacuo*. For the other polymerizations the Me- β -CD/CTA/initiator ratio was kept constant at 5/1/0.2. The DEAAm/CTA ratio was altered and water was added to keep the concentration constant at 3.5 mol·L⁻¹. The experiments with **2** and **3** were conducted in an analogous fashion.

Exemplary Procedure for the Chain Extension of PDEAAm

PDEAAm ($M_{nSEC} = 8500 \text{ g}\cdot\text{mol}^{-1}$, $D_m = 1.11$, 20.0 mg, 0.002 mmol, 1.0 eq.) as macro-CTA, DEAAm (204 mg, 1.60 mmol, 925.0 eq.), VA-044 (0.4 mg, 0.001 mmol, 0.5 eq.), deionized H₂O (0.3 mL) and acetone (0.3 mL) were added to a Schlenk-tube. After three freeze-pump-thaw cycles the tube was placed into an oil bath at 25 °C and kept there for 24 h. The reaction-mixture was cooled with liquid nitrogen, subjected to air and dialysed for 3 days at ambient temperature. The solvent was removed *in vacuo* to give the polymer as a yellow solid (182 mg, 81%, **SEC(DMAc)**: $M_{nSEC} = 83000 \text{ g}\cdot\text{mol}^{-1}$, $D_m = 1.13$).

Exemplary Procedure for Kinetic Measurements of the Polymerization of DEAAm

1 (17.4 mg, 0.049 mmol, 1.0 eq.) and Me- β -CD-solution (40 wt.% in deionized H₂O, 820 mg, 0.250 mmol, 5.1 eq.) were added to a Schlenk-tube. The two-phase mixture was ultrasonicated until a clear yellow solution was obtained. Afterwards DEAAm (1.50 g 11.78 mmol, 240.5 eq.), VA-044 (3.2 mg, 0.010 mmol, 0.2 eq.) and deionized H₂O (3.3 mL) were added. The solution was separated into several tubes containing a stirring-bar and three freeze-pump-thaw cycles were applied. Subsequently the tubes were sealed and placed into an oil bath at 25 °C. After specific time intervals the tubes were cooled with liquid nitrogen. Samples for NMR analysis were withdrawn, a pinch of hydroquinone (approx. 5 mg) was added to inhibit further polymerization and acetone-D₆ was added. The conversion was calculated via comparison of the vinyl-proton integrals with the appropriate integrals of the backbone or side chains of the polymers (see Chapter 9.3 for details). The residual sample in each tube was purified by dialysis for 3 days at ambient temperature and 1 day at 45 °C. The solvent was removed *in vacuo* and the polymer subjected to SEC-analysis.

Exemplary Procedure for the Polymerization of NIPAAm

1 (7.0 mg, 0.020 mmol, 1.0 eq.) and Me- β -CD-solution (40 wt.% in deionized H₂O, 326 mg, 0.100 mmol, 5.0 eq.) were added to a Schlenk-tube. The two-phase mixture was ultrasonicated until a clear yellow solution was obtained. Afterwards stirring-bar, NIPAAm (100 mg, 0.88 mmol, 44.0 eq.), VA-044 (1.3 mg, 0.004 mmol, 0.2 eq.) and deionized H₂O (0.2 mL) were added. After three freeze-pump-thaw cycles the tube was sealed and placed into an oil bath at 25 °C and removed after 18 h. The tube was subsequently cooled with liquid nitrogen to stop the reaction. A NMR-sample was withdrawn for the determination of conversion, inhibited with a pinch of hydroquinone (approx. 5 mg) and acetone-D₆ was added. A conversion of > 99% was calculated based on the NMR data (see Chapter 9.3 for details). The residue was dialysed with a SpectraPor3 membrane (MWCO = 3500 Da) for 3 days at ambient temperature and for 1 day at 45 °C. The solvent was removed *in vacuo* to yield the polymer as a yellow solid (64 mg, 60%, **SEC(DMAc)**: $M_{nSEC} = 9000 \text{ g}\cdot\text{mol}^{-1}$, $D_m = 1.15$).

In the case of short-chain polymers (with targeted M_n below 3500 g·mol⁻¹) the reaction mixture was dialysed with a SpectraPor3 membrane (MWCO = 1000 Da) for three days at ambient temperature. The polymer sample was subsequently diluted with acetic acid/acetate buffer, the α -amylase containing enzyme-mixture Taka-Diastase was added to degrade the residual CDs, the mixture incubated at 37 °C for 24 h and boiled for 10 min. Finally, the mixture was dialysed against water for 3 days at ambient temperature and the solvent removed *in vacuo*. For the other polymerizations the Me- β -CD/CTA/initiator ratio was kept constant at 5/1/0.2. The NIPAAm/CTA ratio was altered and water was added to keep the concentration constant at 2.5 mol·L⁻¹.

Exemplary Procedure for the Chain Extension of PNIPAAm

PNIPAAm ($M_{nSEC} = 9000 \text{ g}\cdot\text{mol}^{-1}$, $D_m = 1.15$, 20.0 mg, 0.002 mmol, 1.0 eq.) as macro-CTA, NIPAAm (172 mg, 1.52 mmol, 760.0 eq.), VA-044 (0.4 mg, 0.001 mmol, 0.5 eq.), deionized H₂O (0.8 mL) and 1,4-dioxane (0.6 mL) were added to a Schlenk-tube. After three freeze-pump-thaw cycles the tube was placed into an oil bath at 25 °C and kept there for 24 h. The reaction-mixture was cooled with liquid nitrogen, subjected to air and dialysed for 3 days at ambient temperature. The solvent was removed *in vacuo* to give the polymer as a yellow solid (180 mg, 94%, **SEC(DMAc)**: $M_{nSEC} = 90000 \text{ g}\cdot\text{mol}^{-1}$, $D_m = 1.11$).

Exemplary Procedure for Kinetic Measurements of the Polymerization of NIPAAm

1 (35.8 mg, 0.101 mmol, 1.0 eq.) and Me- β -CD-solution (40 wt.% in deionized H₂O, 1.65 g, 0.504 mmol, 5.0 eq.) were added to a Schlenk-tube. The two-phase mixture was ultrasonicated until a clear yellow solution was obtained. Afterwards NIPAAm (500 mg, 4.42 mmol, 43.8 eq.), VA-044 (6.5 mg, 0.020 mmol, 0.2 eq.) and deionized H₂O (0.8 mL) were added. The solution was separated into several tubes containing a stirring-bar and three freeze-pump-thaw cycles were applied. Subsequently, the tubes were sealed and placed into an oil bath at 25 °C. After specific time intervals the tubes were cooled with liquid nitrogen. Samples for NMR analysis were withdrawn, a pinch of hydroquinone (approx. 5 mg) was added to inhibit further polymerization and acetone-D₆ was added. The conversion was calculated via comparison of the vinyl-proton integrals with the appropriate integrals of the backbone or side chains of the polymers (see Chapter 9.3 for details). The residual sample in each tube was purified by dialysis for 3 days at ambient temperature and 1 day at 45 °C. The solvent was removed *in vacuo* and the polymer subjected to SEC-analysis.

Supramolecular ABA Triblock Copolymers

4.1 Introduction

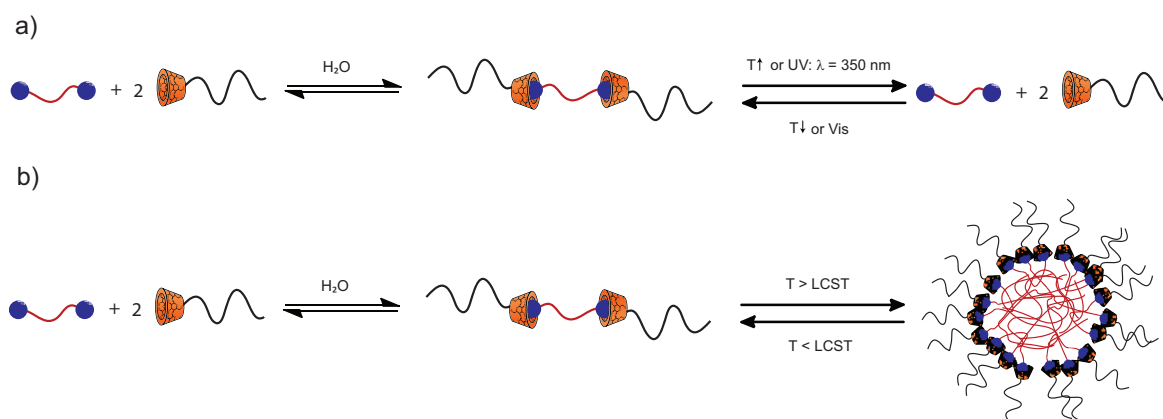
Complex macromolecular architectures constitute an important field in contemporary polymer chemistry. Block copolymers belong to the most studied materials in this field and are subjected to manifold applications.^{244,245} Apart from classical anionic²⁴⁶ and cationic²⁴⁷ polymerization, reversible-deactivation radical polymerizations, *e.g.* NMP,⁹ ATRP,^{11,12} and RAFT polymerization^{13,45} have proven to be a very versatile tool for the generation of new block copolymers with a large variety of different blocks *via* convenient synthetic procedures. Furthermore, modular ligation chemistry had a strong impact on the field of block copolymer synthesis,^{18,20,88} *e.g.* *via* the CuAAc,²⁴⁸ the Diels-Alder²⁴⁹ or the RAFT hetero Diels-Alder reaction,²⁵⁰ which provide numerous opportunities to generate block copolymers as well as more complex architectures.^{249,251}

A common application of CDs in polymer chemistry is the utilization as a linker molecule for the formation of supramolecular block copolymers. Hereby, reversible-deactivation radical polymerization techniques and modular conjugation have proven to be a very powerful tool set for the incorporation of CD-endgroups into polymers. The most frequently applied ligation reaction is CuAAc based on the convenient synthesis of mono azido functionalized β -CD (β -CD-N₃). So far, mostly AB diblock copolymers with different properties have been described, *e.g.* with a light responsive linkage,¹⁷⁴ with a redox responsive linkage,¹⁷³ with a thermoresponsive block¹⁷²

NOESY measurements were performed in collaboration with M. Hetzer and Prof. H. Ritter (Heinrich Heine Universität Düsseldorf). Parts of this chapter were reproduced with permission from Schmidt, B. V. K. J.; Hetzer, M.; Ritter, H.; Barner-Kowollik, C. *Macromolecules* **2013**, *46* (3), 1054-1065 (DOI: 10.1021/ma302386w). Copyright 2013 American Chemical Society.

and even with schizophrenic behavior of the blocks.^{166,171} A further example is a CD-centered star polymer, where two cores are coupled using supramolecular interactions.^{200,201} The variety of possible building blocks and guest-moieties gives the opportunity for several applications. For example, light-controlled supramolecular nanotubes have been described¹⁷⁴ as well as vesicular nanocontainers with voltage-triggered release¹⁷³ or supramolecular linkages for the generation of dynamic core-shell nanoparticles.¹⁶⁴ A further example is a core-shell nano-assembly that shows tumor-triggered release.¹⁵⁸ One can imagine many applications that can be derived from conventional covalently bound block copolymers, *e.g.* self-assembly of supramolecular block copolymers coupled *via* hydrogen bonding motifs in thin-films that mimic the behavior of their covalent analogues.¹⁷⁵

In the current approach, two PHPMA outer blocks are connected with a PDMAAm or PDEAAm inner block *via* a CD host/guest complex to generate a novel supramolecular macromolecular architecture (see Scheme 4.1). PHPMA was chosen due to its potential application in drug delivery.²⁵² PDMAAm was selected to study the thermoresponsive behavior of the host/guest complexation (refer to Scheme 4.1 a), whereas PDEAAm was chosen due to its T_c of close to 30 °C²⁴² and therefore close to physiological temperatures. The T_c of PDEAAm can be utilized to form aggregates in aqueous solution upon heating that are connected *via* supramolecular interactions (see Scheme 4.1 b).



Scheme 4.1: Schematic representation of the formation of supramolecular ABA triblock copolymers *via* CD host/guest complexation (β -CD is depicted orange; the guest groups are depicted blue; the outer PHPMA block is depicted black; the inner PDMAAm- and PDEAAm-blocks are depicted red): a) PDMAAm based supramolecular block copolymers with temperature- and light-responsive complexation *via* azobenzene guest groups and b) PDEAAm based supramolecular block copolymers with T_c triggered aggregate formation.

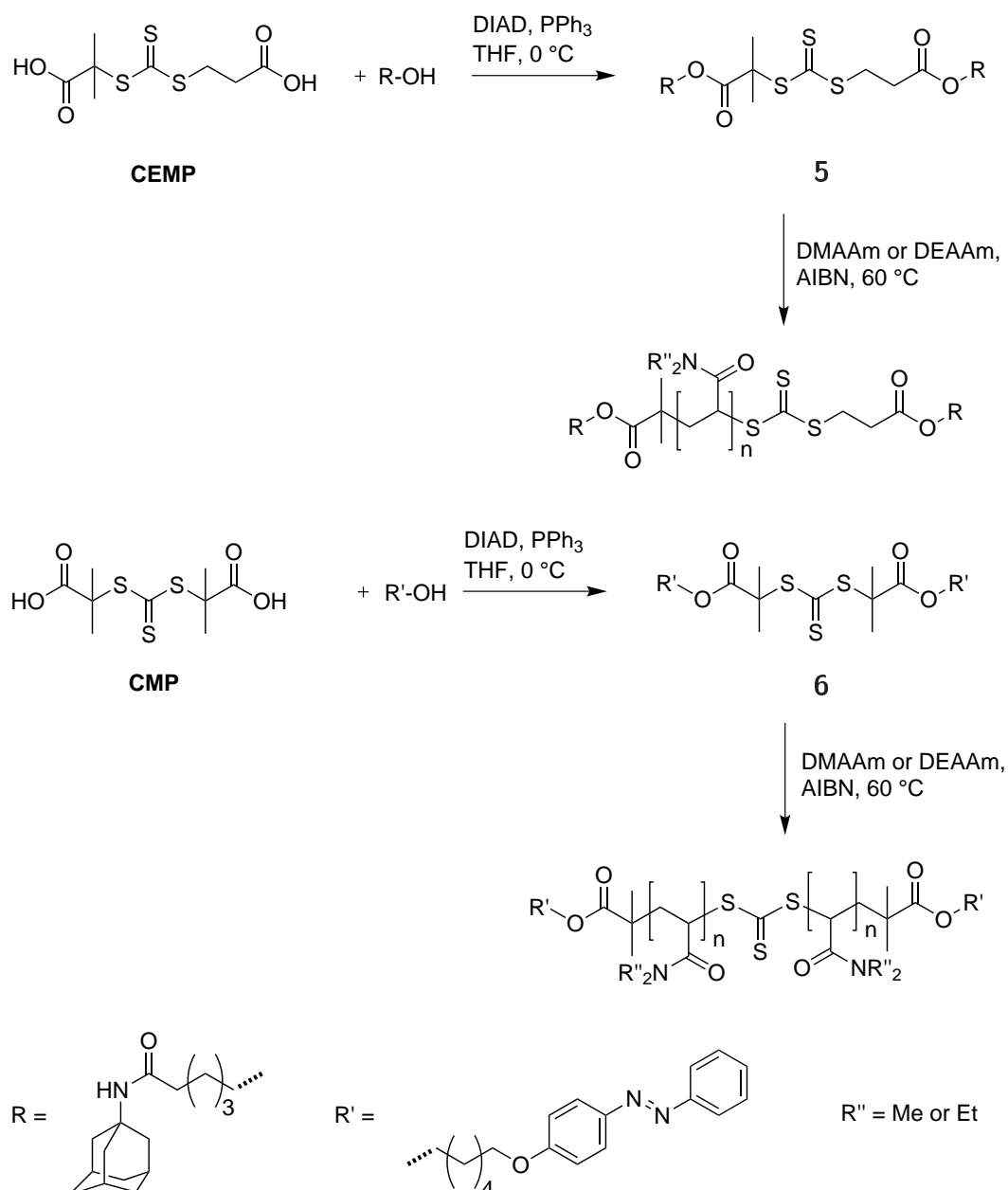
In this chapter the formation of a novel supramolecular ABA triblock copolymer consisting of a PDMAAm or PDEAAm inner block and a biocompatible PHPMA

outer block is reported. The inner building block was synthesized *via* RAFT polymerization employing novel doubly guest-functionalized CTAs featuring adamantyl or photoresponsive azobenzene guest groups. The outer building block was synthesized *via* RAFT polymerization with an alkyne containing CTA and subsequent CuAAC with β -CD-N₃. The building blocks were characterized *via* ¹H-NMR, ESI-MS and SEC. The complex formation was investigated with DLS, turbidimetry measurements and NOESY.

4.2 Results and Discussion

4.2.1 Synthesis of the Building Blocks

For the synthesis of the inner building blocks two doubly guest-functionalized CTAs based on trithiocarbonates were designed. **5** contains two adamantyl groups and **6** contains two azobenzene groups. The adamantyl group was chosen due to its high complexation constant of up to $10^5 \cdot \text{M}^{-1}$ with β -CD.²³⁷ The azobenzene group was chosen due to its ability to change the conformation from *trans* to *cis* in response to light irradiation. This change in conformation leads to a significant change in the complexation constant with β -CD, *i.e.* the guest is expelled from the host-molecule upon irradiation with UV-light. The guest molecules were attached to the core CTA molecule *via* a short spacer group to support its availability in the complex formation. As shown in Scheme 4.2, both guest-functionalized CTAs were synthesized *via* a Mitsunobu reaction from the corresponding acids, **CEMP** in the case of **5** and **CMP** in the case of **6**.



Scheme 4.2: Overview of the synthetic pathway leading to the doubly guest-functionalized inner building block featuring adamantyl- or azobenzene-guest groups.

Subsequently, the novel CTAs were employed in the RAFT polymerization of DMAAm and DEAAm in DMF at 60 °C with AIBN as initiator. DMAAm was selected to investigate the temperature response of the complex formation whereas DEAAm was chosen due to its T_c , providing the opportunity to study the formation of block copolymer aggregates in solution due to a coil to globule transition of PDEAAm above the T_c . For PDMAAm, molecular masses of 6400 g·mol⁻¹ and 15700 g·mol⁻¹ with a D_m of 1.06 and 1.11, respectively, were achieved with **5**, while a molecular weight of 5400 g·mol⁻¹ and 11000 g·mol⁻¹ with a D_m of 1.08 and 1.11, respectively, were reached with **6** (refer to Figure 4.1 a/b and Table 4.1). The polymerization of DEAAm with **5**

afforded polymers with molecular masses ranging from $6500 \text{ g}\cdot\text{mol}^{-1}$ to $12100 \text{ g}\cdot\text{mol}^{-1}$ and D_m ranging from 1.11 to 1.27 (refer to Figure 4.1 c and Table 4.1). Furthermore, PDEAAMs with molecular weights ranging from $5400 \text{ g}\cdot\text{mol}^{-1}$ to $11000 \text{ g}\cdot\text{mol}^{-1}$ and D_m ranging from 1.16 to 1.33 (refer to Figure 4.1 d and Table 4.1) were synthesized with **6**. The structures of the polymers were verified *via* $^1\text{H-NMR}$ and ESI-MS (refer to Appendix Figures B.1 - B.8).

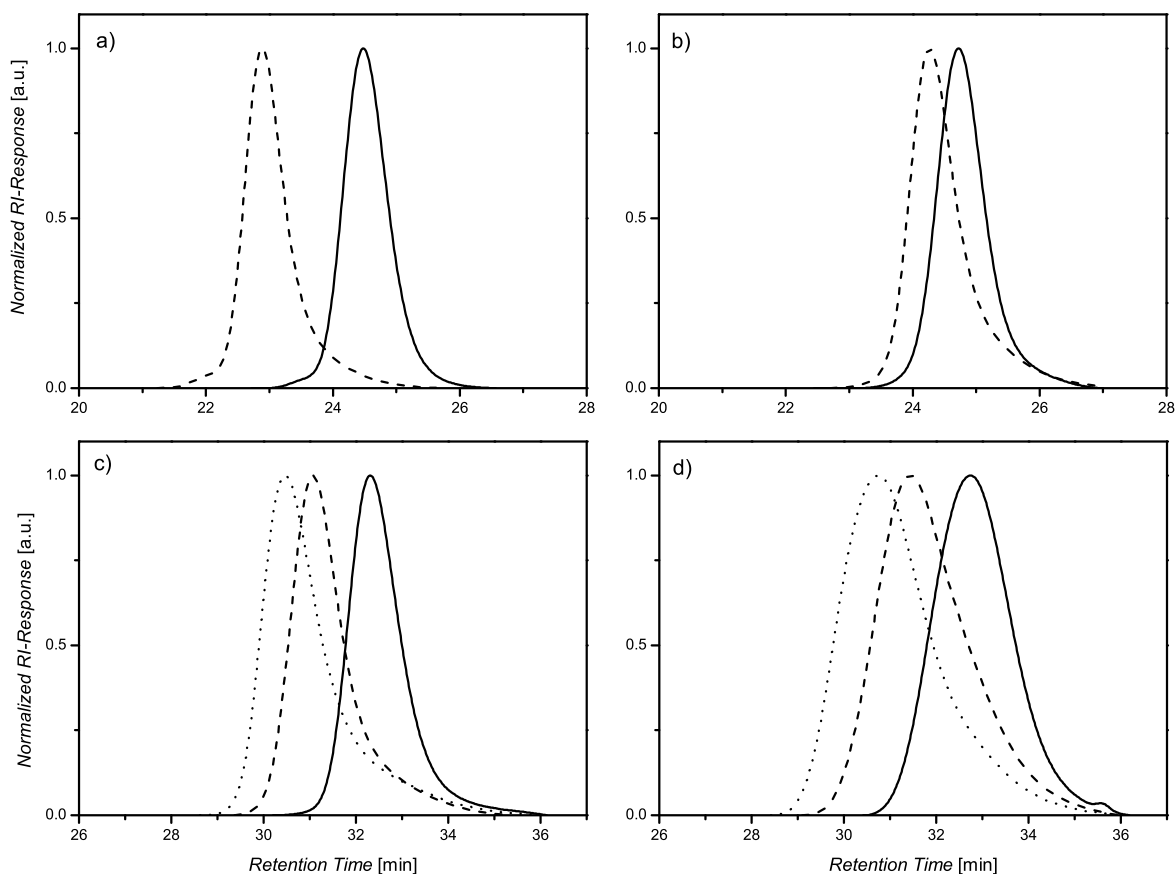


Figure 4.1: SEC traces for a) PDMAAM polymerized with **5** (dashed line PDMAAM₁₅₁-Ad₂; solid line PDMAAM₅₇-Ad₂), b) PDMAAM polymerized with **6** (dashed line: PDMAAM₁₀₃-AzO₂; solid line: PDMAAM₄₆-AzO₂), c) PDEAAM polymerized with **5** (dotted line: PDEAAM₈₉-Ad₂; dashed line: PDEAAM₇₈-Ad₂; solid line: PDEAAM₄₅-Ad₂), d) PDEAAM polymerized with **6** (dotted line: PDEAAM₈₀-AzO₂; dashed line: PDEAAM₅₉-AzO₂; solid line: PDEAAM₃₆-AzO₂).

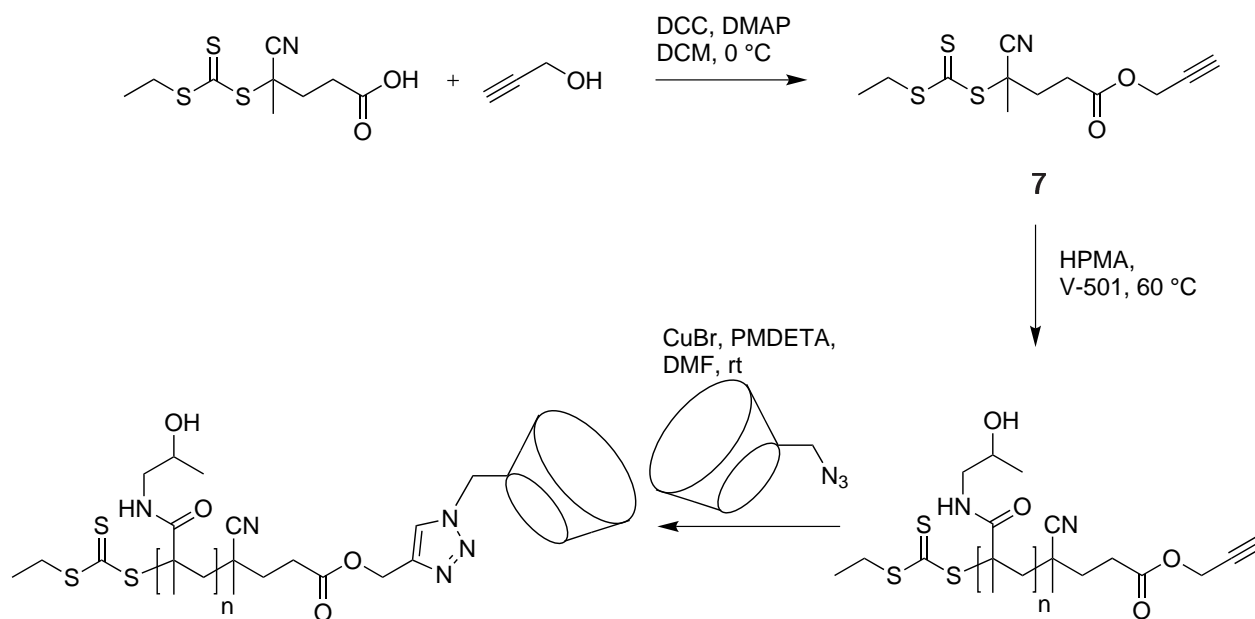
Table 4.1: Results for the living/controlled RAFT polymerization of DMAAm or DEAAm at 60 °C in DMF.

DMAAm/CTA/I	Time / h	Conv.	$M_{n\text{theo}} / \text{g}\cdot\text{mol}^{-1}$	$M_{n\text{SEC}} / \text{g}\cdot\text{mol}^{-1}$	D_m	D_p
5: 34/1/0.2	24	> 99	4200	6400	1.06	57
5: 100/1/0.2	24	> 99	10700	15700	1.11	151
6: 35/1/0.2	24	79	3500	5400	1.08	46
6: 100/1/0.2	24	65	7300	11000	1.15	103

DEAAm/CTA/I	Time / h	Conv.	$M_{n\text{theo}} / \text{g}\cdot\text{mol}^{-1}$	$M_{n\text{SEC}} / \text{g}\cdot\text{mol}^{-1}$	D_m	D_p
5: 56/1/0.2	24	> 99	7900	6500	1.11	45
5: 107/1/0.2	24	98	14300	10700	1.16	78
5: 159/1/0.2	24	97	20900	12100	1.27	89
6: 55/1/0.2	24	76	6100	5400	1.16	36
6: 110/1/0.2	24	72	10900	8300	1.26	59
6: 172/1/0.2	24	76	22800	11000	1.33	80

For the outer building block the biocompatible monomer HPMA was utilized.²⁵² Therefore, a trithiocarbonate CTA with an alkyne moiety was synthesized (refer to Scheme 4.3). A dithiobenzoate CTA, the first choice for methacrylamide and methacrylate monomers, was not further considered as the complex formation between the phenyl-group and β -CD cannot be ruled out. As the utilized CTA contains an unprotected alkyne moiety, the conversion in the RAFT polymerizations was kept at low values to suppress radical transfer to the terminal alkyne.

The polymerization of HPMA was conducted in a mixture of DMF and acetic acid/sodium acetate buffer with V-501 as initiator at 70 °C. The utilization of **7** afforded narrowly distributed alkyne-functionalized PHPMA, *e.g.* a molecular mass of 6500 $\text{g}\cdot\text{mol}^{-1}$ and a D_m of 1.17 (refer to Figure 4.2 and Table 4.2). The structure of the polymer was proven *via* ESI-MS and ¹H-NMR measurements (refer to Appendix B.9/B.10).



Scheme 4.3: Overview of the synthetic pathway leading to the β -CD-functionalized outer PHPMA building block.

Table 4.2: Results for the living/controlled RAFT polymerization of HPMA at 70 °C in DMF/acetic acid sodium acetate buffer with 7.

HPMA/CTA/I	Time / h	Conv.	$M_{n\text{theo}} / \text{g}\cdot\text{mol}^{-1}$	$M_{n\text{SEC}} / \text{g}\cdot\text{mol}^{-1}$	D_m	D_p
35/1/0.2	2	15	1100	3900	1.17	26
35/1/0.2	2	28	1700	4300	1.15	28
36/1/0.2	2	23	5400	6500	1.17	44
71/1/0.2	13	81	8400	9200	1.40	63

The subsequent functionalization with β -CD was accomplished *via* a CuAAC reaction of the alkyne-functionalized PHPMA and β -CD- N_3 . In the SEC trace a shift of the RI-signal to lower retention times is evident, thus proving the increased hydrodynamic volume of the β -CD conjugated PHPMA in comparison with the alkyne-functionalized PHPMA (refer to Figure 4.2 a-d), *e.g.* the M_n of the molecular weight distribution of PHPMA₄₄ increases from 6500 $\text{g}\cdot\text{mol}^{-1}$ to 7300 $\text{g}\cdot\text{mol}^{-1}$, which fits the theory as the β -CD- N_3 moiety has a molecular weight of 1159 $\text{g}\cdot\text{mol}^{-1}$. In other cases with lower molecular weight PHPMA (refer to Table 4.3), the M_n of the distribution remains close to unchanged. Nevertheless, the peak maximum molecular weight (M_p) increases as expected (Table 4.3) and a shift of the full molecular weight distribution is visible (Figure 4.2 a-d). In all cases a broadening of the molecular weight distribution is evident that could be attributed to adsorptive interactions of the β -CD moiety with

the SEC column. The distributions have small shoulders at higher molecular weights that could be due to the conjugation of small amounts of difunctional azido β -CD.

Table 4.3: Results for the CuAAc conjugation of alkyne-functionalized PHPMA and β -CD-N₃.

alkyne-PHPMA			β -CD-PHPMA		
$M_{nSEC} / \text{g}\cdot\text{mol}^{-1}$	$M_{pSEC} / \text{g}\cdot\text{mol}^{-1}$	D_m	$M_{nSEC} / \text{g}\cdot\text{mol}^{-1}$	$M_{pSEC} / \text{g}\cdot\text{mol}^{-1}$	D_m
3900	4400	1.17	3800	5800	1.41
4300	4700	1.15	3800	5800	1.46
6500	7700	1.17	7300	8900	1.29
9200	13900	1.4	10600	15200	1.44

Furthermore, ¹H-NMR spectroscopy shows the formation of the triazole ring as the new signal at 8.1 ppm can be assigned to the triazole-proton (Figure 4.2 e inset). Additionally, the ¹H-NMR spectrum shows signals that can be assigned to both β -CD and PHPMA, *e.g.* the anomeric CD protons between 4.3 and 4.6 ppm, the 2-hydroxyl and the 3-hydroxyl protons between 5.5 and 6.0 ppm, the hydroxyl protons of PHPMA between 4.6 and 4.8 ppm or the amide proton of PHPMA between 7.0 and 7.5 ppm (see Figure 4.2 e).

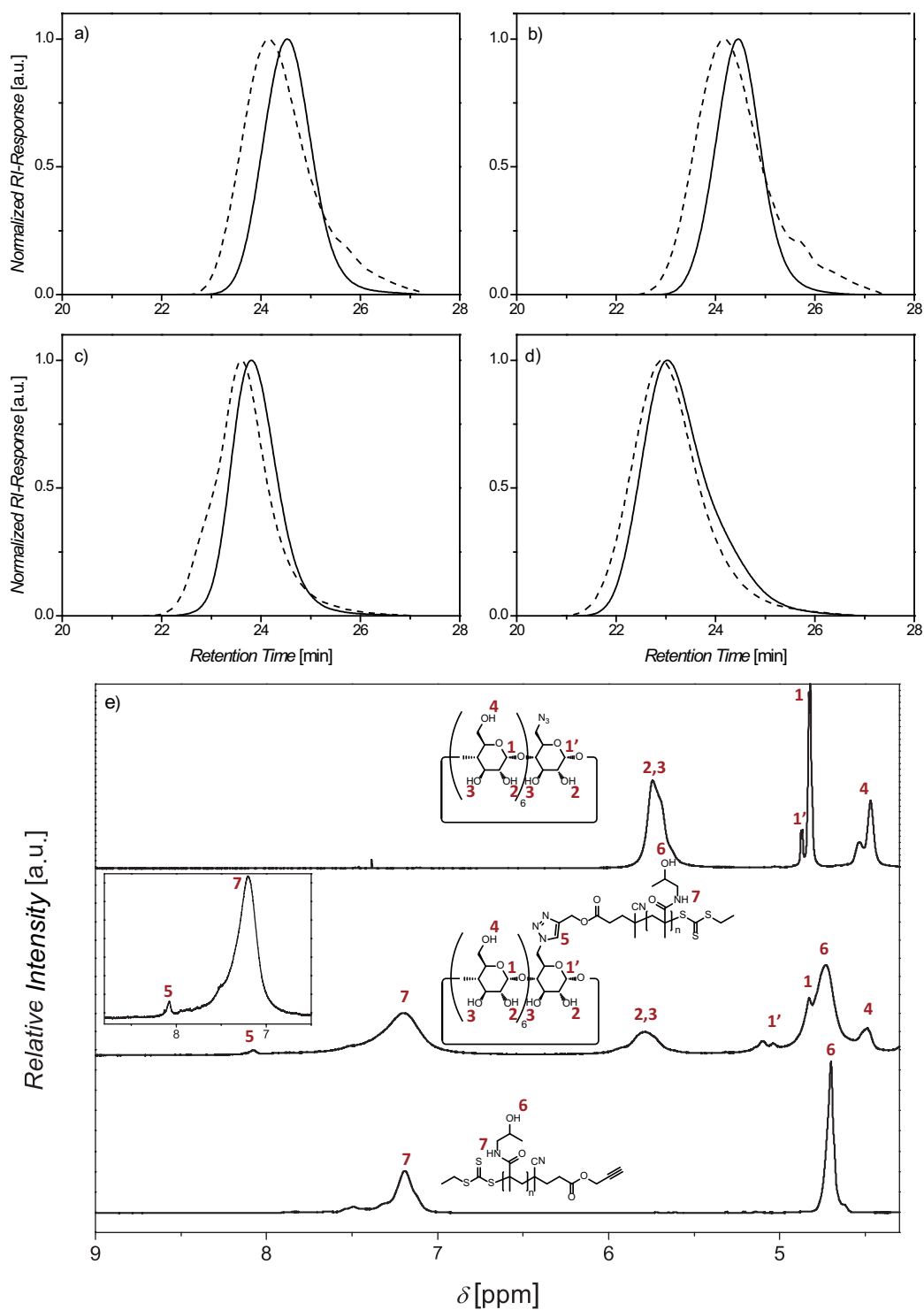


Figure 4.2: a) SEC traces for PHPMA polymerized with 7 (solid line) and the product of the conjugation with β -CD- N_3 (dashed line): a) for PHPMA₂₆-alkyne; b) for PHPMA₂₈-alkyne; c) for PHPMA₄₄-alkyne; d) for PHPMA₆₃-alkyne and e) comparison of the $^1\text{H-NMR}$ spectra of β -CD- N_3 (top), the β -CD-functionalized PHPMA click product (middle: PHPMA₂₈- β -CD) and alkyne-functionalized PHPMA (bottom: PHPMA₂₈-alkyne).

4.2.2 Formation of ABA Triblock Copolymers *via* Self-Assembly

To ensure the availability of the hydrophobic guest groups for the complex formation, the self-assembly of the building blocks was accomplished *via* the dialysis method. In brief, both polymer building blocks were dissolved in an organic solvent, *e.g.* DMF, one solution was added dropwise to the other under vigorous stirring and the organic solvent was removed *via* dialysis. The complexes were finally lyophilized and subsequently characterized *via* DLS and NOESY.

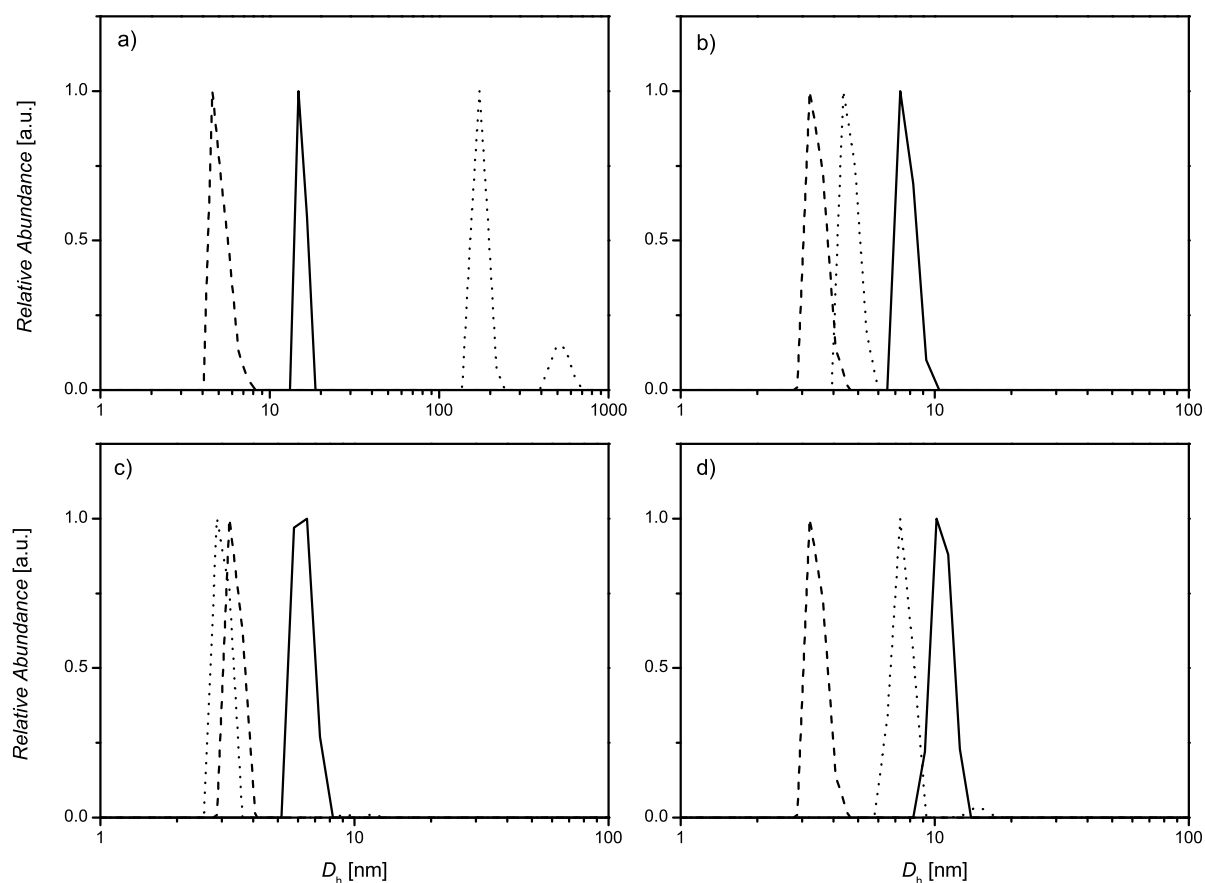


Figure 4.3: Comparison of the number averaged particle size distributions obtained from DLS measurements of the building blocks (dashed line PHPMA and dotted line PDMAAM) and the supramolecular block copolymer (solid line) at a concentration of $1 \text{ mg}\cdot\text{mL}^{-1}$ and at $25 \text{ }^\circ\text{C}$: a) $\text{PHPMA}_{44}\text{-}\beta\text{-CD}$, $\text{PDMAAm}_{57}\text{-Ad}_2$ and $\text{PDMAAm}_{57}\text{-Ad}_2\text{-}b\text{-}(\text{PHPMA}_{44}\text{-}\beta\text{-CD})_2$; b) $\text{PHPMA}_{26}\text{-}\beta\text{-CD}$, $\text{PDMAAm}_{151}\text{-Ad}_2$ and $\text{PDMAAm}_{151}\text{-Ad}_2\text{-}b\text{-}(\text{PHPMA}_{26}\text{-}\beta\text{-CD})_2$; c) $\text{PHPMA}_{26}\text{-}\beta\text{-CD}$, $\text{PDMAAm}_{46}\text{-AzO}_2$ and $\text{PDMAAm}_{46}\text{AzO}_2\text{-}b\text{-}(\text{PHPMA}_{26}\text{-}\beta\text{-CD})_2$; d) $\text{PHPMA}_{26}\text{-}\beta\text{-CD}$, $\text{PDMAAm}_{103}\text{-AzO}_2$ and $\text{PDMAAm}_{103}\text{AzO}_2\text{-}b\text{-}(\text{PHPMA}_{26}\text{-}\beta\text{-CD})_2$.

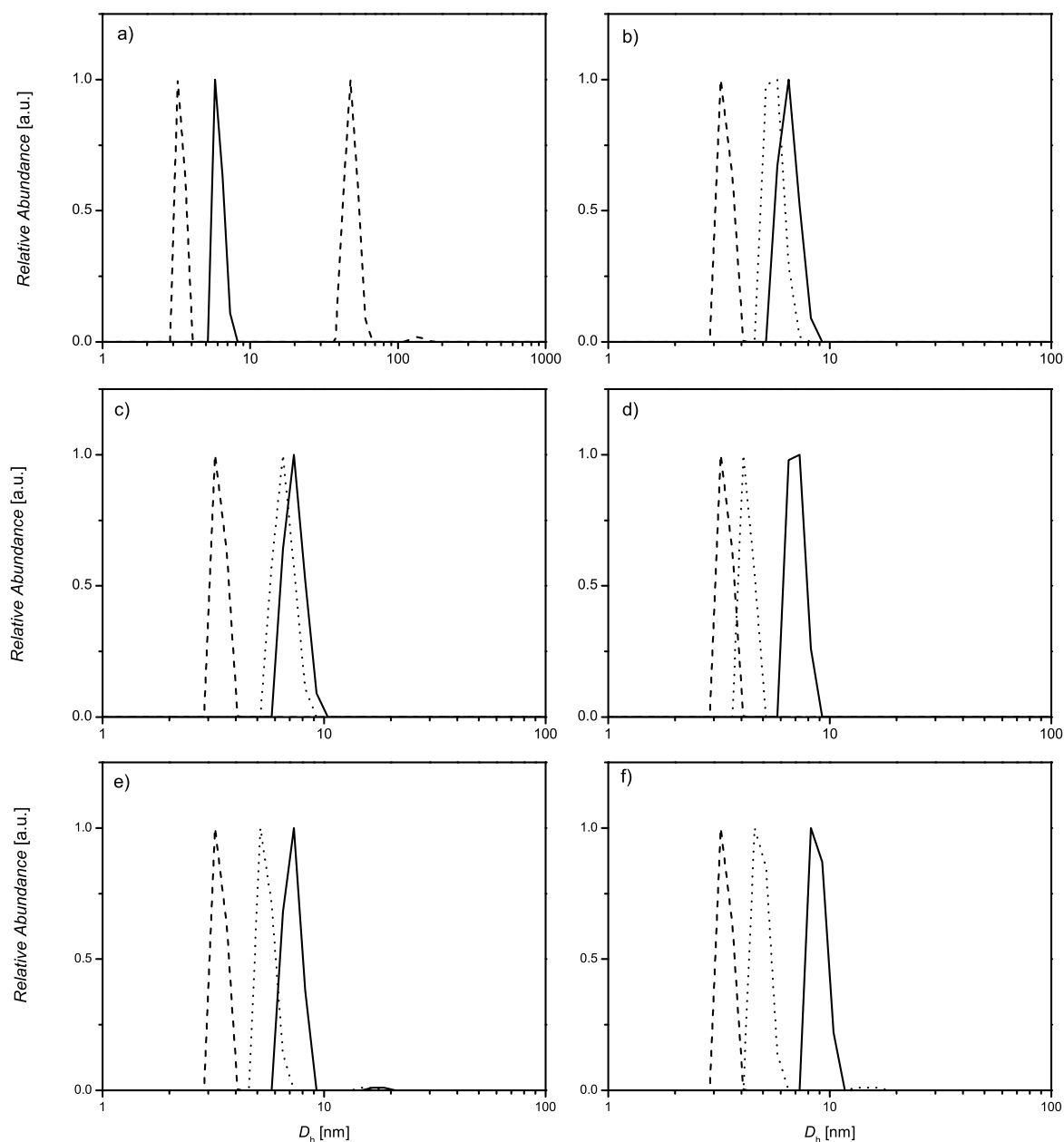


Figure 4.4: Comparison of the number averaged particle size distributions obtained from DLS measurements of the building blocks (dashed line PHPMA and dotted line PDEAAM) and the supramolecular block copolymer (solid line) at a concentration of $1 \text{ mg}\cdot\text{mL}^{-1}$ at $10 \text{ }^\circ\text{C}$: a) $\text{PHPMA}_{28}\text{-}\beta\text{-CD}$, $\text{PDEAAM}_{45}\text{-Ad}_2$ and $\text{PDEAAM}_{45}\text{-Ad}_2\text{-b-(PHPMA}_{28}\text{-}\beta\text{-CD)}_2$; b) $\text{PHPMA}_{28}\text{-}\beta\text{-CD}$, $\text{PDEAAM}_{78}\text{-Ad}_2$ and $\text{PDEAAM}_{78}\text{Ad}_2\text{-b-(PHPMA}_{28}\text{-}\beta\text{-CD)}_2$; c) $\text{PHPMA}_{28}\text{-}\beta\text{-CD}$, $\text{PDEAAM}_{89}\text{-Ad}_2$ and $\text{PDEAAM}_{89}\text{-Ad}_2\text{-b-(PHPMA}_{28}\text{-}\beta\text{-CD)}_2$; d) $\text{PHPMA}_{28}\text{-}\beta\text{-CD}$, $\text{PDEAAM}_{36}\text{-AzO}_2$ and $\text{PDEAAM}_{36}\text{AzO}_2\text{-b-(PHPMA}_{28}\text{-}\beta\text{-CD)}_2$; e) $\text{PHPMA}_{28}\text{-}\beta\text{-CD}$, $\text{PDEAAM}_{59}\text{-AzO}_2$ and $\text{PDEAAM}_{59}\text{AzO}_2\text{-b-(PHPMA}_{28}\text{-}\beta\text{-CD)}_2$; f) $\text{PHPMA}_{28}\text{-}\beta\text{-CD}$, $\text{PDEAAM}_{80}\text{-AzO}_2$ and $\text{PDEAAM}_{80}\text{AzO}_2\text{-b-(PHPMA}_{28}\text{-}\beta\text{-CD)}_2$.

DLS is a versatile tool to investigate the complex formation in solution. In the current investigation DLS was employed to obtain the hydrodynamic diameter (D_h) of

the polymer coils in solution. In principle, the D_h should increase upon complex formation as three polymer chains are included in the complex. The PDMAAm based complexes were measured at 25 °C and the complexes show larger D_h than the individual parts (refer to Figure 4.3 and 4.4), *e.g.* PHPMA₂₆- β -CD has a D_h of 3.4 nm, PDMAAm₁₅₁-Ad₂ has a D_h of 4.7 nm and the supramolecular complex features a D_h of 7.8 nm. An exception is the doubly adamantyl-functionalized PDMAAm with low molecular weight, which has a D_h of 175.0 nm for PDMAAm₅₇-Ad₂, a D_h of 5.1 for PHPMA₄₄- β -CD and a D_h of 15.4 nm for the supramolecular complex PDMAAm₅₇-Ad₂-*b*-(PHPMA₄₄- β -CD)₂. In this case, the hydrophobic guest groups lead to aggregation of or within the homopolymer. The complex shows a smaller D_h , yet the value of 15.4 nm suggests further aggregation probably due to more complicated structures in solution (refer to Figure 4.3 a). An example for doubly azobenzene-functionalized PDEAAm is PDEAAm₈₀Azo₂-*b*-(PHPMA₂₈- β -CD)₂ with a D_h of 8.9 nm. The individual building blocks PDEAAm₈₀Azo₂ and PHPMA₂₈- β -CD have a D_h of 4.9 nm and 3.4 nm, respectively. Due to the T_c of PDEAAm the DLS measurements were performed at 10 °C. A significant increase in D_h was evident in most of the cases (refer to Figure 4.4). An example for doubly adamantyl-functionalized PDEAAm PDEAAm₈₉-Ad₂-*b*-(PHPMA₂₈- β -CD)₂ with a D_h of 7.4 nm consisting of PDEAAm₈₉-Ad₂ with a D_h of 6.6 nm and PHPMA₂₈- β -CD with a D_h of 3.4 nm. Similar to PDMAAm of lower molecular weight, doubly adamantyl-functionalized PDEAAm shows very large D_h (48.4 nm for PDEAAm₄₅-Ad₂) for the homopolymer and a D_h of 6.1 nm after complexation with PHPMA₂₈- β -CD (Figure 4.4 a). For doubly azobenzene-functionalized PDEAAm an increase in D_h from 4.9 nm for the middle-block PDEAAm₈₀-Azo₂ and 3.4 nm for the outer PHPMA₂₈- β -CD blocks to 8.9 nm is observed for the complex. In the case of azobenzene functionalized polymers no higher aggregates were observed for the homopolymers or complexes, which can be attributed to the higher polarity of the azobenzene moiety compared to the adamantyl group.

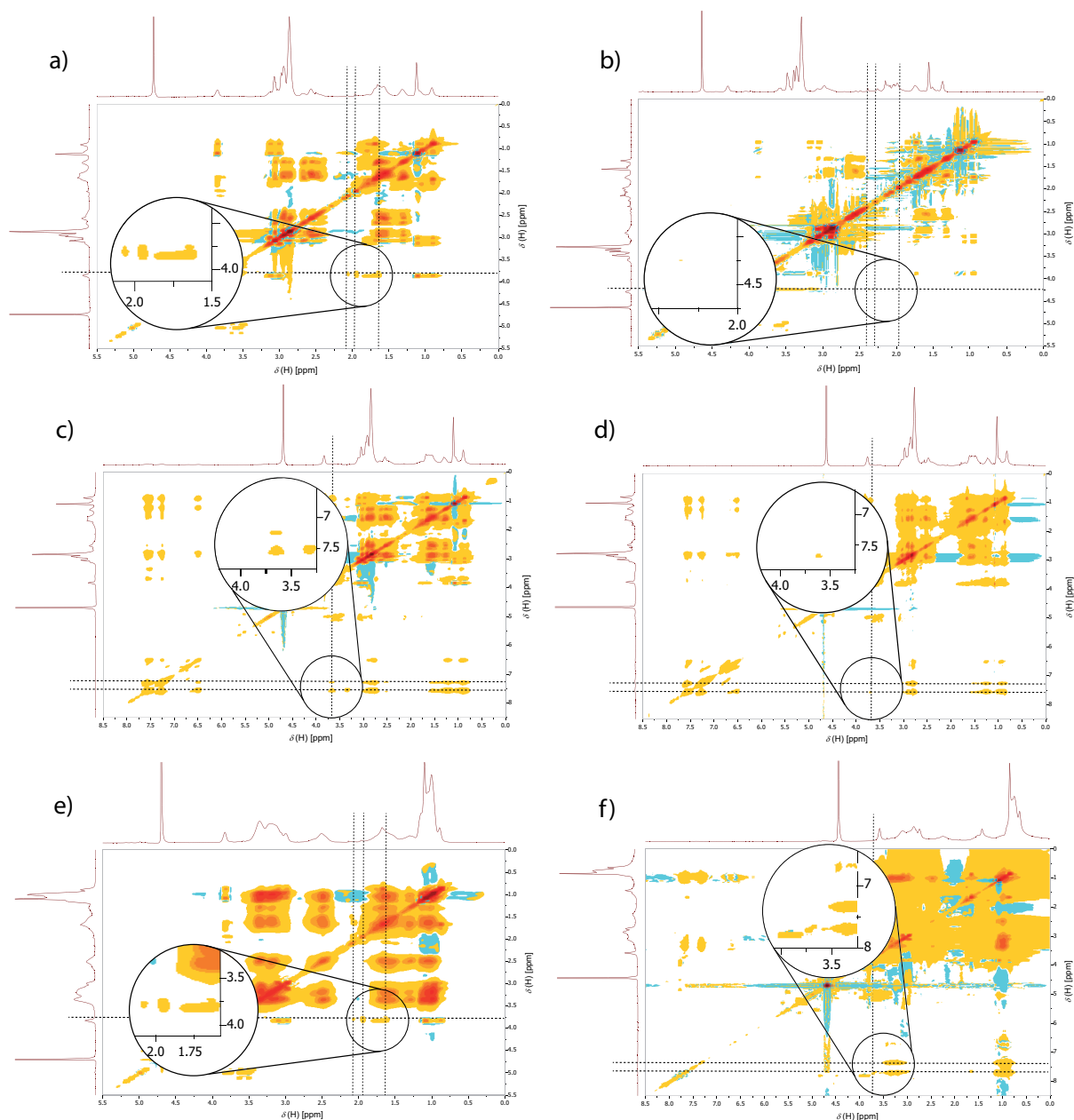


Figure 4.5: 2D NOESY spectra of the supramolecular triblock copolymers in D_2O : a) PDMAAm₁₅₁Ad₂-*b*-(PHPMA₂₆- β -CD)₂ at 25 °C; b) PDMAAm₁₅₁Ad₂-*b*-(PHPMA₂₆- β -CD)₂ at 70 °C; c) PDMAAm₁₀₃AzO₂-*b*-(PHPMA₂₆- β -CD)₂ at 25 °C; d) PDMAAm₁₀₃AzO₂-*b*-(PHPMA₂₆- β -CD)₂ after UV irradiation for 7 minutes at 25 °C; e) PDEAAm₇₈Ad₂-*b*-(PHPMA₂₈- β -CD)₂ at 25 °C and f) PDEAAm₈₀AzO₂-*b*-(PHPMA₂₈- β -CD)₂ at 25 °C.

To evidence the molecular nature of the complex formation NOESY was utilized, which is a well suited tool to study host/guest complex formation. The adamantyl-based systems PDMAAm₁₅₁Ad₂-*b*-(PHPMA₂₆- β -CD)₂ and PDEAAm₇₈Ad₂-*b*-(PHPMA₂₈- β -CD)₂ show cross correlation peaks that correspond to the signals of the adamantyl moiety at 1.7, 2.0 and 2.2 ppm and the inner protons of β -CD between 3.5 and 3.8 ppm (Figure 4.5 a and e). This proves the close spatial proximity of the adamantyl

moiety and the inner CD protons, which is the case for inclusion complexes. NOESY spectra of the azobenzene-based systems show weak cross correlation peaks originating from the azobenzene protons between 7.0 and 7.5 ppm and the inner CD protons (refer to Figure 4.5 c and f). The azobenzene-moiety shows weaker cross correlation peaks in comparison with adamantyl-systems which can be explained with the weaker complexation and the larger distance between the CD protons and the aromatic protons in the azobenzene. Nevertheless, the spectra are a strong hint for inclusion complex formation. In general, the observed cross correlation peaks are weaker in the case of PDEAAm containing samples as the concentration of the NMR samples was lower due to less solubility of the block copolymer in D₂O compared to the PDMAAm based copolymers. It should be noted that the described supramolecular ABA block copolymer is in equilibrium with the building blocks due to its non-covalent nature. Therefore, the existence of AB block copolymers and non-connected building blocks cannot be excluded. However, the formation of the desired structure is governed by the association constants that are rather high in the described systems. Thus, the ABA block copolymer should almost exclusively be present in solution.

4.2.3 Investigations of the Stimuli-Responsive Behavior

The prepared CD-based host/guest complexes show thermoresponsivity due to the usually negative enthalpy of complex formation (refer to Chapter 2.2.3).^{116,253} To evidence the thermoresponsivity of the host/guest supramolecular triblock copolymers guest-functionalized PDMAAm was synthesized that features no T_c . As shown in Figure 4.6, both the adamantyl- and azobenzene-based triblock copolymers show a significant decrease in D_h from 7.8 to 4.2 nm for an adamantyl-guest in the case of PDMAAm₁₅₁Ad₂-*b*-(PHPMA₂₆- β -CD)₂ and from 11.2 to 5.4 nm in the case of azobenzene in PDMAAm₁₀₃Azo₂-*b*-(PHPMA₂₆- β -CD)₂ upon heating to 70 °C. Furthermore, the complexes form again after remaining at ambient temperature which is proven by an increase in D_h close to the original values. In the case of lower molecular weight PDMAAm, the D_h increases with heating which is due to the formation of aggregates in solution as the complex dissociates (Figure 4.6 a and b). These aggregates could be formed due to the hydrophobic guest-groups that are unmasked which changes the solubility of the PDMAAm. In analogy to the higher molecular weight PDMAAm, the complexes re-form again after remaining at ambient temperature for 3 to 4 days and the D_h decreases. The rate of the re-formation of the complexes can be followed by DLS. It seems that azobenzene-based complexes form faster, which may be attributed to the increased polarity of azobenzene compared to adamantane, which enhances the accessibility of the guest moiety in aqueous solution. Moreover, the re-formation of the complexes is faster with a higher degree of polymerization of PDMAAm. An

explanation for the effect is the overall solubility of the polymer chain that changes drastically after the complex dissociation for lower molecular weight polymers and the earlier mentioned aggregates disturb the complex re-formation.

Furthermore, The temperature triggered dissociation of the supramolecular complexes could be observed *via* 2D NOESY at 70 °C (see Figure 4.5 b). In comparison with the sample at 25 °C, no relevant cross-correlation peaks are observable. It should be noted that due to the increased temperature the chemical shifts of the respective signals change.

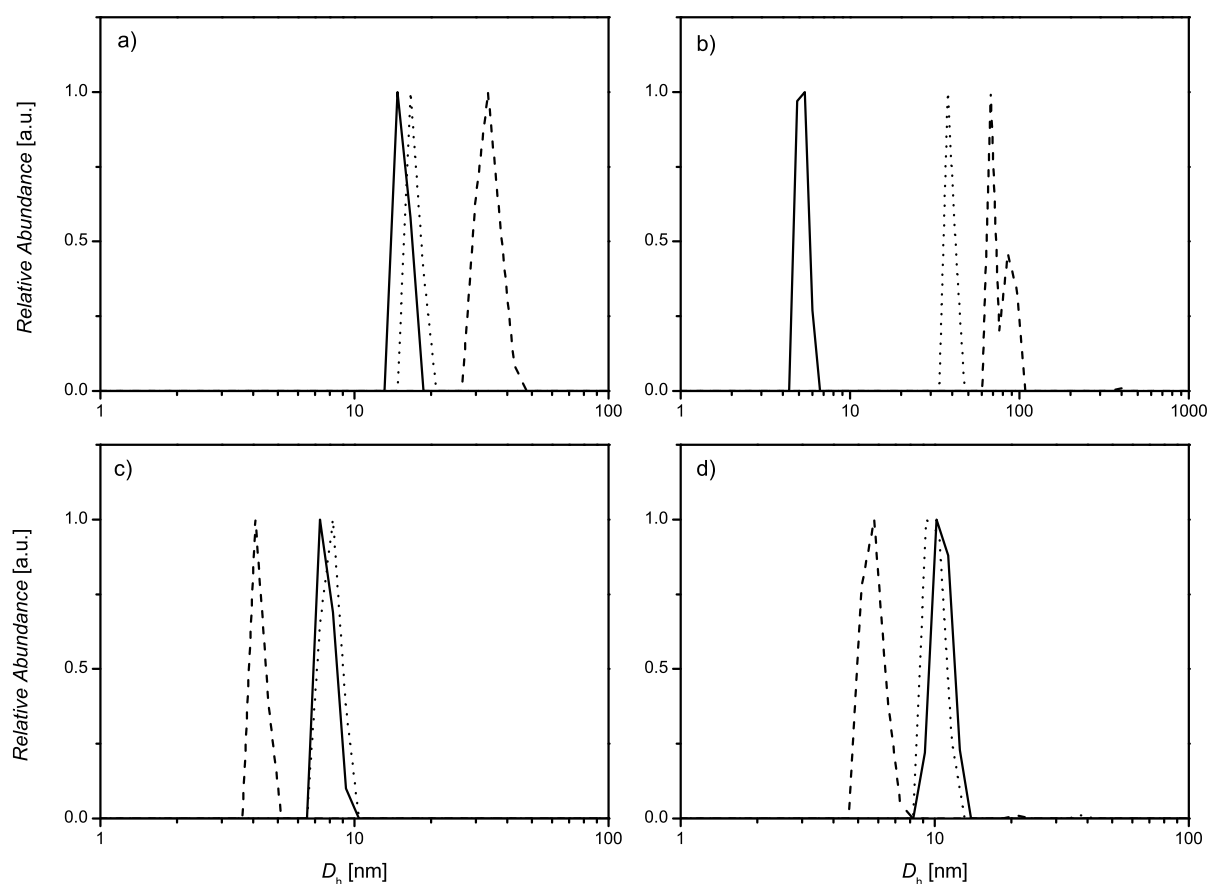


Figure 4.6: Number averaged particle size distributions obtained from DLS measurements before heating to 70 °C (solid line), at 70 °C (dashed line) and after keeping at ambient temperature for the specified time (dotted line): a) complex PDMAAm₅₇Ad₂-b-(PHPMA₄₄-β-CD)₂ before heating, at 70 °C and after 4 days; b) complex PDMAAm₄₆AzO₂-b-(PHPMA₂₆-β-CD)₂ before heating, at 70 °C and after 3 days; c) complex PDMAAm₁₅₁Ad₂-b-(PHPMA₂₆-β-CD)₂ before heating, at 70 °C and after 3 days; d) complex PDMAAm₁₀₃AzO₂-b-(PHPMA₂₆-β-CD)₂ before heating, at 70 °C and after 1 day.

In addition to the thermoresponsivity of the employed host/guest complexes, azobenzenes provide the opportunity to generate structures that are sensitive to light irradiation, as azobenzenes show a transition from the thermodynamically more sta-

ble *trans*- to the *cis*-conformation at wavelengths close to 360 nm. This photoisomerization is reversible and the reversion can be induced by heat or light with wavelengths close to 430 nm. Furthermore, the complexation constants are higher for the *trans*-conformation compared to the *cis*-conformation (460 M^{-1} for a *trans*-azobenzene test-compound and 2.5 M^{-1} for a *cis* azobenzene test-compound).¹⁵¹ In general, higher complexation constants (up to 10^4 M^{-1})¹⁴⁷ and differences between *cis* and *trans*-conformations could be achieved *via* the utilization of α -CD instead of β -CD. In here, azobenzene-based β -CD complexes were irradiated with UV light at 350 nm for 30 min and the change in D_h was monitored *via* DLS. A significant decrease was evident, *e.g.* from 8.9 to 4.8 nm after irradiation in the case of PDEAAm₈₀Azo₂-*b*-(PHPMA₂₈- β -CD)₂ (see Figure 4.7), evidencing that the block copolymers are debonded in a photoresponsive fashion. After keeping the samples at ambient temperature and daylight, the block copolymers formed again as proven by an increased D_h value, *e.g.* 8.2 nm compared to the original value of 8.9 nm in the case of PDEAAm₈₀Azo₂-*b*-(PHPMA₂₈- β -CD)₂ and 10.1 nm compared to 11.2 nm before in the case of PDMAAm₁₀₃Azo₂-*b*-(PHPMA₂₆- β -CD)₂. In almost all cases the D_h after standing in daylight is close to the initial value. As shown in Figure 4.6 and 4.7, the azobenzene-based PDMAAm block copolymers are double responsively bound as their supramolecular connection is sensitive to heat and light.

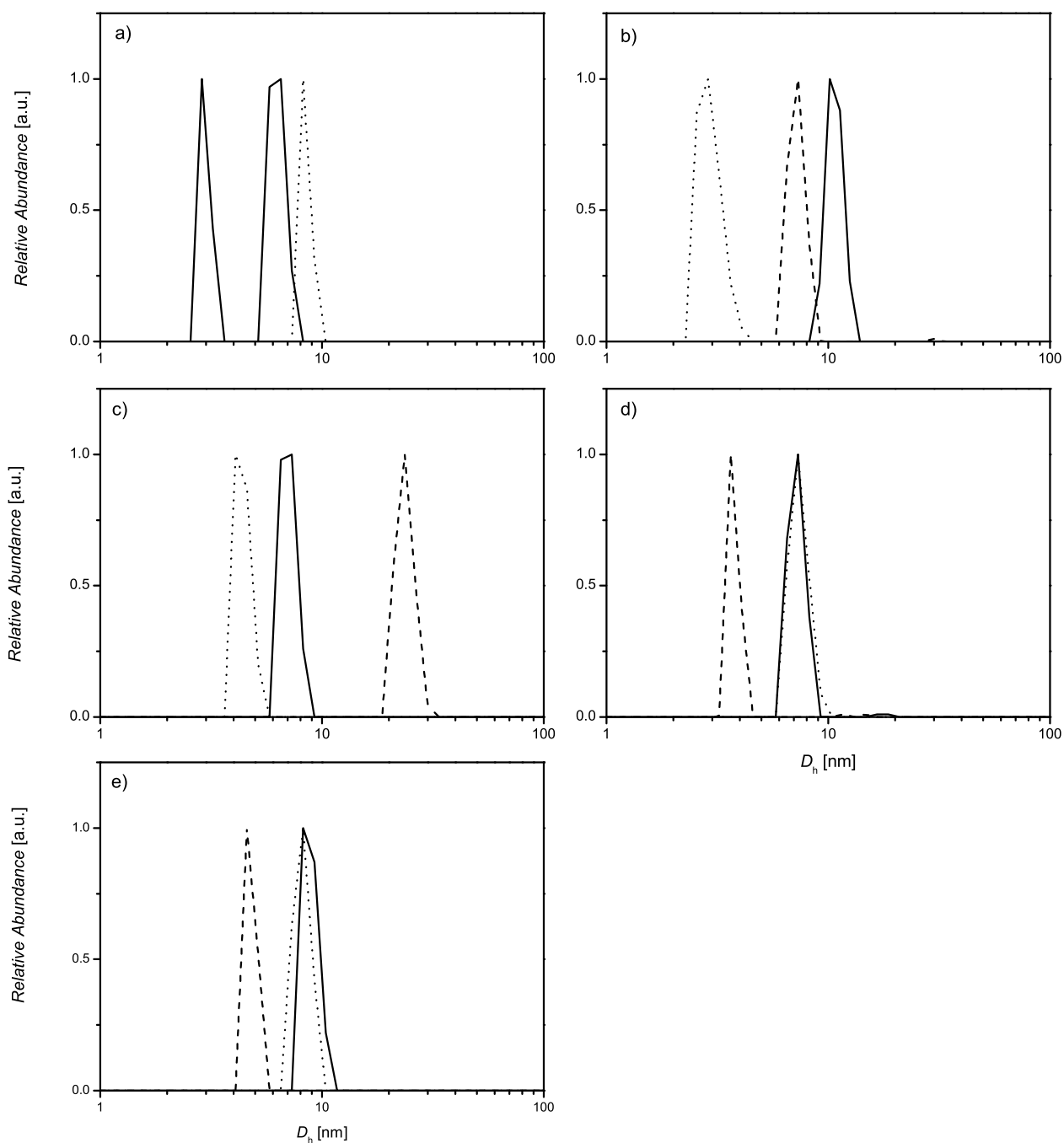


Figure 4.7: Number averaged particle size distributions obtained from DLS measurements before applying the stimulus (solid line), directly after UV irradiation at 350 nm for 30 min (dashed line) and in daylight for the specified time (dotted line): a) complex PDMAAm₄₆AzO₂-*b*-(PHPMA₂₆-β-CD)₂ before irradiation, directly after irradiation and after 3 days; b) complex PDMAAm₁₀₃AzO₂-*b*-(PHPMA₂₆-β-CD)₂ before irradiation, directly after irradiation and after 1 day; c) complex PDEAAm₃₆AzO₂-*b*-(PHPMA₂₈-β-CD)₂ before irradiation, directly after irradiation and after 3 days; d) complex PDEAAm₅₉AzO₂-*b*-(PHPMA₂₈-β-CD)₂ before irradiation, directly after irradiation and after 2 days; e) complex PDEAAm₈₀AzO₂-*b*-(PHPMA₂₈-β-CD)₂ before irradiation, directly after irradiation and after 2 days.

The light triggered complex dissociation could be observed furthermore *via* 2D NOESY (see Figure 4.5 d). The intensity of the corresponding cross correlation peaks decreases significantly after irradiation of UV light for 7 min. Nevertheless, the peaks do not vanish completely. This can be attributed to the fact that the complexes could re-form during the NOESY measurement with a measuring time of around 9 hours. Furthermore an equilibrium between *cis*- and *trans*-azobenzenes is formed where small amounts of *trans*-azobenzenes with higher association constant remain in the solution and the irradiation time is limited as RAFT polymers are sensitive to UV irradiation.

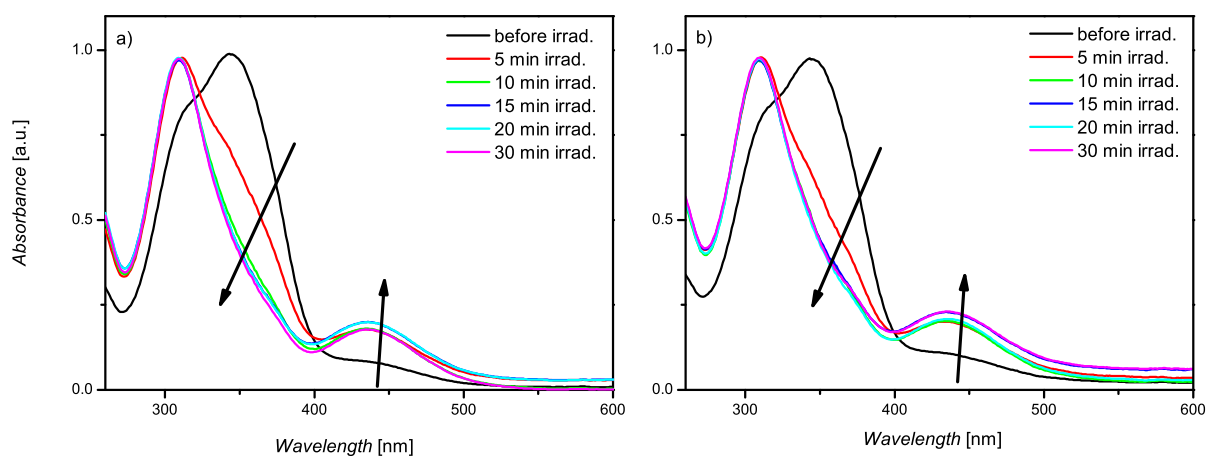


Figure 4.8: Overlay of the UV spectra before irradiation (black curve), after irradiation at 350 nm for 5 min (red curve) and after irradiation at 350 nm for longer than 5 min (other curves) at 10 °C: a) PDEAAm₅₉Azo₂; b) PDEAAm₅₉Azo₂-b-(PHPMA₂₈-β-CD)₂.

The formation of *cis*-azobenzenes can be monitored *via* UV spectroscopy as well. The UV spectra of all samples show a significant increase of the absorption at 440 nm after irradiation at 350 nm for 30 minutes (see Figure 4.8 and Appendix B.11 and B.12). Concomitantly, the absorption of *trans*-azobenzene moieties at 340 nm decreases drastically. As the absorption of *trans*-azobenzene is overlapping with the absorption of the trithiocarbonate, a quantitative statement with respect to the *trans*- and *cis*-azobenzene content in solution is difficult. Nevertheless, judging from the shape of the absorption band after irradiation, only minor amounts of *trans*-azobenzene remain.

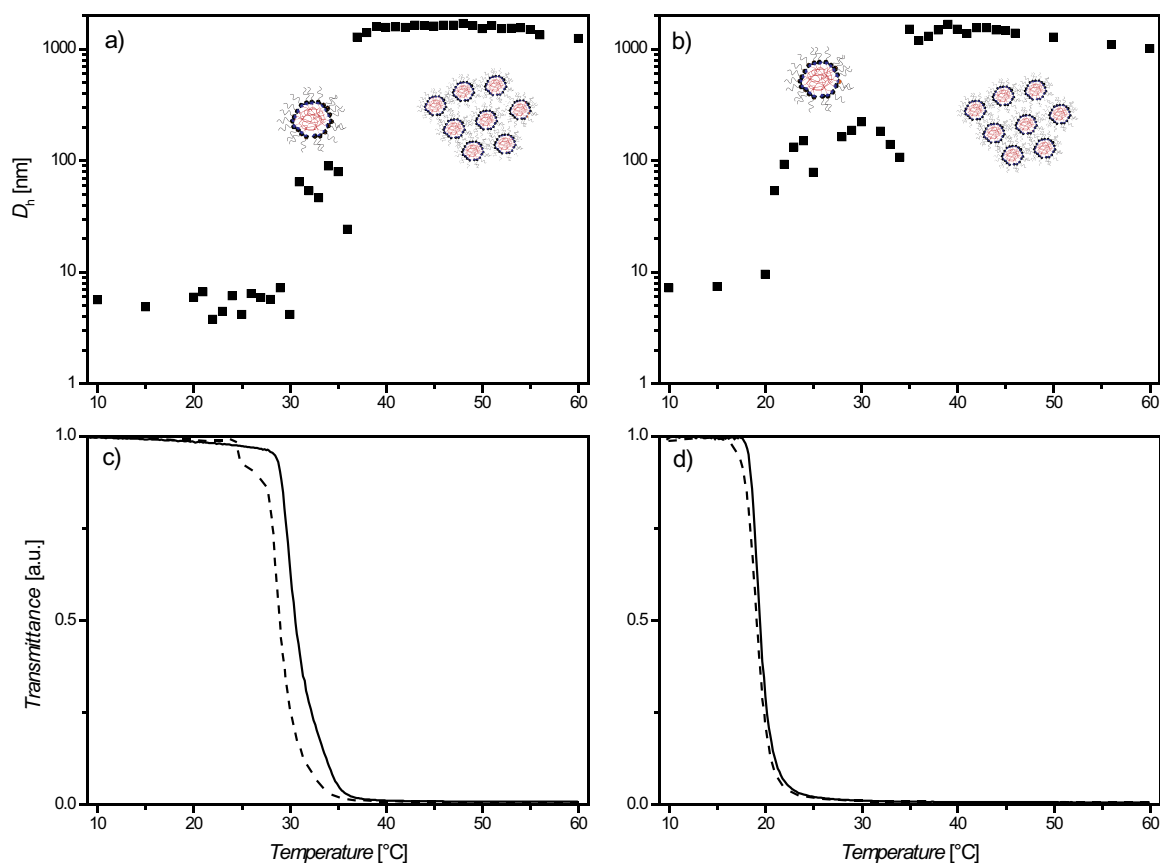


Figure 4.9: a) Temperature sequenced DLS measurement of PDEAAm₇₈Ad₂-*b*-(PHPMA₂₈-β-CD)₂ at a heating rate of 0.2 °C·min⁻¹ and a concentration of 1 mg·mL⁻¹; b) temperature sequenced DLS measurement of PDEAAm₅₉Azo₂-*b*-(PHPMA₂₈-β-CD)₂ at a heating rate of 0.2 °C·min⁻¹ and a concentration of 1 mg·mL⁻¹; c) turbidity measurements for PDEAAm₇₈Ad₂ (dashed line) and the supramolecular triblock copolymer PDEAAm₇₈Ad₂-*b*-(PHPMA₂₈-β-CD)₂ (solid line) at a cooling rate of 0.32 °C·min⁻¹ and a concentration of mg·mL⁻¹; d) turbidity measurements for PDEAAm₅₉Azo₂ (dashed line) and the supramolecular triblock copolymer PDEAAm₅₉Azo₂-*b*-(PHPMA₂₈-β-CD)₂ (solid line) at a cooling rate of 0.32 °C·min⁻¹ and a concentration of 1 mg·mL⁻¹.

The utilization of PDEAAm as the inner block provides the opportunity for temperature-induced aggregation.^{166,171,201} As shown in Figure 4.9, the block copolymers are present as random coils at lower temperatures, *e.g.* a D_h of around 7 nm for PDEAAm₇₈Ad₂-*b*-(PHPMA₂₈-β-CD)₂ up to 30 °C or a D_h around 8 nm for PDEAAm₅₉Azo₂-*b*-(PHPMA₂₈-β-CD)₂ up to 20 °C (Figure 4.9 a/b). The situation changes upon heating over the T_c where aggregates are formed. In the case of PDEAAm₇₈Ad₂-*b*-(PHPMA₂₈-β-CD)₂ aggregates with D_h between 24 and 90 nm are formed between 31 and 36 °C. A broader temperature range from 21 to 34 °C is covered with PDEAAm₅₉Azo₂-*b*-(PHPMA₂₈-β-CD)₂, where D_h between 54 and 222 nm are observed. With further heating these aggregates agglomerate, leading to particles with sizes over 1000 nm. The other examined block copolymers show similar behavior. In the first

stage, unimers were observed, whereas aggregates with D_h ranging from 37 to 210 nm were observed after heating above the T_c . The onset of the aggregate formation varies with different chain length of the middle block as well as the nature of the guest group. Agglomerate sizes ranging from $D_h = 1000 - 1700$ nm were found in the third stage of the temperature sequenced DLS measurements except of PDEAAm₃₆Azo₂-*b*-(PHPMA₂₈- β -CD)₂ where particles between 500 and 1000 nm are found (refer to Appendix Figure B.13). In general all samples show the described D_h profile with a change of the temperature. The behavior of these triblock copolymers resembles the behavior of literature known systems where a plateau as well as further agglomeration is described.^{166,201} One possible explanation for agglomeration at higher temperatures is the decreased complex stability, making a dynamic exchange of the building blocks possible. Thus, the stabilization effect of the PHPMA corona on the PDEAAm cores is decreasing and finally the aggregates begin to agglomerate. The DLS data are in agreement with the plots of turbidimetry, which is evident *via* the direct comparison in Figure 4.9 a/c and b/d.

Turbidity measurements show in almost all cases an increased T_c of the complexes compared to the uncomplexed PDEAAm blocks (refer to Figure 4.9 and Appendix B.14), which is an expected behavior of supramolecular block copolymers with a thermoresponsive block.^{166,201} A possible explanation for such a behavior is the shielding of the hydrophobic endgroups by the CD moiety. In the case of doubly adamantyl-functionalized polymers the difference in the T_{cs} lies between 4 and 2 °C whereas the difference with azobenzene-functionalized polymers is rather small and the T_{cs} are almost the same. A reason for the different behavior of the guest groups may be the enhanced polarity of the azobenzene moiety and the weaker association with β -CD. Furthermore an increase of the T_c with molecular weight is evident as well.

4.3 Conclusions

The synthesis of a novel macromolecular architecture based on CD host/guest chemistry, *i.e.* an ABA triblock copolymer was accomplished. A doubly guest-functionalized, namely adamantyl- and azobenzene-functionalized inner block was synthesized *via* RAFT polymerization of DMAAm and DEAAm. The host functionalized block was synthesized *via* RAFT polymerization of the monomer HPMA, affording the biocompatible PHPMA, and a CuAAc conjugation with β -CD-N₃. The individual blocks were characterized *via* SEC, ¹H-NMR and ESI-MS. Subsequently, the triblock copolymers were formed in aqueous solution and the complex formation was evidenced *via* DLS, 2D NOESY as well as turbidity measurements. Furthermore, the triblock copolymer formation was responsive to temperature and in the case of azobenzene-guests

to irradiation of light at 350 nm in a reversible fashion as disassembly after the stimuli and reassembly of the triblock copolymers was unambiguously evidenced. In the case of PDEAAm, the temperature induced aggregation was investigated after heating above the T_c of the PDEAAm block.

4.4 Experimental Part

Synthesis of 6-(adamantan-1-ylamino)-6-oxohexyl 2-(((3-((6-(-adamantan-1-ylamino)-6-oxohexyl)oxy)-3-oxopropyl)thio)carbonothioyl)thio)-2-methylpropanoate (5)

According to a literature procedure,²⁵⁴ **CEMP** (0.61 g, 2.26 mmol, 1.0 eq.), *N*-(adamantan-1-yl)-6-hydroxyhexanamide (**8**) (1.50 g, 5.65 mmol, 2.5 eq.) and triphenylphosphine (1.48 g, 5.65 mmol, 2.5 eq.) were dissolved in anhydrous THF (15 mL). At 0 °C DIAD (1.3 mL, 5.65 mmol, 2.5 eq.) in anhydrous THF (5 mL) was added dropwise. The reaction mixture was stirred at ambient temperature over night and subsequently for 3 h at 40 °C. After cooling to ambient temperature, DCM (50 mL) was added and the organic phase was washed twice with saturated NaHCO₃-solution (50 mL). The organic phase was dried over Na₂SO₄, filtered and the solvent evaporated *in vacuo*. The residue was subjected to column chromatography on silica-gel with *n*-hexane:ethyl acetate as eluent that was gradually changed from 1:1 to 1:2. The product was obtained as a yellow oil (0.88 g, 1.15 mmol, 51%).

¹H-NMR (400 MHz, CDCl₃): [δ , ppm] = 1.15 - 1.28 (m, 4H, 2x CH₂-CH₂-CH₂-C=O), 1.28 - 1.46 (m, 4H, 2x CH₂-CH₂-O), 1.48 - 1.75 (m, 28H, 4x (CH₃)₂-C, 2x CH₂-CH₂-C=O; 6x CH_{2,adamantyl}), 1.92 - 2.01 (m, 12H, 6x CH_{2,adamantyl}-C-NH), 2.04 - 2.10 (m, 10 H, 6x CH_{adamantyl}; 2x CH₂-C=O), 2.70 (t, ³J = 6.9 Hz, CH₂-CH₂-S), 3.52 (t, 2H, ³J = 6.9 Hz, CH₂-S), 4.08 (q, 4H, ³J = 6.4 Hz, CH₂-O-C=O), 5.19 (m, 2H, NH). ¹³C-NMR (100 MHz, CDCl₃): [δ , ppm] = 25.5, 25.7 and 25.8 (2x CH₂-CH₂-CH₂-C=O; 2x CH₂-CH₂-C=O, 2x (CH₃)₂-C), 28.3 and 28.5 (2x CH₂-CH₂-O-C=O), 29.6 (6x CH_{adamantyl}), 31.4 (CH₂-CH₂-S), 33.2 (CH₂-S), 36.5 (6x CH_{2,adamantyl}), 37.7 (2x CH₂-C=O), 41.9 (6x CH_{2,adamantyl}-C-NH), 51.9 (2x C-NH), 56.4 (2x C(CH₃)₂), 65.0 and 66.1 (2x CH₂-O-C=O), 171.5, 172.0, 172.1 and 172.9 (4x C=O), 220.9 (C=S). **ESI-MS**: [M + Na⁺]_{exp} = 785.58 m/z and [M + Na⁺]_{calc} = 785.37 m/z.

Synthesis of bis(6-(4-(phenyldiazenyl)phenoxy)hexyl) 2,2'-(thiocarbonylbis(sulfane-diyl))bis(2-methylpropanoate) (6)

Based on a literature procedure,²⁵⁴ **CMP** (1.00 g, 3.54 mmol, 1.0 eq.), 6-(4-(phenyldiazenyl)phenoxy)hexan-1-ol (**9**) (3.38 g, 11.33 mmol, 3.2 eq.) and triphenylphosphine (2.97 g, 11.32 mmol, 3.2 eq.) were dissolved in anhydrous THF (20 mL). At 0 °C DIAD (2.2 mL, 11.21 mmol, 3.2 eq.) in anhydrous THF (20 mL) was added dropwise. The reaction mixture was stirred at ambient temperature over night and subsequently for 3 h at 40 °C. After cooling to ambient temperature, DCM (100 mL) was added and the organic phase was washed twice with saturated NaHCO₃-solution (100 mL). The organic phase was dried over Na₂SO₄, filtered and the solvent evaporated *in vacuo*. The residue was subjected to column chromatography on silica-gel with *n*-hexane:ethyl acetate as eluent that was gradually changed from 10:1 to 8:1. The product was obtained as an orange oil which solidified on cooling (2.77 g, 3.30 mmol, 93%).

¹H-NMR (400 MHz, CDCl₃): [δ, ppm] = 1.37 - 1.57 (m, 4H, 2x CH₂-CH₂-CH₂-O), 1.58 - 1.72 (m, 16H, 4x C-CH₃; 2x O=C-O-CH₂-CH₂), 1.77 - 1.87 (m, 4H, 2x O-CH₂-CH₂), 4.03 (t, 4H, ³J = 6.5 Hz, 2x CH₂-O), 4.09 (t, 4H, ³J = 6.5 Hz, 2x CH₂-O-C=O), 7.00 (d, 4H, ³J = 9.0 Hz, 4x CH_{arom}), 7.40 - 7.46 (m, 2H, 2x CH_{arom}), 7.47 - 7.56 (m, 4H, 4x CH_{arom}), 7.82 - 7.97 (m, 8H, 8x CH_{arom}). ¹³C-NMR (100 MHz, CDCl₃): [δ, ppm] = 25.3 (4x CH₃-C), 25.8 and 25.9 (4x CH₂-CH₂-CH₂-O), 28.4 (2x O-CH₂-CH₂), 29.2 (2x O=C-O-CH₂-CH₂), 56.3 (2x C(CH₃)₂), 66.1 (2x O=C-O-CH₂), 68.3 (2x O-CH₂), 114.8 (2x O-C_{arom}-CH_{arom}), 122.7 (2x CH_{arom}), 124.9 (4x CH_{arom}), 129.2 (4x CH_{arom}), 130.4 (2x CH_{arom}), 147.0 (2x C_{arom}-N=N), 152.9 (2x C_{arom}-N=N), 161.8 (2x O-C_{arom}), 172.9 (2x C=O), 218.6 (C=S). ESI-MS: [M + H⁺]_{exp} = 843.33 m/z and [M + H⁺]_{calc} = 843.33 m/z.

Synthesis of prop-2-yn-1-yl 4-cyano-4-(((ethylthio)carbonothioyl)thio)pentanoate (7)

In a 100 mL Schlenk-flask, **CEP** (1.00 g, 3.80 mmol, 1.0 eq.), propargylalcohol (0.5 mL, 8.65 mmol, 2.3 eq.) and DMAP (0.09 g, 0.77 mmol, 0.2 eq.) were dissolved in anhydrous DCM (20 mL). At 0 °C a solution of DCC (1.57 g, 7.61 mmol, 2.0 eq.) in anhydrous DCM (10 mL) was added. After one hour the solution was warmed to ambient temperature, stirred overnight, filtered and concentrated under reduced pressure. The residue was purified *via* column chromatography on silica-gel with *n*-hexane:ethyl acetate 10:1 as eluent. The product was obtained as a yellow oil (0.94 g, 3.13 mmol, 82%). ¹H-NMR (400 MHz, CDCl₃): [δ, ppm] = 1.35 (t, 3H, ³J = 7.4 Hz, CH₂-CH₃), 1.87 (s, 3H, C-CH₃), 2.27 - 2.59 (m, 3H, CH, CH₂-COO), 2.62 - 2.76 (m, 2H, C-CH₂), 3.34 (q, 2H, ³J = 7.4 Hz, CH₃-CH₂), 4.71 (d, 2H, ⁴J = 2.5 Hz, CH₂-C-CH). ¹³C-NMR (100 MHz, CDCl₃): [δ, ppm] = 12.9 (CH₃), 25.0 (C-CH₃), 29.7 (CH₂-COO), 31.5 (C-CH₂), 33.8

(CH₃-CH₂), 46.4 (C-CH₂), 52.6 (CH₂-C-CH), 75.4 (CH₂-C-CH), 77.4 (CH₂-C-CH), 119.0 (C-N), 170.8 (C=O), 216.8 (C=S). **ESI-MS:** [M + Na⁺]_{exp} = 324.08 m/z and [M + Na⁺]_{calc} = 324.02 m/z.

Exemplary Procedure for the RAFT Polymerization of DEAAm

5 (54.9 mg, 0.07 mmol, 1.0 eq.), DEAAm (500.0 mg, 3.94 mmol, 56.3 eq.), AIBN (4.2 mg, 0.03 mmol, 0.4 eq.), DMF (3.3 mL) and a stirring-bar were added into a Schlenk-tube. After three freeze-pump-thaw cycles the tube was backfilled with argon, sealed, placed into an oil bath at 60 °C and removed after 24 h. The tube was subsequently cooled with liquid nitrogen to stop the reaction. An NMR-sample was withdrawn for the determination of conversion, inhibited with a pinch of hydroquinone (approx. 5 mg) and CDCl₃ was added. Quantitative conversion was estimated based on the NMR data (see Section 9.3 for details of the calculation). The residue was dialyzed against deionized water with a SpectraPor3 membrane (MWCO = 1000 Da) for 3 days at ambient temperature. The solvent was removed *in vacuo* to yield the polymer as a yellow solid (422.0 mg, 76%, **SEC(THF):** $M_{nSEC} = 6500 \text{ g}\cdot\text{mol}^{-1}$, $D_m = 1.11$).

Exemplary Procedure for the RAFT Polymerization of HPMA

7 (60.5 mg, 0.20 mmol, 1.0 eq.), HPMA (2.00 g, 14.18 mmol, 35.5 eq.), V-501 (11.6 mg, 0.04 mmol, 0.2 eq.), DMF (6.0 mL), acetic acid/sodium acetate buffer (pH 5.2, 0.27 M acetic acid and 0.73 M sodium acetate; 6.0 mL) and a stirring-bar were added into a Schlenk-tube. After three freeze-pump-thaw cycles the tube was backfilled with argon, sealed, placed into an oil bath at 70 °C and removed after 2 h. The tube was subsequently cooled with liquid nitrogen to stop the reaction. A NMR-sample was withdrawn for the determination of conversion, inhibited with a pinch of hydroquinone (approx. 5 mg) and D₂O was added. A conversion of 23% was estimated based on the NMR data (see Section 9.3 for details of the calculation). The residue was dialyzed against deionized water with a SpectraPor3 membrane (MWCO = 1000 Da) for 3 days at ambient temperature. The solvent was removed *in vacuo* to yield the polymer as a yellow solid (0.37 g, 80%, **SEC(DMAc):** $M_{nSEC} = 6500 \text{ g}\cdot\text{mol}^{-1}$, $D_m = 1.17$).

Exemplary Click-Reaction of Alkyne-Functionalized PHPMA with β -CD-N₃

Alkyne-functionalized PHPMA ($M_{nSEC} = 6500 \text{ g}\cdot\text{mol}^{-1}$; 150.0 mg, 0.023 mmol, 1.0 eq.), β -CD-N₃ (133.8 mg, 0.115 mmol 5.0 eq.), PMDETA (34 μl , 0.163 mmol, 7.1 eq.), DMF (5.3 mL) and a stirring-bar were introduced into a Schlenk-tube. After three freeze-pump-thaw cycles the tube was filled with argon and CuBr (19.8 mg, 0.138 mmol, 6.0 eq.) was added under a stream of argon. Subsequently, two freeze-pump-thaw cycles were performed, the tube was backfilled with argon and the mixture stirred at ambient temperature for 24 h. EDTA-solution (5 wt.%, 1 mL) was added and the residue was dialyzed against deionized water with a SpectraPor3 membrane (MWCO = 2000 Da) for 3 days at ambient temperature. The solvent was removed *in vacuo* to yield the CD-functionalized polymer as a yellow solid (96.0 mg, 55%, SEC(DMAc): $M_{nSEC} = 7300 \text{ g}\cdot\text{mol}^{-1}$, $D_m = 1.29$).

Exemplary Supramolecular ABA Block Copolymer-Formation *via* CD/Guest Interaction

CD-functionalized PHPMA ($M_{nSEC} = 7300 \text{ g}\cdot\text{mol}^{-1}$; 70.0 mg, 0.0096 mmol, 2.0 eq.) was dissolved in DMF (4 mL) and added dropwise to a solution of doubly adamantyl-functionalized PDMAAm ($M_{nSEC} = 6400 \text{ g}\cdot\text{mol}^{-1}$; 30.0 mg, 0.0047 mmol, 1.0 eq.) in DMF (2 mL) under vigorous stirring. The resulting solution was dialysed against a deionized water/DMF-mixture with a SpectraPor3 (MWCO = 1000 Da) membrane at 4 °C. The water-content was gradually changed from 70% to 100% over 1 day and the dialysis was continued for 3 days with deionized water at 4 °C. The solvent was removed *in vacuo* to yield the supramolecular complex in quantitative yield.

Supramolecular Three Armed Star Polymers

5.1 Introduction

Star polymers are an important class of polymers that have attracted significant attention in the last years.^{255–257} This can be attributed to unique properties originating from their condensed structure, non-linear shape, and multiple chain ends per macromolecule. Many applications for such systems have been discussed in the literature, *e.g.* as unimolecular nanocontainers,²⁵⁸ for drug-delivery²⁵⁹ or in organic light-emitting diodes.²⁶⁰

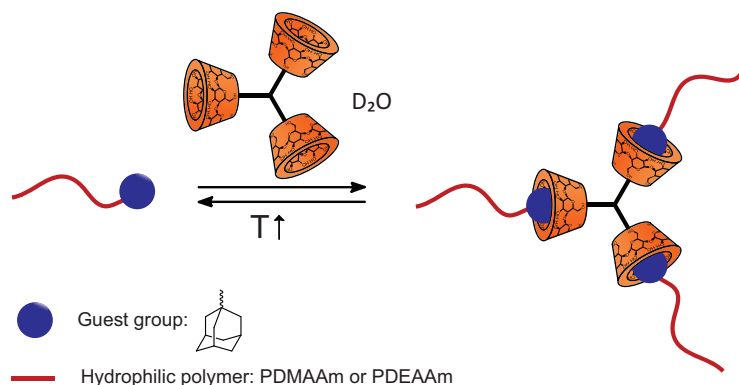
Traditionally, the synthesis of star polymers has been carried out *via* living polymerization techniques, *i.e.* anionic²⁵⁷ or cationic^{261,262} methodologies. According to these synthetic strategies, one can distinguish between multifunctional initiators, *i.e.* the core-first approach,²⁶³ or multifunctional termination agents, *i.e.* the arm-first approach.²⁶⁴ Especially the introduction of controlled radical polymerization techniques, *i.e.* NMP,⁹ ATRP,⁴² and RAFT polymerization,^{13,45} have led to the generation of a broad range of star polymers in core-first approaches *via* multifunctional initiators or CTAs.^{265–267} As an alternative, modular conjugation reactions can be employed for the synthesis of such architectures, *e.g.* *via* click chemistry^{256,268} in an arm-first approach. Several methods have been employed in that regard benefiting from high efficiency, short reaction times, and possible equimolarity of the reactions that fulfil the respective criteria.¹⁷ Some examples include the copper-catalyzed azide-alkyne cy-

DLS measurements were performed in collaboration with T. Rudolph and Prof. F. H. Schacher (Friedrich Schiller Universität Jena). ROESY measurements were performed in collaboration with M. Hetzer and Prof. H. Ritter (Heinrich Heine Universität Düsseldorf). Parts of this chapter were reproduced from Schmidt, B. V. K. J.; Rudolph, T.; Hetzer, M.; Ritter, H.; Schacher, F. H.; Barner-Kowollik, C. *Polym. Chem.* **2012**, 3, 3139–3154 (DOI: 10.1039/C2PY20293J) with permission from the Royal Society of Chemistry.

claddition (CuAAC),^{192,269} the thiol-ene reaction,²⁷⁰ or the RAFT hetero Diels–Alder reaction.²⁷¹ As these strategies represent orthogonal approaches, they are nowadays also widely employed for the synthesis of miktoarm star polymers.^{256,268,272}

New opportunities arise from the synthesis of supramolecular star polymers. Here, the formation of the star polymer is driven by supramolecular interactions that offer reversible and potentially stimuli-responsive bond-formation amongst other properties. The mainly utilized types of supramolecular interactions comprise hydrogen-bonding,^{273–275} metal-ligand-coordination^{276–278} or host/guest complexation.²⁷⁹ An important class of hosts in the realm of host/guest complexations are CDs due to their availability and the ease of chemical modification. Considering star polymer synthesis the ability of CDs to form inclusion complexes with hydrophobic guest molecules enables the formation of new materials. Apart from the formation of new macromolecular architectures, this ability is widely used in polymer chemistry, *e.g.* for drug- or siRNA-delivery,^{32,280,281} or to solubilize hydrophobic monomers.^{224,227,229} In the case of star polymers CD has been mainly used as a core molecule in the past, *e.g.* in ATRP,¹⁸⁶ RAFT,¹⁸⁸ or in a combination of ATRP and NMP.¹⁹⁶ Here, however, the arms were covalently attached to the CD core. In an alternative example CD-centered star polymers were reported, where two cores are bound employing supramolecular interactions.^{200,201}

In Chapter 5 the formation of supramolecular three-armed star polymers using CD host/guest interactions is presented. The materials consist of adamantyl-functionalized polyacrylamides as arms and a threefold β -CD-functionalized core molecule (refer to Scheme 5.1). An adamantyl-functionalized CTA was utilized in the RAFT polymerization of DMAAm and DEAAm for the synthesis of the arms, which were subsequently characterized *via* ESI-MS, NMR and SEC. In aqueous solution, supramolecular complexes were formed and the existence of three-armed star polymers was proven *via* ROESY as well as DLS.

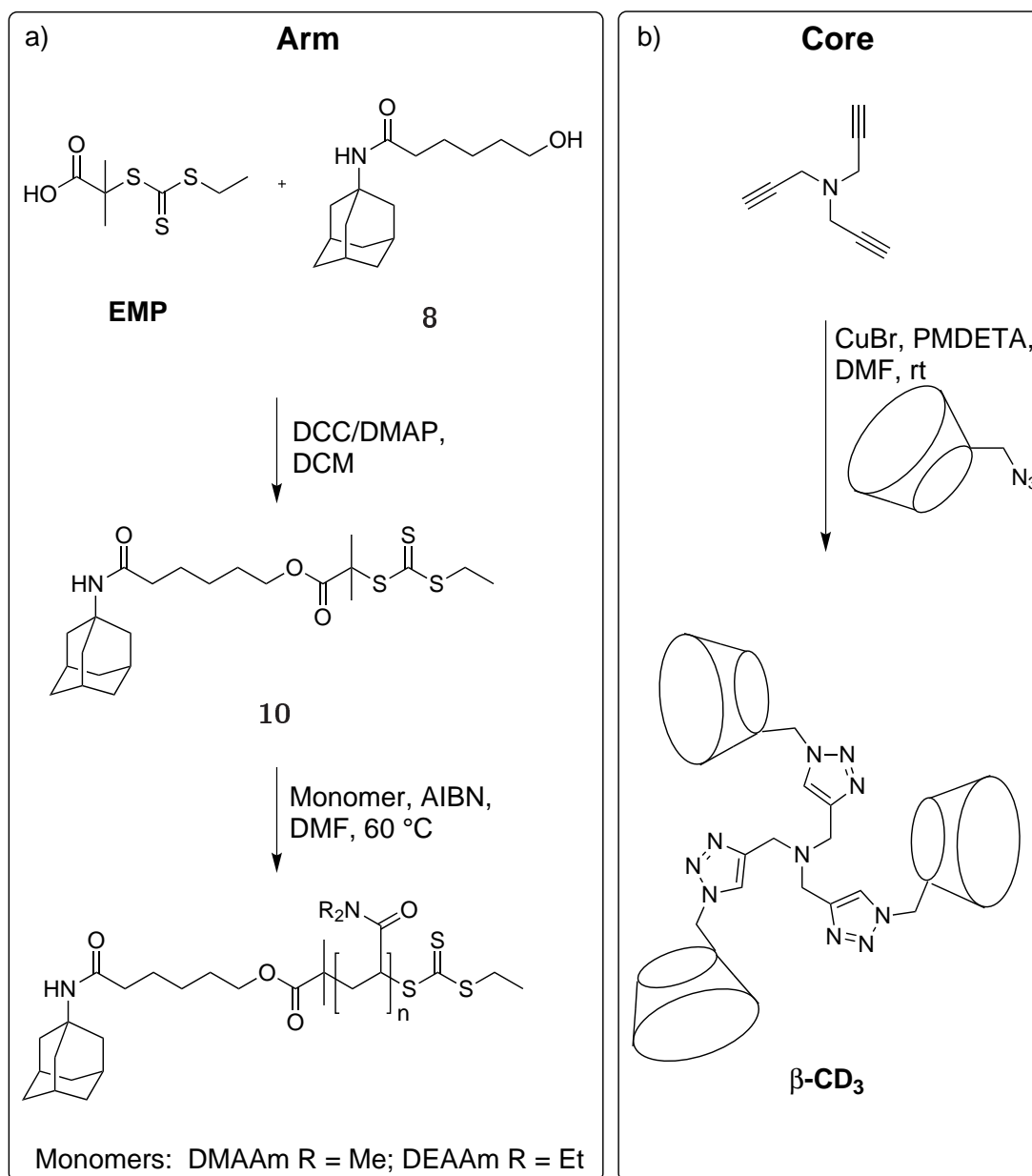


Scheme 5.1: Schematic representation of supramolecular star polymer formation *via* host/guest inclusion complexes between adamantyl-functionalized polyacrylamides (polymer: red; adamantyl-group: blue) and a three-pronged β -CD linker (orange).

5.2 Results and Discussion

5.2.1 Synthesis and Characterization of the Building Blocks

For the formation of supramolecular star polymers two types of building blocks were synthesized (Scheme 5.2): adamantyl end-functionalized polymers as arms (guest) and a three-pronged β -CD-functionalized core as the host.



Scheme 5.2: Synthesis of the building blocks utilized for star polymer formation: a) adamantyl-functionalized RAFT-agent (**10**), followed by the synthesis of polyacrylamides; b) synthesis of the three-pronged β -CD core (β -CD₃).

The adamantyl-functionalized polymers were synthesized *via* RAFT-polymerization using a trithiocarbonate-containing CTA **10**. The prominent adamantyl moiety was chosen as guest-group due to its high complexation constants with β -CD of up to 10^5 M^{-1} .²³⁷ The CTA was synthesized starting from an adamantyl-containing alcohol *via* DCC-coupling with **EMP** as shown in Scheme 5.2 a. The adamantyl moiety was separated from the trithiocarbonate group with a C₅-spacer to improve its accessibility for the inclusion process. Subsequently, RAFT polymerizations were conducted with DMAAm and DEAAm utilizing several CTA/monomer ratios. Polymer-

ization degrees ranging from 31 to 202 with M_n ranging from 3500 to 20500 $\text{g}\cdot\text{mol}^{-1}$ and low $D_m < 1.25$ were achieved for PDMAAm. Furthermore, the thermoresponsive adamantyl-functionalized PDEAAm was prepared *via* RAFT polymerization with **10** affording a polymerization degree of 87 with a M_n of 11500 $\text{g}\cdot\text{mol}^{-1}$ and a low D_m (see Table 5.1).

Table 5.1: Results for the RAFT polymerization of DMAAm (top) and DEAAm (bottom) with **10** at 60 °C in DMF with AIBn as initiator.

DMAAm/ 10 /I	Time / h	Conv.	$M_{n\text{theo}} / \text{g}\cdot\text{mol}^{-1}$	$M_{n\text{SEC}} / \text{g}\cdot\text{mol}^{-1}$	D_m	D_p
21/1/0.1	24	quant.	2550	3500	1.08	31
100/1/0.2	24	quant.	10370	14600	1.12	143
241/1/0.2	24	96%	23400	20500	1.23	202

DEAAm/ 10 /I	Time / h	Conv.	$M_{n\text{theo}} / \text{g}\cdot\text{mol}^{-1}$	$M_{n\text{SEC}} / \text{g}\cdot\text{mol}^{-1}$	D_m	D_p
101/1/0.2	24	quant.	13300	11500	1.11	87

The RAFT polymerization of DMAAm and DEAAm with **10** yielded unimodal molecular mass distributions (Figure 5.1). For higher molecular masses a certain tailing to higher elution volumes was observed, presumably due to interactions with the column during SEC. The structure of the obtained polymers was verified *via* $^1\text{H-NMR}$ and ESI-MS (refer to the Appendix Figures C.1-C.4).

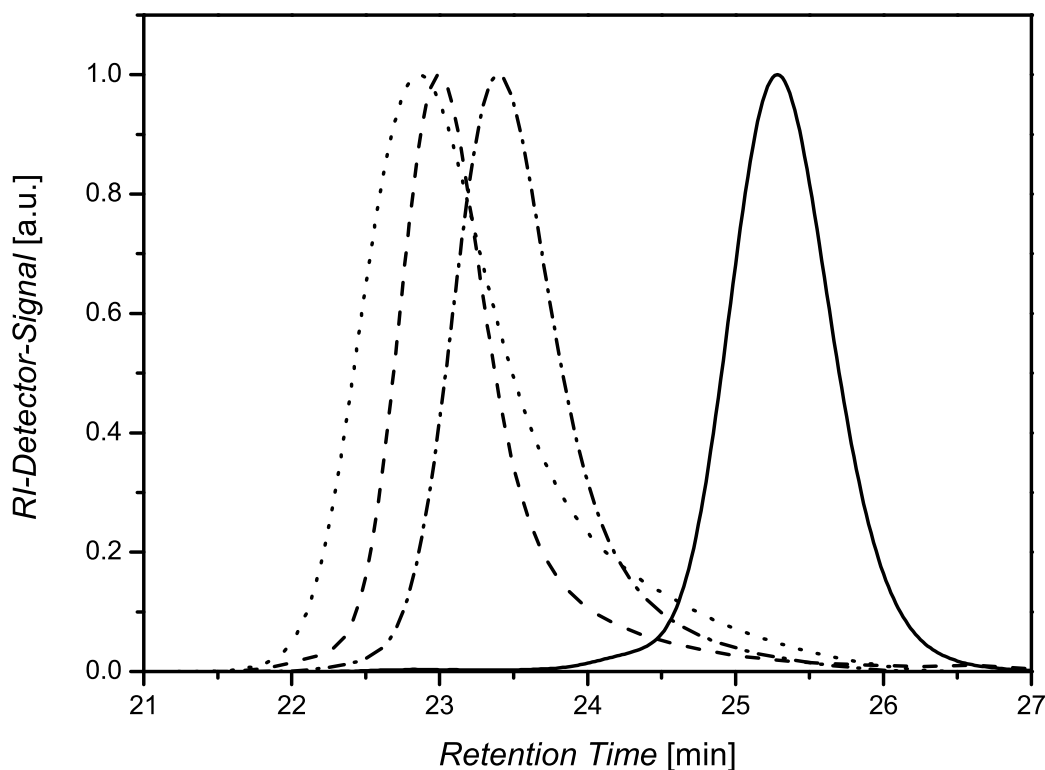


Figure 5.1: SEC-traces for PDMAAm₃₁-Ad (solid black line), PDMAAm₁₄₃-Ad (dashed black line), PDMAAm₂₀₂-Ad (dotted black line), and PDEAAm₈₇-Ad (solid dashed-dotted line).

The three-pronged CD-functional building block β -CD₃ was synthesized *via* CuAAC starting from tripropargylamine and β -CD-N₃ (Scheme 5.2 b).²⁸² The product was analyzed *via* ¹H-NMR and ESI-MS (Appendix C.5/C.6).

5.2.2 Star Polymer Formation: Investigations using Light Scattering

Light scattering experiments are a powerful method for the *in situ* investigation of polymeric systems in solution. Before mixing the arms and the core moiety, all individual compounds were analyzed *via* DLS at ambient temperature in H₂O and D₂O. Surprisingly, all polyacrylamide-compounds seemed to be better soluble in D₂O, resulting in an increase of $\sim 20\%$ of the hydrodynamic radius (R_h) (Figure 5.2), while for β -CD₃ no difference was observed. Such an effect has also been observed for PNI-PAAm,^{283–285} although the reason was not fully understood. The increased hydrodynamic volumes of the polymer chains should, however, lead to a better accessibility of the adamantyl moiety for the inclusion process with the β -CD₃ core. Therefore, all following experiments were performed in D₂O at a polymer concentration of 5 mg·mL⁻¹. In addition, control experiments in H₂O were carried out (Figure 5.3 a).

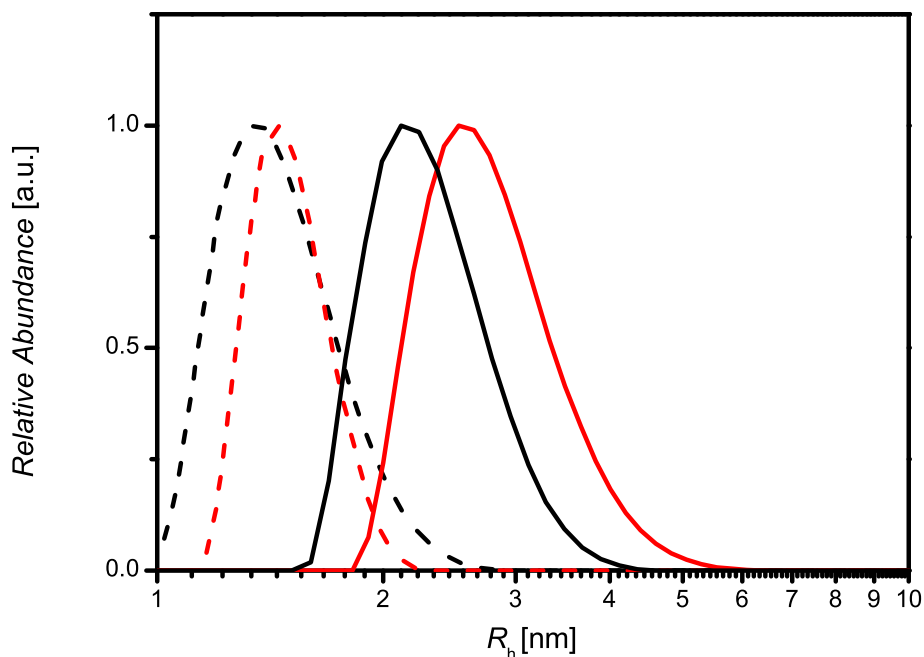
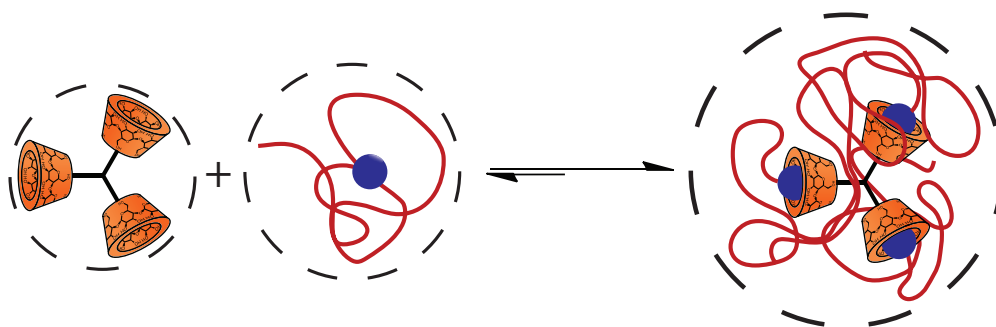


Figure 5.2: Comparison of the number averaged hydrodynamic radii for the core β -CD₃ (dashed line) and PDMAAm₁₄₃-Ad (solid line) in different solvents: H₂O (black line) and D₂O (red line) at 25 °C.

Table 5.2: DLS results (number averaged hydrodynamic radii) for the individual building blocks, the supramolecular star polymers after self-assembly, and the respective expansion ratio at 25 °C in D₂O.

Polymer	$R_{h,crude\ polymer} / nm$	$R_{h,polymer@-\beta-CD_3} / nm$	expansion ratio
β -CD ₃	1.3	-	-
PDMAAm ₃₁ -Ad	1.8	2.3	1.3
PDMAAm ₁₄₃ -Ad	2.5	3.7	1.5
PDMAAm ₂₀₂ -Ad	3.3	4.6	1.4
PDEAAm ₈₇ -Ad	2.4	3.8	1.6



Scheme 5.3: Schematic representation of the formation of supramolecular star polymers, indicating the expected changes in hydrodynamic radius (R_h dashed circles).

Adamantyl-functionalized PDMAAm with three different molar masses were combined in stoichiometric amounts (3:1) with the β -CD₃ core, dissolved in D₂O, stirred and analyzed using DLS after 12 and 24 hours (also after several days, Figure 5.5), showing a clear shift to higher hydrodynamic radii with time. For PDMAAm₃₁ ($M_{nSEC} = 3500 \text{ g}\cdot\text{mol}^{-1}$) an apparent hydrodynamic radius $R_h = 1.8 \text{ nm}$ was observed, while the β -CD₃ exhibits a radius of $R_h = 1.3 \text{ nm}$. After 12 hours at ambient temperature, an increase in size to $R_h = 2.3 \text{ nm}$ was found, which remained constant over several days. This corresponds to an expansion ratio of 1.3. The same procedure was utilized for PDMAAm₁₄₃ and PDMAAm₂₀₂ and a R_h of 2.5 and 3.3 nm for the unimolecular polymer chains was observed, respectively. After stoichiometric mixing in a molar ratio of 3:1 with the CD-core moiety, a distinct increase in size can be observed in both cases. For PDMAAm₁₄₃, supramolecular star polymers with $R_h = 3.7 \text{ nm}$ were observed whereas in case of PDMAAm₂₀₂ the aggregate size was even larger, with $R_h = 4.6 \text{ nm}$, owing to longer polyacrylamide arms. An expansion ratio of 1.5 and 1.4 (Table 5.2) was deduced. In all cases, monomodal number-weighted size distributions were observed, indicating full inclusion of the guest-polymer chains into the CD core (Figure 5.4). The proposed structure formation mechanism is depicted in Scheme 5.3, which also illustrates the rather small observed expansion ratios. As the arms of the formed supramolecular star polymers form coils in solution in three dimensions, the observed R_h of the star polymers is smaller than the sum of the individual parts. For all investigated combinations of the arms with the core, an increase of the hydrodynamic radius was observed, hinting at the formation of star-shaped aggregates. The expansion ratio (Table 5.2) yields comparable values for all polymers investigated. Adamantyl-functionalized polymers with higher a molecular mass leads to higher hydrodynamic radii. Furthermore, the size distributions of the adamantyl-functionalized polymers were measured after the addition of crude β -CD (refer to Figure 5.3 b) to prove that the increase in R_h is due to the three-pronged nature of β -CD₃.

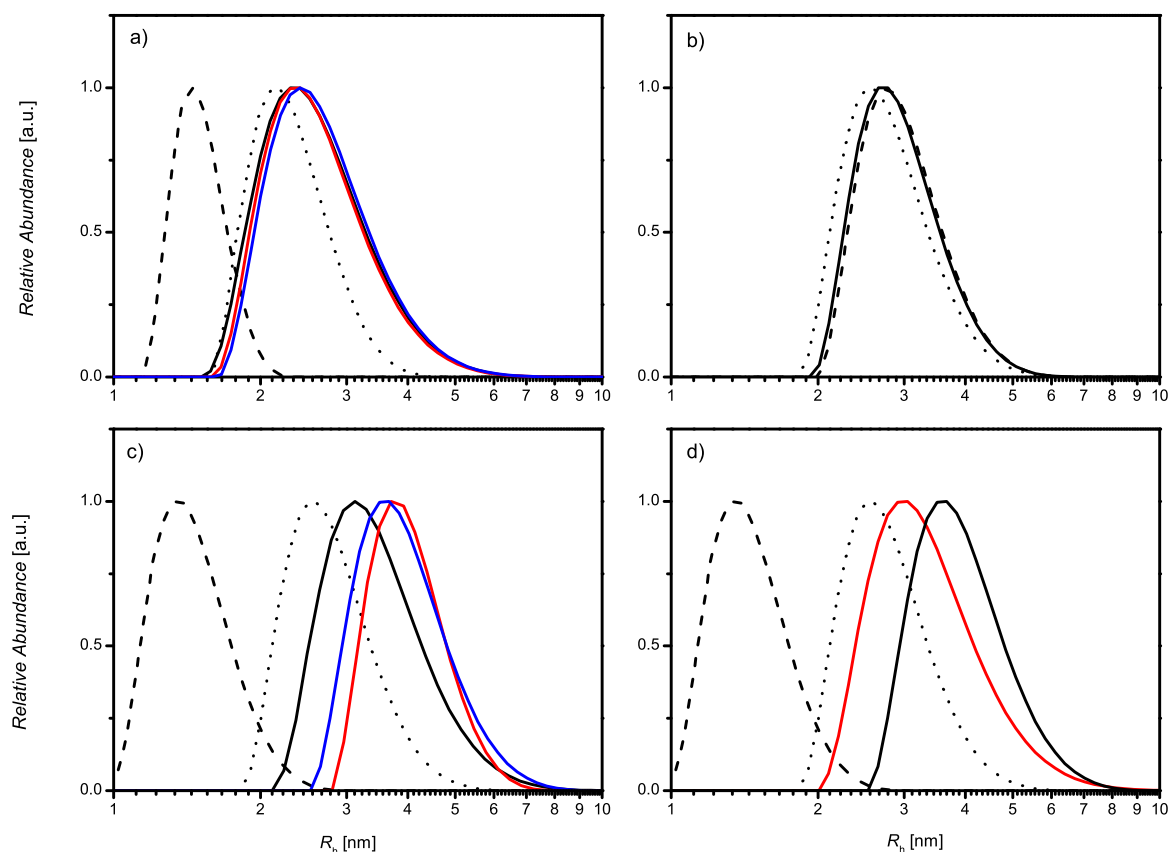


Figure 5.3: Number averaged hydrodynamic radii obtained from DLS measurements a) for PDMAAm₁₄₃-Ad (black dotted line) mixed with the β -CD₃ core (black dashed line) and the resulting supramolecular star polymers over several days in H₂O at 25 °C (1 day: black solid line; 5 days: red solid line; 9 days: blue solid line); b) for PDMAAm₁₄₃-Ad mixed (dotted line) with β -CD at 25 °C in D₂O (stoichiometric β -CD: solid line; excess β -CD: dashed line); c) for PDMAAm₁₄₃-Ad (black dotted line) mixed with the β -CD₃ core (black dashed line) in a time dependent investigation of the self-assembly process (10 min: black solid line; 1 hour: red solid line; 12 hours: blue solid line); d) for PDMAAm₁₄₃-Ad (black dotted line) mixed with the β -CD₃ core (black dashed line) for a 1:1 mixture of PDMAAm₁₄₃-Ad (red solid line) and the β -CD₃ core with a molar ratio of 3:1 (black solid line) (D₂O, 25 °C).

For control experiments, the linear polymer was dissolved together with the linker molecule β -CD₃ in H₂O and analyzed over several days without any change in the R_h being observed (Figure 5.3 a). In Figure 5.3 c the increase of R_h with time is depicted. A growth of R_h with time is visible. After 10 minutes the complex formation progressed to a large extend and after 5 hours the complex formation is finished. As a further control the β -CD₃ was mixed in an excess with the polymer (Figure 5.3 d), which shows no significant increase in R_h . This can be attributed to a formation of only one supramolecular connection per guest functionalized chain and thus the size of the aggregate is smaller compared to the incorporation of three guest functionalized polymer chains in the complex.

The reversibility of star polymer formation at higher temperatures was also investigated *via* DLS (Figure 5.4 d). Therefore, the temperature was increased from 25 °C in 2 hours and the sample was kept at this temperature for further 30 min. As a result, a decrease of the R_h from 3.7 nm to 2.8 nm was observed. This might well correspond to the expulsion of the adamantyl moiety from the β -CD₃ core (Figure 5.4 d, red solid line). Afterwards, the sample solution was cooled down to 25 °C and, subsequently, the R_h increased again.

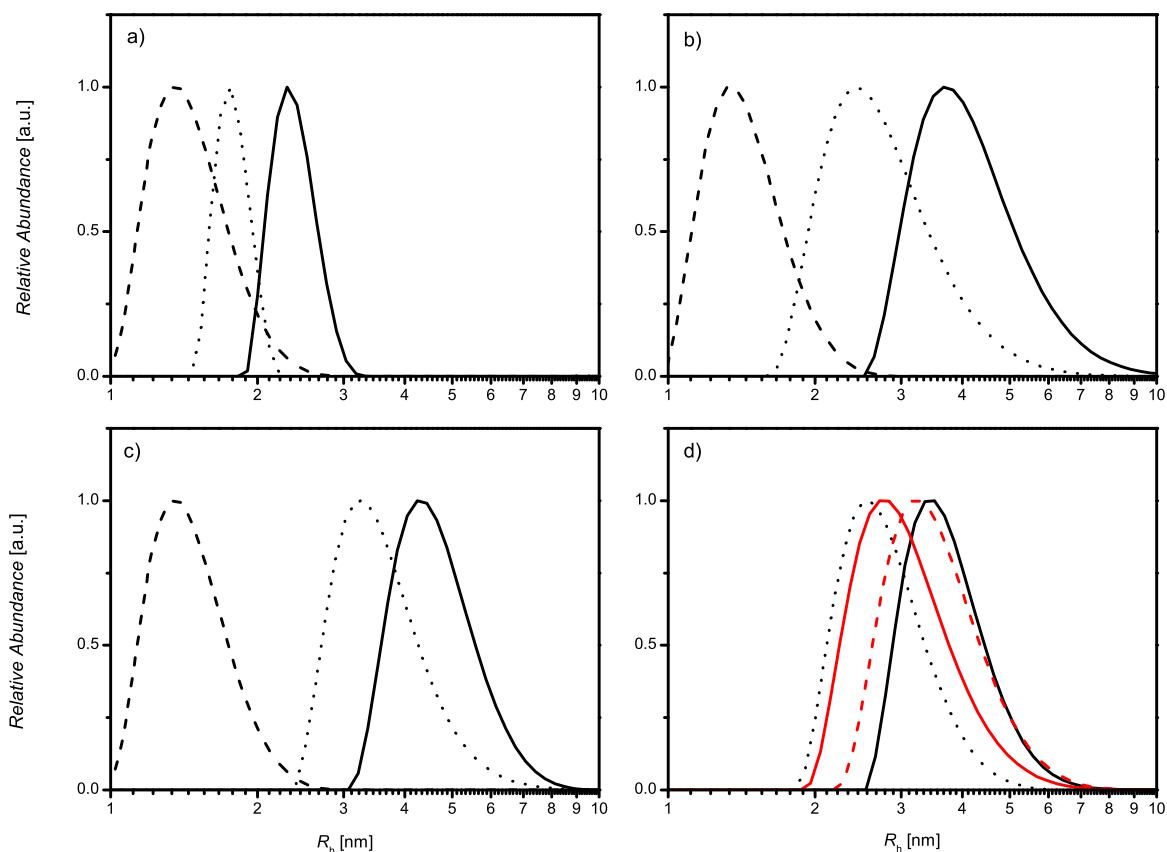


Figure 5.4: Number averaged hydrodynamic radii obtained from DLS measurements for PDMAAm_x: a) $x = 31$, b) $x = 143$ and c) $x = 202$ (dotted lines), the β -CD₃ core molecule (dashed lines), and the resulting supramolecular star polymers in a molar ratio of 3:1 after 24 hours in D₂O at 25 °C (solid lines); d) Investigations regarding the reversibility of the inclusion process by heating the complex from 25 °C (black solid line) to 70 °C (red solid line), followed by cooling and re-formation of the aggregates (red dotted line) (black dotted line: arm polymer for comparison).

Comparable investigations were carried out using PDEAAm₈₇ (Figure 5.5 a), a polymer which exhibits cloud point behaviour.²⁴² Depending on the molar mass and the respective end group, PDEAAm materials undergo a coil-to-globule transition in the temperature range of 25 to 40 °C.^{231,242} Again, stoichiometric amounts of PDEA-

Am₈₇-Ad and the CD-core were mixed in D₂O and the resulting assemblies were investigated using DLS. An increase in R_h from 2.4 to 3.8 nm was observed, corresponding to an expansion ratio of 1.6, similar values if compared to the earlier discussed PDMAAm systems (Figure 5.5 a).

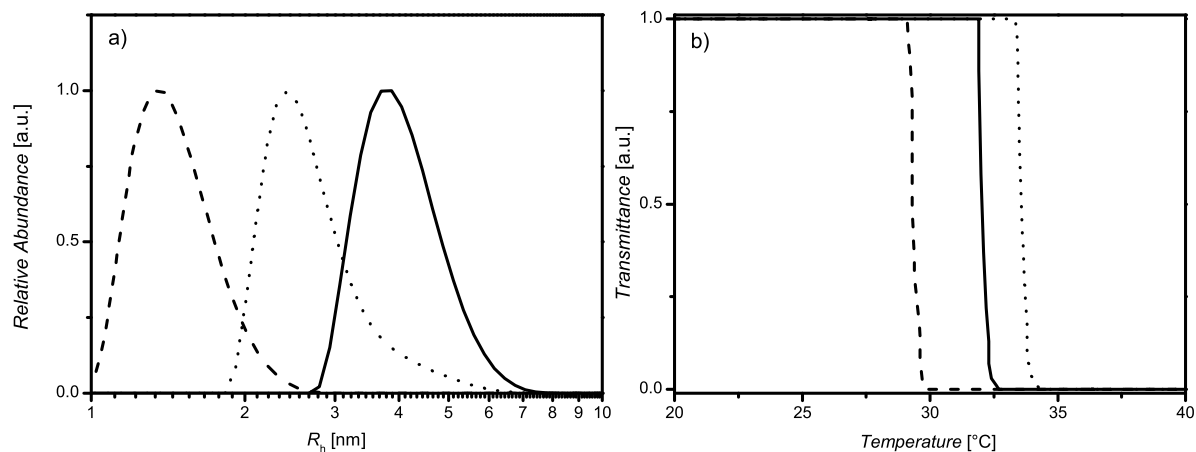


Figure 5.5: a) Number averaged size distributions obtained from DLS measurements for the supramolecular star polymer (solid line), PDEAAM₈₇-Ad (dotted line), and the β -CD₃ core (dashed line) in a molar ratio of 3:1 after 24 hours at 25 °C; b) turbidity measurements for PDEAAM₈₇-Ad (dotted line), the supramolecular star polymer (solid line), and a mixture of PDEAAM₈₇-Ad and β -CD (dashed line) mixture in D₂O.

To elucidate the temperature-dependent solubility of the PDEAAM-based supramolecular star polymers in water, turbidimetry measurements were carried out. Any changes in temperature were performed with a heating/cooling rate of 1 °C·min⁻¹. The cloud point temperature (T_c) was determined at a transmittance of 50%. Three samples, PDEAAM₈₇-Ad, the supramolecular star polymer, and a mixture of β -CD and PDEAAM₈₇, were investigated in a temperature range of 5 - 100 °C in D₂O. For PDEAAM₈₇, a T_c of 29.3 °C was found, while the mixture with CD led to a higher value ($T_c = 33.6$ °C). Such an observation can be explained by the complexation of the adamantyl moiety by β -CD and therefore the formation of a less hydrophobic end-group. In case of the star-shaped system a cloud point at 32.0 °C was observed in between the values for PDEAAM₈₇-Ad and the β -CD containing mixture (Figure 5.5 b). This might be explained by a shielding of the hydrophobic adamantyl groups due to the inclusion complex formation and – at the same time – a decrease in the conformational freedom of the individual polymer chains by connecting three arms to one core moiety. The sharp decrease of the transmittance and the reversibility of the turbidimetry measurements (at least three times) are an additional indication for the successful formation of supramolecular star polymers *via* host/guest inclusion complexes. The collapse of the PDEAAM arms leads to an inclusion of the β -CD₃ into the collapsed

polymer coil at a temperature far below the dissociation of the host/guest complex (~ 70 °C, as demonstrated using DLS in Figure 5.4 d).

5.2.3 Investigations of the Self-Assembly *via* ROESY

ROESY is a perfectly suitable tool to investigate the formation of inclusion complexes. The cross-correlation peaks in the ROESY spectrum can be assigned to protons that are closely situated (< 4 Å).¹²¹ While DLS experiments probe the molecular nature of the star polymers, ROESY was performed to demonstrate the formation of the inclusion complex between the adamantyl moiety of polymer arms and the β -CD₃ core. The 2D ROESY spectrum (Figure 5.6 a) shows six cross-correlation peaks that can be assigned to the adamantyl moiety and the β -CD moiety. The a, b and c protons of the adamantyl group feature resonances at 1.7, 2.0 and 2.1 ppm, respectively, whereas the inner protons H3 and H5 of β -CD have resonances at 3.7 and 3.8 ppm. In the 2D spectrum, the signals are located at the corresponding intersections that are expected for an inclusion complex of β -CD and the adamantyl moiety. Thus, a close distance between the protons of the adamantyl and β -CD moiety can be concluded, confirming the formation of an inclusion complex.¹⁶⁶ To exclude complex formation between the CD and the side chains of PDMAAm, a control sample of PDMAAm polymerized with **EMP** without the adamantyl moiety and β -CD was investigated as well, where the respective cross-correlation peaks were absent in the 2D NMR (Figure 5.6 b). Instead cross-correlation peaks between CD and the isobutyric acid or ethyl endgroups arise (cross-correlation peaks at 1.0 - 1.3 and 1.7 with 3.7 and 3.8 ppm). Nevertheless these signals are not present, when adamantyl functionalized polymers are added. This could be due to the increased association constant of the adamantyl moiety compared to an isobutyric acid or ethyl group.

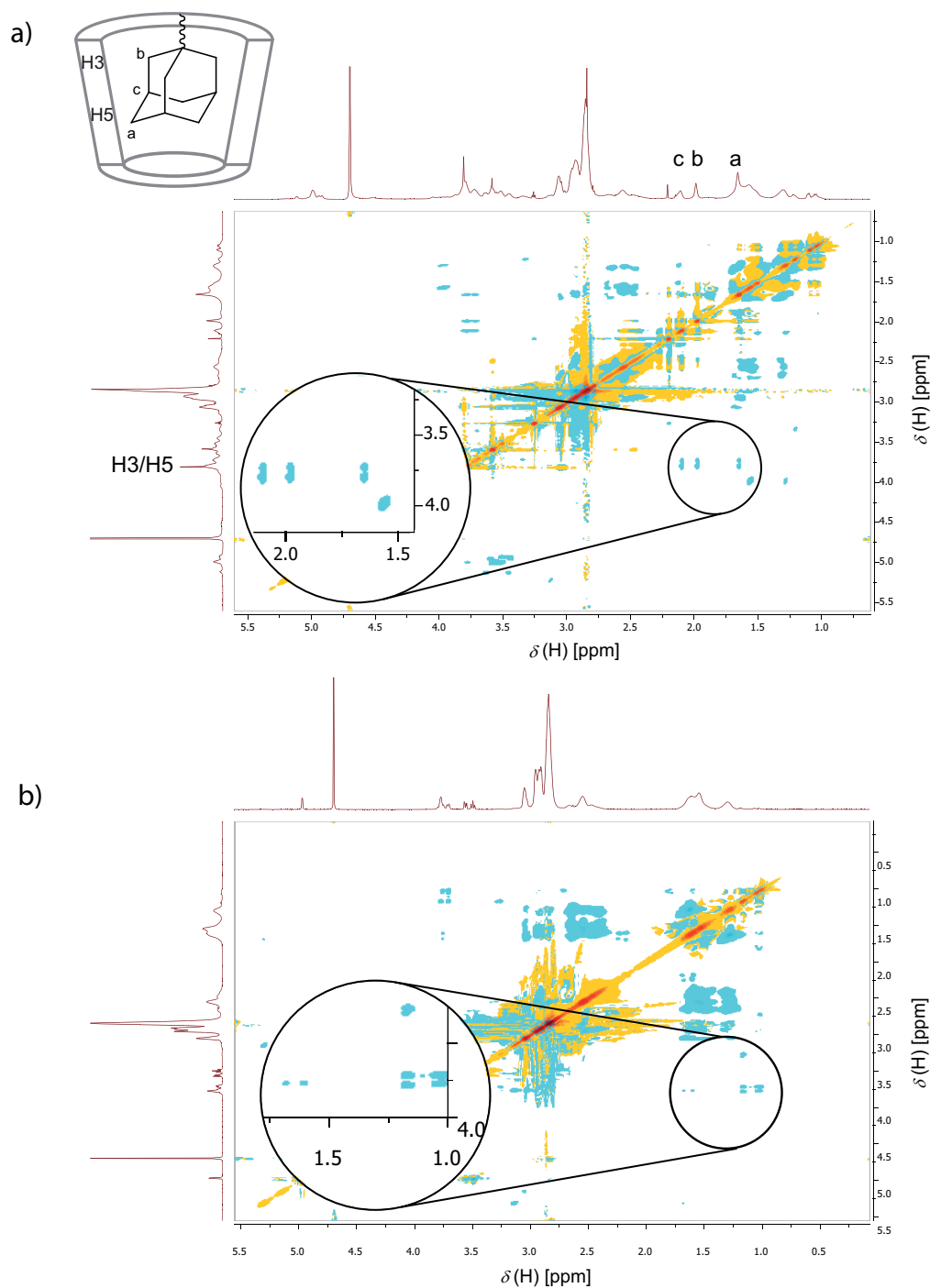


Figure 5.6: 2D ROESY spectrum (the insets show a magnification of the relevant peaks) in D_2O at 25 °C of a) 3:1 molar mixture of PDMAAm₃₁-Ad ($M_{nSEC} = 3500 \text{ g}\cdot\text{mol}^{-1}$, $D_m = 1.08$) and the $\beta\text{-CD}_3$ core; b) 1:1.1 molar mixture of PDMAAm ($M_{nSEC} = 12800 \text{ g}\cdot\text{mol}^{-1}$, $D_m = 1.10$) polymerized with EMP and $\beta\text{-CD}$.

5.3 Conclusions

In summary, the formation of supramolecular star polymers *via* the formation of inclusion complexes between adamantyl-functionalized polyacrylamides and a three-pronged CD-core was performed. The synthesis of PDMAAm-Ad and PDEAAm-Ad was carried out *via* RAFT polymerization with a novel adamantyl-functionalized chain transfer agent (**10**). The core, β -CD₃, was synthesized *via* CuAAC techniques. All building blocks were characterized *via* SEC, ¹H-NMR and ESI-MS.

The formation of supramolecular star polymers was carried out in D₂O and evidenced *via* a combination of DLS and 2D ROESY. In the case of star polymers with PDEAAm arms, additional turbidity measurements revealed a change in temperature-dependent solution behaviour. The star polymer formation was shown to be reversible, as heating to 70 °C leads to an expulsion of the individual polymer arms and cooling to 25 °C to re-formation of the complex.

5.4 Experimental Part

Synthesis of 6-(Adamantan-1-ylamino)-6-oxohexyl 2-(((ethylthio)carbonothioyl)-thio)-2-methylpropanoate (**10**)

In a 50 mL Schlenk-flask, EMP (0.84 g, 3.75 mmol, 1.0 eq.), *N*-(adamantan-1-yl)-6-hydroxyhexanamide (**8**) (1.00 g, 3.77 mmol, 1.0 eq.) and DMAP (0.09 g, 0.74 mmol, 0.2 eq.) were dissolved in anhydrous DCM (15 mL). At 0 °C a solution of DCC (1.17 g, 5.67 mmol, 1.5 eq.) in anhydrous DCM (10 mL) was added. After one hour the solution was warmed to ambient temperature, stirred overnight, filtered and concentrated under reduced pressure. The residual oil was purified *via* column chromatography on silica-gel with a 5:1 mixture of *n*-hexane:ethyl acetate as eluent. The product was obtained as yellow oil (1.08 g, 2.29 mmol, 61%).

¹H-NMR (400 MHz, CDCl₃): [δ , ppm] = 1.27 - 1.43 (m, 5H, CH₃-CH₂; CH₂-CH₂-CH₂-O), 1.53 - 1.73 (m, 16H, 2x C-CH₃; CH₂-CH₂-O; CH₂-CH₂-C=O; 3x CH_{2,adamantyl}), 1.98 (d, 6H, ³J = 2.8 Hz, 3x NH-C-CH_{2,adamantyl}), 2.02 - 2.10 (m, 5H, 3x CH_{adamantyl}; CH₂-C=O-NH), 3.28 (q, 2H, ³J = 7.4 Hz, CH₂-CH₃), 4.08 (t, 2H, ³J = 6.5 Hz, CH₂-O), 5.11 (br s, 1H, NH). ¹³C-NMR (100 MHz, CDCl₃): [δ , ppm] = 13.1 (CH₃-CH₂), 25.5, 25.7 and 28.3 (CH₂-CH₂-C=O; CH₂-CH₂-CH₂-C=O; CH₂-CH₂-C=O-NH; 2x CH₃-C=O), 29.6 (3x CH_{adamantyl}), 31.3 (CH₃-CH₂), 36.5 (3x CH_{2,adamantyl}), 37.8 (CH₂-C=O-NH), 41.9 (3x CCH_{2,adamantyl}-C-NH), 52.0 (C-NH), 56.2 (C(CH₃)₂), 66.0 (CH₂-CH₂-O), 172.1 (NH-C=O), 173.1 (O-C=O), 221.4 (C=S). ESI-MS: [M + Na⁺]_{exp} = 494.42 m/z and

$$[M + Na^+]_{\text{calc}} = 494.18 \text{ m/z.}$$

Synthesis of *N,N,N*-(tris-1-(mono-(6-desoxy)- β -CD)-1*H*-1,2,3-triazol-4-yl)methan-amine (β -CD₃)

The preparation of this compound was modified from a literature procedure.²⁸² In a 50 mL Schlenk-tube tripropargylamine (34 mg, 0.26 mmol, 1.0 eq.), PMDETA (0.16 mL, 0.77 mmol, 3.0 eq.) and β -CD-N₃ (1.00 g, 0.86 mmol, 3.3 eq.) were dissolved in DMF (11 mL). After three freeze-pump-thaw cycles the tube was backfilled with argon and CuBr (112 mg, 0.78 mmol, 3.0 eq.) was added under a flow of argon. The tube was sealed again and subjected to two freeze-pump-thaw cycles. Subsequently the tube was backfilled with argon and immersed in an oil bath at 70 °C for 4 days. After cooling to ambient temperature the product was precipitated in an excess of acetone. The product was filtered, dissolved in 10 mL EDTA-solution (5 wt.%) and dialyzed with a SpectraPor3 membrane (MWCO = 2000 Da) for 3 days at ambient temperature. Finally the solvent was removed *in vacuo* to yield β -CD₃ (574 mg, 0.16 mmol, 61%) as an off-white solid.

¹H-NMR (400 MHz, D₂O): [δ , ppm] = 3.18 (d, 3H, ³J = 11.5 Hz, N-NCH(gem)₂), 3.32 (t, 3H, ³J = 6.3 Hz, N-NCH(gem)₂), 3.37 - 4.14 (m, 124H, CD-H_{2,3,4,5,6}), 4.24 (t, 3H, ³J = 8.8 Hz, NCH(gem)₂-C), 4.66 (dd, 3H, ³J = 14.2, 8.4 Hz, NCH(gem)₂-C), 4.93 - 5.25 (m, 21H, CD-H1), 8.02 (s, 3H, H_{triazole}). ESI-MS: [M + 2Na²⁺]_{exp} = 1828.33 m/z and [M + 2Na²⁺]_{calc} = 1828.09 m/z (refer to Appendix Figure C.6 for a more detailed ESI-MS characterization)

Exemplary Procedure for the RAFT Polymerization

10 (60.0 mg, 0.13 mmol, 1.0 eq.), DMAAm (1.26 g, 12.72 mol, 97.9 eq.), AIBN (4.2 mg, 0.03 mmol, 0.2 eq.), DMF (6.0 mL) and a stirring-bar were added into a Schlenk-tube. After three freeze-pump-thaw cycles the tube was backfilled with argon, sealed, placed into an oil bath at 60 °C and removed after 24 h. The tube was subsequently cooled with liquid nitrogen to stop the reaction. A NMR-sample was withdrawn for the determination of conversion, inhibited with a pinch of hydroquinone (approx. 5 mg) and CDCl₃ was added. A quantitative conversion was calculated based on the NMR data (see Section 9.3 for details). The residue was dialyzed with a SpectraPor3 membrane (MWCO = 1000 Da) for 3 days at ambient temperature. The solvent was removed *in vacuo* to yield the polymer as a yellow solid (1.20 g, 99%, SEC(DMAc): $M_{n\text{SEC}} = 14600 \text{ g}\cdot\text{mol}^{-1}$, $D_m = 1.12$).

Exemplary Procedure for the Self-Assembly of the Adamantyl-Functionalized PDMAAm with β -CD₃

Adamantyl-functionalized PDMAAm ($M_{nSEC} = 13200 \text{ g}\cdot\text{mol}^{-1}$, 55.4 mg, 0.0042 mmol, 3.0 eq.) and β -CD₃ (5.0 mg, 0.0014 mmol, 1.0 eq.) were dissolved in D₂O (0.5 mL, $c = 120 \text{ mg}\cdot\text{mL}^{-1}$) and stirred at ambient temperature overnight. Subsequently, the formed complex was characterized *via* 2D ROESY.

Preparation for Dynamic Light Scattering Experiments

Adamantyl-functionalized polymer, *e.g.* PDMAAm ($M_{nSEC} = 14600 \text{ g}\cdot\text{mol}^{-1}$, 12.4 mg, 3.0 eq.) and β -CD₃ (1.4 mg, 1.0 eq.) were dissolved in D₂O or Milli-Q water (1 mL, $c = 5 \text{ mg}\cdot\text{mL}^{-1}$) and stirred at 25 °C.

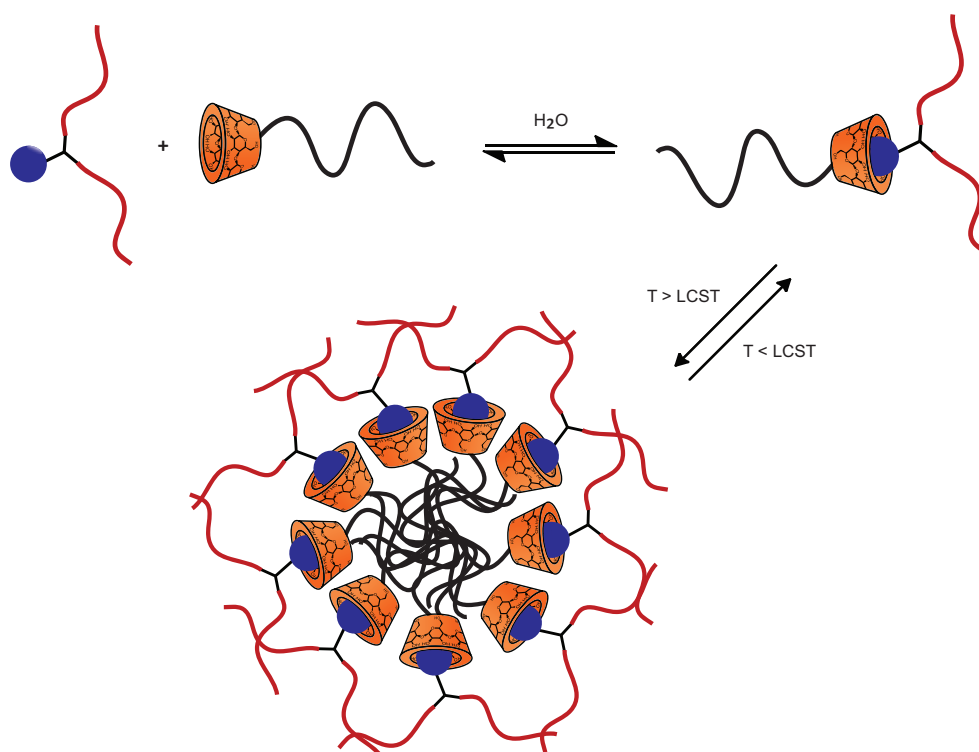
AB₂ Miktoarm Star Polymers

6.1 Introduction

The generation of novel macromolecular architectures utilizing the concept of supramolecular chemistry has driven synthetic polymer chemistry significantly in the last years.²⁷ Hydrogen bonding,^{286,287} metal complexes²⁸⁸ and inclusion complexes²⁸⁹ are widely employed. An important class of supramolecular hosts that have the ability to form inclusion complexes are CDs. This ability has found manifold utilization in polymer chemistry, *e.g.* for drug-delivery²⁸¹ or to dissolve hydrophobic monomers.²²⁷ From the view of macromolecular architectures, CDs give the opportunity for the formation of macromolecular architectures that are governed by supramolecular interactions in an aqueous environment.²⁸ Examples for the utilization of CDs for the formation of complex macromolecular architectures cover a broad range of architectures *e.g.* linear diblockcopolymers,^{166,171–174} supramolecular gels,^{34,290} CD-centered star polymers connected to linear polymers^{200,201} or supramolecular grafts for polymer brushes.^{168,178}

In Chapter 6 the formation of supramolecular miktoarm star polymers is presented, *i.e.* star polymers that have arms consisting of more than one polymer type, utilizing CD- and adamantyl-functionalized acrylamido polymers. The precursor polymers were synthesized *via* RAFT polymerization – based on a novel two-arm adamantyl bearing trithiocarbonate – of DMAAm and DEAAm and were thoroughly characterized *via* ESI-MS, NMR and SEC in DMAc. The subsequent formation of the supramolecular complex in water was proven *via* 2D ROESY and is supported by DLS data.

ROESY measurements were performed in collaboration with M. Hetzer and Prof. H. Ritter (Heinrich Heine Universität Düsseldorf). Parts of this chapter were reproduced from Schmidt, B. V. K. J.; Hetzer, M.; Ritter, H.; Barner-Kowollik, C. *Polym. Chem.* **2012**, *3*, 3064-3067 (DOI: 10.1039/C2PY20214J) with permission from the Royal Society of Chemistry.

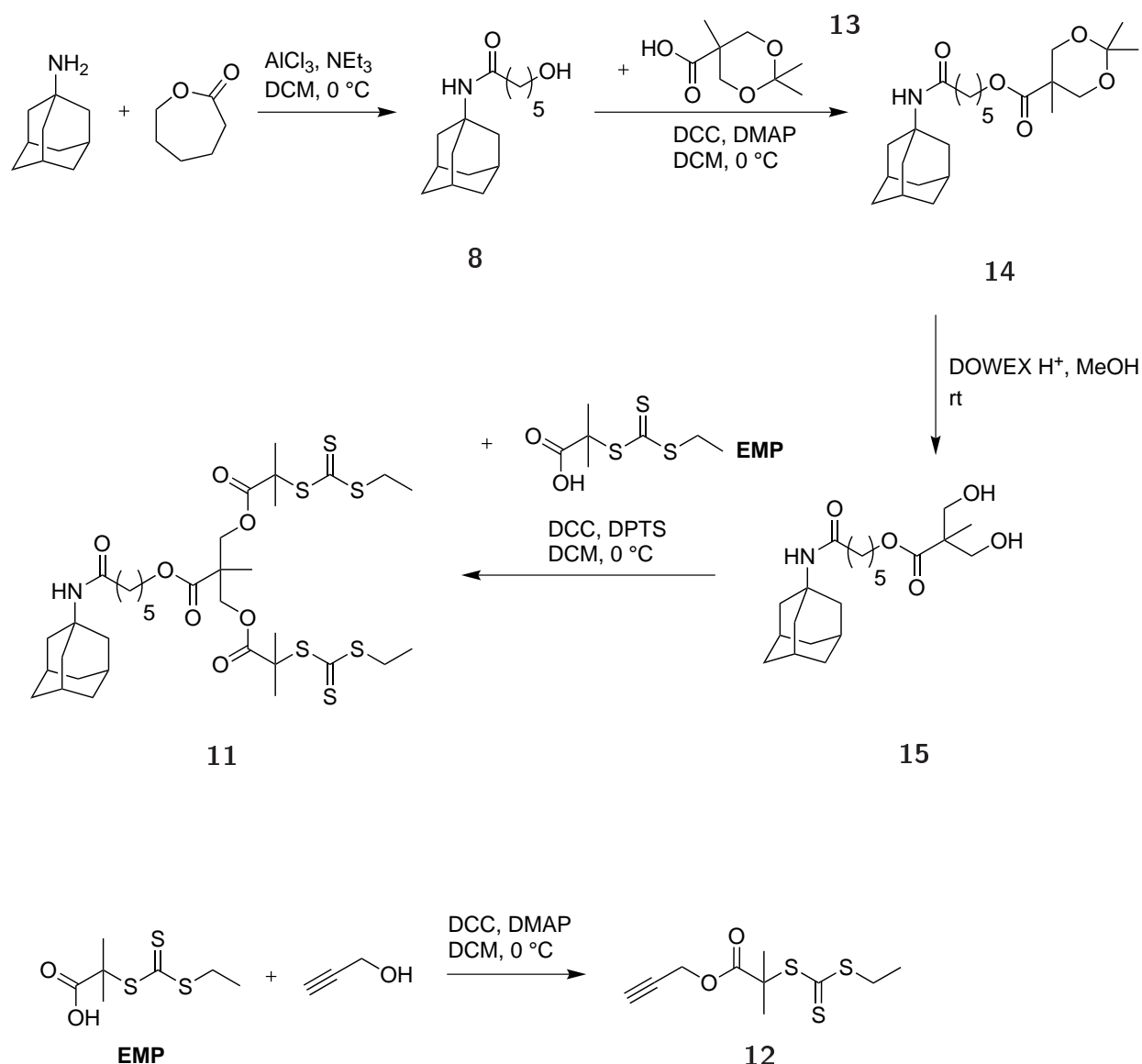


Scheme 6.1: Synthetic pathway for the supramolecular miktoarm star polymer (PDEAAm is depicted in black, PDMAAm is depicted in red, the β -CD moiety is depicted orange and the adamantyl group is depicted in dark blue).

6.2 Results and Discussion

6.2.1 Synthesis of the Building Blocks

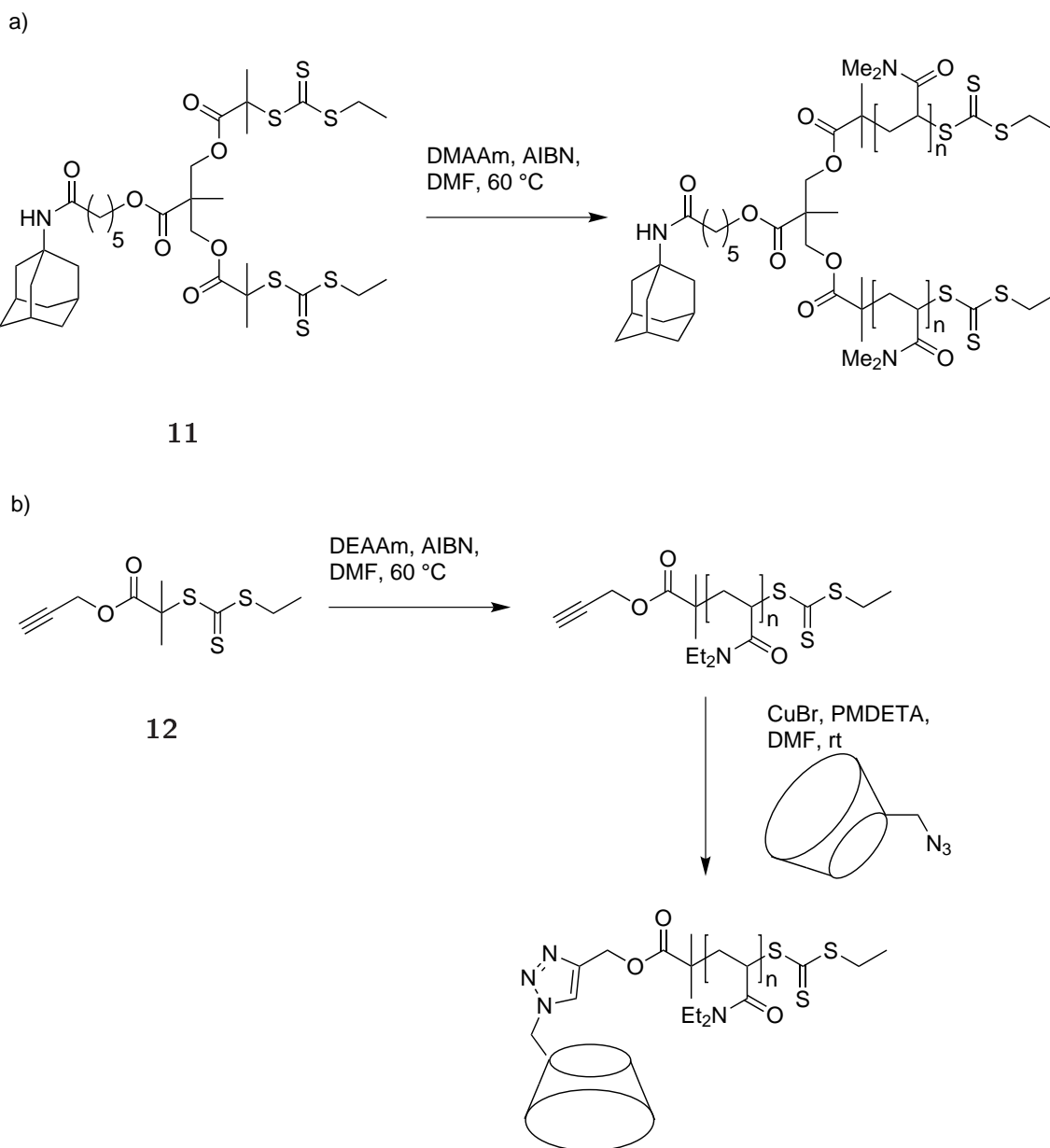
A RAFT agent with an adamantyl moiety between two trithiocarbonate-groups was synthesized (Scheme 6.1 and Scheme 6.2), to achieve a mid-chain guest-functionalized polymer. The prominent adamantyl moiety was chosen as guest-group due to its high complexation constants of up to $10^5 M^{-1}$.²³⁷ To increase the mobility and accessibility of the pendant adamantyl-group a C_5 -spacer was incorporated. The adamantyl moiety was coupled to isopropylidene-2,2-bis(methoxy)propionic acid **13** with DCC. After deprotection, an acid-functionalized trithiocarbonate RAFT-agent was attached *via* DCC-coupling to yield **11**.



Scheme 6.2: Synthesis of the utilized CTAs (**EMP**: 2-(((ethylthio)carbonothioyl)thio)-2-methylpropanoic acid).

The subsequent RAFT-polymerizations of DMAAm with were conducted in DMF employing AIBN as initiator at $60\text{ }^\circ\text{C}$ leading to narrow unimodal molecular weight distributions with low \bar{D}_m (Scheme 6.3, Figure 6.1 and Table 6.1). The tailing of the elugram is probably due to adsorptive interactions of the polymers with the SEC column. The molecular structure of the polymers was verified *via* ESI-MS and $^1\text{H-NMR}$ (Appendix D.1/D.2). The ability of the adamantyl-functionalized PDMAAm to form an inclusion complex with β -CD was proven *via* 2D ROESY (Figures 6.7 b). The resonances between the adamantyl-protons (1.65, 1.95 and 2.05 ppm) and the inner protons of β -CD (3.7 and 3.8 ppm) show the inclusion of the guest-group. Furthermore, a minor correlation between the methyl-endgroups and the inner CD protons is visible. A mixture of β -CD and non-adamantyl-functionalized PDMAAm displays no

comparable peaks (Figure 6.7 a) evidencing that no other protons in PDMAAm show correlation signals in the region of the adamantyl protons.



Scheme 6.3: RAFT polymerization for the synthesis of a) mid-chain adamantyl-functionalized PDMAAm; b) alkyne-functionalized PDEAAm and the subsequent CuAAC to form β -CD-functionalized PDEAAm.

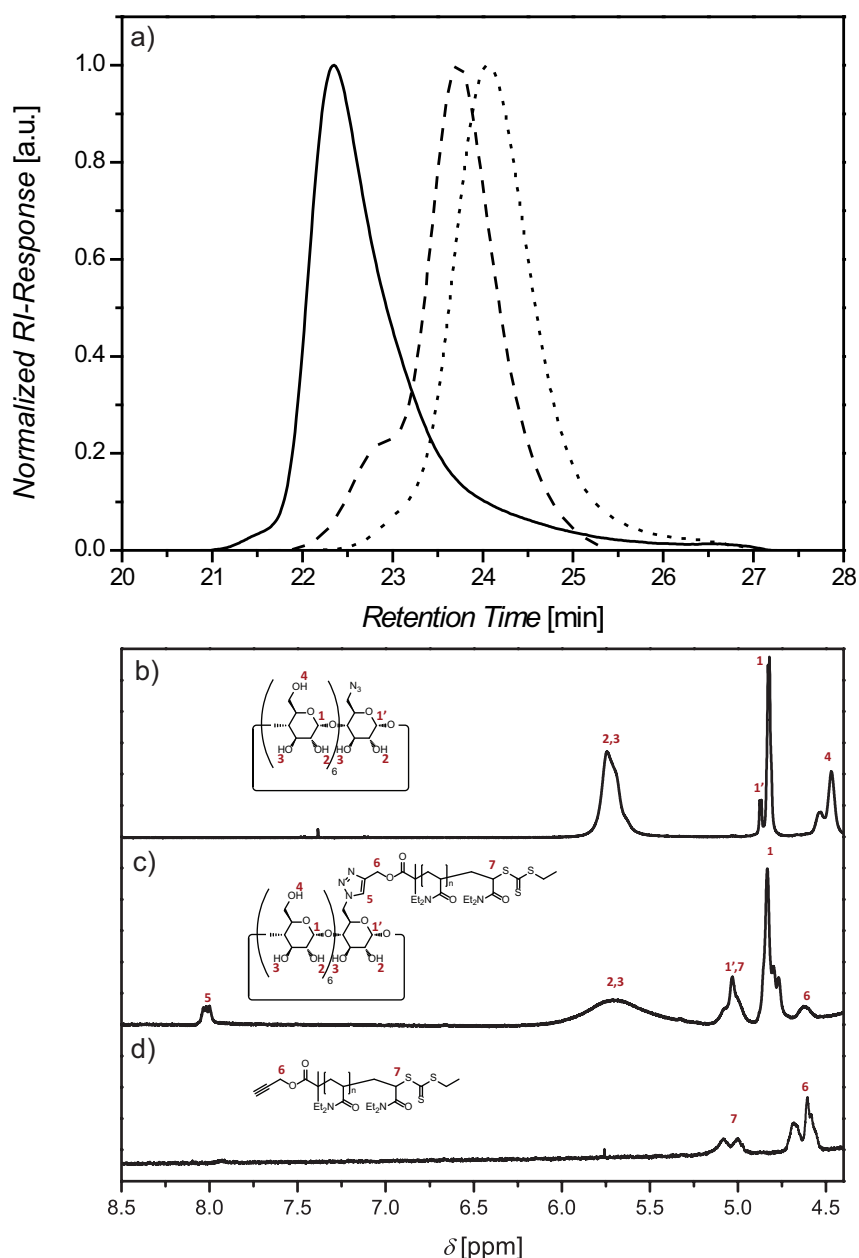


Figure 6.1: a) SEC-traces of the utilized PDMAAm₁₅₅-Ad (solid line; $M_{nSEC} = 15800 \text{ g}\cdot\text{mol}^{-1}$, $D_m = 1.41$), PDEAAm₅₇-alkyne (dotted line; $M_{nSEC} = 7500 \text{ g}\cdot\text{mol}^{-1}$, $D_m = 1.14$) and PDEAAm₅₇- β -CD (dashed line; $M_{nSEC} = 10300 \text{ g}\cdot\text{mol}^{-1}$, $D_m = 1.12$) in DMAc; comparison of the ^1H -NMR region from 4.3 ppm to 8.5 ppm b) β -CD- N_3 , c) the click-product PDEAAm₅₇- β -CD ($M_{nSEC} = 8000 \text{ g}\cdot\text{mol}^{-1}$, $D_m = 1.27$) and d) PDEAAm₅₇-alkyne ($M_{nSEC} = 7500 \text{ g}\cdot\text{mol}^{-1}$, $D_m = 1.14$).

An alkyne-endfunctionalized PDEAAm was synthesized with a terminal alkyne-containing RAFT-agent (**12**) in DMF with AIBN as initiator at 60 °C (Scheme 6.2). It should be noted that the monomer conversion was kept low to avoid undesired side-reactions, *e.g.* radical transfer to the alkyne-moiety. Unimodal molecular weight

distributions with narrow D_m were achieved according to SEC in DMAc (Figure 6.1 and Table 6.1).

Table 6.1: Results for the RAFT polymerization of DMAAm (top) with **11** and DEAAm (bottom) with **12** at 60 °C in DMF.

Monomer/CTA/I	Time / h	Conv.	$M_{n\text{theo}} / \text{g}\cdot\text{mol}^{-1}$	$M_{n\text{SEC}} / \text{g}\cdot\text{mol}^{-1}$	D_m	D_p
199/1/0.1	24	90%	18300	15800	1.41	155
76/1/0.1	6	60%	6000	7500	1.14	57

The alkyne-functionalized PDEAAm was further characterized *via* $^1\text{H-NMR}$ and ESI-MS showing a high endgroup fidelity (Appendix D.3/D.4). The host-functionalized polymer was subsequently synthesized *via* CuAAC of the alkyne-endfunctionalized polymer with $\beta\text{-CD-N}_3$ (Scheme 6.2). The successful ligation can be followed by the shift of the full molecular weight distribution determined by SEC in DMAc (Figure 6.1) as well as the emerging peak at 8 ppm from the triazole proton in the $^1\text{H-NMR}$ and the new peaks corresponding to the $\beta\text{-CD}$ moiety (Figure 6.1 c). The SEC elugram indicates a shoulder at higher molecular weights that may be attributed to coupling products due to small amounts of difunctional $\beta\text{-CD-N}_3$.

Turbidimetry measurements show an increase in the T_c from 32.5 °C to 38.1 °C (heating ramp) upon addition of the strongly hydrophilic $\beta\text{-CD}$ moiety (Figure 6.2). Furthermore, a slower transition is observed, which gives an indication that the $\beta\text{-CD}$ moiety also has an effect on the kinetics of the thermoresponsive behavior of PDEAAm.

6.2.2 Characterization of the Supramolecular Miktoarm Star Polymer

The supramolecular miktoarm star polymer was prepared *via* the dialysis method. Both blocks (Table 6.1) were dissolved in THF and one solution was added dropwise to the other under vigorous stirring. The organic solvent was removed *via* dialysis. After lyophilization of the sample the complex was dissolved in D_2O or H_2O to perform ROESY or DLS. The measurement of the T_c s of the supramolecular complex and the $\beta\text{-CD}$ functionalized PDEAAm show a difference of 2.3 °C from 38.1 °C to 40.4 °C (heating ramp) (Figure 6.2). The above is an expected result, as the non-thermoresponsive PDMAAm block leads to an increased hydrophilicity of the complex and thus the T_c is shifted to higher values. The supramolecular complex also shows a slower transition in contrast to non-CD functionalized PDEAAm featuring a rather sharp transition (Figure 6.2), which can be attributed to the interactions of both

the CD moiety and the PDMAAm block with the PDEAAm-block.

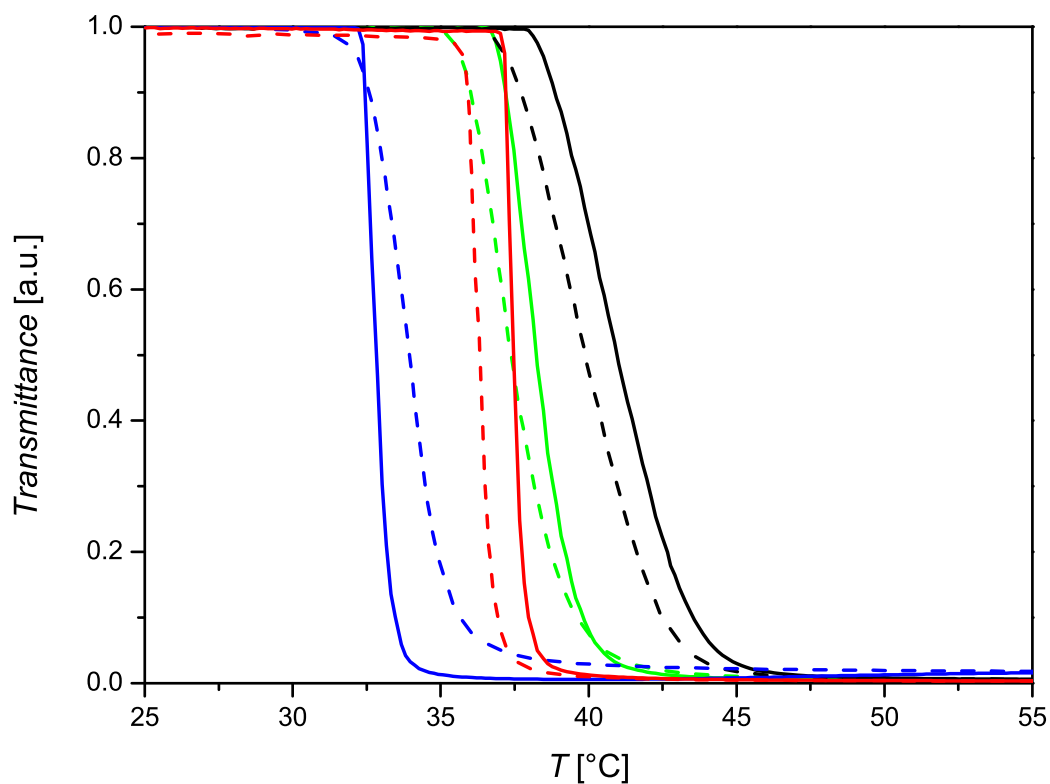


Figure 6.2: Turbidimetry measurement (cooling: dotted line; heating: solid line) of the supramolecular miktoarm star complex (black curves), PDEAAm₅₇- β -CD (green curves; $M_{nSEC} = 10300 \text{ g}\cdot\text{mol}^{-1}$, $D_m = 1.12$); PDEAAm₅₇-alkyne (blue curves; $M_{nSEC} = 7500 \text{ g}\cdot\text{mol}^{-1}$, $D_m = 1.14$) and acid-functionalized PDEAAm (red curves; $M_{nSEC} = 7900 \text{ g}\cdot\text{mol}^{-1}$, $D_m = 1.20$) at a concentration of $1 \text{ mg}\cdot\text{mL}^{-1}$.

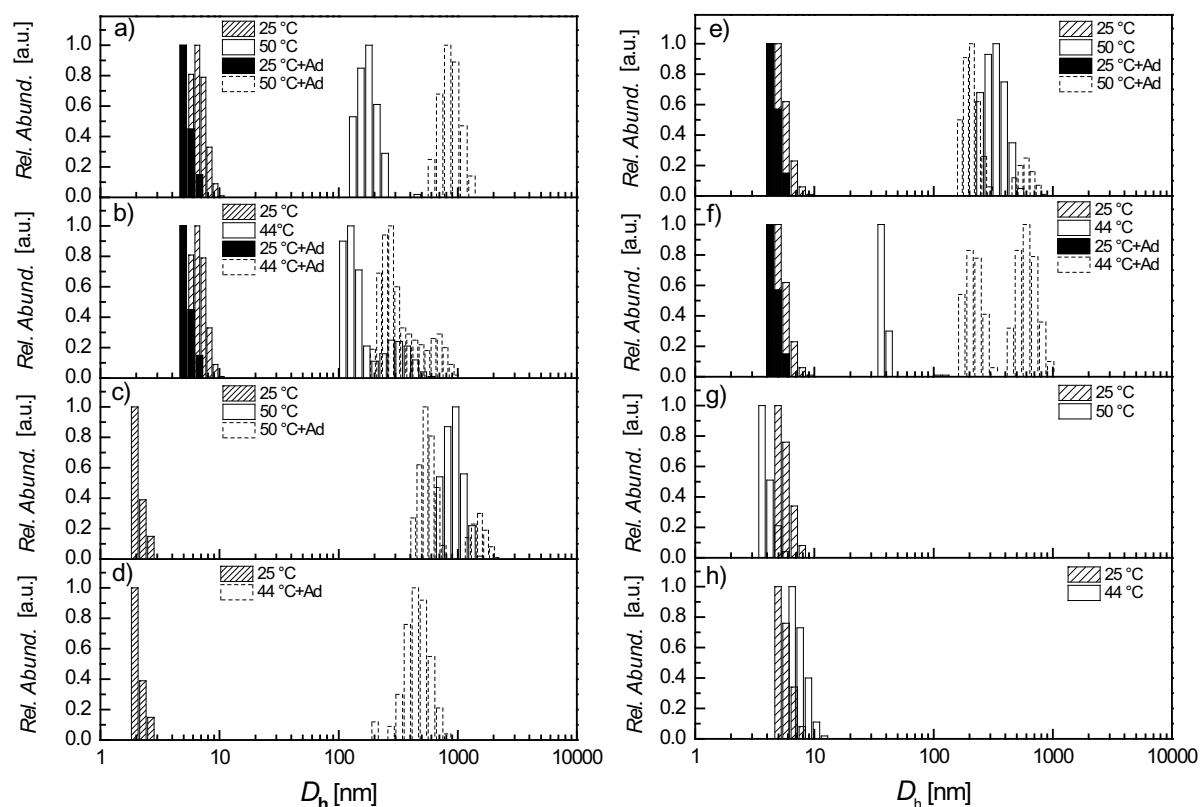


Figure 6.3: Comparison of the number averaged particle size distributions obtained from DLS measurements at a concentration of $1 \text{ mg}\cdot\text{mL}^{-1}$ with or without 1-adamantylamine hydrochloride (Ad): a) the supramolecular complex at $25 \text{ }^\circ\text{C}$ and $50 \text{ }^\circ\text{C}$; b) the supramolecular complex at $25 \text{ }^\circ\text{C}$ and $44 \text{ }^\circ\text{C}$; c) PDEAAm₅₇- β -CD at $25 \text{ }^\circ\text{C}$ and $50 \text{ }^\circ\text{C}$; d) PDEAAm₅₇- β -CD at $25 \text{ }^\circ\text{C}$ and $44 \text{ }^\circ\text{C}$; e) the control sample P4 at $25 \text{ }^\circ\text{C}$ and $50 \text{ }^\circ\text{C}$; f) the control sample P4 at $25 \text{ }^\circ\text{C}$ and $44 \text{ }^\circ\text{C}$; g) PDMAAm₁₅₅-Ad at $25 \text{ }^\circ\text{C}$ and $50 \text{ }^\circ\text{C}$; h) PDMAAm₁₅₅-Ad at $25 \text{ }^\circ\text{C}$ and $44 \text{ }^\circ\text{C}$.

DLS gives the opportunity to study the properties of the formed supramolecular complexes in solution (Figure 6.3). A comparison of the D_h of the single parts and the complex in water at $25 \text{ }^\circ\text{C}$ shows only minor differences (Figures 6.3). The adamantyl-functionalized PDMAAm shows a D_h at $25 \text{ }^\circ\text{C}$ of 5.6 nm and the β -CD-functionalized PDEAAm shows a D_h of 2.1 nm at $25 \text{ }^\circ\text{C}$ whereas the supramolecular miktoarm star polymer shows a D_h of 6.8 nm at $25 \text{ }^\circ\text{C}$. A variation of the molar ratios of the two utilized building blocks shows a maximum diameter at a molar ratio of 1:1 (Figure 6.4). This gives an indication for complex formation at $25 \text{ }^\circ\text{C}$.

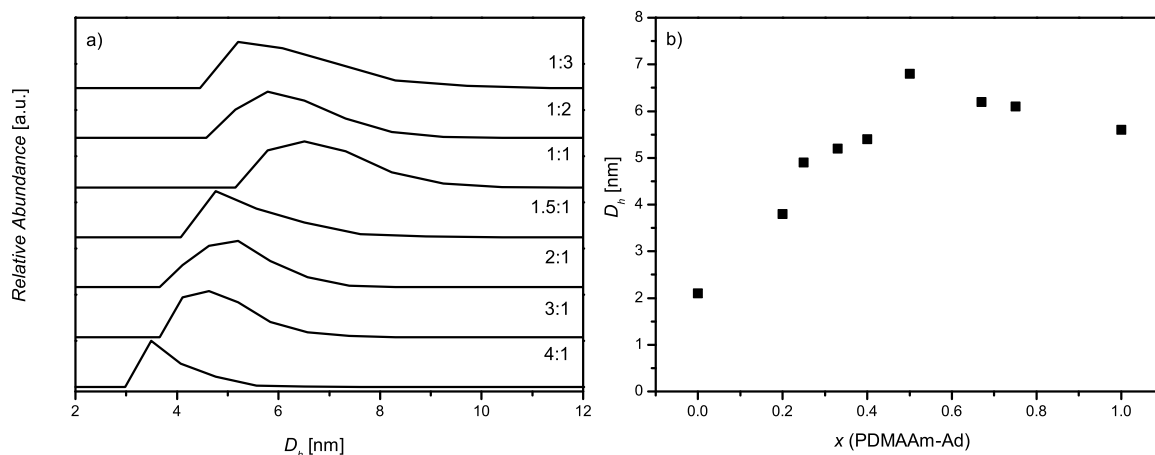


Figure 6.4: a) Comparison of the number averaged particle size distributions obtained from DLS measurements at $1 \text{ mg}\cdot\text{mL}^{-1}$ at $25 \text{ }^\circ\text{C}$ and different molar ratios of PDMAAm₁₅₅-Ad:PDEAAm₅₇- β -CD and b) comparison of the number averaged hydrodynamic diameter at $1 \text{ mg}\cdot\text{mL}^{-1}$ at $25 \text{ }^\circ\text{C}$ of mixtures of PDMAAm₁₅₅-Ad and PDEAAm₅₇- β -CD in dependence of the molar fraction x of PDMAAm₁₅₅-Ad.

A significant difference between the building blocks and the supramolecular complex is observed when the samples are heated above the T_c of the thermoresponsive PDEAAm-block (Appendix D.5). Micellization of thermoresponsive supramolecular block copolymers has been used in the literature relatively often, *e.g.* to prove the formation of the desired architectures or to generate multi-stimuli responsive micelles.^{166,171,291} At $44 \text{ }^\circ\text{C}$ and $50 \text{ }^\circ\text{C}$ the D_h of the adamantyl-functionalized PDMAAm is not changing significantly as expected for a non T_c -polymer (Figure 6.3). The β -CD-functionalized PDEAAm shows large aggregates with a D_h of 937 nm at $50 \text{ }^\circ\text{C}$. In contrast, the complex has a D_h of 132 nm and 275 nm at $44 \text{ }^\circ\text{C}$ and $50 \text{ }^\circ\text{C}$ respectively. A control sample that was prepared from a non adamantyl-functionalized PDMAAm and the β -CD-functionalized PDEAAm features a D_h of 38 nm at $44 \text{ }^\circ\text{C}$ and 333 nm at $50 \text{ }^\circ\text{C}$. The comparison indicates that the supramolecular miktoarm star polymer forms larger aggregates than the control sample. As it has been concluded from the turbidimetry measurements, the PDEAAm block interacts with both the β -CD moiety and the PDMAAm. This is apparent again from the DLS results, where heating of the control sample leads to one distribution, giving rise to the assumption that the free PDMAAm is associated with the PDEAAm aggregates. Keeping that in mind, the difference in D_h between the supramolecular miktoarm star polymer and the control sample has to be considered carefully. Nevertheless, the difference is still significant and a strong indication for complex formation. The observed particle sizes are larger than expected for a usual micellar system. It is possible that at $44 \text{ }^\circ\text{C}$ agglomeration of the formed aggregates already commences. On the other hand, in the literature mi-

cellular systems with similar size are described.^{201,292}

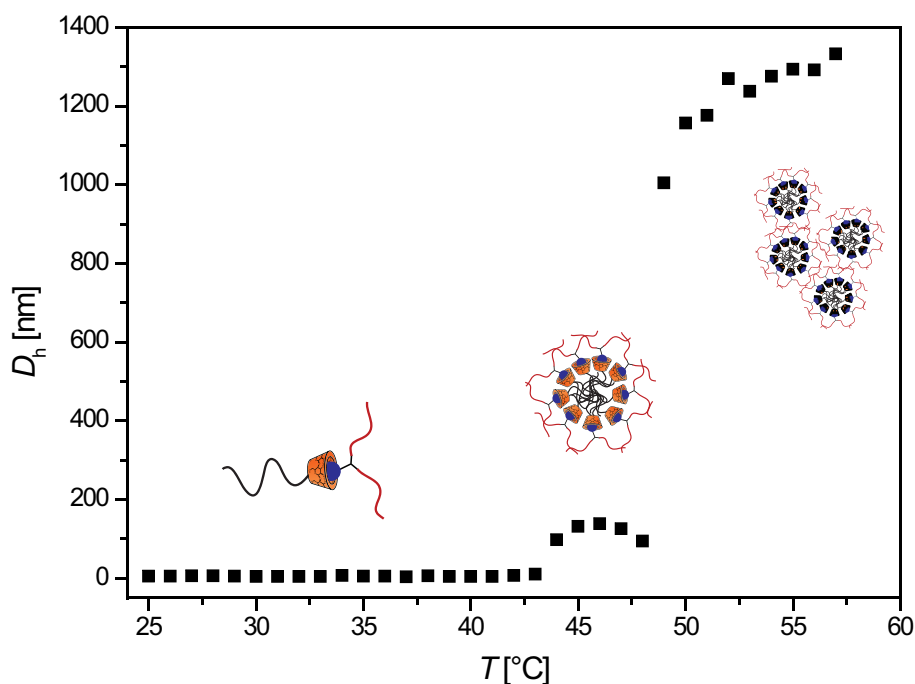


Figure 6.5: Temperature sequenced DLS measurement showing the relation between the D_h from the number averaged particle size distribution and the temperature.

The addition of an excess of 1-adamantylamine hydrochloride (Ad) leads to an insignificant decrease of the D_h at 25 °C of 1.4 nm whereas large differences are observed at elevated temperatures. Instead of 132 and 275 nm larger particles with D_h of 275 nm and 881 nm are found upon heating at 44 °C and 50 °C, respectively. At 50 °C a D_h of 881 nm is formed, which is close to the D_h of β -CD-functionalized PDEAAm with 937 nm. This result is in agreement with the expectation that the addition of an excess of guest molecules leads to the disruption of the supramolecular miktoarm star polymer complex and therefore different aggregates are formed in solution upon heating. It should be noted that the addition of guest molecules also alters the thermoresponsive behavior of the control sample. In this case also larger aggregates are formed with multi-modal particle size distributions, which can be attributed to a change in the hydrophilicity of the CD endgroups when an inclusion complex is formed (Figure 6.3).

To further investigate the formation of the aggregates a temperature sequenced DLS measurement of the supramolecular complex was performed which shows three regimes (Figure 6.5). From 25 °C to 43 °C, the complexes are present as unimolecular coils with an average D_h of 5.4 nm. From 44 °C to 48 °C defined aggregates are formed with an average D_h of 118 nm as the PDEAAm-block becomes insoluble due

to its T_c . The formation of defined aggregates is a strong hint for the supramolecular connection between both blocks. A further increase in temperature leads to further agglomeration (> 1000 nm) as it has been discussed in the literature with a similar system consisting of a linear linker with an adamantyl-group on every end and two β -CD-centered stars attached *via* supramolecular interactions.²⁰¹ This effect could be attributed to the weaker complexation at elevated temperatures, which leads to partial disruption of the complexes, a loss or rearrangement of stabilizing PDMAAm chains in the corona and agglomeration of multiple particles. It is striking that the size of the formed aggregates depends strongly on the heating rate (Figure 6.6). Direct heating from 25 °C to 50 °C leads to smaller aggregates (275 nm) than slow heating (> 1000 nm). The above behavior could be due to effects of the kinetics of the aggregate formation.²⁹³

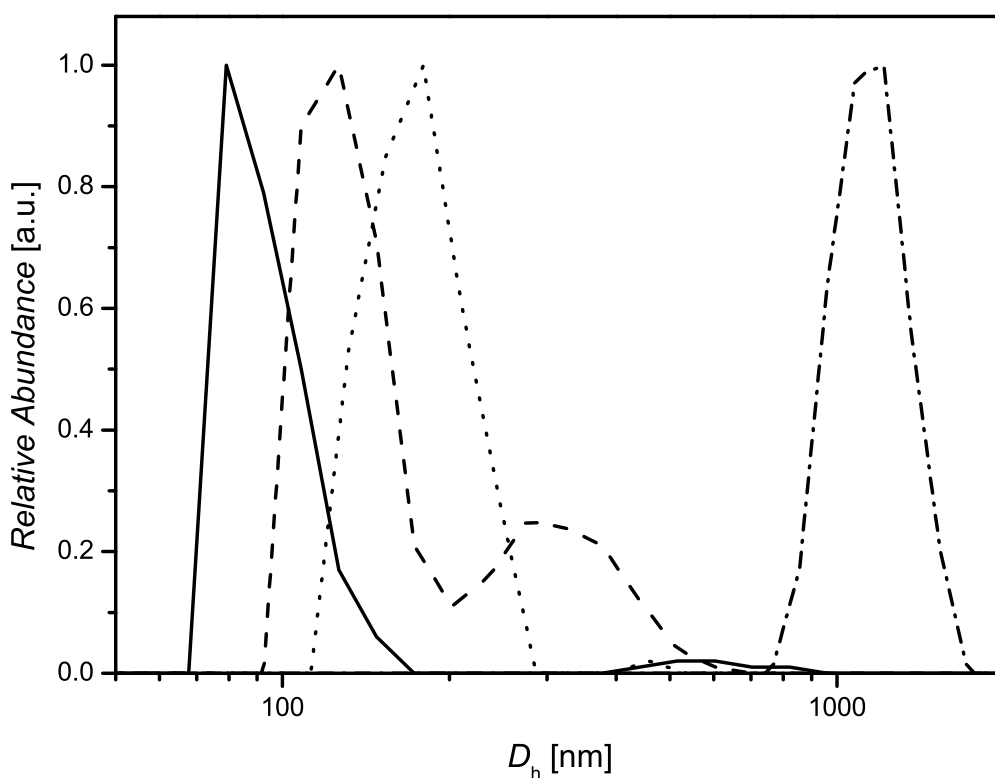


Figure 6.6: Comparison of the number averaged particle size distributions of the supramolecular miktoarm star polymer obtained from DLS measurements with slow heating at 44 °C (solid line) and 50 °C (dashed-dotted line) and after fast heating at 44 °C (dashed line) and 50 °C (dotted line).

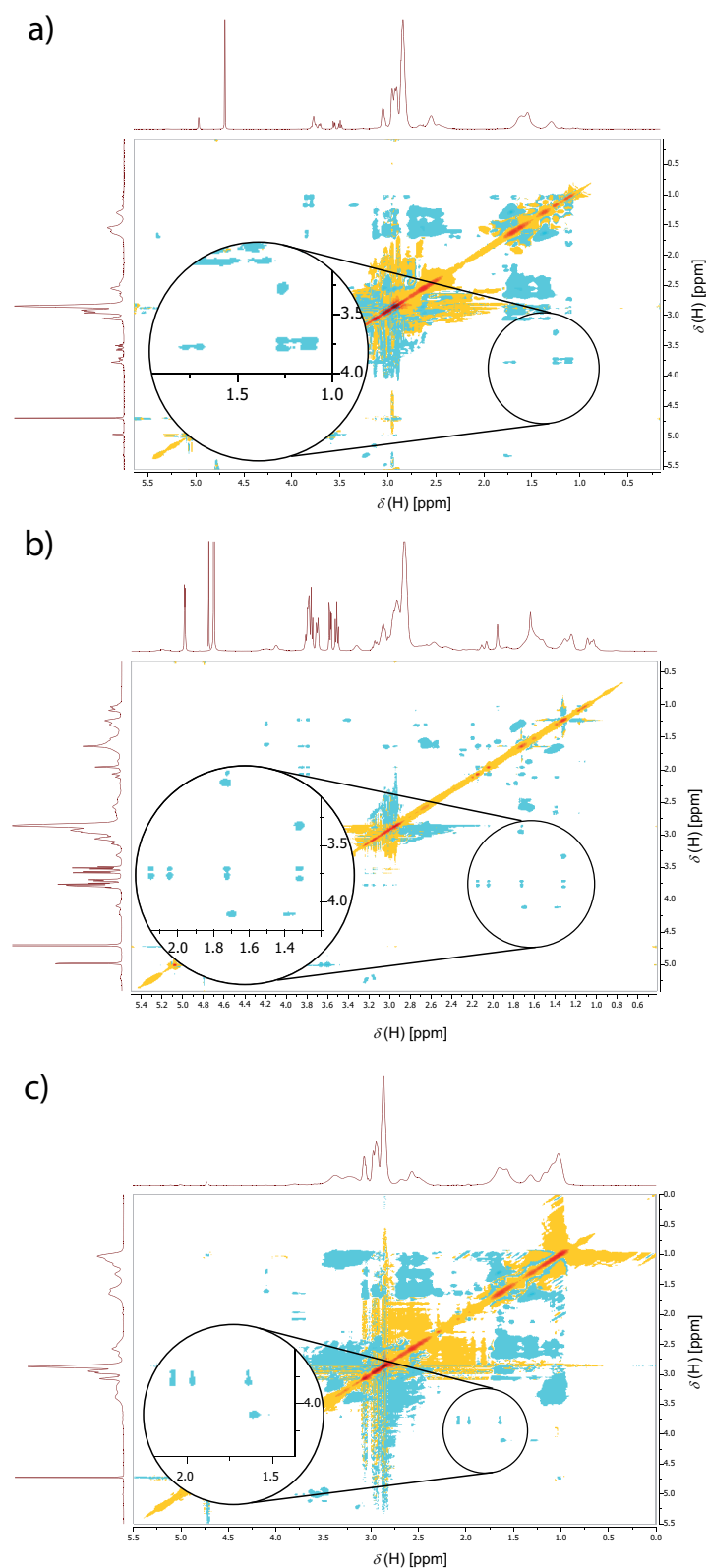


Figure 6.7: 2D ROESY spectra in D₂O at 25 °C with magnification of the relevant signals of a) 1:1.1 molar mixture of PDMAAm ($M_{nSEC} = 12800 \text{ g}\cdot\text{mol}^{-1}$, $D_m = 1.10$) polymerized with EMP and β -CD; b) 1:1.1 molar mixture of a mid-chain adamantyl-functionalized PDMAAm ($M_{nSEC} = 4000 \text{ g}\cdot\text{mol}^{-1}$, $D_m = 1.09$) polymerized with **11** and β -CD; c) the supramolecular mikroarm star polymer in D₂O at 25 °C.

The DLS results are an indication that the expected supramolecular complex is formed. Nevertheless, the connection of both blocks *via* the CD/adamantyl pair has to be proven. ROESY is a powerful tool to study inclusion complexes. The ROESY spectrum of the supramolecular complex proves the inclusion of the mid-chain adamantyl moiety in the PDMAAm into the pendant CD units of the PDEAAm thus proving the formation of a supramolecular miktoarm star polymer (Figure 6.7 c). Six correlation peaks at 1.72, 2.04 and 2.16 ppm can be assigned to the interaction of the adamantyl group with the inner protons of β -CD at 3.7 and 3.8 ppm.¹⁶⁶ No other significant correlation peaks are found in the respective regions, which proves that no other interactions are present that could lead to different architectures. A similar spectrum was found with the adamantyl-functionalized PDMAAm and native β -CD (Figure 6.7 b). Furthermore the additional correlation peaks between 1.2 ppm and 3.7 and 3.8 ppm that were found with native β -CD are absent in the ROESY spectrum of the miktoarm star polymer. Thus, the formation of the miktoarm star architecture can be assumed.

6.3 Conclusions

The formation of a novel supramolecular miktoarm star polymer that is based on CD-host/guest chemistry was described. A mid-chain adamantyl-containing PDMAAm and an alkyne-endgroup-containing PDEAAm were prepared *via* the RAFT process. The terminal alkyne was transferred into a β -CD-endgroup *via* CuAAC with β -CD-N₃. The supramolecular miktoarm star polymer architecture was formed subsequently *via* a CD/adamantyl inclusion-complex. The complex formation was proven *via* DLS and ROESY. The thermoresponsive behavior of the formed supramolecular miktoarm star polymers were studied *via* turbidimetry measurements showing significant changes in the T_c s of complexed polymers and the native building blocks. Furthermore, temperature sequenced DLS was performed to study the temperature induced micellization of the supramolecular miktoarm star polymers with regard to the size of formed aggregates. It could be shown that addition of free guest molecules leads to disruption of the formed supramolecular complexes with significant changes in the thermoresponsive behavior.

6.4 Experimental Part

Synthesis of 6-(adamantan-1-ylamino)-6-oxohexyl-2,2,5-trimethyl-1,3-dioxane-5-carboxylate (14)

In a 50 mL Schlenk-flask isopropylidene-2,2-bis(methoxy)propionic acid (**13**) (1.04 g, 8.04 mmol, 1.2 eq.), *N*-(adamantan-1-yl)-6-hydroxyhexanamide (**8**) (1.78 g, 6.72 mmol, 1.0 eq.) and DMAP (0.16 g, 1.31 mmol, 0.2 eq.) were dissolved in anhydrous DCM (14 mL). At 0 °C a solution of DCC (1.66 g, 8.04 mmol, 1.2 eq.) in anhydrous DCM (8 mL) was added. After one hour the solution was warmed to ambient temperature, stirred overnight, filtered and concentrated under reduced pressure. The residual oil was purified *via* column chromatography on silica-gel with a mixture of *n*-hexane:ethyl acetate as eluent that was gradually changed from 5:1 to 4:1. The product was obtained as colorless oil (2.70 g, 6.41 mmol, 95%).

¹H-NMR (400 MHz, CDCl₃): [δ, ppm] = 1.18 (s, 3H, CH₃-C-C=O), 1.30 - 1.50 (m, 8H, 2x C-CH₃, CH₂-CH₂-C-O), 1.56 - 1.73 (m, 10H, 2x CH_{2,alkyl}; 3x CH_{2,adamantyl}), 1.97 (d, 6H, ³J = 2.8 Hz, 3x NH-C-CH_{2,adamantyl}), 2.02 - 2.12 (m, 5H, 3x CH_{adamantyl}; CH₂-C=O-NH), 3.62 (d, 2H, J = 11.8 Hz, CH₂-O-C), 3.98 - 4.36 (m, 4H, 2x CH₂-O-C), 5.10 (br s, 1H, NH). ¹³C-NMR (100 MHz, CDCl₃): [δ, ppm] = 18.9 (C-CH₃), 23.0 and 24.6 (2x CH₃-C-O), 25.4 and 25.6 (CH₂-CH₂-C=O; CH₂-CH₂-CH₂-C=O), 28.5 (CH₂-CH₂-C=O-NH), 29.6 (3x CH_{adamantyl}), 36.5 (3x CH_{2,adamantyl}), 37.7 (CH₂-C=O-NH), 41.8 (3x CH_{2,adamantyl}-C-NH), 41.9 (O-CH₂-C-C=O), 51.9 (C-NH), 64.9 (CH₂-CH₂-O), 66.2 (2x C-CH₂-O), 98.2 (CH₂-O-C(CH₃)₂-O-CH₂), 172.0 (NH-C=O), 174.4 (O-C=O). ESI-MS: [M + Na⁺]_{exp} = 444.48 m/z and [M + Na⁺]_{calc} = 444.27 m/z.

Synthesis of 6-(adamantan-1-ylamino)-6-oxohexyl 3-hydroxy-2-(hydroxymethyl)-2-methylpropanoate (15)

6-(adamantan-1-ylamino)-6-oxohexyl-2,2,5-trimethyl-1,3-dioxane-5-carboxylate (**14**) (2.50 g, 5.94 mmol, 1.0 eq.) was dissolved in methanol (20 mL). Subsequently one spoon of Dowex H⁺ resin was added and the mixture stirred at ambient temperature over night. The mixture was filtered and washed with methanol. After evaporation of the solvent *in vacuo* 2.15 g (5.64 mmol, 95%) of the product were obtained as colorless oil.

¹H-NMR (400 MHz, CDCl₃): [δ, ppm] = 1.06 (s, 3H, CH₃-C-C=O), 1.29 - 1.50 (m, 2H, CH₂-CH₂-C-O), 1.52 - 1.77 (m, 10H, 2x CH_{2,alkyl}; 3x CH_{2,adamantyl}), 1.97 - 2.14 (m, 11H, 3x CH_{adamantyl}; CH₂-C=O-NH; 3x NH-C-CH_{2,adamantyl}), 2.83 (br s, 2H, OH), 3.72 (d, 2H, ³J = 11.2 Hz, CH₂-O-C), 3.87 (d, 2H, ³J = 11.2 Hz, CH₂-O-C), 4.16 (t, 2H, ³J = 6.4 Hz, CH₂-CH₂-O-C), 5.21 (br s, 1H, NH). ¹³C-NMR (100 MHz, CDCl₃): [δ, ppm]

= 17.4 (C-CH₃), 25.2 and 25.7 (CH₂-CH₂-C=O; CH₂-CH₂-CH₂-C=O), 28.3 (CH₂-CH₂-C=O-NH), 29.6 (3x CH_{adamantyl}), 36.5 (3x CH_{2,adamantyl}), 37.5 (CH₂-C=O-NH), 41.8 (3x CH_{2,adamantyl}-C-NH), 49.4 (O=C-C-(CH₂-O)₂), 52.1 (C-NH), 64.9 (CH₂-CH₂-O), 68.3 (2x C-CH₂-O), 172.3 (NH-C=O), 176.2 (O-C=O). **ESI-MS:** [M + Na⁺]_{exp} = 404.44 m/z and [M + Na⁺]_{calc} = 404.50 m/z.

Synthesis of 2-(((6-(adamantan-1-ylamino)-6-oxohexyl)oxy)carbonyl)-2-methylpropane-1,3-diyl bis(2-(((ethylthio)carbonothioyl)thio)-2-methylpropanoate (11)

In a 50 mL round bottom-flask 6-(adamantan-1-ylamino)-6-oxohexyl 3-hydroxy-2-(hydroxymethyl)-2-methylpropanoate (**15**) (2.00 g, 5.25 mmol, 1.0 eq.), **EMP** (2.47 g, 11.02 mmol, 2.1 eq.) and **DPTS** (0.62 g, 2.11 mmol, 0.4 eq.) were dissolved in anhydrous DCM (20 mL). At 0 °C a solution of **DCC** (3.25 g, 15.75 mmol, 3.0 eq.) in anhydrous DCM (20 mL) was added. After one hour the solution was warmed to ambient temperature, stirred for 2 days, filtered and concentrated under reduced pressure. The residual oil was purified *via* column chromatography on silica-gel with a mixture of *n*-hexane:ethyl acetate as eluent that was gradually changed from 4:1 to 3:1. The product was obtained as yellow oil (2.25 g, 2.84 mmol, 54%).

¹H-NMR (400 MHz, CDCl₃): [δ, ppm] = 1.02 - 1.47 (m, 11H, CH₂-CH₂-C-O; CH₃-C=O; 2x CH₃-CH₂), 1.51 - 1.85 (m, 22H, 2x CH_{2,alkyl}; 3x CH_{2,adamantyl}; 4x C-CH₃), 1.89 - 2.22 (m, 11H, 3x CH_{adamantyl}; CH₂-C=O-NH; 3x NH-C-CH_{2,adamantyl}), 3.26 (q, 4H, ³J = 7.4 Hz, CH₂-S), 3.31 - 3.90 (m, 6H, CH₂-O-C, CH₂-O-C; CH₂-CH₂-O-C), 5.15 (br s, 1H, NH). **¹³C-NMR** (100 MHz, CDCl₃): [δ, ppm] = 13.0 (4x CH₂-CH₃), 17.9 (C-CH₃), 25.4, 25.5 and 25.7 (4x C-CH₃; CH₂-CH₂-C=O; CH₂-CH₂-CH₂-C=O), 28.5 (CH₂-CH₂-C=O-NH), 29.6 (3x CH_{adamantyl}), 31.3 (2x CH₂-S), 36.5 (3x CH_{2,adamantyl}), 37.6 (CH₂-C=O-NH), 41.8 (3x CH_{2,adamantyl}-C-NH), 46.2 (O=C-C-(CH₂-O)₂), 52.0 (C-NH), 56.0 (C-(CH₃)₂), 65.3 and 67.0 (CH₂-CH₂-O; 2x C-CH₂-O), 172.0, 172.4 and 172.6 (2x O-C=O, NH-C=O), 221.4 (2x C=S). **ESI-MS:** [M + Na⁺]_{exp} = 816.32 m/z and [M + Na⁺]_{calc} = 816.22 m/z.

Synthesis of prop-2-yn-1-yl 2-(((ethylthio)carbonothioyl)thio)-2-methylpropanoate (12)

In a 250 mL Schlenk-flask **EMP** (4.00 g, 17.86 mmol, 1.0 eq.), propargyl alcohol (2.1 mL, 36.34 mmol, 2.0 eq.) and **DMAP** (0.88 g, 7.20 mmol, 0.4 eq.) were dissolved in anhydrous DCM (80 mL). At 0 °C a solution of **DCC** (7.40 g, 35.86 mmol, 2.0 eq.) in anhydrous DCM (40 mL) was added. After one hour the solution was warmed to ambient temperature, stirred overnight, filtered and concentrated under reduced pressure. The residual oil was purified *via* column chromatography on silica-gel with a 20:1 mixture

of *n*-hexane:ethyl acetate. The product was obtained as yellow oil (3.92 g, 14.94 mmol, 84%).

¹H-NMR (400 MHz, CDCl₃): [δ , ppm] = 1.32 (t, 3H, ³J = 7.4 Hz, CH₃-CH₂), 1.70 (s, 6H, 2x C-CH₃), 2.46 (t, ³J = 2.5 Hz, 1H, CH), 3.28 (q, 2H, ³J = 7.4 Hz, CH₃-CH₂), 4.69 (d, ³J = 2.5 Hz, 2H, CH₂-O). **¹³C-NMR** (100 MHz, CDCl₃): [δ , ppm] = 13.0 (CH₂-CH₃), 25.3 (2x C-CH₃), 31.4 (CH₂-CH₃), 53.5 (C-CH₃), 55.7 (CH₂-O), 75.2 (CH), 77.4 (C-CH), 172.5 (C=O), 221.0 (C=S). **ESI-MS**: [M + Na⁺]_{exp} = 284.88 m/z and [M + Na⁺]_{calc} = 285.01 m/z.

Exemplary Synthesis of Mid-Chain Adamantyl-Functionalized PDMAAm

11 (60.0 mg, 0.076 mmol, 1.0 eq.), DMAAm (1.50 g, 15.14 mmol, 199.2 eq.), AIBN (2.5 mg, 0.015 mmol, 0.2 eq.), DMF (15.0 mL) and a stirring-bar were added into a Schlenk-tube. After three freeze-pump-thaw cycles the tube was backfilled with argon, sealed, placed in an oil bath at 60 °C and removed after 24 h. The tube was subsequently cooled with liquid nitrogen to stop the reaction. A NMR-sample was withdrawn for the determination of conversion, inhibited with a pinch of hydroquinone (approx. 5 mg) and CDCl₃ was added. A conversion of 90% was calculated based on the NMR data (see Section 9.3 for details of the calculation). The residue was dialyzed against deionized water with a SpectraPor3 membrane (MWCO = 1000 Da) for 3 days at ambient temperature. The solvent was removed *in vacuo* to yield the polymer as a yellow solid (1.40 g, 99%, $M_{\text{ntheo}} = 18500 \text{ g}\cdot\text{mol}^{-1}$, **SEC(DMAc)**: $M_{\text{nSEC}} = 15800 \text{ g}\cdot\text{mol}^{-1}$, $D_{\text{m}} = 1.41$).

Exemplary Synthesis of Alkyne-Functionalized PDEAAm

12 (269.0 mg, 1.03 mmol, 1.0 eq.), DEAAm (10.00 g, 78.62 mmol, 76.3 eq.), AIBN (15.0 mg, 0.091 mmol, 0.1 eq.), DMF (45 mL) and a stirring-bar were added into a Schlenk-tube. After three freeze-pump-thaw cycles the tube was backfilled with argon, sealed, placed in an oil bath at 60 °C and removed after 6 h. The tube was subsequently cooled with liquid nitrogen to stop the reaction. A NMR-sample was withdrawn for the determination of conversion, inhibited with a pinch of hydroquinone (approx. 5 mg) and CDCl₃ was added. A conversion of 82% was calculated based on the NMR data (see Section 9.3 for details of the calculation). The residue was dialyzed against deionized water with a SpectraPor3 membrane (MWCO = 1000 Da) for 3 days at ambient temperature. The solvent was removed *in vacuo* to yield the polymer as yellow solid (7.34 g, 87%, $M_{\text{ntheo}} = 8200 \text{ g}\cdot\text{mol}^{-1}$, **SEC(DMAc)**: $M_{\text{nSEC}} = 7500 \text{ g}\cdot\text{mol}^{-1}$, $D_{\text{m}} = 1.14$).

Exemplary Click-Reaction of Alkyne-Functionalized PDEAAm with β -CD-N₃

Alkyne functionalized PDEAAm ($M_{nSEC} = 7500 \text{ g}\cdot\text{mol}^{-1}$; 2.00 g, 0.27 mmol, 1.0 eq.), β -CD-N₃ (1.25 g, 1.08 mmol 4.0 eq.), PMDETA (56 μl , 0.27 mmol, 1.0 eq.), DMF (25 mL) and a stirring-bar were introduced into a Schlenk-tube. After three freeze-pump-thaw cycles the tube was filled with argon and CuBr (38.0 mg, 0.27 mmol, 1.0 eq.) was added under a stream of argon. Subsequently, two freeze-pump-thaw cycles were performed, the tube backfilled with argon and the mixtures stirred at ambient temperature for 24 h. EDTA-solution (5 wt.%, 1 mL) was added and the residue was dialysed against deionized water with a SpectraPor3 membrane (MWCO = 2000 Da) for 3 days at ambient temperature. The solvent was removed *in vacuo* to yield the CD-functionalized polymer as a yellow solid (1.58 g, 68%, SEC(DMAc): $M_{nSEC} = 10300 \text{ g}\cdot\text{mol}^{-1}$, $D_m = 1.12$).

Exemplary Supramolecular Miktoarm Star Polymer-Formation via CD/Guest Interaction

Mid-chain adamantyl functionalized PDMAAm ($M_{nSEC} = 15800 \text{ g}\cdot\text{mol}^{-1}$; 100.0 mg, 0.006 mmol, 1.0 eq.) was dissolved in THF (2 mL) and added dropwise to a solution of CD-functionalized PDEAAm ($M_{nSEC} = 8000 \text{ g}\cdot\text{mol}^{-1}$; 50.6 mg, 0.006 mmol, 1.0 eq.) under vigorous stirring. The resulting solution was dialyzed against a deionized water/THF-mixture. The water-content was gradually changed from 70% to 100% over 1 day and the dialysis was continued for 3 days with deionized water at ambient temperature. The solvent was removed *in vacuo* to yield the supramolecular complex in quantitative yield. In a similar manner a control sample was prepared consisting of a CD-functionalized PDEAAm ($M_{nSEC} = 8000 \text{ g}\cdot\text{mol}^{-1}$; 25.0 mg, 0.003 mmol, 1.0 eq.) and non-adamantyl functionalized PDMAAm ($M_{nSEC} = 12300 \text{ g}\cdot\text{mol}^{-1}$; 38.4 mg, 0.003 mmol, 1.0 eq.) that was polymerized with EMP.

Modulation of the Thermoresponsivity of PDEAAm via CD Addition

7.1 Introduction

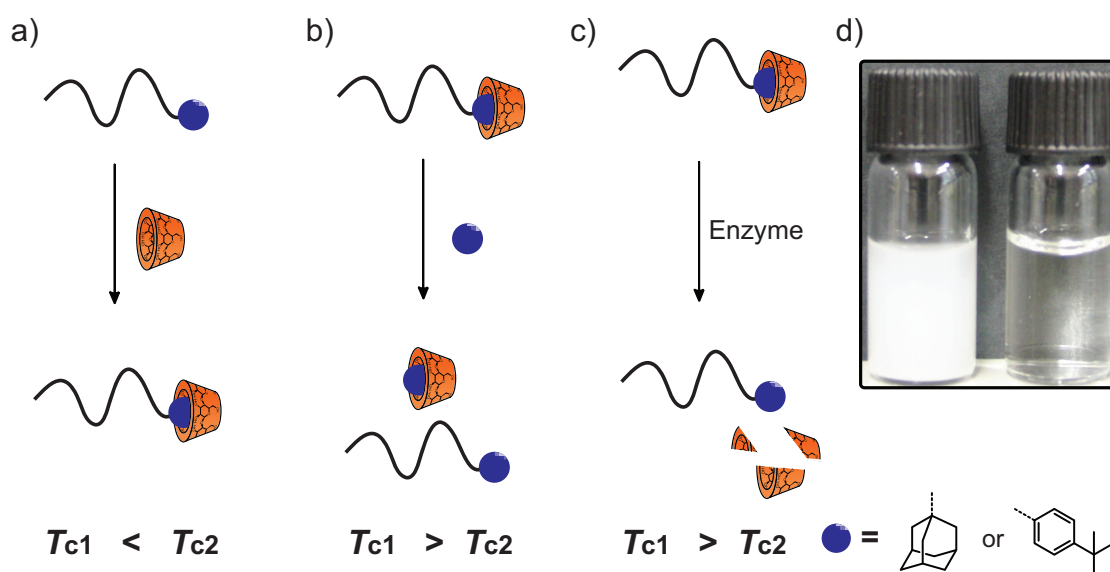
Thermoresponsive water soluble polymers have attracted much attention in the last years.^{294–297} This is especially due to a broad range of envisaged applications, in *e.g.* drug²⁹⁸ or gene delivery.²⁹⁹ Several polymer classes have been in the focus of polymer scientists, *e.g.* poly(oxazolines),³⁰⁰ poly(acrylamides) or poly(acrylates) with oligo(ethyleneglycol) sidechains.³⁰¹ In addition thermoresponsive blocks have been utilized in polymers with multiple stimuli responses, *i.e.* schizophrenic behavior.²²⁰ A common property of thermoresponsive water soluble polymers is a coil to globule transition at a certain critical temperature, *i.e.* the cloud point T_c . Either the polymers lose their water solubility upon heating to a certain temperature (LCST) or they dissolve upon heating (UCST). There are manifold examples of these two classes, *e.g.* PNIPAAm³⁰² for LCST-polymers or poly(*N*-acryloylglycinamide)³⁰³ for UCST-polymers. The T_c is governed by several factors such as ionic strength,³⁰⁴ polymer endgroups,²³³ polymer concentration, polymer topology³⁰⁵ or the addition of supramolecular hosts, *e.g.* β -CD via complexation of endgroups^{306,307} or polymer sidegroups.³⁰⁸ The variation of the polymer endgroup gives rise to modulations of the T_c , which can also be combined with external triggers or additional compounds, *e.g.* the masking of a hydrophobic endgroup with cucurbit[8]uril,³⁰⁹ the cleavage of a

NOESY measurements were performed in collaboration with M. Hetzer and Prof. H. Ritter (Heinrich Heine Universität Düsseldorf). Parts of this chapter were reproduced with permission from Schmidt, B. V. K. J.; Hetzer, M.; Ritter, H.; Barner-Kowollik, C. *Macromol. Rapid Commun.* **2013**, *34* (16), 1306-1311 (DOI: 10.1002/marc.201300478). Copyright 2013 John Wiley & Sons.

disulfide to remove a hydrophobic endgroup³¹⁰ or the photoisomerization of polymer endgroups³¹¹ via UV-light.

In the present chapter the modulation of the T_c of PDEAAm via the formation of supramolecular inclusion complexes between the guest-functionalized polymers and Me- β -CD or β -CD (Scheme 7.1) is described. The change in the T_c upon complexation was determined via turbidimetry measurements. Furthermore, the complexes were characterized via 2D NOESY. The modulation of the T_c could be reversed via addition of competing guest molecules or for the first time via enzymatic degradation of the added CDs, which is an outstanding property with regard to biomedical applications.

In the research on CD-complexed RAFT reagents for the reversible-deactivation radical polymerization of various acrylamides in aqueous solution (refer to Chapter 3) it was noticed that in the case of DEAAm a homogenous polymerization mixture was retained throughout the reaction time. Nevertheless, some of the obtained polymers showed no water solubility after the removal of Me- β -CD. This effect was assigned to the masking of the hydrophobic endgroups by the CD moiety and is investigated further in the present chapter.



Scheme 7.1: Overview of the examined concept. a) Increase of the T_c of PDEAAm (black) via addition of Me- β -CD or β -CD (orange); b) decrease of T_c after addition of competing guest molecules; c) decrease of T_c after degradation of CD upon enzyme addition; d) picture of crude doubly adamantyl functionalized PDEAAm ($M_n = 3000 \text{ g}\cdot\text{mol}^{-1}$) (left) and the polymer after complex formation with 2 eq. of Me- β -CD (right) at 10°C .

7.2 Results and Discussion

7.2.1 Synthesis of Guest Endfunctionalized PDEAAM

PDEAAM with different chain lengths and endgroups was prepared via RAFT polymerization in DMF at 60 °C using AIBN as initiator (Scheme 7.2). As endgroups for single and double functionalized polymers *tert*-butyl phenyl (via **1** and **2**), adamantyl (via **10** and **5**) or azobenzene (via **16** and **6**) were utilized (Figure 7.1). The obtained polymers were analyzed via SEC and subsequently subjected to measurements of the T_c (refer to Appendix E.1-E.7).

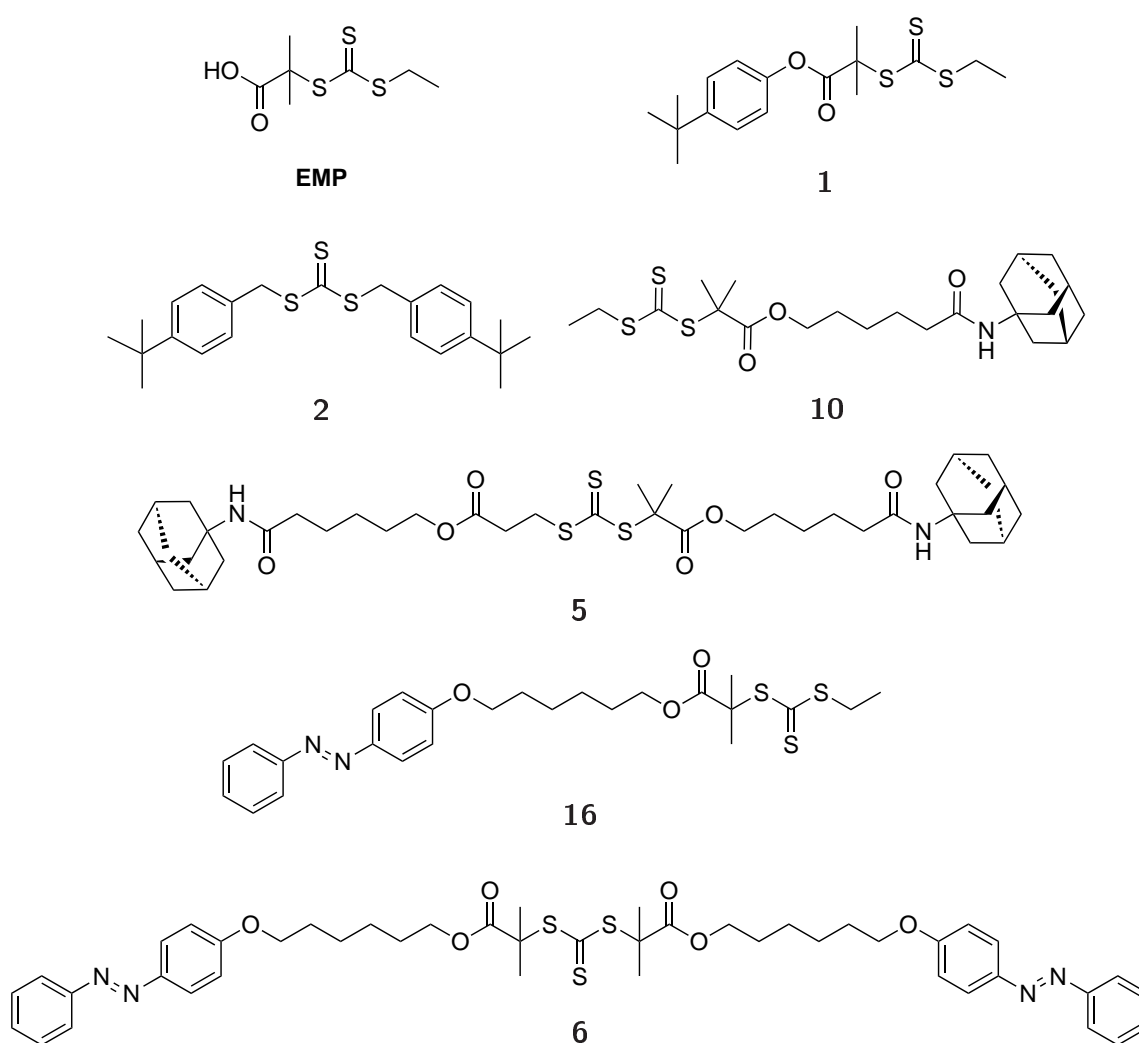
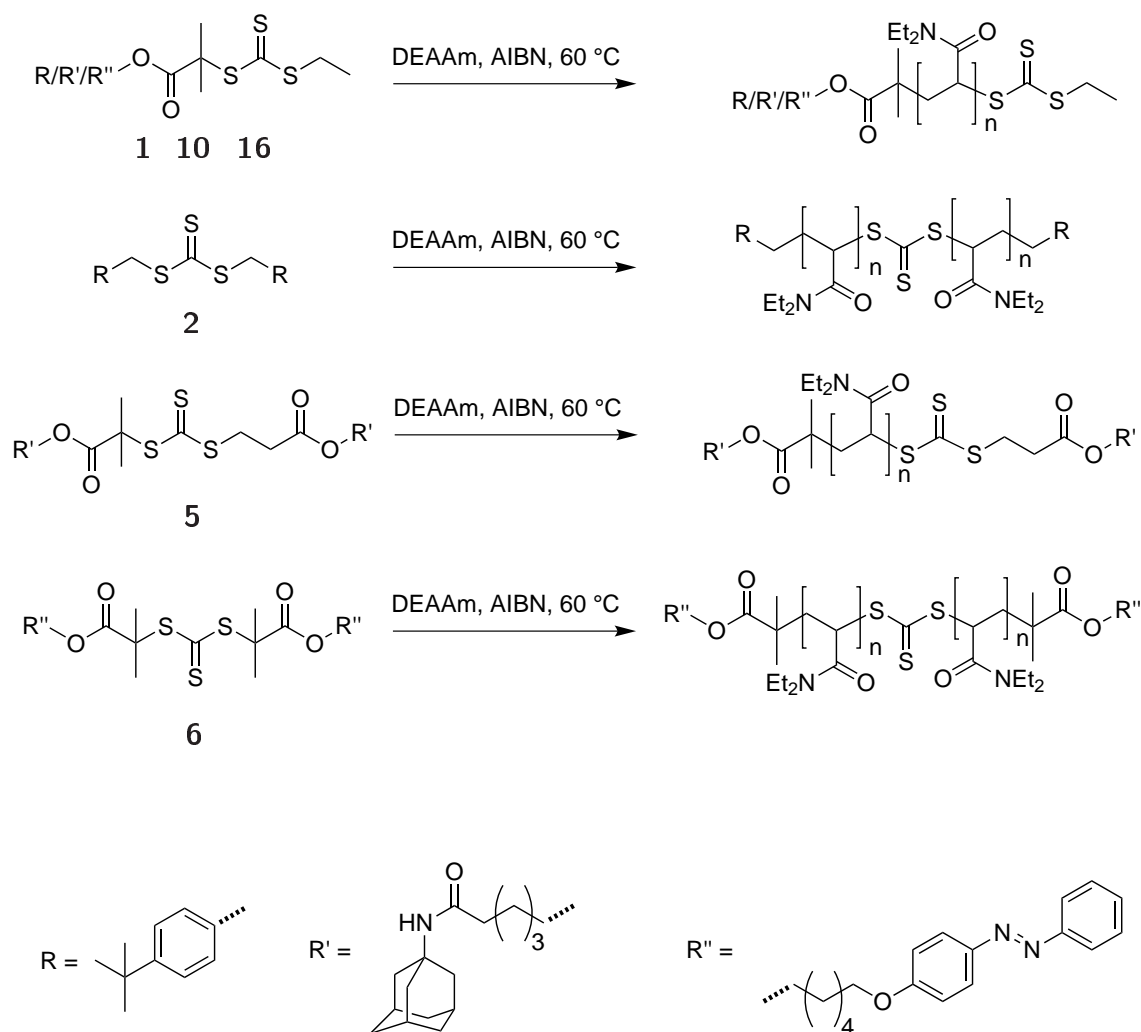


Figure 7.1: Structures of the utilized CTAs



Scheme 7.2: Polymerization of DEAAm in DMF at 60 °C with the respective CTA to generate the desired endfunctionalized polymers.

The effect of CDs on the solubility of PDEAAm can be readily visualized when a short chain PDEAAm with hydrophobic guest groups is considered, *e.g.* double adamantyl functionalized PDEAAm ($M_n = 3000 \text{ g}\cdot\text{mol}^{-1}$). Without the addition of Me- β -CD, the polymer is insoluble in water even at 4 °C, whereas after addition of Me- β -CD a clear solution of PDEAAm in water is obtained (refer to Scheme 7.1 d). The inclusion complex formation of the polymer endgroup with Me- β -CD can be proven via NOESY. In the case of *tert*-butyl phenyl guests, the expected cross correlation peaks between the signals of the inner CD protons at 3.6 and 3.8 ppm and the *tert*-butyl phenyl-protons at 1.3, 6.9 and 7.3 ppm (refer to Figure 7.2 a and b) are observed. For adamantyl guests cross correlation peaks between the inner CD protons and the adamantyl protons at 1.7, 2.0 and 2.2 ppm are evident (refer to Figure 7.2 c and d). Mixtures of azobenzene functionalized PDEAAm with Me- β -CD or α -CD show cross correlation peaks between the inner CD protons and the signals of the protons of the azobenzene moiety between 7.0 and 7.5 ppm. A control sample of carboxyl termi-

nated PDEAAm shows no cross correlation peaks in the respective regions (refer to Appendix E.1).

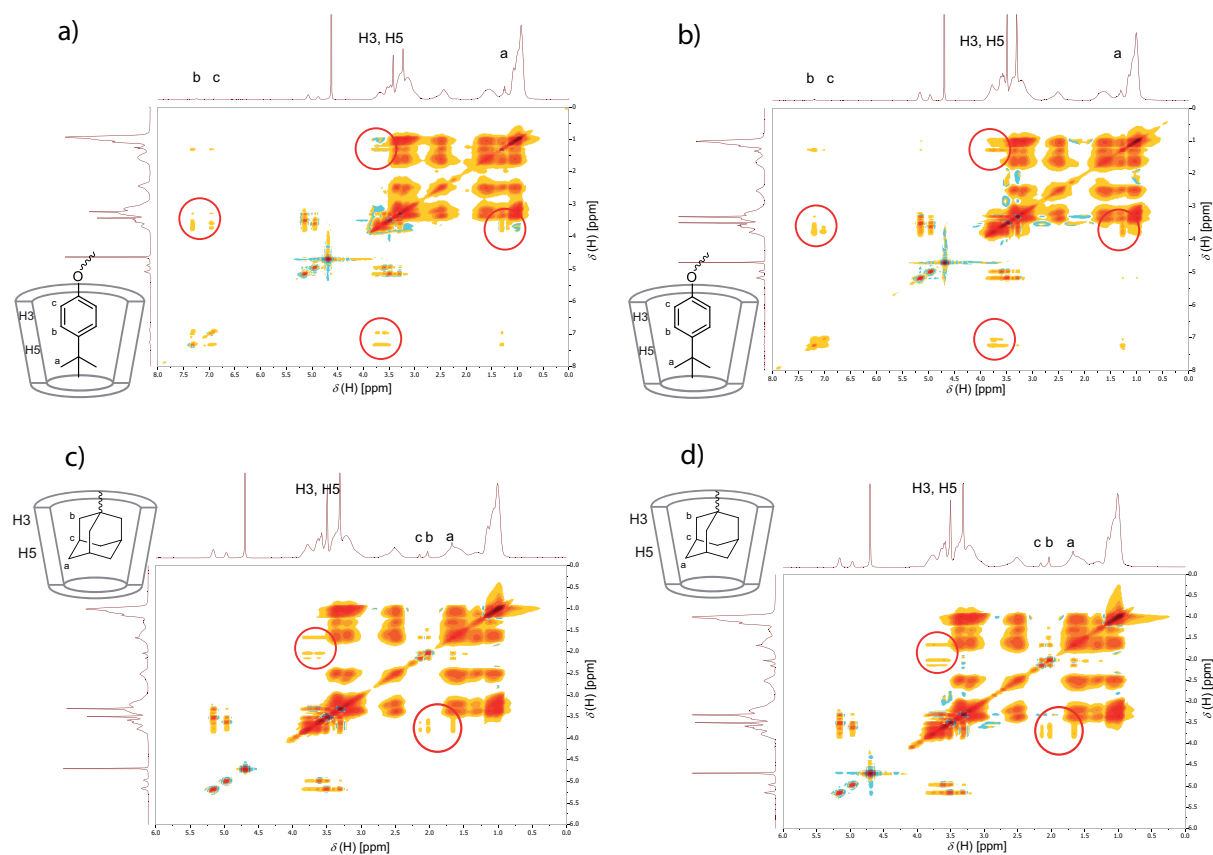


Figure 7.2: NOESY spectrum in D_2O at $25\text{ }^\circ\text{C}$ of a mixture of a) single *tert*-butyl phenyl functionalized PDEAAm ($M_n = 6500\text{ g}\cdot\text{mol}^{-1}$) and 2 eq. of Me- β -CD; b) double *tert*-butyl phenyl functionalized PDEAAm ($M_n = 5600\text{ g}\cdot\text{mol}^{-1}$) and 4 eq. of Me- β -CD; c) single adamantyl functionalized PDEAAm ($M_n = 4900\text{ g}\cdot\text{mol}^{-1}$) and 2 eq. of Me- β -CD; d) double adamantyl functionalized PDEAAm ($M_n = 7700\text{ g}\cdot\text{mol}^{-1}$) and 4 eq. of Me- β -CD.

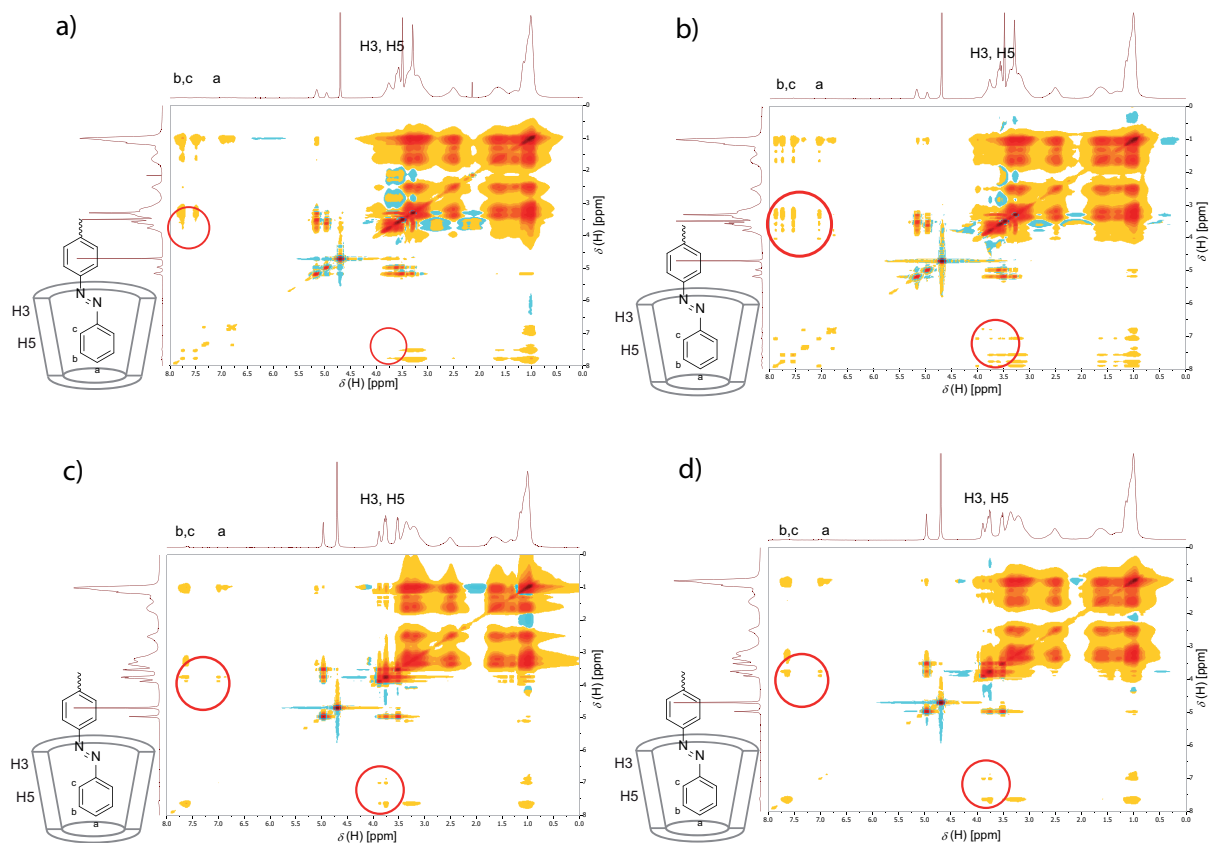


Figure 7.3: NOESY spectrum in D₂O at 25 °C of a mixture of a) single azobenzene functionalized PDEAAm ($M_n = 5000 \text{ g}\cdot\text{mol}^{-1}$) and 2 eq. of Me- β -CD; b) double azobenzene functionalized PDEAAm ($M_n = 11500 \text{ g}\cdot\text{mol}^{-1}$) and 4 eq. of Me- β -CD; c) single azobenzene functionalized PDEAAm ($M_n = 5000 \text{ g}\cdot\text{mol}^{-1}$) and 2 eq. of α -CD; d) double azobenzene functionalized PDEAAm ($M_n = 11500 \text{ g}\cdot\text{mol}^{-1}$) and 4 eq. of α -CD.

7.2.2 Turbidimetric Measurements: Influence of Guest Groups, Chain Length and CD/Endgroup Ratio

Apart from macroscopic observations, the apparent T_c s were measured via turbidimetry with and without the addition of Me- β -CD. Firstly, the effect of different guest groups and their quantity was probed. Transmittance versus temperature plots of exemplary chain lengths close to $5000 \text{ g}\cdot\text{mol}^{-1}$ are depicted in Figure 7.4 a. As expected, doubly guest functionalized PDEAAm exhibits a lower T_c compared to single functionalized PDEAAm due to the increased hydrophobicity of the chains, e.g. a T_c of 28.4 °C is observed for single *tert*-butyl phenyl functionalization and a T_c of 26.8 °C for double *tert*-butyl phenyl functionalization. Single adamantyl functionalized PDEAAm has a T_c of 29.8 °C and double adamantyl functionalized PDEAAm is not soluble in water over 4 °C. After addition of Me- β -CD, an increase of the T_c is observed that is also dependent on the respective guest group. For adamantyl guest

groups, large changes are evident, *e.g.* from 29.8 °C to 35.1 °C in the case of $M_n = 4900 \text{ g}\cdot\text{mol}^{-1}$. A completely different situation is observed in the case of azobenzene guests, as no significant changes in the T_c upon complexation are evident. This effect could be due to the more hydrophilic nature of azobenzenes and the weaker complexation with β -CD (refer to Appendix E.6 and E.7). Thus, the effect of addition of α -CD on the T_c of azobenzene functionalized PDEAAm was investigated due to higher association constants of α -CD with azobenzenes.² After addition of α -CD, similar T_c s of non-complexed and Me- β -CD complexed PDEAAm were observed (refer to Appendix E.8 and E.9). The observed T_c is increasing with increasing chain length. Nevertheless the T_c is not rising over 30 °C even for molecular masses over $10000 \text{ g}\cdot\text{mol}^{-1}$.

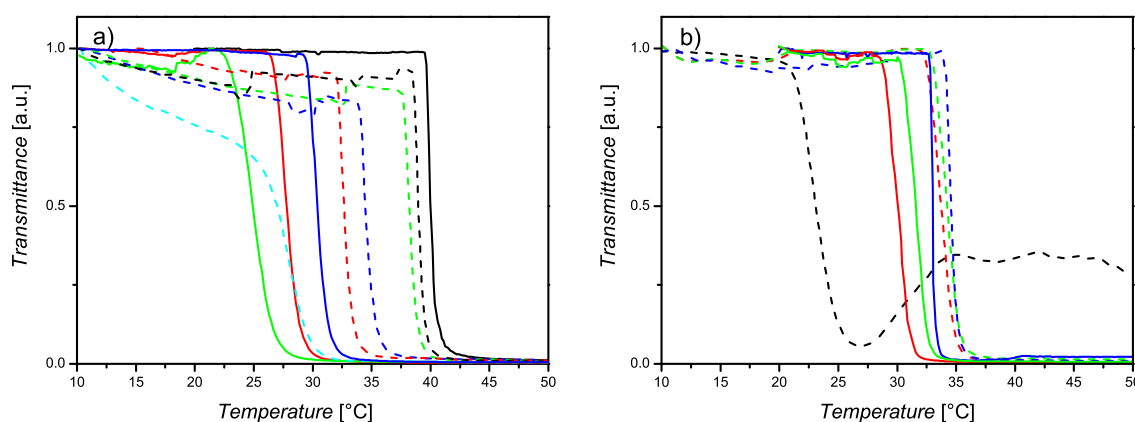


Figure 7.4: a) Turbidimetric measurements of PDEAAm with different guest groups (solid line: without Me- β -CD; dashed line: with Me- β -CD) and a M_n of approx. $5000 \text{ g}\cdot\text{mol}^{-1}$: carboxylic acid (black), double *tert*-butyl phenyl (green), single adamantyl (blue), single *tert*-butyl phenyl (red) and double adamantyl (turquoise, note: without Me- β -CD the T_c is below 4 °C); b) Turbidimetric measurements of PDEAAm with different M_n and single *tert*-butyl phenyl endgroup (solid line: without Me- β -CD; dashed line: with Me- β -CD): $M_n = 1800 \text{ g}\cdot\text{mol}^{-1}$ (black, note: without Me- β -CD the T_c is below 4 °C), $6500 \text{ g}\cdot\text{mol}^{-1}$ (red), $7700 \text{ g}\cdot\text{mol}^{-1}$ (green) and $11200 \text{ g}\cdot\text{mol}^{-1}$ (blue).

Furthermore, the dependence of the T_c from the polymer chain length was investigated (Figure 7.4 b). In general, T_c increases with increasing chain length for guest functionalized systems, *e.g.* the T_c comprises a range from insoluble at 4 °C to 33.0 °C from a molecular mass of 1800 to $11200 \text{ g}\cdot\text{mol}^{-1}$ in the case of single *tert*-butyl phenyl functionalized PDEAAm without the addition of Me- β -CD. The complex formation with Me- β -CD leads to an increase of the T_c from 6.0 °C to 1.5 °C resulting in a range of observed T_c s from 22.9 °C to 34.5 °C (refer to Figure 3b and an additional discussion in the Supporting Information Section for the other guest systems). The differences in the T_c between Me- β -CD associated and non-associated PDEAAm decrease with molar mass of the polymers. This is due to the weaker influence of the hydrophobic end-

groups with a larger hydrophilic fraction in the polymer. In the case of carboxylic acid functionalized PDEAAm, the T_c is almost constant around 37.5 °C to 41.1 °C regardless of the addition of Me- β -CD which leads to T_c s from 38.8 °C to 41.6 °C. In general, the possible ranges of T_c modulation with CD complexes is dependent on the chain length, the hydrophobicity of the guest group and the number of guest groups (Figure 7.5). As stated already, T_c increases with increasing chain length of PDEAAm. In the case of double *tert*-butyl phenyl functionalized PDEAAm, the observed T_c increases from insoluble with a M_n of 1800 g·mol⁻¹ to 30.7 °C for a M_n of 7400 g·mol⁻¹. After addition of 2 equivalents of Me- β -CD, the T_c shifts to 33.5 °C for a M_n of 1800 g·mol⁻¹ and to 36.7 °C for a M_n of 7400 g·mol⁻¹. Single adamantyl functionalized PDEAAm shows T_c s of 27.3 °C for a M_n of 3200 g·mol⁻¹ and 33.7 °C for a M_n of 8300 g·mol⁻¹. The association of the endgroups with Me- β -CD leads to a T_c of 33.4 °C for a M_n of 3200 g·mol⁻¹ and 35.6 °C for a M_n of 8300 g·mol⁻¹. For the double adamantyl functionalized PDEAAm samples only PDEAAm with higher molecular mass of 12700 g·mol⁻¹ is soluble in water with a T_c of 33.0 °C. The addition of Me- β -CD leads to solubilization of all samples. For a M_n of 5100 g·mol⁻¹, a T_c of 27.8 °C is observed, while a T_c of 36.1 °C is observed for a M_n of 12700 g·mol⁻¹. Similar trends are observable for both guest systems. In the case of the *tert*-butyl phenyl and adamantyl endgroups, the T_c converges at molecular masses exceeding 8000 g·mol⁻¹ to a value of approximately 33 °C, which is close to the reported value in the literature.²⁴² It is noteworthy that carboxylic acid functionalized PDEAAm has even higher T_c s close to 40 °C, probably due to additional hydrogen bonding interactions. The addition of Me- β -CD leads to a shift in the observed T_c from approximately 37 °C to 40 °C. For shorter chain polymers with M_n below 8000 g·mol⁻¹, T_c s of approximately 33 °C are observed. Interestingly, at chain lengths over 8000 g·mol⁻¹ the T_c still increases after Me- β -CD and converges to the value of carboxylic acid functionalized PDEAAm, which shows that the addition of CDs does not only shield the hydrophilic endgroups but also increases the hydrophilicity of the chain ends (Figure 7.5).

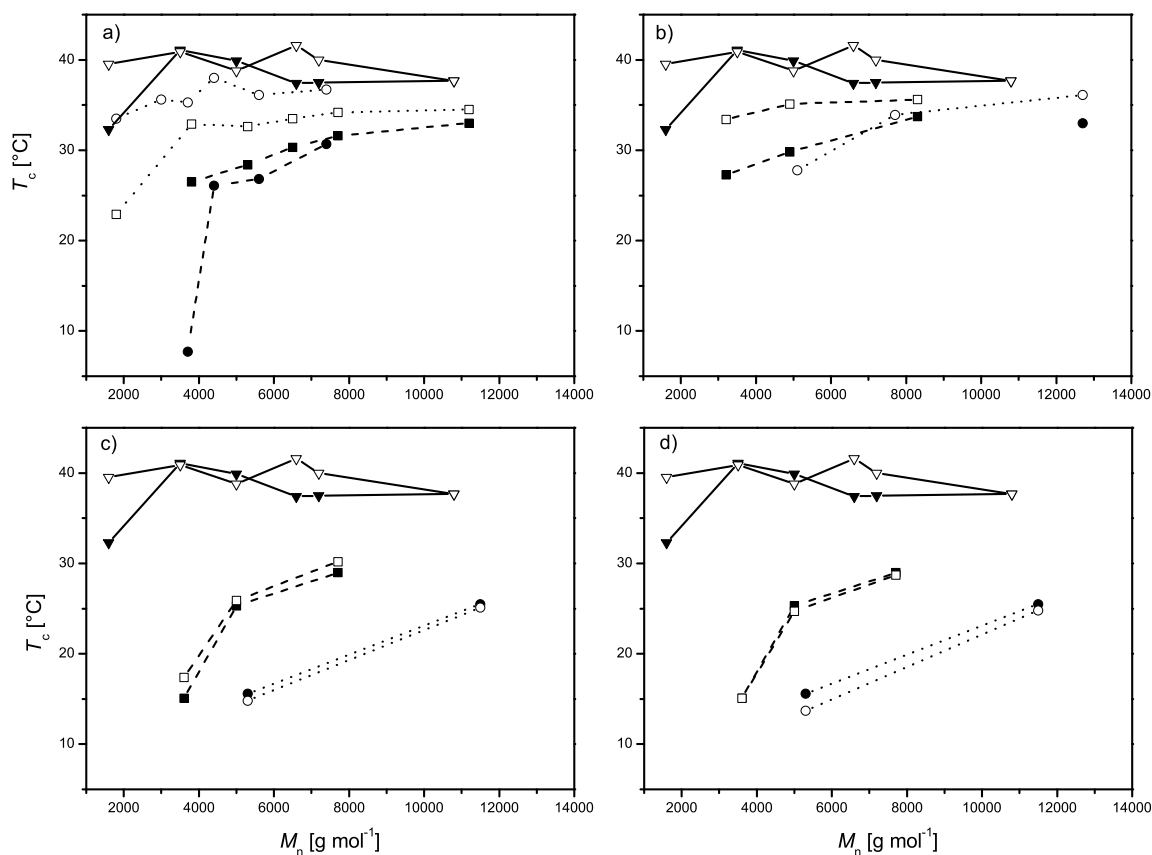


Figure 7.5: Observed T_c s as a function of M_n for PDEAAm (filled symbols) and complexed PDEAAm (open symbols; a), b), c) Me- β -CD addition and d) α -CD addition): a) single *tert*-butyl phenyl guest (squares), double *tert*-butyl phenyl guests (circles) and carboxylic acid functionalization (triangles); b) single adamantyl guest (squares), double adamantyl guests (circles) and carboxylic acid functionalization (triangles); c) and d) single azobenzene guest (squares), double azobenzene guests (circles) and carboxylic acid functionalization (triangles).

The dependence of endgroup / Me- β -CD ratio on the T_c was investigated as well (Figure 7.6 and Appendix E.10). Initially for short chain guest functionalized polymers ($M_n = 3800 \text{ g}\cdot\text{mol}^{-1}$) upon Me- β -CD addition the transmittance versus temperature plot shows the expected sharp increase in turbidity at the T_c . Unexpectedly, the turbidity decreases again after further heating (see also Figure 7.4 b and 7.7 b: black dashed line). The variation of the Me- β -CD / polymer endgroup ratio reveals an unexpected behavior. For short chain guest functionalized polymers with pendant complexed Me- β -CD ($M_n = 3800 \text{ g}\cdot\text{mol}^{-1}$), the transmittance versus temperature plot shows the expected sharp increase in turbidity at the T_c . The turbidity decreases again after further heating, whereas control samples with carboxylic acid endfunctionalization and comparable M_n do not show such a behavior. This effect clearly indicates that the behavior is due to host/guest complexation. The cooling curve does not show such a behavior, yet a slower transition is observed resulting in a large discrepancy of the T_c from heating ramp and cooling ramp. With a longer chain guest functional

PDEAAm ($M_n = 6500 \text{ g}\cdot\text{mol}^{-1}$), only minor discrepancies of the T_c between the heating and cooling ramp are observed. Nevertheless, the decreasing turbidity after the first sharp increase is observed, yet to a weaker extent as well. A possible explanation is that after the phase transition at the T_c the complexes begin to break up, which leads to free Me- β -CD molecules in solution that interact with the insoluble polymers and change the turbidity of the solution.

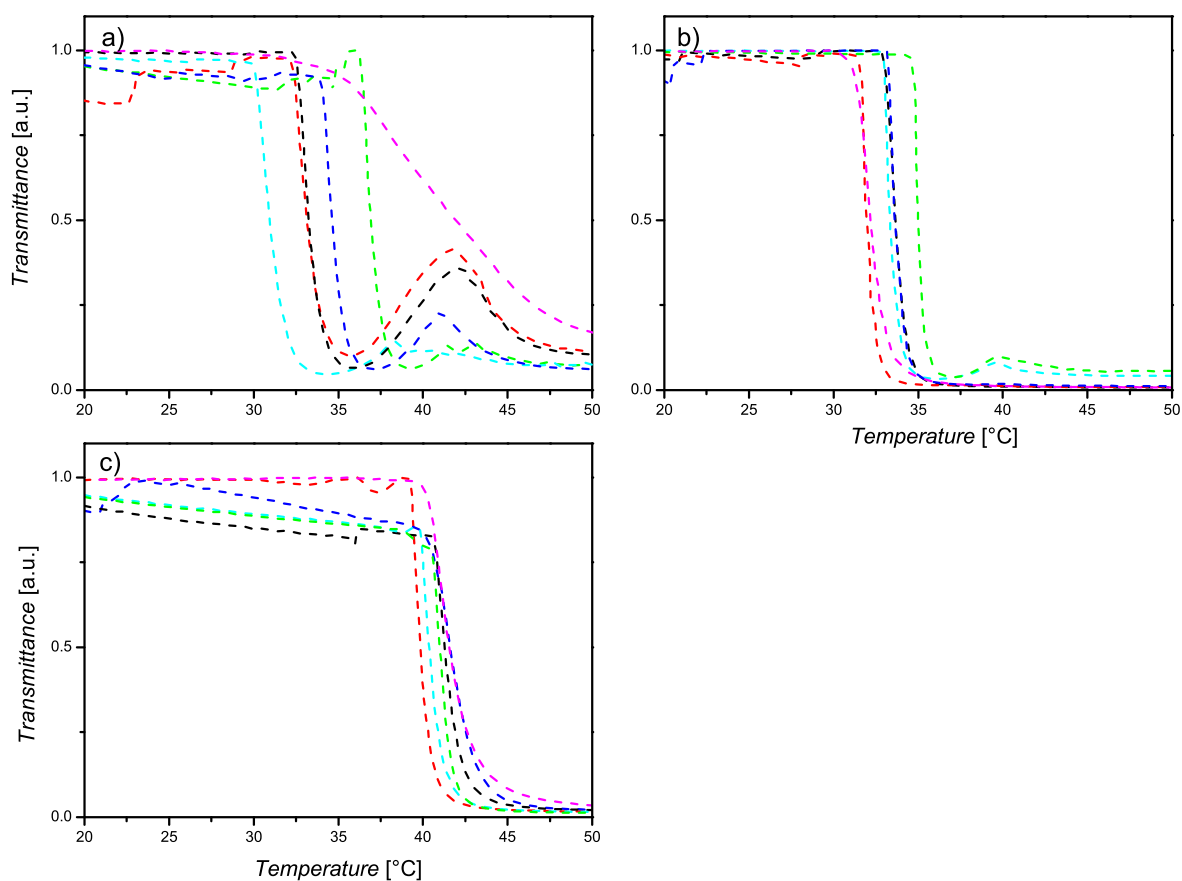


Figure 7.6: Turbidimetric measurements of PDEAAm with different Me- β -CD equivalents (heating ramps: 1.0 eq. red curve; 1.5 eq. turquoise curve; 2.0 eq. black curve; 3.0 eq. blue curve; 5.0 eq. green curve; cooling ramp: 2.0 eq. magenta curve): a) single *tert*-butyl phenyl group ($M_n = 3800 \text{ g}\cdot\text{mol}^{-1}$), b) single *tert*-butyl phenyl group ($M_n = 6500 \text{ g}\cdot\text{mol}^{-1}$) and c) carboxylic acid group ($M_n = 3500 \text{ g}\cdot\text{mol}^{-1}$).

7.2.3 Reversal of the Effect via External Stimuli

As the addition of Me- β -CD leads to significant changes in the observed T_c s, removal of the CD moieties should give the opportunity to decrease the T_c again or even to precipitate the uncomplexed PDEAAm strands. One possibility is the addition of an excess of guest molecules that should shift the equilibrium to uncomplexed polymers and therefore change the observed T_c (refer to Figure 7.7 a and b). As an example, single *tert*-butyl phenyl ($M_n = 3800 \text{ g}\cdot\text{mol}^{-1}$) and double *tert*-butyl phenyl ($M_n = 5600 \text{ g}\cdot\text{mol}^{-1}$) functionalized PDEAAm was complexed with 2 equiv. of Me- β -CD and an excess of 16 equiv. 1-adamantyl amine hydrochloride was added. A decrease in the T_c towards the T_c of uncomplexed PDEAAm was observed, *i.e.* from 32.9 °C to 27.9 °C for single *tert*-butyl phenyl functionalized PDEAAm ($M_n = 3800 \text{ g}\cdot\text{mol}^{-1}$) (refer to Appendix E.11).

Apart from the addition of competing guests, destruction of the added CD molecules should lead to a shift in T_c as well. An enzymatic pathway is a valid and biocompatible choice, *e.g.* via hydrolysis of the α -1,4-glycosidic bond in CD with α -amylase. Incubation of beforehand β -CD complexed PDEAAm with Taka diastase from *aspergillus oryzae* leads to a significant shift in T_c from 30.4 °C to 26.5 °C in the case of double *tert*-butyl phenyl functionalized PDEAAm ($M_n = 4400 \text{ g}\cdot\text{mol}^{-1}$) (refer to Figure 7.7 c and Appendix E.12), which is close to the obtained T_c for the respective uncomplexed sample. For a control sample with non-guest functionalized PDEAAm, no shift was observed (Figure 7.7 d). Thus not only an increase in T_c upon complex formation was observed, but the situation could be reversed via addition of a competing guest or enzymatically.

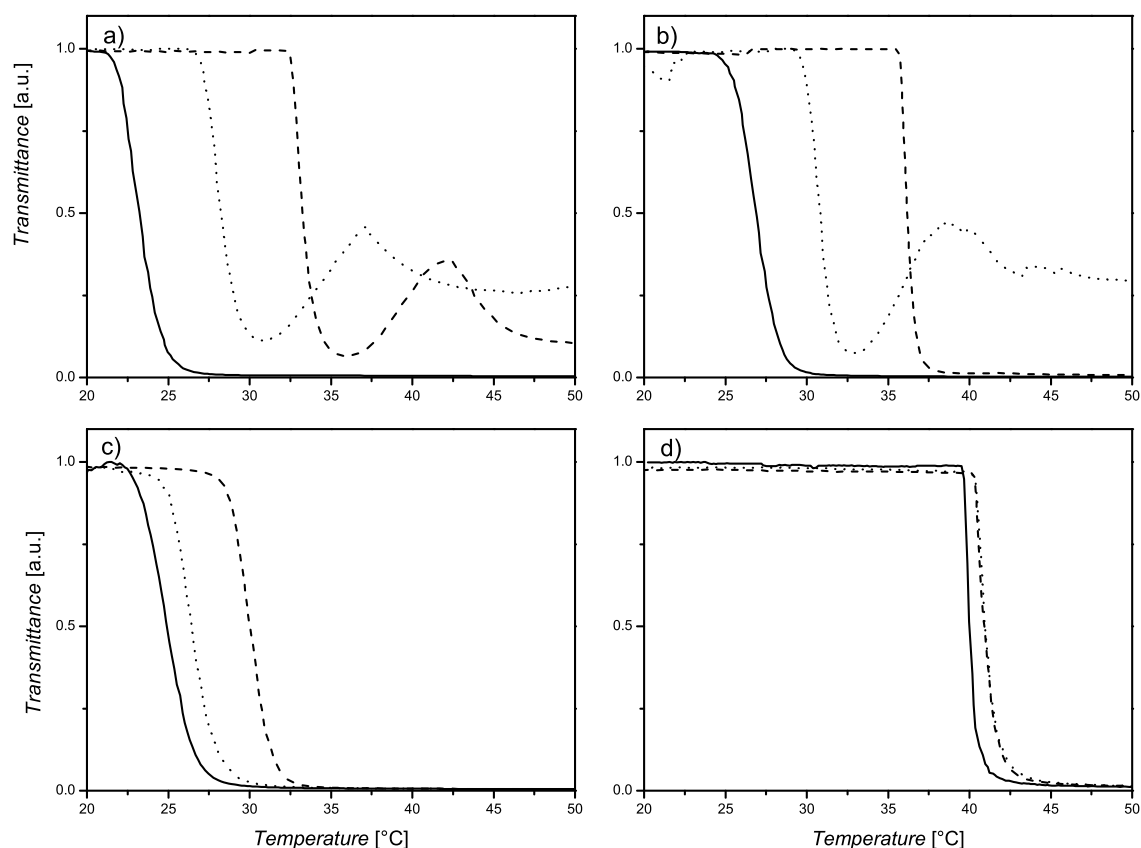


Figure 7.7: a) Turbidimetric measurements of PDEAAm with single *tert*-butyl phenyl group ($M_n = 3800 \text{ g}\cdot\text{mol}^{-1}$): without Me- β -CD (solid line), with 2 eq. Me- β -CD (dashed line) and after addition of 16 eq. 1-adamantylamine hydrochloride (dotted line); b) turbidimetric measurements of PDEAAm with double *tert*-butyl phenyl group ($M_n = 5600 \text{ g}\cdot\text{mol}^{-1}$): without Me- β -CD (solid line), with 2 eq. Me- β -CD (dashed line) and after addition of 16 eq. 1-adamantylamine hydrochloride (dotted line); c) turbidimetric measurements of PDEAAm with double *tert*-butyl phenyl group ($M_n = 4400 \text{ g}\cdot\text{mol}^{-1}$): without β -CD (solid line), with 2 eq. β -CD (dashed line) and after enzymatic treatment (dotted line); d) turbidimetric measurements of PDEAAm with carboxylic acid group ($M_n = 5000 \text{ g}\cdot\text{mol}^{-1}$): without β -CD (solid line), with 2 eq. β -CD (dashed line) and after enzymatic treatment (dotted line).

7.3 Conclusions

In summary, we have evidenced that the T_c of aqueous guest functionalized PDEAAm solutions is responsive to the addition of CD host molecules. The formation of supramolecular host/guest complexes of the hydrophobic polymer endgroups with CDs leads to a shielding of the hydrophobic nature of the pendant guests. Furthermore, the effect of different guest groups, the chain length and the endgroup / CD ratio was investigated, showing a broad tuneability of the T_c . Addition of competing guest molecules or CD degrading enzymes gives the opportunity to reverse the observed

change of the T_c in a straightforward and – in the case of enzymatic treatment – bio-compatible fashion.

7.4 Experimental Part

Synthesis of 6-(4-(phenyldiazenyl)phenoxy)hexyl 2-(((ethylthio)carbonothioyl)thio)-2-methylpropano-ate (16)

In a 50 mL Schlenk-flask **EMP** (0.75 g, 3.35 mmol, 1.0 eq.), 6-(4-(phenyldiazenyl)phenoxy)hexan-1-ol (1.25 g, 5.02 mmol, 1.5 eq.) and DMAP (0.08 g, 0.67 mmol, 0.2 eq.) were dissolved in anhydrous DCM (15 mL). At 0 °C, a solution of DCC (1.04 g, 5.02 mmol, 1.5 eq.) in anhydrous DCM (10 mL) was added. After one hour the solution was warmed to ambient temperature, stirred overnight, filtered and concentrated under reduced pressure. The residual oil was purified via column chromatography on silica-gel with a 20:1 mixture that was changed gradually to 15:1 of *n*-hexane:ethyl acetate as eluent. The product-containing fractions were concentrated and the residue recrystallized from *n*-hexane:ethyl acetate. The product was obtained as orange crystals (1.10 g, 2.42 mmol, 72%).

$^1\text{H-NMR}$ (400 MHz, CDCl_3): [δ , ppm] = 1.31 (t, $^3J = 7.4$ Hz, 3H, $\text{CH}_3\text{-CH}_2$), 1.38 - 1.56 (m, 4H, 2x $\text{CH}_2\text{-CH}_2\text{-CH}_2\text{-O}$), 1.57 - 1.75 (m, 10H, 2x C-CH_3 ; $\text{O=C-O-CH}_2\text{-CH}_2$), 1.81 (m, 2H, $\text{O-CH}_2\text{-CH}_2$), 3.27 (q, $^3J = 7.4$ Hz, 2H, $\text{CH}_3\text{-CH}_2$), 4.04 (t, $^3J = 6.4$ Hz, 2H, $\text{CH}_2\text{-O}$), 4.12 (t, $^3J = 6.4$ Hz, 2H, $\text{CH}_2\text{-O-C=O}$), 7.00 (d, $^3J = 8.9$ Hz, 2H, $\text{CH}_{\text{arom.}}$), 7.40 - 7.55 (m, 3H, $\text{CH}_{\text{arom.}}$), 7.82 - 7.97 (m, 4H, $\text{CH}_{\text{arom.}}$). $^{13}\text{C-NMR}$ (100 MHz, CDCl_3): [δ , ppm] = 13.1 ($\text{CH}_2\text{-CH}_3$), 25.5 (2x $\text{CH}_3\text{-C}$), 25.8 and 25.9 (2x $\text{CH}_2\text{-CH}_2\text{-CH}_2\text{-O}$), 28.4 ($\text{O-CH}_2\text{-CH}_2$), 29.2 ($\text{O=C-O-CH}_2\text{-CH}_2$), 31.3 ($\text{CH}_2\text{-CH}_3$), 56.1 ($\text{C}(\text{CH}_3)_2$), 66.1 (O=C-O-CH_2), 68.3 (O-CH_2), 114.8 (2x $\text{O-CH}_{\text{arom.}}\text{-CH}_{\text{arom.}}$), 122.7 (2x $\text{CH}_{\text{arom.}}$), 124.9 (2x $\text{CH}_{\text{arom.}}$), 129.2 (2x $\text{CH}_{\text{arom.}}$), 130.4 ($\text{CH}_{\text{arom.}}$), 147.0 ($\text{C}_{\text{arom.}}\text{-N=N}$), 152.9 ($\text{C}_{\text{arom.}}\text{-N=N}$), 161.8 ($\text{O-C}_{\text{arom.}}$), 173.1 (C=O), 221.4 (C=S). **ESI-MS**: [$\text{M} + \text{H}^+$] $_{\text{exp}} = 505.25$ m/z and [$\text{M} + \text{H}^+$] $_{\text{calc}} = 505.17$ m/z.

Exemplary Synthesis of Endfunctionalized PDEAAm

1 (26.1 mg, 0.073 mmol, 1.0 eq.), DEAAm (311 mg, 2.49 mmol, 33.0 eq.), AIBN (2.4 mg, 0.015 mmol, 0.2 eq.), DMF (2.0 mL) and a stirring-bar were added into a Schlenk-tube. After three freeze-pump-thaw cycles the tube was backfilled with argon, sealed, placed in an oil bath at 60 °C and removed after 24 h. The tube was subsequently cooled with liquid nitrogen to stop the reaction. A NMR-sample was withdrawn for the determination of the conversion, inhibited with a pinch of hydroquinone (approx. 5 mg) and CDCl₃ was added. A conversion of 99% was calculated based on the NMR data (see Characterization Methods for details of the calculation). The residue was dialysed against deionized water with a SpectraPor3 membrane (MWCO = 1000 Da) for 3 days at ambient temperature. The solvent was removed *in vacuo* to yield the polymer as a yellow solid (243 mg, 72%, $M_{\text{ntheo}} = 4500 \text{ g}\cdot\text{mol}^{-1}$, SEC(THF): $M_{\text{nSEC}} = 3800 \text{ g}\cdot\text{mol}^{-1}$, $D_{\text{m}} = 1.08$).

Exemplary Procedure for the Preparation of the Complexes for the Measurement of T_c

PDEAAm polymerized with **1** ($M_{\text{nSEC}} = 6500 \text{ g}\cdot\text{mol}^{-1}$; 3.0 mg, 0.46 μmol , 1.0 eq.) and Me- β -CD (1.2 mg, 0.96 μmol , 2.0 eq.) were added into a vial. Deionized H₂O (3 mL) was added and the solution stirred for 1 day at ambient temperature and kept in the fridge for 1 day. Subsequently, the T_c was measured according to the Characterization Methods Section.

Exemplary Procedure for the Shifting of the T_c via addition of Competing Guests

PDEAAm polymerized with **1** ($M_{\text{nSEC}} = 3800 \text{ g}\cdot\text{mol}^{-1}$; 3.0 mg, 0.79 μmol , 1.0 eq.) and Me- β -CD (1.8 mg, 1.37 μmol , 1.7 eq.) were added into a vial. Deionized H₂O (3 mL) was added and the solution stirred for 1 day at ambient temperature and kept in the fridge for 1 day. Subsequently, 1-adamantyl amine hydrochloride (2.4 mg, 12.78 μmol , 16.0 eq.) was added and the solution stirred for 2 days at ambient temperature. Finally, the T_c was measured according to the Characterization Methods Section.

Exemplary Procedure for the Shifting of the T_c via Enzymatic Treatment

PDEAAm polymerized with **17** ($M_{nSEC} = 4400 \text{ g}\cdot\text{mol}^{-1}$; 3.0 mg, 0.69 μmol , 1.0 eq.) and β -CD (1.5 mg, 1.36 μmol , 2.0 eq.) were added into a vial. Deionized H_2O (3 mL) was added and the solution stirred for 1 day at ambient temperature and kept in the fridge for 1 day. Subsequently, Taka Diastase from *aspergillus oryzae* (approx. 0.5 mg) was added and the solution was stirred for 2 days at 33 °C. Finally, the sample was cooled in the fridge, filtered and the T_c was measured according to the Characterization Methods Section.

Conclusions and Outlook

Supramolecular chemistry has emerged as an important tool in contemporary polymer science. The utilization of supramolecular motifs, *e.g.* hydrogen bonding, metal-complexes or inclusion complexes, has led to a broad range of materials with novel properties and promising applications in the life and material sciences. The development of reversible-deactivation radical polymerization techniques had a very significant impact on polymer science as well, especially for the preparation of novel complex macromolecular architectures. The combination of both concepts to generate supramolecular driven complex macromolecular architectures is a highly important research topic from the view of fundamental science, yet with regard to applications as well.

One reasonable approach for the formation of complex macromolecular architectures governed by supramolecular interactions is the incorporation of supramolecular motifs into polymers *via* end functionalization, which can be conducted *via* click chemistry or the synthesis of the respective controlling agents. The control over polymer functionality is essential in such an approach and is certainly possible *via* RAFT polymerization. Such a functionality guided attempt facilitates the formation of complex macromolecular topologies and thus the combination of variable building blocks enables the formation of complex macromolecular architectures. Another key feature of the supramolecular approach is the possibility to combine the building blocks in a modular fashion. As different building blocks are combined to form complex architectures *via* specific supramolecular recognition motifs, it is easily possible to exchange the respective building blocks, *e.g.* with different polymer-types and thus to change the properties of the obtained materials easily.

In the current thesis, CDs were utilized as supramolecular motifs that are capable of forming inclusion complexes with hydrophobic molecules in aqueous solution.

Their complexation ability was exploited in a new method to solubilize hydrophobic RAFT agents and subsequently perform RAFT polymerizations of several acrylamides, *i.e.* DMAAm, DEAAm and NIPAAm, in aqueous solution. Thus, hydrophilic polymers with hydrophobic endgroups were prepared in water in one step. In addition to the novel method for controlling chain endfunctionality, CDs were incorporated in polymers as endgroup. In combination with guest functionalized polymers, several complex macromolecular architectures were formed. Mono CD functionalized PHPMA was conjugated supramolecularly with doubly guest functionalized PDMAAm or PDEAAm to form supramolecular ABA block copolymers. In this case the stimuli responsive behavior of the supramolecular linkage was probed, *i.e. via* a temperature- and light-response. Thus, the formed triblock copolymers were disassembled upon external stimuli. Furthermore, the thermo-responsive PDEAAm block allowed the investigation of temperature-induced micellization. In the area of star architectures a three fold CD functional core was attached to guest endfunctionalized polymers to form three arm star polymers that showed disassembly of the stars at increased temperatures and re-formation of the supramolecular assemblies after cooling. An AB₂ miktoarm star polymer was prepared with CD-functionalized PDEAAm and a mid-chain guest functionalized PDMAAm. Again, the thermoresponsive nature of PDEAAm was utilized to form temperature-induced aggregates. Additionally, the thermoresponsive behavior of PDEAAm was modulated *via* complexation of hydrophobic endgroups with CD. This effect could be reversed *via* the addition of competing guest molecules or in a biocompatible way *via* enzymatic degradation of the CD molecules.

In conclusion, CD driven macromolecular architectures were put on a new level: From control over endgroups to complex architectures such as block copolymers or star polymers. Especially incorporation of stimuli-responsive linkages have proven to be a powerful property of the presented systems, especially if future applications are considered, *e.g.* drug-delivery or the formation of nano-objects. Furthermore, the utilization of thermoresponsive building blocks allows temperature-induced aggregation, which has again uses in drug-delivery. The next step with the materials presented in this thesis, is to put them to use in first application oriented studies, *e.g.* drug encapsulation and release or microphase separation of block copolymers.

CD-based macromolecular architectures are an interesting area of research that is at a turning point. Almost every conceivable architecture has been prepared so far and the focus of polymer scientists is turning from the fundamental level to more application oriented research. Biomedical science is the most promising area for applications in that regard, *e.g.* for drug-delivery. CDs are a viable choice in that case as native CDs are biocompatible and are already employed in food technology or drug-delivery. Furthermore, the association of CDs and guest molecules is performed in an aque-

ous environment, which is the solvent of choice for biological applications. From the point of view of biomedical applications, the frequently utilized CuAAC, which is certainly used so frequently due to the convenient preparation of mono azido functional CD, has to be exchanged with biocompatible click reactions, *e.g.* thiol-ene reactions or Diels-Alder processes. Branched structures and hydrogels have proven to be an important area of CD-based polymer science. This area will be important with regard to applications in the future as well, *e.g.* the formation of microgels, hydrogels for drug-delivery or self-healing materials. Another area of rising importance in polymer science is the modification of surfaces and first steps of supramolecular surface modifications with CDs have been undertaken already in the Barner-Kowollik group and other research groups as well. Nevertheless, there are many opportunities left for different applications of supramolecularly attached molecules on surfaces.

Experimental Part

Experiments employing anhydrous solvents were conducted with standard Schlenk-techniques under an atmosphere of argon. The glassware was dried with a heat-gun under high vacuum and the flasks were backfilled with argon prior to addition of reagents.

9.1 Materials

Acetic acid (Roth, 99%), 1-adamantylamine hydrochloride (ABCR, 99%), aluminium chloride (ABCR, 99%), 2-amino-1-propanol (TCI, 98%), 4,4'-azobis(4-cyanovaleric acid) (V-501; Sigma Aldrich, 98%), β -cyclodextrin (β -CD; Wacker, pharmaceutical grade), 2,2-bis(hydroxymethyl)propionic acid (Sigma Aldrich, 98%), 2-bromoisobutyric acid (Sigma Aldrich, 98%), 3-bromopropionyl chloride (ABCR, 90%), carbon disulfide (Acros, 99.9%), 1-chloro-6-hydroxyhexane (Acros, 95%), copper bromide (Sigma Aldrich, 99%), deuterated acetone (acetone-D₆; Euriso-top, 99.8%), deuterated chloroform (CD-Cl₃; Euriso-top, 99.9%), deuterated dimethylsulfoxide (DMSO-D₆; Euriso-top, 99.8%), deuterium oxide (D₂O; Euriso-top, 99.9%), diisopropylazodicarboxylate (DIAD; ABCR, 94%), *N,N'*-dicyclohexylcarbodiimide (DCC; ABCR, 99%), *N,N*-dimethylamino-pyridine (DMAP; Sigma Aldrich, 99%), *N,N*-dimethylformamide (DMF; ABCR, 99%), Dowex 50WX2-100 ion-exchange resin (Sigma Aldrich), ϵ -caprolactone (CL; Alfa Aesar, 99%), ethanethiol (Acros, 99%), ethylenediaminetetraacetic acid disodium salt (EDTA; ABCR, 99%), hydroquinone (Fluka, 99%), iodine (Acros, 99.5%), 3-mercaptopropionic acid (Acros, 99%), methacryloyl chloride (Sigma Aldrich, 97%), 4-*tert*-butyl benzylbromide (Acros, 97%), 4-*tert*-butyl phenol (Sigma Aldrich, 99%), 4-*tert*-butyl aniline (Acros, 99%), 4-*tert*-butylbenzyl mercaptan (Sigma Aldrich, 99%), *p*-toluenesulfonic acid monohydrate (Sigma Aldrich, 99%), *p*-toluenesulfonyl chloride (ABCR, 98%), *N,N,N',N'',N''*-pentamethyldiethyltriamine (PMDETA; Merck, 99.9%), 4-phenyl-

azophenol (ABCR, 98%), potassium carbonate (VWR, rectapur), potassium iodide (Sigma Aldrich, 99%), potassium phosphate monohydrate (Sigma Aldrich, puriss.), propargylalcohol (Alfa Aesar, 99%), randomly methylated β -cyclodextrin (Me- β -CD, average methylation grade 1.8 per glucose unit, pharmaceutical grade, was a gift from Wacker), silica gel (Merck, Geduran SI60 0.063 - 0.200 mm), sodium acetate (Roth, 99%), sodium azide (Acros, 99%), sodium hydroxide (Roth, 99%), Taka-Diastase from *aspergillus oryzae* (Sigma Aldrich, 126 u·mg⁻¹), tetrabutyl ammonium hydrogen sulfate (Sigma Aldrich, 97%), triethylamine (Acros, 99%), trifluoroacetic acid (TFA; ABCR, 99%), triphenylphosphine (Merck, 99%), tripropargylamine (Sigma Aldrich, 98%) were used as received. Anhydrous dichloromethane (DCM), *N,N*-dimethylformamide (DMF) and tetrahydrofuran (THF) were purchased from Acros (extra dry over molecular sieves) and used as received. Diethyl ether (VWR Analpur) was dried over CaH₂ and distilled before use. 1,4-Dioxane (VWR, HPLC-grade) was passed over a short column of basic alumina prior to use. All other solvents were of analytical grade and used as received. 2,2'-Azobis[2-(2-imidazolin-2-yl)propane]dihydrochloride (VA-044; Wako, 99%) and 2,2'-azobis(2-methylpropionitrile) (AIBN; Fluka, 99%) were recrystallized twice from methanol. *N,N*-Diethylacrylamide (DEAAm; TCI, 98%) and *N,N*-dimethylacrylamide (DMAAm; TCI, 99%) were passed over a short column of basic alumina prior to use. *N*-Isopropylacrylamide (NIPAAm, Acros, 99%) was recrystallized twice from *n*-hexane. Milli-Q water was obtained from a Milli-Q Advantage A10 Ultrapure Water Purification System (Millipore, USA). Acetic acid/acetate buffer had a pH of 5.2 with an acetic acid concentration of 0.27 mol·L⁻¹ and a sodium acetate concentration of 0.73 mol·L⁻¹. 4-(Dimethylamino)-pyridinium *p*-toluenesulfonate (DPTS)³¹² and isopropylidene-2,2-bis(methoxy)propionic acid (**13**)³¹³ were prepared according to the literature.

9.2 Additional Experimental Procedures

In the following, procedures are described that were utilized for the preparation of starting materials in the previous chapters.

Synthesis of mono-(6-*O*-(*p*-toluene sulfonyl))- β -CD (18)

According to the literature,¹⁵⁹ β -CD (50.0 g, 44.05 mmol, 1.0 eq.) was dissolved in sodium hydroxide solution (500 mL, 0.4 M) and cooled to 5 °C in an ice-bath. The solution was stirred vigorously and *p*-toluenesulfonyl chloride (35.0 g, 183.53 mmol, 4.2 eq.) was added in small portions, over a period of 5 min. The mixture was stirred at 5 °C for 30 min and filtered subsequently. The filtrate was neutralized with conc. HCl and stirred for 1 h. A white precipitate formed, was filtered off and washed three times with deionized H₂O. The white precipitate was freeze dried to yield the product as white solid (14.1 g, 10.91 mmol, 25%).

¹H-NMR (400 MHz, DMSO-D₆): [δ , ppm] = 2.43 (s, 3H, CH₃), 3.14 - 3.76 (m, 42H, H_{2,3,4,5,6}), 4.07 - 4.60 (m, 6H, OH₆), 4.70 - 4.87 (m, 7H, ³J = 3.2 Hz, H₁), 5.57 - 5.94 (br s, 14H, OH_{2,3}), 7.43 (s, 2H, ³J = 8.2 Hz, H_{arom}), 7.75 (s, 2H, ³J = 8.2 Hz, H_{arom}).

Synthesis of mono-(6-azido-6-desoxy)- β -CD (β -CD-N₃)

Based on a literature procedure,¹⁵⁹ mono-(6-*O*-(*p*-toluene sulfonyl))- β -CD (18) (10.0 g, 7.76 mmol, 1.0 eq.) was suspended in deionized H₂O (100 mL) and heated to 80 °C. Sodium azide (2.2 g, 33.85 mmol, 4.4 eq.) was added and the mixture was stirred at 80 °C over night, the solution was filtered and the product precipitated in cold acetone (600 mL). The white precipitate was filtered off and dried under high vacuum. The white solid was recrystallized from deionized H₂O to give the product as white crystals (3.9 g, 3.41 mmol, 44%).

¹H-NMR (400 MHz, DMSO-D₆): [δ , ppm] = 3.22 - 3.46 (m, 14H, H_{2,4}), 3.48 - 3.81 (br m, 28H, H_{3,5,6}), 4.39 - 4.58 (m, 6H, OH₆), 4.83 (d, 6H, ³J = 3.2 Hz, H₁), 4.87 (d, 1H, ³J = 3.4 Hz, H₁), 5.73 (br s, 14H, OH_{2,3}). ESI-MS: [M + Na⁺]_{exp} = 1182.50 m/z and [M + Na⁺]_{calc} = 1182.37 m/z.

Synthesis of 2-(((ethylthio)carbonothioyl)thio)-2-methylpropanoic acid (EMP)

Based on a literature procedure,²³⁴ in a 100 mL round-bottom-flask ethanethiol (1.4 mL, 18.91 mmol, 1.2 eq.) was dissolved in a suspension of K₃PO₄·H₂O (4.27 g, 18.57 mmol, 1.1 eq.) in acetone (60 mL) at ambient temperature. After stirring for 20 min carbon disulfide (3.0 mL, 49.69 mmol, 3.0 eq.) was added and the solution turned yellow. 2-Bromoisobutyric acid (2.74 g, 16.41 mmol, 1.0 eq.) was added after 20 min and the mixture stirred at ambient temperature overnight. 1M HCl (200 mL) was added and the aqueous phase was extracted with DCM (2 × 150 mL). The combined organic extracts were washed with deionized H₂O (75 mL), brine (75 mL), dried over Na₂SO₄ and filtered. After evaporation of the solvent the yellow oily residue was purified *via*

column chromatography on silica-gel with *n*-hexane:ethyl acetate 2:1 as eluent. The yellow fractions were combined, evaporated and the residue recrystallized from *n*-hexane at 40 °C to give the product as yellow crystals (2.71 g, 12.09 mmol, 74%).

¹H-NMR (400 MHz, CDCl₃): [δ , ppm] = 1.27 (t, 3H, ³J = 7.4 Hz, CH₃), 1.66 (s, 6H, C-(CH₃)₂), 3.23 (q, 2H, ³J = 7.4 Hz, CH₂). **¹³C-NMR** (100 MHz, CDCl₃): [δ , ppm] = 11.9 (CH₃), 24.2 (C-(CH₃)₂), 30.3 (CH₂), 54.6 (C-(CH₃)₂), 177.9 (C=O), 219.6 (C=S). **ESI-MS**: [M + Na⁺]_{exp} = 247.09 m/z and [M + Na⁺]_{calc} = 246.99 m/z.

Synthesis of 2-((((2-carboxyethyl)thio)carbonothioyl)thio)-2-methylpropanoic acid (CEMP)

Based on a literature procedure,²³⁴ in a 250 mL round-bottom-flask 3-mercaptopropionic acid (1.2 mL, 13.77 mmol, 1.1 eq.) was dissolved in a suspension of K₃PO₄·H₂O (3.19 g, 13.86 mmol, 1.1 eq.) in acetone (80 mL) at ambient temperature. After stirring for 20 min at ambient temperature carbon disulfide (2.5 mL, 41.40 mmol, 3.3 eq.) was added and the solution turned yellow. 2-Bromoisobutyric acid (2.09 g, 12.53 mmol, 1.0 eq.) was added after 20 min and the mixture was stirred at ambient temperature overnight. 1M HCl (200 mL) was added and the aqueous phase was extracted with DCM (2 × 150 mL). The combined organic extracts were washed with deionized H₂O (150 mL), brine (150 mL), dried over Na₂SO₄ and filtered. After evaporation of the solvent the yellow solid was recrystallized from acetone to give the product as yellow crystals in two fractions (1.92 g, 6.48 mmol, 52%).

¹H-NMR (400 MHz, DMSO-D₆): [δ , ppm] = 1.62 (s, 6H, C-(CH₃)₂), 2.64 (t, 2H, ³J = 6.9 Hz, O=C-CH₂), 3.45 (t, 2H, ³J = 6.9 Hz, S-CH₂), 12.73 (br s, 2H, 2x COOH). **¹³C-NMR** (100 MHz, DMSO-D₆): [δ , ppm] = 25.0 (C-(CH₃)₂), 31.4 (O=C-CH₂), 32.3 (S-CH₂), 56.3 (C-(CH₃)₂), 172.4 and 173.1 (C=O), 221.5 (C=S). **ESI-MS**: [M + Na⁺]_{exp} = 291.08 m/z and [M + Na⁺]_{calc} = 290.98 m/z.

Synthesis of 2-(1-carboxy-1-methylethylsulfanylthiocarbonylsulfanyl)-2-methylpropanoic acid (CMP)

In modification of the literature,⁸⁷ carbon disulfide (9.2 mL, 152.37 mmol, 1.0 eq.), chloroform (30.5 mL, 378.12 mmol, 2.5 eq.), acetone (27.9 mL, 379.49 mmol, 2.5 eq.) and tetrabutylammonium hydrogen sulfate (1.02 g, 3.00 mmol, 0.02 eq.) were mixed in petrolether (51 mL). At 0 °C sodium hydroxide solution (50 wt.% in deionized water; 85 g, 1063 mmol, 7.0 eq.) were added dropwise over 90 min. The mixture was stirred overnight and deionized water (380 mL) was added. Finally conc. HCl (51 mL) was added cautiously as gas was formed during the addition. The mixture was stirred for 30 min with argon purge. The residue was extracted twice with diethyl ether (300 mL).

The organic phase was washed with 1N HCl (300 mL), brine (300 mL), dried over Na₂SO₄ and the solvent was subsequently removed *in vacuo*. The crude product was recrystallized from acetone to give the product as a yellow crystalline solid in two fractions (8.71 g, 30.84 mmol, 20%).

¹H-NMR (400 MHz, DMSO-D₆): [δ , ppm] = 1.60 (s, 12H, C-(CH₃)₂), 12.91 (br s, 2H, COOH). **¹³C-NMR** (100 MHz, DMSO-D₆): [δ , ppm] = 24.9 (C-(CH₃)₂), 56.2 (O=C-CH₃), 173.1 (C=O), 219.0 (C=S). **ESI-MS**: [M + Na⁺]_{exp} = 305.08 m/z and [M + Na⁺]_{calc} = 305.00 m/z.

Synthesis of 4-cyano-4-(((ethylthio)carbonothioyl)thio)pentanoate (CEP)

According to the literature procedure,³¹⁴ in a 250 mL Schlenk-flask ethanethiol (2.8 mL, 37.85 mmol, 1.0 eq.) was added dropwise to a suspension of sodium hydride (60 wt.% in mineral oil, 1.64 g, 41.00 mmol, 1.1 eq.) in anhydrous diethyl ether (75 mL). Subsequently carbon disulfide (2.4 mL, 39.75 mmol, 1.05 eq.) was added dropwise resulting in a yellow precipitate. The precipitate was filtered off and washed with *n*-hexane. Furthermore the resulting filtrate was treated with *n*-hexane leading to further precipitation that was filtered off as well. The two fractions were combined to yield ethyl sodium carbonotrithioate as a yellow solid (5.84 g, 36.53 mmol, 97%). Subsequently the product was suspended in diethyl ether (70 mL) and iodine (4.30 g, 16.94 mmol, 0.5 eq.) was added in portions. After stirring for 1 hour at ambient temperature a white precipitate was filtered off. The filtrate was washed with saturated Na₂S₂O₃ solution (100 mL), dried over Na₂SO₄ and filtered. Evaporation of the solvent yielded diethyl carbonotrithioate disulfide as yellow oil (3.99 g, 14.55 mmol, 80%) that was used subsequently in the next step. The disulfide was dissolved in ethyl acetate (150 mL) and V-501 (6.11 g, 21.91 mmol, 1.5 eq.) was added. The mixture was degassed *via* two freeze-pump-thaw cycles and heated to reflux under argon for 18 hours. After cooling to ambient temperature the solvent was evaporated *in vacuo* and the residual oil was subjected to a filtration on a silica pad with *n*-hexane:ethyl acetate as eluent that was gradually changed from 1:1 to 1:20. The product was obtained after evaporation of the solvent as a yellow solid (7.05 g, 26.91 mmol, 92%).

¹H-NMR (400 MHz, DMSO-D₆): [δ , ppm] = 1.36 (t, 3H, ³J = 7.3 Hz, CH₂-CH₃), 1.88 (s, 3H, C-CH₃), 2.29 - 2.60 (m, 2H, O=C-CH₂), 3.35 (q, 2H, ³J = 7.3 Hz, CH₂-CH₃), 11.00 (br s, 1H, COOH). **¹³C-NMR** (100 MHz, DMSO-D₆): [δ , ppm] = 12.9 (CH₂-CH₃), 25.0 (C-CH₃), 29.7 (O=C-CH₂), 31.5 (O=C-CH₂-CH₂), 33.6 (S-CH₂), 46.3 (C-CN), 119.0 (C-N), 177.5 (C=O), 216.8 (C=S). **ESI-MS**: [M + Na⁺]_{exp} = 286.08 m/z and [M + Na⁺]_{calc} = 286.00 m/z.

Synthesis of *N*-(adamantan-1-yl)-6-hydroxyhexanamide (8)

According to the literature procedure,³¹⁵ aluminium chloride (11.8 g, 88.50 mmol, 2.2 eq.) were suspended in anhydrous DCM (100 mL). At 0 °C triethylamine (17.2 mL, 124.08 mmol, 3.1 eq.) were added dropwise *via* a syringe. After stirring for 15 minutes at 0 °C, the mixture was warmed to ambient temperature. Subsequently, a solution of ϵ -caprolactone (4.2 mL, 39.74 mmol, 1.0 eq.), triethylamine (6.1 mL, 46.89 mmol, 1.2 eq.) and adamantylamine hydrochloride (8.25 g, 43.95 mmol, 1.1 eq.) in anhydrous DCM (100 mL) was added dropwise. The mixture was stirred over night and subsequently poured into an ice cold solution of sodium carbonate (30 g) in ice water (300 mL). The organic phase was separated and the aqueous phase extracted three times with DCM (200 mL). The combined organic extracts were washed with deionized water (500 mL), brine (500 mL), dried over Na₂SO₄, filtered and concentrated *in vacuo*. The resulting solid was recrystallized from an acetonitrile/methanol mixture to give 7.09 g (26.72 mmol, 67%) of the product as off-white crystals.

¹H-NMR (400 MHz, CDCl₃): [δ , ppm] = 1.31 - 1.43 (m, 2H, CH₂-CH₂-CH₂-O), 1.51 - 1.73 (m, 10H, CH₂-CH₂-O; CH₂-CH₂-C=O; 3x CH_{2,adamantyl}), 1.92 - 2.00 (m, 6H, 3x NH-C-CH_{2,adamantyl}), 2.01 - 2.12 (m, 5H, 3x CH_{adamantyl}; CH₂-C=O-NH), 3.63 (t, 2H, ³J = 6.5 Hz, CH₂-OH), 5.17 (br s, 1H, NH). ¹³C-NMR (100 MHz, CDCl₃): [δ , ppm] = 25.4 (CH₂-CH₂-C=O; CH₂-CH₂-CH₂-C=O), 29.6 (3x CH_{adamantyl}), 32.4 (CH₂-CH₂-OH), 36.5 (3x CH_{2,adamantyl}), 37.7 (CH₂-C=O), 41.8 (3x CH_{2,adamantyl}-C-NH), 51.9 (C-NH), 62.6 (CH₂-OH), 172.3 (C=O). ESI-MS: [M + Na⁺]_{exp} = 288.36 m/z and [M + Na⁺]_{calc} = 288.19 m/z.

Synthesis of *N*-(2-hydroxypropyl)methacrylamide (HPMA)

According to the literature,³¹⁶ in a 250 mL Schlenk-flask 1-amino-2-propanol (48.6 mL, 621.17 mmol, 2.0 eq.) was dissolved in anhydrous DCM (20 mL). At 0 °C methacryloyl chloride (30.0 mL, 307.09 mmol, 1.0 eq.) in anhydrous DCM (20 mL) was added dropwise over 1 hour. After 1 hour the ice bath was removed and the mixture was stirred for further 30 min at ambient temperature. The mixture was cooled to -20 °C in a freezer. The formed precipitate was treated with DCM at 40 °C. Any remaining insoluble salt was removed by filtration and the product crystallized at -20 °C. This procedure was repeated three times to obtain *N*-(2-hydroxypropyl)methacrylamide as a white crystalline solid (22.91 g, 162.45 mmol, 53%).

¹H-NMR (400 MHz, D₂O+DSS): [δ , ppm] = 1.17 (d, 3H, ³J = 6.4 Hz, CH-CH₃), 1.93 (s, 3H, O=C-C-CH₃), 3.20 - 3.38 (m, 2H, CH₂), 3.86 - 4.05 (m, 1H, CH-CH₃), 5.46 (s, 1H, CH_{trans}), 5.71 (s, 1H, CH_{cis}). ¹³C-NMR (100 MHz, D₂O+DSS): [δ , ppm] = 20.4 (O=C-C-CH₃), 22.1 (CH-CH₃), 48.9 (CH₂-NH), 68.9 (CH-OH), 123.7 (C-CH₂), 141.7 (O=C-C-

CH₃), 174.8 (C=O).

Synthesis of 6-(4-(phenyldiazenyl)phenoxy)hexan-1-ol (9)

According to the literature,³¹⁷ 1-chloro-6-hydroxyhexane (8.1 mL, 60.72 mmol, 1.5 eq.), 4-phenylazophenol (8.00 g, 40.34 mmol, 1.0 eq.), K₂CO₃ (8.40 g, 60.78 mmol, 1.5 eq.) and potassium iodide (0.20 g, 1.21 mmol, 0.03 eq.) were suspended in anhydrous DMF (24 mL). The mixture was heated to 120 °C for 24 hours. After cooling to ambient temperature the mixture was added to deionized water (400 mL) under stirring. The resulting orange precipitate was filtered off, dried and dissolved in ethyl acetate (400 mL). The organic phase was washed with deionized water (400 mL), brine (400 mL) and subsequently dried over Na₂SO₄. After filtration and removal of the solvent *in vacuo* the crude product was recrystallized from methanol to give the product as orange solid (8.90 g, 29.78 mmol, 74%).

¹H-NMR (400 MHz, CDCl₃): [δ , ppm] = 1.35 - 1.55 (m, 4H, CH₂-CH₂-CH₂-O; CH₂-CH₂-CH₂-O), 1.56 - 1.66 (m, 2H, HO-CH₂-CH₂), 1.78 - 1.89 (m, 2H, CH_{arom}-O-CH₂-CH₂), 3.67 (t, 2H, ³J = 6.5 Hz, CH₂-OH), 4.04 (t, 2H, ³J = 6.5 Hz, CH₂-O-CH_{arom}), 7.00 (d, 2H, ³J = 9.0 Hz, CH_{arom}), 7.40 - 7.46 (m, 2H, CH_{arom}), 7.47 - 7.53 (m, 2H, CH_{arom}), 7.82 - 7.95 (m, 4H, 2x CH_{arom}). ¹³C-NMR (100 MHz, CDCl₃): [δ , ppm] = 25.7 and 26.0 (2x CH₂-CH₂-CH₂-O), 29.3 (CH_{arom}-O-CH₂-CH₂), 32.8 (HO-CH₂-CH₂), 63.0 (HO-CH₂), 68.3 (O-CH₂), 114.8 (O-C_{arom}-CH_{arom}), 122.7 (CH_{arom}), 124.9 (2x CH_{arom}), 129.2 (2x CH_{arom}), 130.4 (2x CH_{arom}), 147.0 (C_{arom}-N=N), 152.9 (C_{arom}-N=N), 161.8 (O-C_{arom}). ESI-MS: [M + H⁺]_{exp} = 299.33 m/z and [M + H⁺]_{calc} = 299.18 m/z.

9.3 Characterization and Methods

Nuclear magnetic resonance (NMR) measurements were conducted on a Bruker AM-250 spectrometer at 250 MHz for hydrogen nuclei for kinetic measurements, a Bruker Avance III 300 spectrometer at 300 MHz for hydrogen nuclei for kinetic measurements and a Bruker AM400 spectrometer at 400 MHz for hydrogen-nuclei and at 100 MHz for carbon-nuclei for structure verification. ROESY (rotating frame nuclear Overhauser effect spectroscopy) and NOESY (nuclear Overhauser effect spectroscopy) NMR-spectra were measured on a Bruker Avance III 300 spectrometer at 300 MHz or a Bruker Avance III 600 spectrometer at 600 MHz. For the determination of the conversion of DMAAm the integrals of one vinylic proton (5.78 - 5.89 ppm) and the methyl sidechain protons (2.87 - 3.28 ppm) were employed. The conversion of DEAAM was determined with the integral of one vinylic proton (5.57 - 5.73 ppm) and with the integral of the sidechain methyl groups and backbone protons (0.81 - 1.97 ppm). The cal-

ulation of the NIPAAm conversion was carried out with the integrals of one vinylic proton (5.47 - 5.59 ppm) and the integral of the sidechain methyl groups and the backbone protons (0.92 - 1.95 ppm). The conversion of HPMA was calculated with the integral of one vinylic proton (5.48 - 5.58 ppm) and with the integral of one side-chain proton (3.86 - 4.14 ppm).

Size exclusion chromatography (SEC) employing *N,N*-dimethylacetamide (DMAc) as eluent containing 0.03 wt.% LiBr was performed for PDMAAm and PHPMA on a Polymer Laboratories PL-GPC 50 Plus Integrated System, comprising an autosampler, a PLgel 5 μm bead-size guard column (50 \times 7.5 mm) followed by three PLgel 5 μm MixedC columns (300 \times 7.5 mm) and a differential refractive index detector at 50 °C with a flow rate of 1.0 mL \cdot min⁻¹. The SEC system was calibrated against linear PSty standards with molecular weights ranging from 160 to 6 \cdot 10⁶ g \cdot mol⁻¹ or PMMA standards with molecular weights ranging from 700 to 2 \cdot 10⁶ g \cdot mol⁻¹. All SEC calculations for PDMAAm and PNIPAAm were carried out relative to a PSty calibration. The SEC calculations for PHPMA were carried out relative to a PMMA calibration.

SEC employing tetrahydrofuran (THF) as eluent containing 200 ppm 2,6-di-*tert*-butyl-4-methylphenol for PDEAAm was performed on a Polymer Laboratories PL-GPC 50 Plus Integrated System, comprising an autosampler, a PLgel 5 μm bead-size guard column (50 \times 7.5 mm) followed by three PLgel 5 μm MixedC columns (300 \times 7.5 mm), a PLgel 5 μm MixedE column (300 \times 7.5 mm) and a differential refractive index detector at 35 °C with a flow rate of 1.0 mL \cdot min⁻¹. The SEC system was calibrated against linear PSty standards with molecular weights ranging from 160 to 6 \cdot 10⁶ g \cdot mol⁻¹. All SEC calculations for PDEAAm were carried out relative to PSty. The molecular-weight dispersity is abbreviated as D_m .

Electrospray ionization mass spectrometry (ESI-MS) was performed on a LXQmass spectrometer (ThermoFisher Scientific, San Jose, CA) equipped with an atmospheric pressure ionization source operating in the nebulizer-assisted electrospray mode. The instrument was calibrated in the m/z range 195-1822 Da using a standard containing caffeine, Met-Arg-Phe-Ala acetate (MRFA), and a mixture of fluorinated phosphazenes (Ultramark 1621) (all from Aldrich). A constant spray voltage of 4.5 kV was used, and nitrogen at a dimensionless sweep gas flow rate of 2 (\sim 3 L \cdot min⁻¹) and a dimensionless sheath gas flow rate of 12 (\sim 1 L \cdot min⁻¹) were applied. The capillary voltage, the tube lens offset voltage, and the capillary temperature were set to 60 V, 110 V, and 300 °C respectively.

Turbidity measurements (Chapter 6 and 4) were performed on a Cary 300 Bio UV/VIS spectrophotometer (Varian) at 600 nm. The heating rate was set to 0.32 °C \cdot min⁻¹ and the concentration was 1 mg \cdot mL⁻¹. For the determination of the LCST the point of inflection of the transmittance vs. temperature plot was used.

Turbidity measurements (Chapter 5) were performed in a temperature range from 5 °C to 100 °C with a heating and cooling ramp of 1 °C · min⁻¹ under stirring (700 rpm). During these controlled heating/cooling cycles, the transmission was monitored in a Crystal 16 TM (Avantium Technologies) instrument.

Dynamic light scattering (DLS) (Chapter 4) was performed on a 380 DLS spectrometer (Particle Sizing Systems, Santa Barbara, USA) with a 90 mW laser diode operating at 658 nm equipped with an avalanche photo diode detector. Every measurement was performed four times at 10 °C for samples containing PDEAAm and at 25 °C for samples containing PDMAAm. The data was evaluated with an inverse Laplace algorithm. The scattered light was recorded at an angle of 90° to the incident beam. For the temperature sequenced measurements the sample was equilibrated at the specific temperature for 5 minutes, then the DLS measurement was performed three times for three minutes and the temperature changed again. The entire procedure was performed three times and the data points were finally averaged. All hydrodynamic diameters (D_h) in the text are the averages of the number weighted distributions. The samples were prepared in Milli-Q water and filtered with a 0.2 µm regenerated cellulose syringe filter (Roth, Rotilabo).

DLS (Chapter 6) was performed on a 380 DLS spectrometer (Particle Sizing Systems, Santa Barbara, USA) with a 90 mW laser diode operating at 658 nm equipped with an avalanche photo diode detector. Every measurement was performed 4 times at 25 °C, 44 °C or 50 °C and the data was evaluated with an inverse Laplace algorithm. The scattered light was recorded at an angle of 90° to the incident beam. For the temperature sequenced measurements the sample was equilibrated at the specific temperature for 3 minutes, then the DLS measurement was performed 2 times for 5 minutes and the temperature changed again. The entire procedure was performed 3 times and the data points were finally averaged. All hydrodynamic diameters (D_h) in the text are the averages of the number weighted distributions. The samples were prepared in Milli-Q water and filtered with a 0.2 µm regenerated cellulose syringe filter (Roth, Rotilabo).

DLS (Chapter 5) was performed at a scattering angle of 90° on an ALV CGS-3 instrument and a He-Ne laser operating at a wavelength of $\lambda = 633$ nm at 25 °C. The CONTIN algorithm was applied to analyze the obtained correlation functions. For temperature dependent measurements the DLS is equipped with a Lauda thermostat. Apparent hydrodynamic radii were calculated according to the Stokes-Einstein equation. All CONTIN plots are number-weighted distributions.

UV/VIS spectra were measured on a Cary 300 Bio UV/VIS spectrophotometer (Varian) at a temperature of 25 °C or 10 °C depending on the sample.

UV irradiation for investigation of photoresponse was applied *via* a BLB-8 UV lamp (8 W, Camag) with an emission maximum at 350 nm for the DLS samples and *via*

a UVASPOT 2000RF2 (2000 W, Hönle technology) with its main irradiation between 315-420 nm for NMR samples.

Theoretical molecular weights (M_{theo}) were calculated according to equation 2.8 and 9.1 with the following equation, with m_{M} as the molar mass of the monomer, m_{CTA} as the molar mass of the CTA and $[\text{M}]_0$ or $[\text{CTA}]_0$ as the initial concentration of the respective compounds:

$$M_{\text{theo}} = \text{conversion} \cdot m_{\text{M}} \cdot \frac{[\text{M}]_0}{[\text{CTA}]_0} + m_{\text{CTA}} \quad (9.1)$$

Bibliography

- [1] Hawker, C. J.; Wooley, K. L. *Science* **2005**, *209*, 1200–1205.
- [2] Hadjichristidis, N., Hiraio, A., Tezuka, Y., Du Prez, F., Eds. *Complex Macromolecular Architectures: Synthesis, Characterization, and Self-Assembly*; John Wiley & Sons (Asia) Pte Ltd, 2011.
- [3] Gregory, A.; Stenzel, M. H. *Prog. Polym. Sci.* **2012**, *37*, 38–105.
- [4] Hedrick, J. L.; Magbitang, T.; Connor, E. F.; Glauser, T.; Volksen, W.; Hawker, C. J.; Lee, V. Y.; Miller, R. D. *Chem. Eur. J.* **2002**, *8*, 3308–3319.
- [5] Grayson, S. M.; Godbey, W. T. *J. Drug Targeting* **2008**, *16*, 329–356.
- [6] Tian, H.; Tang, Z.; Zhuang, X.; Chen, X.; Jing, X. *Prog. Polym. Sci.* **2012**, *37*, 237–280.
- [7] Neugebauer, D.; Zhang, Y.; Pakula, T.; Sheiko, S. S.; Matyjaszewski, K. *Macromolecules* **2003**, *36*, 6746–6755.
- [8] Soler-Illia, G. J. A. A.; Azzaroni, O. *Chem. Soc. Rev.* **2011**, *40*, 1107–1150.
- [9] Hawker, C. J.; Bosman, A. W.; Harth, E. *Chem. Rev.* **2001**, *101*, 3661–3688.
- [10] Nicolas, J.; Guillaneuf, Y.; Lefay, C.; Bertin, D.; Gigmès, D.; Charleux, B. *Prog. Polym. Sci.* **2013**, *38*, 63–235.
- [11] Ouchi, M.; Terashima, T.; Sawamoto, M. *Chem. Rev.* **2009**, *109*, 4963–5050.
- [12] Matyjaszewski, K. *Macromolecules* **2012**, *45*, 4015–4039.
- [13] Barner-Kowollik, C. *Handbook of RAFT-Polymerization*; Wiley-VCH, Weinheim, 2008.

- [14] Barner-Kowollik, C.; Perrier, S. J. *Polym. Sci. Part A: Polym. Chem.* **2008**, *46*, 5715–5723.
- [15] Moad, G.; Rizzardo, E.; Thang, S. H. *Aust. J. Chem.* **2012**, *65*, 985–1076.
- [16] Kolb, H. C.; Finn, M. G.; Sharpless, K. B. *Angew. Chem. Int. Ed.* **2001**, *40*, 2004–2021.
- [17] Barner-Kowollik, C.; Du Prez, F. E.; Espeel, P.; Hawker, C. J.; Junkers, T.; Schlaad, H.; Van Camp, W. *Angew. Chem. Int. Ed.* **2011**, *50*, 60–62.
- [18] Kempe, K.; Krieg, A.; Becer, C. R.; Schubert, U. S. *Chem. Soc. Rev.* **2012**, *41*, 176–191.
- [19] Binder, W. H.; Sachsenhofer, R. *Macromol. Rapid. Commun.* **2007**, *28*, 15–54.
- [20] Lutz, J. F. *Angew. Chem. Int. Ed.* **2007**, *46*, 1018–1025.
- [21] Hoyle, C.; Bowman, C. *Angew. Chem. Int. Ed.* **2010**, *49*, 1540–1573.
- [22] Lowe, A. B. *Polym. Chem.* **2010**, *1*, 17–36.
- [23] Tasdelen, M. A. *Polym. Chem.* **2011**, *2*, 2133–2145.
- [24] Wilson, A. J. *Soft Matter* **2007**, *3*, 409–425.
- [25] Bertrand, A.; Lortie, F.; Bernard, J. *Macromol. Rapid. Commun.* **2012**, *33*, 2062–2091.
- [26] Kurth, D. G.; Higuchi, M. *Soft Matter* **2006**, *2*, 915–927.
- [27] Zayed, J. M.; Nouvel, N.; Rauwald, U.; Scherman, O. A. *Chem. Soc. Rev.* **2010**, *39*, 2806–2816.
- [28] Chen, G.; Jiang, M. *Chem. Soc. Rev.* **2011**, *40*, 2254–2266.
- [29] Zheng, B.; Wang, F.; Dong, S.; Huang, F. *Chem. Soc. Rev.* **2012**, *41*, 1621–1636.
- [30] van de Manakker, F.; Vermonden, T.; van Nostrum, C. F.; Hennink, W. E. *Biomacromolecules* **2009**, *10*, 3157–3175.
- [31] Yhaya, F.; Gregory, A. M.; Stenzel, M. H. *Aust. J. Chem.* **2010**, *63*, 195–210.
- [32] Zhou, J.; Ritter, H. *Polym. Chem.* **2010**, *1*, 1552–1559.
- [33] Harada, A.; Takashima, Y.; Yamaguchi, H. *Chem. Soc. Rev.* **2009**, *38*, 875–882.
- [34] Nakahata, M.; Takashima, Y.; Yamaguchi, H.; Harada, A. *Nat. Commun.* **2011**, *2*, 511.

- [35] Zhang, X.; Wang, C. *Chem. Soc. Rev.* **2011**, *40*, 94–101.
- [36] Chen, Y.; Liu, Y. *Chem. Soc. Rev.* **2010**, *39*, 495–505.
- [37] Szwarc, M. *Living Polymers and Mechanisms of Anionic Polymerization*; Adv. Polym. Sci.; Springer, Berlin, 1983; Vol. 49.
- [38] Hsieh, H. L.; Quirk, R. P. *Anionic Polymerization: Principles and Practical Applications*, 1st ed.; Marcel Dekker, New York, 1996.
- [39] Moad, G.; Rizzardo, E.; Thang, S. H. *Acc. Chem. Res.* **2008**, *41*, 1133–1142.
- [40] Szwarc, M. *Ionic Polymerization and Living Polymers*, 1st ed.; Chapman & Hall, New York, 1993.
- [41] Matyjaszewski, K.; Xia, J. *Chem. Rev.* **2001**, *101*, 2921–2990.
- [42] Braunecker, W. A.; Matyjaszewski, K. *Prog. Polym. Sci.* **2007**, *32*, 93–146.
- [43] Solomon, D. H.; Rizzardo, E.; Cacioli, P. US Patent US4581429. 1986.
- [44] Grubbs, R. B. *Polym. Rev.* **2011**, *51*, 104–137.
- [45] Chiefari, J.; Chong, Y. K.; Ercole, F.; Krstina, J.; Jeffery, J.; Le, T. P. T.; Mayadunne, R. T. A.; Meijs, G. F.; Moad, C. L.; Moad, G.; Rizzardo, E.; Thang, S. H. *Macromolecules* **1998**, *31*, 5559–5562.
- [46] Barner-Kowollik, C.; Perrier, S. J. *Polym. Sci. Part A: Polym. Chem.* **2008**, *46*, 5715–5723.
- [47] Moad, G.; Rizzardo, E.; Thang, S. H. *Polymer* **2008**, *49*, 1079–1131.
- [48] Moad, G.; Rizzardo, E.; Thang, S. H. *Aust. J. Chem.* **2009**, *62*, 1402–1472.
- [49] Odian, G. *Principles of Polymerization*, 4th ed.; John Wiley & Sons, New York, 2004.
- [50] Le, T. P.; Moad, G.; Rizzardo, E.; Thang, S. H. Int. Patent WO9801478. 1998.
- [51] Corpart, P.; Charmot, D.; Biadatti, T.; Zard, S. Z.; Michelet, D. Int. Patent WO9858974. 1998.
- [52] Chiefari, J.; Mayadunne, R. T. A.; Moad, C. L.; Moad, G.; Rizzardo, E.; Postma, A.; Skidmore, M. A.; Thang, S. H. *Macromolecules* **2003**, *36*, 2273–2283.
- [53] Chong, Y. K.; Krstina, J.; Le, T. P. T.; Moad, G.; Postma, A.; Rizzardo, E.; Thang, S. H. *Macromolecules* **2003**, *36*, 2256–2272.

- [54] Perrier, S.; Takolpuckdee, P. J. *Polym. Sci. Part A: Polym. Chem.* **2005**, *43*, 5347–5393.
- [55] Barner-Kowollik, C.; Buback, M.; Charleux, B.; Coote, M. L.; Drache, M.; Fukuda, T.; Goto, A.; Klumperman, B.; Lowe, A. B.; Mcleary, J. B.; Moad, G.; Monteiro, M. J.; Sanderson, R. D.; Tonge, M. P.; Vana, P. J. *Polym. Sci. Part A: Polym. Chem.* **2006**, *44*, 5809–5831.
- [56] Moad, G.; Chiefari, J.; Chong, Y.; Krstina, J.; Mayadunne, R. T.; Postma, A.; Rizzardo, E.; Thang, S. H. *Polym. Int.* **2000**, *49*, 993–1001.
- [57] Mori, H.; Ookuma, H.; Nakano, S.; Endo, T. *Macromol. Chem. Phys.* **2006**, *207*, 1005–1017.
- [58] Stenzel-Rosenbaum, M.; Davis, T. P.; Chen, V.; Fane, A. G. *J. Polym. Sci. Part A: Polym. Chem.* **2001**, *39*, 2777–2783.
- [59] Quinn, J. F.; Barner, L.; Barner-Kowollik, C.; Rizzardo, E.; Davis, T. P. *Macromolecules* **2002**, *35*, 7620–7627.
- [60] Hongand, C.-Y.; You, Y.-Z.; Bai, R.-K.; Pan, C.-Y.; Borjihan, G. *J. Polym. Sci. Part A: Polym. Chem.* **2001**, *33*, 3934–3939.
- [61] Chen, G.; Zhu, X.; Zhu, J.; Cheng, Z. *Macromol. Rapid Commun.* **2004**, *25*, 818–824.
- [62] Lowe, A. B.; McCormick, C. L. *Prog. Polym. Sci.* **2007**, *32*, 283–351.
- [63] Mitsukami, Y.; Donovan, M. S.; Lowe, A. B.; McCormick, C. L. *Macromolecules* **2001**, *34*, 2248–2256.
- [64] Sumerlin, B. S.; Donovan, M. S.; Mitsukami, Y.; Lowe, A. B.; McCormick, C. L. *Macromolecules* **2001**, *34*, 6561–6564.
- [65] Rodriguez-Emmenegger, C.; Schmidt, B. V. K. J.; Sedlakova, Z.; Subr, V.; Alles, A. B.; Brynda, E.; Barner-Kowollik, C. *Macromol. Rapid Commun.* **2011**, *32*, 958–965.
- [66] Convertine, A. J.; Lokitz, B. S.; Lowe, A. B.; Scales, C. W.; Myrick, L. J.; McCormick, C. L. *Macromol. Rapid Commun.* **2005**, *26*, 791–795.
- [67] Thomas, D. B.; Convertine, A. J.; Hester, R. D.; Lowe, A. B.; McCormick, C. L. *Macromolecules* **2004**, *37*, 1735–1741.
- [68] Levesque, G.; Arsène, P.; Fanneau-Bellenger, V.; Pham, T.-N. *Biomacromolecules* **2000**, *1*, 400–406.

- [69] Thomas, D. B.; Convertine, A. J.; Myrick, L. J.; Scales, C. W.; Smith, A. E.; Lowe, A. B.; Vasilieva, Y. A.; Ayres, N.; McCormick, C. L. *Macromolecules* **2004**, *37*, 8941–8950.
- [70] Thomas, D. B.; Sumerlin, B. S.; Lowe, A. B.; McCormick, C. L. *Macromolecules* **2003**, *36*, 1436–1439.
- [71] Smith, A. E.; Xu, X.; McCormick, C. L. *Prog. Polym. Sci.* **2010**, *35*, 45–93.
- [72] Millard, P.-E.; Barner, L.; Stenzel, M. H.; Davis, T. P.; Barner-Kowollik, C.; Müller, A. H. E. *Macromol. Rapid Commun.* **2006**, *27*, 821–828.
- [73] Convertine, A. J.; Sumerlin, B. S.; Thomas, D. B.; Lowe, A. B.; McCormick, C. L. *Macromolecules* **2003**, *36*, 4679–4681.
- [74] Yuan, J.-J.; Ma, R.; Gao, Q.; Wang, Y.-F.; Cheng, S.-Y.; Feng, L.-X.; Fan, Z.-Q.; Jiang, L. *J. Appl. Polym. Sci.* **2003**, *89*, 1017–1025.
- [75] Sahnoun, M.; Charreyre, M.-T.; Veron, L.; Delair, T.; D'Agosto, F. *J. Polym. Sci. Part A: Polym. Chem.* **2005**, *43*, 3551–3565.
- [76] Xiong, Q.; Ni, P.; Zhang, F.; Yu, Z. *Polym. Bull.* **2004**, *53*, 1–8.
- [77] Donovan, M. S.; Sumerlin, B. S.; Lowe, A. B.; McCormick, C. L. *Macromolecules* **2002**, *35*, 8663–8666.
- [78] Delaittre, G.; Rieger, J.; Charleux, B. *Macromolecules* **2011**, *44*, 462–470.
- [79] Convertine, A. J.; Lokitz, B. S.; Vasileva, Y.; Myrick, L. J.; Scales, C. W.; Lowe, A. B.; McCormick, C. L. *Macromolecules* **2006**, *39*, 1724–1730.
- [80] Scales, C. W.; Vasilieva, Y. A.; Convertine, A. J.; Lowe, A. B.; McCormick, C. L. *Biomacromolecules* **2005**, *6*, 1846–1850.
- [81] Barner, L.; Davis, T. P.; Stenzel, M. H.; Barner-Kowollik, C. *Macromol. Rapid Commun.* **2007**, *28*, 539–559.
- [82] Quémener, D.; Davis, T. P.; Barner-Kowollik, C.; Stenzel, M. H. *Chem. Commun.* **2006**, 5051–5053.
- [83] Gondi, S. R.; Vogt, A. P.; Sumerlin, B. S. *Macromolecules* **2007**, *40*, 474–481.
- [84] Postma, A.; Davis, T. P.; Evans, R. A.; Li, G.; Moad, G.; O'Shea, M. S. *Macromolecules* **2006**, *39*, 5293–5306.
- [85] Liu, J.; Hong, C.-Y.; Pan, C.-Y. *Polymer* **2004**, *45*, 4413–4421.

- [86] Lima, V.; Jiang, X.; Brokken-Zijp, J.; Schoenmakers, P. J.; Klumperman, B.; Linde, R. V. D. *J. Polym. Sci. Part A: Polym. Chem.* **2005**, *43*, 959–973.
- [87] Lai, J. T.; Filla, D.; Shea, R. *Macromolecules* **2002**, *35*, 6754–6756.
- [88] Barner-Kowollik, C.; Inglis, A. J. *Macromol. Chem. Phys.* **2009**, *210*, 987–992.
- [89] Perrier, S.; Takolpuckdee, P.; Mars, C. A. *Macromolecules* **2005**, *38*, 2033–2036.
- [90] Llauro, M.; Loiseau, J.; Boisson, F.; Delolme, F.; Ladavière, C.; Claverie, J. *J. Polym. Sci. Part A: Polym. Chem.* **2004**, *42*, 5439–5462.
- [91] Lowe, A. B.; Sumerlin, B. S.; Donovan, M. S.; McCormick, C. L. *J. Am. Chem. Soc.* **2002**, *124*, 11562–11563.
- [92] Vana, P.; Albertin, L.; Barner, L.; Davis, T. P.; Barner-Kowollik, C. *J. Polym. Sci. Part A: Polym. Chem.* **2002**, *40*, 4032–4037.
- [93] Lu, L.; Zhang, H.; Yang, N.; Cai, Y. *Macromolecules* **2006**, *39*, 3770–3776.
- [94] Mayadunne, R. T. A.; Rizzardo, E.; Chiefari, J.; Krstina, J.; Moad, G.; Postma, A.; Thang, S. H. *Macromolecules* **2000**, *33*, 243–245.
- [95] Benaglia, M.; Chiefari, J.; Chong, Y. K.; Moad, G.; Rizzardo, E.; Thang, S. H. *J. Am. Chem. Soc.* **2009**, *131*, 6914–6915.
- [96] Bernard, J.; Favier, A.; Zhang, L.; Nilasaroya, A.; Davis, T. P.; Barner-Kowollik, C.; Stenzel, M. H. *Macromolecules* **2005**, *38*, 5475–5484.
- [97] Mayadunne, R. T. A.; Jeffery, J.; Moad, G.; Rizzardo, E. *Macromolecules* **2003**, *36*, 1505–1513.
- [98] Stenzel, M. H.; Zhang, L.; Huck, W. T. S. *Macromol. Rapid Commun.* **2006**, *27*, 1121–1126.
- [99] Darcos, V.; Duréault, A.; Taton, D.; Gnanou, Y.; Marchand, P.; Caminade, A.-M.; Majoral, J.-P.; Destarac, M.; Leising, F. *Chem. Commun.* **2004**, 2110–2111.
- [100] Mertoglu, M.; Laschewsky, A.; Skrabania, K.; Wieland, C. *Macromolecules* **2005**, *38*, 3601–3614.
- [101] Lehn, J. M. *Acc. Chem. Res.* **1978**, *11*, 49–57.
- [102] Lehn, J.-M. *Angew. Chem. Int. Ed.* **1988**, *27*, 89–112.
- [103] Lehn, J.-M. *Supramolecular Chemistry*; Wiley VCH, Weinheim, 1995.

- [104] Lehn, J.-M. In *Supramolecular Polymers*; Ciferri, A., Ed.; CRC Press, Boca Raton, 2005; Chapter 1, p 3.
- [105] Steed, J. W.; Atwood, J. L. *Supramolecular Chemistry*; John Wiley & Sons, New York, 2009.
- [106] Connors, K. A. *Chem. Rev.* **1997**, *97*, 1325–1358.
- [107] Biwer, A.; Antranikian, G.; Heinzle, E. *Appl. Microbiol. Biotechnol.* **2002**, *59*, 609–617.
- [108] Sängler, W. *Angew. Chem.* **1980**, *92*, 343–361.
- [109] van Etten, R. L.; Clowes, G. A.; Sebastian, J. F.; Bender, M. L. *J. Am. Chem. Soc.* **1967**, *89*, 3253–3262.
- [110] da Silva, W. A.; Rodrigues, M. T.; Shankaraiah, N.; Ferreira, R. B.; Andrade, C. K. Z.; Pilli, R. A.; Santos, L. S. *Org. Lett.* **2009**, *11*, 3238–3241.
- [111] Loftsson, T.; Jarho, P.; Måsson, M.; Järvinen, T. *Expert Opin. Drug Deliv.* **2005**, *2*, 335–351.
- [112] Szejtli, J. *J. Mater. Chem.* **1997**, *7*, 575–587.
- [113] Nishi, H.; Fukuyama, T.; Terabe, S. *J. Chrom. A* **1991**, *553*, 503–516.
- [114] Szente, L.; Szejtli, J. *Trends Food Sci. Technol.* **2004**, *15*, 137–142.
- [115] Dodziuk, H. In *Cyclodextrins and Their Complexes*; Dodziuk, H., Ed.; Wiley VCH, 2006; Chapter 1, pp 1–26.
- [116] Del Valle, E. M. M. *Process Biochem.* **2004**, *39*, 1033–1046.
- [117] Hedges, A. R. *Chem. Rev.* **1998**, *98*, 2035–2044.
- [118] Loftsson, T.; Brewster, M. E. *J. Pharm. Sci.* **1996**, *85*, 1017–1025.
- [119] Kaya, E.; Mathias, L. J. *J. Polym. Sci. Part A: Polym. Chem.* **2010**, *48*, 581–592.
- [120] Cramer, F.; Sängler, W.; Spatz, H.-C. *J. Am. Chem. Soc.* **1967**, *89*, 14–20.
- [121] Schneider, H.-J.; Hacket, F.; Rüdiger, V.; Ikeda, H. *Chem. Rev.* **1998**, *98*, 1755–1786.
- [122] Béni, S.; Szakács, Z.; Csernák, O.; Barcza, L.; Noszál, B. *Eur. J. Pharm. Sci.* **2007**, *30*, 167–174.
- [123] Zhang, Y.; Liu, Y.; Liu, W.; Gan, Y.; Zhou, C. *J. Inclusion Phenom. Macrocyclic Chem.* **2010**, *67*, 177–182.

- [124] Guo, P.; Su, Y.; Cheng, Q.; Pan, Q.; Li, H. *Carbohydr. Res.* **2011**, *346*, 986–990.
- [125] Ivanov, P. M.; Salvatierra, D.; Jaime, C. J. *Org. Chem.* **1996**, *61*, 7012–7017.
- [126] Chen, B.; Liu, K. L.; Zhang, Z.; Ni, X.; Goh, S. H.; Li, J. *Chem. Commun.* **2012**, *48*, 5638–5640.
- [127] Yoroazu, T.; Hoshino, M.; Imamura, M. *J. Phys. Chem.* **1982**, *86*, 4426–4429.
- [128] Cruz, J. R.; Becker, B. A.; Morris, K. F.; Larive, C. K. *Magn. Reson. Chem.* **2008**, *46*, 838–845.
- [129] Wenz, G.; Han, B.-H.; Müller, A. *Chem. Rev.* **2006**, *106*, 782–817.
- [130] Zhao, Y.-L.; Dichtel, W. R.; Trabolsi, A.; Saha, S.; Aprahamian, I.; Stoddart, J. F. *J. Am. Chem. Soc.* **2008**, *130*, 11294–11296.
- [131] Armspach, D.; Ashton, P. R.; Ballardini, R.; Balzani, V.; Godi, A.; Moore, C. P.; Prodi, L.; Spencer, N.; Stoddart, J. F.; Tolley, M. S.; Wear, T. J.; Williams, D. J. *Chem. Eur. J.* **1995**, *1*, 31–55.
- [132] Harada, A.; Kamachi, M. *Macromolecules* **1990**, *23*, 2821–2823.
- [133] Harada, A.; Okada, M.; Li, J.; Kamachi, M. *Macromolecules* **1995**, *28*, 8406–8411.
- [134] Harada, A.; Li, J.; Nakamitsu, T.; Kamachi, M. *J. Org. Chem.* **1993**, *58*, 7524–7528.
- [135] He, L.; Huang, J.; Chen, Y.; Xu, X.; Liu, L. *Macromolecules* **2005**, *38*, 3845–3851.
- [136] Born, M.; Ritter, H. *Angew. Chem. Int. Ed.* **1995**, *34*, 309–311.
- [137] Gibson, H. W.; Ge, Z.; Jones, J. W.; Harich, K.; Pederson, A.; Dorn, H. C. *J. Polym. Sci. Part A: Polym. Chem.* **2009**, *47*, 6472–6495.
- [138] Sabadini, E.; Cosgrove, T. *Langmuir* **2003**, *19*, 9680–9683.
- [139] Harada, A.; Takashima, Y.; Yamaguchi, H. *Chem. Soc. Rev.* **2009**, *38*, 875–882.
- [140] Liao, X.; Chen, G.; Liu, X.; Chen, W.; Chen, F.; Jiang, M. *Angew. Chem. Int. Ed.* **2010**, *49*, 4409–4413.
- [141] De Bo, G.; De Winter, J.; Gerbaux, P.; Fustin, C.-A. *Angew. Chem. Int. Ed.* **2011**, *50*, 9093–9096.
- [142] Stoll, R. S.; Friedman, D. C.; Stoddart, J. F. *Org. Lett.* **2011**, *13*, 2706–2709.
- [143] Houk, K. N.; Leach, A. G.; Kim, S. P.; Zhang, X. *Angew. Chem. Int. Ed.* **2003**, *42*, 4872–4897.

- [144] Benesi, H. A.; Hildebrand, J. H. *J. Am. Chem. Soc.* **1949**, *71*, 2703–2707.
- [145] Kuntz, I. D.; Gasparro, F. P.; Johnston, M. D.; Taylor, R. P. *J. Am. Chem. Soc.* **1968**, *90*, 4778–4781.
- [146] Yang, C.; Liu, L.; Mu, T.-W.; Guo, Q.-X. *Anal. Sci.* **2000**, *16*, 537–539.
- [147] Tomatsu, I.; Hashidzume, A.; Harada, A. *Macromolecules* **2005**, *38*, 5223–5227.
- [148] Tamesue, S.; Takashima, Y.; Yamaguchi, H.; Shinkai, S.; Harada, A. *Angew. Chem. Int. Ed.* **2010**, *49*, 7461–7464.
- [149] Lewis, E. A.; Hansen, L. D. *J. Chem. Soc., Perkin Trans. 2* **1973**, 2081–2085.
- [150] Miyaji, T.; Kurono, Y.; Uekama, K.; Ikeda, K. *Chem. Pharm. Bull.* **1976**, *24*, 1155–1159.
- [151] Takashima, Y.; Nakayama, T.; Miyauchi, M.; Kawaguchi, Y.; Yamaguchi, H.; Harada, A. *Chem. Lett.* **2004**, *33*, 890–891.
- [152] Höfler, T.; Wenz, G. *J. Inclusion Phenom. Macrocyclic Chem.* **1996**, *25*, 81–84.
- [153] Boger, J.; Corcoran, R. J.; Lehn, J.-M. *Helv. Chim. Acta* **1978**, *61*, 2190–2218.
- [154] Khan, A. R.; Forgo, P.; Stine, K. J.; D'Souza, V. T. *Chem. Rev.* **1998**, *98*, 1977–1996.
- [155] Tang, W.; Ng, S.-C. *Nat. Protoc.* **2008**, *3*, 691–697.
- [156] Hamasaki, K.; Ikeda, H.; Nakamura, A.; Ueno, A.; Toda, F.; Suzuki, I.; Osa, T. *J. Am. Chem. Soc.* **1993**, *115*, 5035–5040.
- [157] Melton, L. D.; Slessor, K. N. *Carbohydr. Res.* **1971**, *18*, 29–37.
- [158] Quan, C.-Y.; Chen, J.-X.; Wang, H.-Y.; Li, C.; Chang, C.; Zhang, X.-Z.; Zhuo, R.-X. *ACS Nano* **2010**, *4*, 4211–4219.
- [159] Amajjahe, S.; Choi, S.; Munteanu, M.; Ritter, H. *Angew. Chem. Int. Ed.* **2008**, *47*, 3435–3437.
- [160] Kuzuya, A.; Ohnishi, T.; Wasano, T.; Nagaoka, S.; Sumaoka, J.; Ihara, T.; Jyo, A.; Komiyama, M. *Bioconjugate Chem.* **2009**, *20*, 1643–1649.
- [161] Bonomo, R. P.; Cucinotta, V.; Impellizzeri, F. D. A. G.; Maccarrone, G.; Rizzarelli, E.; Vecchio, G. *J. Inclusion Phenom. Molecular Recognit.* **1993**, *15*, 167–180.
- [162] Fujita, K.; Ueda, T.; Imoto, T.; Tabushi, I.; Toh, N.; Koga, T. *Bioorg. Chem.* **1982**, *11*, 72–84.

- [163] Huan, X.; Wang, D.; Dong, R.; Tu, C.; Zhu, B.; Yan, D.; Zhu, X. *Macromolecules* **2012**, *45*, 5941–5947.
- [164] Yhaya, F.; Binauld, S.; Callari, M.; Stenzel, M. H. *Aust. J. Chem.* **2012**, *65*, 1095–1103.
- [165] Giacomelli, C.; Schmidt, V.; Putaux, J.-L.; Narumi, A.; Kakuchi, T.; Borsali, R. *Biomacromolecules* **2009**, *10*, 449–453.
- [166] Liu, H.; Zhang, Y.; Hu, J.; Li, C.; Liu, S. *Macromol. Chem. Phys.* **2009**, *210*, 2125–2137.
- [167] Cai, T.; Yang, W. J.; Zhang, Z.; Zhu, X.; Neoh, K.-G.; Kang, E.-T. *Soft Matter* **2012**, *8*, 5612–5620.
- [168] Bertrand, A.; Stenzel, M.; Fleury, E.; Bernard, J. *Polym. Chem.* **2012**, *3*, 377–383.
- [169] Martina, K.; Trotta, F.; Robaldo, B.; Belliardi, N.; Jicsinszky, L.; Cravotto, G. *Tetrahedron Lett.* **2007**, *48*, 9185–9189.
- [170] Casati, C.; Franchi, P.; Pievo, R.; Mezzina, E.; Lucarini, M. *J. Am. Chem. Soc.* **2012**, *134*, 19108–19117.
- [171] Zeng, J.; Shi, K.; Zhang, Y.; Sun, X.; Zhang, B. *Chem. Commun.* **2008**, 3753–3755.
- [172] Stadermann, J.; Komber, H.; Erber, M.; Däbritz, F.; Ritter, H.; Voit, B. *Macromolecules* **2011**, *44*, 3250–3259.
- [173] Yan, Q.; Yuan, J.; Cai, Z.; Xin, Y.; Kang, Y.; Yin, Y. *J. Am. Chem. Soc.* **2010**, *132*, 9268–9270.
- [174] Yan, Q.; Xin, Y.; Zhou, R.; Yin, Y.; Yuan, J. *Chem. Commun.* **2011**, *47*, 9594–9596.
- [175] Rao, J.; Paunescu, E.; Mirmohades, M.; Gadwal, I.; Khaydarov, A.; Hawker, C. J.; Bang, J.; Khan, A. *Polym. Chem.* **2012**, *3*, 2050–2056.
- [176] Ren, S.; Chen, D.; Jiang, M. *J. Polym. Sci. Part A: Polym. Chem.* **2009**, *47*, 4267–4278.
- [177] Yan, J.; Zhang, X.; Li, W.; Zhang, X.; Liu, K.; Wu, P.; Zhang, A. *Soft Matter* **2012**, *8*, 6371–6377.
- [178] Zhao, Q.; Wang, S.; Cheng, X.; Yam, R. C. M.; Kong, D.; Li, R. K. Y. *Biomacromolecules* **2010**, *11*, 1364–1369.
- [179] Huskens, J.; Deij, M. A.; Reinhoudt, D. N. *Angew. Chem. Int. Ed.* **2002**, *41*, 4467–4471.

- [180] Auletta, T. et al. *Angew. Chem. Int. Ed.* **2004**, *43*, 369–373.
- [181] Hsu, S.-H.; Yilmaz, M. D.; Blum, C.; Subramaniam, V.; Reinhoudt, D. N.; Velders, A. H.; Huskens, J. *J. Am. Chem. Soc.* **2009**, *131*, 12567–12569.
- [182] González-Campo, A.; Hsu, S.-H.; Puig, L.; Huskens, J.; Reinhoudt, D. N.; Velders, A. H. *J. Am. Chem. Soc.* **2010**, *132*, 11434–11436.
- [183] Ludden, M. J. W.; Mulder, A.; Tampé, R.; Reinhoudt, D. N.; Huskens, J. *Angew. Chem. Int. Ed.* **2007**, *46*, 4104–4107.
- [184] Uhlenheuer, D. A.; Wasserberg, D.; Haase, C.; Nguyen, H. D.; Schenkel, J. H.; Huskens, J.; Ravoo, B. J.; Jonkheijm, P.; Brunsveld, L. *Chem. Eur. J.* **2012**, *18*, 6788–6794.
- [185] Gong, Y.-H.; Li, C.; Yang, J.; Wang, H.-Y.; Zhuo, R.-X.; Zhang, X.-Z. *Macromolecules* **2011**, *44*, 7499–7502.
- [186] Ohno, K.; Wong, B.; Haddleton, D. M. *J. Polym. Sci. Part A: Polym. Chem.* **2001**, *39*, 2206–2214.
- [187] Stenzel-Rosenbaum, M. H.; Davis, T. P.; Chen, V.; Fane, A. G. *Macromolecules* **2001**, *34*, 5433–5438.
- [188] Stenzel, M. H.; Davis, T. P. *J. Polym. Sci. Part A: Polym. Chem.* **2002**, *40*, 4498–4512.
- [189] Karaky, K.; Reynaud, S.; Billon, L.; François, J.; Chreim, Y. *J. Polym. Sci. Part A: Polym. Chem.* **2005**, *43*, 5186–5194.
- [190] Yang, C.; Li, H.; Goh, S. H.; Li, J. *Biomaterials* **2007**, *28*, 3245–3254.
- [191] He, T.; Hu, T.; Zhang, X.; Zhong, G.; Zhang, H. *J. Appl. Polym. Sci.* **2009**, *112*, 2120–2126.
- [192] Fijten, M. W. M.; Haensch, C.; van Lankvelt, B. M.; Hoogenboom, R.; Schubert, U. S. *Macromol. Chem. Phys.* **2008**, *209*, 1887–1895.
- [193] Zhang, L.; Stenzel, M. H. *Aust. J. Chem.* **2009**, *62*, 813–822.
- [194] Xu, J.; Liu, S. *J. Polym. Sci. Part A: Polym. Chem.* **2009**, *47*, 404–419.
- [195] Zhang, H.; Yan, Q.; Kang, Y.; Zhou, L.; Zhou, H.; Yuan, J.; Wu, S. *Polymer* **2012**, *53*, 3719–3725.
- [196] Miura, Y.; Narumi, A.; Matsuya, S.; Satoh, T.; Duan, Q.; Kaga, H.; Kakuchi, T. *J. Polym. Sci. Part A: Polym. Chem.* **2005**, *43*, 4271–4279.

- [197] Zhang, Q.; Li, G.-Z.; Becer, C. R.; Haddleton, D. M. *Chem. Commun.* **2012**, *48*, 8063–8065.
- [198] Teuchert, C.; Michel, C.; Hausen, F.; Park, D.-Y.; Beckham, H. W.; Wenz, G. *Macromolecules* **2013**, *46*, 2–7.
- [199] Nagahama, K.; Aoki, R.; Saito, T.; Ouchi, T.; Ohya, Y.; Yui, N. *Polym. Chem.* **2013**, *4*, 1769–1773.
- [200] Zhang, Z.-X.; Liu, X.; Xu, F. J.; Loh, X. J.; Kang, E.-T.; Neoh, K.-G.; Li, J. *Macromolecules* **2008**, *41*, 5967–5970.
- [201] Zhang, Z.-X.; Liu, K. L.; Li, J. *Macromolecules* **2011**, *44*, 1182–1193.
- [202] Yan, J.; Zhang, X.; Zhang, X.; Liu, K.; Li, W.; Wu, P.; Zhang, A. *Macromol. Chem. Phys.* **2012**, *213*, 2003–2010.
- [203] Guo, M.; Jiang, M.; Pispas, S.; Yu, W.; Zhou, C. *Macromolecules* **2008**, *41*, 9744–9749.
- [204] Liu, J.; Chen, G.; Guo, M.; Jiang, M. *Macromolecules* **2010**, *43*, 8086–8093.
- [205] Du, P.; Liu, J.; Chen, G.; Jiang, M. *Langmuir* **2011**, *27*, 9602–9608.
- [206] Wei, K.; Li, J.; Liu, J.; Chen, G.; Jiang, M. *Soft Matter* **2012**, *8*, 3300–3303.
- [207] Luo, C.; Zuo, F.; Zheng, Z.; Cheng, X.; Ding, X.; Peng, Y. *Macromol. Rapid Commun.* **2008**, *29*, 149–154.
- [208] Li, J. In *Inclusion Polymers*; Wenz, G., Ed.; Advances in Polymer Science; Springer Berlin Heidelberg, 2009; Vol. 222; pp 175–203.
- [209] Li, J.; Loh, X. J. *Adv. Drug Delivery Rev.* **2008**, *60*, 1000–1017.
- [210] Li, J. *NPG Asia Materials* **2010**, *2*, 112–118.
- [211] Ren, L.; He, L.; Sun, T.; Dong, X.; Chen, Y.; Huang, J.; Wang, C. *Macromol. Biosci.* **2009**, *9*, 902–910.
- [212] Sui, K.; Shan, X.; Gao, S.; Xia, Y.; Zheng, Q.; Xie, D. *J. Polym. Sci. Part A: Polym. Chem.* **2010**, *48*, 2143–2153.
- [213] Li, Z.; Yin, H.; Zhang, Z.; Liu, K. L.; Li, J. *Biomacromolecules* **2012**, *13*, 3162–3172.
- [214] Wu, Y.; Ni, P.; Zhang, M.; Zhu, X. *Soft Matter* **2010**, *6*, 3751–3758.
- [215] Zou, J.; Guan, B.; Liao, X.; Jiang, M.; Tao, F. *Macromolecules* **2009**, *42*, 7465–7473.

- [216] Guo, M.; Jiang, M.; Zhang, G. *Langmuir* **2008**, *24*, 10583–10586.
- [217] Inoue, Y.; Kuad, P.; Okumura, Y.; Takashima, Y.; Yamaguchi, H.; Harada, A. *J. Am. Chem. Soc.* **2007**, *129*, 6396–6397.
- [218] Felici, M.; Marzá-Pérez, M.; Hatzakis, N. S.; Nolte, R. J. M.; Feiters, M. C. *Chem. Eur. J.* **2008**, *14*, 9914–9920.
- [219] Millard, P.-E.; Barner, L.; Reinhardt, J.; Buchmeiser, M. R.; Barner-Kowollik, C.; Müller, A. H. E. *Polymer* **2010**, *51*, 4319–4328.
- [220] Smith, A. E.; Xu, X.; Kirkland-York, S. E.; Savin, D. A.; McCormick, C. L. *Macromolecules* **2010**, *43*, 1210–1217.
- [221] Garnier, S.; Laschewsky, A. *Macromolecules* **2005**, *38*, 7580–7592.
- [222] Glatzel, S.; Badi, N.; Pach, M.; Laschewsky, A.; Lutz, J.-F. *Chem. Commun.* **2010**, *46*, 4517–4519.
- [223] Schwarz-Barac, S.; Ritter, H. *J. Macromol. Sci., Part A: Pure Appl. Chem.* **2003**, *A40*, 437–448.
- [224] Ritter, H.; Mondrzik, B. E.; Rehahn, M.; Gallei, M. *Beilstein J. Org. Chem.* **2010**, *6*, No. 60.
- [225] Storsberg, J.; Hartenstein, M.; Müller, A. H. E.; Ritter, H. *Macromol. Rapid Commun.* **2000**, *21*, 1342–1346.
- [226] Köllisch, H. S.; Barner-Kowollik, C.; Ritter, H. *Macromol. Rapid Commun.* **2006**, *27*, 848–853.
- [227] Köllisch, H. S.; Barner-Kowollik, C.; Ritter, H. *Chem. Commun.* **2009**, 1097–1099.
- [228] Pang, Y.; Ritter, H.; Tabatabai, M. *Macromolecules* **2003**, *36*, 7090–7093.
- [229] Ding, L.; Li, Y.; Deng, J.; Yang, W. *Polym. Chem.* **2011**, *2*, 694–701.
- [230] Weickenmeier, M.; Wenz, G.; Huff, J. *Macromol. Rapid Commun.* **1997**, *18*, 1117–1123.
- [231] Kujawa, P.; Segui, F.; Shaban, S.; Diab, C.; Okada, Y.; Tanaka, F.; Winnik, F. M. *Macromolecules* **2005**, *39*, 341–348.
- [232] Vogt, A. P.; Sumerlin, B. S. *Macromolecules* **2008**, *41*, 7368–7373.
- [233] Li, H.; Yu, B.; Matsushima, H.; Hoyle, C. E.; Lowe, A. B. *Macromolecules* **2009**, *42*, 6537–6542.

- [234] Skey, J.; O'Reilly, R. K. *Chem. Commun.* **2008**, 4183–4185.
- [235] Glockner, P.; Schollmeyer, D.; Ritter, H. *Des. Monomers Polym.* **2002**, *5*, 163–172.
- [236] Funasaki, N.; Yodo, H.; Hada, S.; Neya, S. *Bull. Chem. Soc. Jpn.* **1992**, *65*, 1323–1330.
- [237] Rekharsky, M. V.; Inoue, Y. *Chem. Rev.* **1998**, *98*, 1875–1918.
- [238] Baussard, J.-F.; Habib-Jiwan, J.-L.; Laschewsky, A.; Mertoglu, M.; Storsberg, J. *Polymer* **2004**, *45*, 3615–3626.
- [239] Suetsugu, N.; Koyama, S.; Takeo, K.; Kuge, T. *J. Biochem.* **1974**, *76*, 57–63.
- [240] Jodái, I.; Kandra, L.; Harangi, J.; Nánási, P.; Szejtli, J. *Starch - Stärke* **1984**, *36*, 140–143.
- [241] Fetzner, A.; Böhm, S.; Schreder, S.; Schubert, R. *Eur. J. Pharm. Biopharm.* **2004**, *58*, 91–97.
- [242] Gan, L. H.; Cai, W.; Tam, K. C. *Eur. Polym. J.* **2001**, *37*, 1773–1778.
- [243] Heskins, M.; Guillet, J. E. *J. Macromol. Sci., Part A: Pure Appl. Chem.* **1968**, *2*, 1441–1455.
- [244] Lodge, T. P. *Macromol. Chem. Phys.* **2003**, *204*, 265–273.
- [245] Ruzette, A.-V.; Leibler, L. *Nat. Mater.* **2005**, *4*, 19–31.
- [246] Ishizone, T.; Hirao, A. In *Synthesis of Polymers: New Structures and Methods*; Schlüter, A. D., Hawker, C. J., Sakamoto, J., Eds.; Wiley-VCH, Weinheim, 2012; Chapter Anionic Polymerization: Recent Advances, pp 81–134.
- [247] Aoshima, S.; Kanaoka, S. *Chem. Rev.* **2009**, *109*, 5245–5287.
- [248] Opsteen, J. A.; van Hest, J. C. M. *Chem. Commun.* **2005**, 57–59.
- [249] Hizal, G.; Tunca, U.; Sanyal, A. *J. Polym. Sci. Part A: Polym. Chem.* **2011**, *49*, 4103–4120.
- [250] Inglis, A. J.; Stenzel, M. H.; Barner-Kowollik, C. *Macromol. Rapid Commun.* **2009**, *30*, 1792–1798.
- [251] Schmidt, B. V. K. J.; Fechler, N.; Falkenhagen, J.; Lutz, J. F. *Nat. Chem.* **2011**, *3*, 234–238.
- [252] Fleige, E.; Quadir, M. A.; Haag, R. *Adv. Drug Delivery Rev.* **2012**, *64*, 866–884.

- [253] Ross, P. D.; Rekharsky, M. V. *Biophys. J.* **1996**, *71*, 2144–2154.
- [254] Kwak, R. N. Y.; Matyjaszewski, K. *Macromolecules* **2008**, *41*, 4585–4596.
- [255] Inoue, K. *Prog. Polym. Sci.* **2000**, *25*, 453–571.
- [256] Khanna, K.; Varshney, S.; Kakkar, A. *Polym. Chem.* **2010**, *1*, 1171–1185.
- [257] Higashihara, T.; Hayashi, M.; Hirao, A. *Prog. Polym. Sci.* **2011**, *36*, 323–375.
- [258] Kreutzer, G.; Ternat, C.; Nguyen, T. Q.; Plummer, C. J. G.; Månson, J.-A. E.; Castelletto, V.; Hamley, I. W.; Sun, F.; Sheiko, S. S.; Herrmann, A.; Ouali, L.; Sommer, H.; Fieber, W.; Velazco, M. I.; Klok, H.-A. *Macromolecules* **2006**, *39*, 4507–4516.
- [259] Liu, J.; Duong, H.; Whittaker, M. R.; Davis, T. P.; Boyer, C. *Macromol. Rapid Commun.* **2012**, *33*, 760–766.
- [260] Chen, L.; Li, P.; Tong, H.; Xie, Z.; Wang, L.; Jing, X.; Wang, F. *J. Polym. Sci. Part A: Polym. Chem.* **2012**, *50*, 2854–2862.
- [261] Kanaoka, S.; Sawamoto, M.; Higashimura, T. *Macromolecules* **1991**, *24*, 2309–2313.
- [262] Schlaad, H.; Diehl, C.; Gress, A.; Meyer, M.; Demirel, A. L.; Nur, Y.; Bertin, A. *Macromol. Rapid Commun.* **2010**, *31*, 511–525.
- [263] Hirano, T.; Yoo, H. S.; Ozama, Y.; Abou El-Magd, A.; Sugiyama, K.; Hirao, A. *J. Inorg. Organomet. Polym. Mater.* **2010**, *20*, 445–456.
- [264] Roovers, J. E. L.; Bywater, S. *Macromolecules* **1974**, *7*, 443–449.
- [265] Hawker, C. J. *Angew. Chem. Int. Ed.* **1995**, *34*, 1456–1459.
- [266] Jankova, K.; Bednarek, M.; Hvilsted, S. *J. Polym. Sci. Part A: Polym. Chem.* **2005**, *43*, 3748–3759.
- [267] Barner-Kowollik, C.; Davis, T. P.; Stenzel, M. H. *Aust. J. Chem.* **2006**, *59*, 719–727.
- [268] Altintas, O.; Vogt, A. P.; Barner-Kowollik, C.; Tunca, U. *Polym. Chem.* **2012**, *3*, 34–45.
- [269] Gao, H.; Matyjaszewski, K. *Macromolecules* **2006**, *39*, 4960–4965.
- [270] Chan, J. W.; Yu, B.; Hoyle, C. E.; Lowe, A. B. *Chem. Commun.* **2008**, 4959–4961.
- [271] Inglis, A. J.; Sinnwell, S.; Stenzel, M. H.; Barner-Kowollik, C. *Angew. Chem. Int. Ed.* **2009**, *48*, 2411–2414.

- [272] Iskin, B.; Yilmaz, G.; Yagci, Y. *Polym. Chem.* **2011**, *2*, 2865–2871.
- [273] Bernard, J.; Lortie, F.; Fenet, B. *Macromol. Rapid Commun.* **2009**, *30*, 83–88.
- [274] Likhitsup, A.; Yu, S.; Ng, Y.-H.; Chai, C. L. L.; Tam, E. K. W. *Chem. Commun.* **2009**, 4070–4072.
- [275] Altintas, O.; Muller, T.; Lejeune, E.; Plietzsch, O.; Bräse, S.; Barner-Kowollik, C. *Macromol. Rapid Commun.* **2012**, *33*, 977–983.
- [276] Wu, X.; Fraser, C. L. *Macromolecules* **2000**, *33*, 7776–7785.
- [277] Schubert, U. S.; Heller, M. *Chem. Eur. J.* **2001**, *7*, 5252–5259.
- [278] Gadwal, I.; De, S.; Stuparu, M. C.; Amir, R. J.; Jang, S. G.; Khan, A. J. *Polym. Sci. Part A: Polym. Chem.* **2012**, *50*, 1844–1850.
- [279] Huang, F.; Nagvekar, D. S.; Slebodnick, C.; Gibson, H. W. *J. Am. Chem. Soc.* **2004**, *127*, 484–485.
- [280] Davis, M. E. *Mol. Pharm.* **2009**, *6*, 659–668.
- [281] Yhaya, F.; Lim, J.; Kim, Y.; Liang, M.; Gregory, A. M.; Stenzel, M. H. *Macromolecules* **2011**, *44*, 8433–8445.
- [282] Dong, R.; Liu, Y.; Zhou, Y.; Yan, D.; Zhu, X. *Polym. Chem.* **2011**, *2*, 2771–2774.
- [283] Wang, X.; Wu, C. *Macromolecules* **1999**, *32*, 4299–4301.
- [284] Kujawa, P.; Winnik, F. M. *Macromolecules* **2001**, *34*, 4130–4135.
- [285] Mao, H.; Li, C.; Zhang, Y.; Furyk, S.; Cremer, P. S.; Bergbreiter, D. E. *Macromolecules* **2004**, *37*, 1031–1036.
- [286] Chen, S.; Bertrand, A.; Chang, X.; Alcouffe, P.; Ladavière, C.; Gérard, J.-F.; Lortie, F.; Bernard, J. *Macromolecules* **2010**, *43*, 5981–5988.
- [287] Altintas, O.; Tunca, U.; Barner-Kowollik, C. *Polym. Chem.* **2011**, *2*, 1146–1155.
- [288] Fustin, C. A.; Guillet, P.; Schubert, U. S.; Gohy, J. F. *Adv. Mater.* **2007**, *19*, 1665–1673.
- [289] Rauwald, U.; Scherman, O. *Angew. Chem. Int. Ed.* **2008**, *47*, 3950–3953.
- [290] Kretschmann, O.; Choi, S. W.; Miyauchi, M.; Tomatsu, I.; Harada, A.; Ritter, H. *Angew. Chem. Int. Ed.* **2006**, *45*, 4361–4365.

- [291] Bigot, J.; Charleux, B.; Cooke, G.; Delattre, F.; Fournier, D.; Lyskawa, J.; Sambe, L.; Stoffelbach, F.; Woisel, P. *J. Am. Chem. Soc.* **2010**, *132*, 10796–10801.
- [292] Li, L.-Y.; He, W.-D.; Li, J.; Zhang, B.-Y.; Pan, T.-T.; Sun, X.-L.; Ding, Z.-L. *Biomacromolecules* **2010**, *11*, 1882–1890.
- [293] Sakai, F.; Chen, G.; Jiang, M. *Polym. Chem.* **2012**, *3*, 954–961.
- [294] Alarcon, C. d. I. H.; Pennadam, S.; Alexander, C. *Chem. Soc. Rev.* **2005**, *34*, 276–285.
- [295] Li, Y.; Lokitz, B. S.; McCormick, C. L. *Angew. Chem. Int. Ed.* **2006**, *45*, 5792–5795.
- [296] Liu, F.; Urban, M. W. *Prog. Polym. Sci.* **2010**, *35*, 3–23.
- [297] Roy, D.; Brooks, W. L. A.; Sumerlin, B. S. *Chem. Soc. Rev.* **2013**, DOI:10.1039/C3CS35499G.
- [298] Schmaljohann, D. *Adv. Drug Delivery Rev.* **2006**, *58*, 1655–1670.
- [299] York, A. W.; Kirkland, S. E.; McCormick, C. L. *Adv. Drug Delivery Rev.* **2008**, *60*, 1018–1036.
- [300] Hoogenboom, R.; Thijs, H. M. L.; Jochems, M. J. H. C.; van Lankvelt, B. M.; Fijten, M. W. M.; Schubert, U. S. *Chem. Commun.* **2008**, 5758–5760.
- [301] Lutz, J.-F. *Adv. Mater.* **2011**, *23*, 2237–2243.
- [302] Hirokawa, Y.; Tanaka, T. *J. Chem. Phys.* **1984**, *81*, 6379–6380.
- [303] Glatzel, S.; Laschewsky, A.; Lutz, J.-F. *Macromolecules* **2010**, *44*, 413–415.
- [304] Idziak, I.; Avoce, D.; Lessard, D.; Gravel, D.; Zhu, X. X. *Macromolecules* **1999**, *32*, 1260–1263.
- [305] Zhao, Y.; Tremblay, L.; Zhao, Y. *Macromolecules* **2011**, *44*, 4007–4011.
- [306] Duan, Q.; Miura, Y.; Narumi, A.; Shen, X.; Sato, S.-I.; Satoh, T.; Kakuchi, T. *J. Polym. Sci. Part A: Polym. Chem.* **2006**, *44*, 1117–1124.
- [307] Maatz, G.; Maciollek, A.; Ritter, H. *Beilstein J. Org. Chem.* **2012**, *8*, 1929–1935.
- [308] Ritter, H.; Sadowski, O.; Tepper, E. *Angew. Chem. Int. Ed.* **2003**, *42*, 3171–3173.
- [309] Rauwald, U.; Barrio, J. d.; Loh, X. J.; Scherman, O. A. *Chem. Commun.* **2011**, *47*, 6000–6002.
- [310] Summers, M. J.; Phillips, D. J.; Gibson, M. I. *Chem. Commun.* **2013**, *49*, 4223–4225.

- [311] Jochum, F. D.; zur Borg, L.; Roth, P. J.; Theato, P. *Macromolecules* **2009**, *42*, 7854–7862.
- [312] Moore, J. S.; Stupp, S. I. *Macromolecules* **1990**, *23*, 65–70.
- [313] Ihre, H.; Hult, A.; Fréchet, J. M. J.; Gitsov, I. *Macromolecules* **1998**, *31*, 4061–4068.
- [314] Moad, G.; Chong, Y. K.; Postma, A.; Rizzardo, E.; Thang, S. H. *Polymer* **2005**, *46*, 8458–8468.
- [315] Yu, Z.; Sawkar, A. R.; Whalen, L. J.; Wong, C.-H.; Kelly, J. W. *J. Med. Chem.* **2006**, *50*, 94–100.
- [316] Apostolovic, B.; Deacon, S. P. E.; Duncan, R.; Klok, H.-A. *Biomacromolecules* **2010**, *11*, 1187–1195.
- [317] Li, C.; Lo, C.-W.; Zhu, D.; Li, C.; Liu, Y.; Jiang, H. *Macromol. Rapid Commun.* **2009**, *30*, 1928–1935.

List of Abbreviations

2VP.....	2-vinylpyridine
4VP.....	4-vinylpyridine
AA.....	acrylic acid
AAm.....	acrylamide
Ad.....	adamantyl
AIBN.....	2,2'-azobis(2-methylpropionitrile)
AFM.....	atomic force microscopy
AMPS.....	2-acrylamido-2-methylpropanesulfonic acid
arom.....	aromatic
ATRP.....	atom transfer radical polymerization
β_{mn}	overall association constant
β -CD-N ₃	mono azido functionalized β -CD
CBMAA-3.....	3-(methacryloylamino-propyl)-(2-carboxy-ethyl)-dimethyl-ammonium carboxybetaine methacrylamide
CD.....	cyclodextrin
ConA.....	concanavalin A
CL.....	ϵ -caprolactone
CMP.....	2-(1-carboxy-1-methylethylsulfanylthiocarbonylsulfanyl)-2-methylpropionic acid
CPDB.....	2-cyano-2-propyl benzodithioate
CTA.....	chain transfer agent
C_{tr}	chain transfer constant
CTP.....	4-cyano-4-(phenylcarbonothioylthio)pentanoic acid
CuAAC.....	copper (I) catalyzed azide-alkyne cycloaddition
d	average number of chains formed in a termination reaction
D_h	hydrodynamic diameter
D_m	molar mass dispersity

D_p	degree of polymerization
DCC.....	<i>N,N'</i> -dicyclohexylcarbodiimide
DCM.....	dichloromethane
DEAAm.....	<i>N,N</i> -diethylacrylamide
DIAD.....	diisopropylazodicarboxylate
DLS.....	dynamic light scattering
DMF.....	<i>N,N</i> -dimethylformamide
DMAAm.....	<i>N,N</i> -dimethylacrylamide
DMAc.....	<i>N,N</i> -dimethylacetamide
DMAEMA.....	<i>N,N</i> -dimethylaminoethyl methacrylate
DMAP.....	4-dimethylaminopyridine
DMAPS.....	3-dimethyl(methacryloyloxyethyl) ammonium propane sulfonate
DMP.....	2-(dodecylthiocarbonothioylthio)-2-methylpropionic acid
DMSO.....	dimethylsulfoxide
DNA.....	desoxyribonucleic acid
Dopat.....	2-((dodecylsulfanyl)carbonothioyl)sulfanyl propionic acid
DOSY.....	diffusion-ordered NMR spectroscopy
Dox.....	Doxorubicin
DPTS.....	4-(dimethylamino)-pyridinium <i>p</i> -toluenesulfonate
ECD.....	PEG- <i>b</i> -PCL- <i>b</i> -PDMAEMA
EDTA.....	ethylenediaminetetraacetic acid disodium salt
EMP.....	2-(((ethylthio)carbonothioyl)thio)-2-methylpropanoic acid
EPX.....	ethyl 2-((ethoxycarbonothioyl)thio)propanoate
eq.....	equivalents
ESI-MS.....	electrospray ionization mass spectrometry
<i>f</i>	initiator efficiency
FT-IR.....	Fourier transform infrared
GAPDH.....	glyceraldehyde 3-phosphate dehydrogenase
$\Delta H_{\text{complex}}$	complex association enthalpy
HEA.....	hydroxy ethylacrylate
HPMA.....	<i>N</i> -(2-hydroxypropyl)methacrylamide
ITC.....	isothermal titration calorimetry
<i>J</i>	coupling constant
K_{ij}	association constant of <i>i</i> and <i>j</i>
k_{add}	rate coefficient of addition
k_{β}	rate coefficient of fragmentation
k_{de}	rate coefficient of initiator decay
k_{ini}	rate coefficient of initiation

k_p	rate coefficient of propagation
k_{trec}	rate coefficient of termination by recombination
k_{td}	rate coefficient of termination by disproportionation
λ	wavelength
LCST	lower critical solution temperature
MADIX	macromolecular design via the interchange of xanthates
Me- β -CD	randomly methylated β -cyclodextrin
m_{CTA}	molar mass of CTA
m_M	molar mass of monomer
M_n	number-average molecular weight
MPEG	methoxy poly(ethylene glycol)
MS	mass spectrometry
MWCO	molecular weight cut off
NAS	<i>N</i> -acryloxysuccinimide
NCCM	noncovalently connected micelle
NIPAAm	<i>N</i> -isopropylacrylamide
NMP	nitroxide mediated polymerization
NMR	nuclear magnetic resonance
NOESY	nuclear Overhauser enhancement spectroscopy
OEGMA	oligo ethylene glycol methacrylate
PAA	poly(acrylic acid)
PCL	poly(ϵ -caprolactone)
PDEAAm	poly(<i>N,N</i> -diethylacrylamide)
pDNA	plasmid DNA
PDMAAm	poly(<i>N,N</i> -dimethylacrylamide)
PDMAEMA	poly(2-(dimethylamino)ethyl methacrylate)
PEG	poly(ethylene glycol)
PHEA	poly(hydroxy ethylacrylate)
PHPMA	poly(<i>N</i> -(2-hydroxypropyl)methacrylamide)
PLA	poly(lactic acid)
PMDETA	<i>N,N,N',N'',N''</i> -pentamethyldiethyltriamine
PMMA	poly(methyl methacrylate)
PNIPAAm	poly(<i>N</i> -isopropylacrylamide)
PPG	poly(propylene glycol)
PSty	poly(styrene)
R_h	hydrodynamic radius
RAFT	reversible addition-fragmentation chain transfer
RI	refractive index

ROESY	rotating frame nuclear Overhauser enhancement spectroscopy
ROP	ring opening polymerization
$\Delta S_{\text{complex}}$	complex association entropy
SEC	size exclusion chromatography
SEM	scanning electron microscopy
SLS	static light scattering
siRNA	small interfering ribonucleic acid
TEM	transmission electron microscopy
TFA	trifluoroacetic acid
TGA	thermo gravimetric analysis
THF	tetrahydrofuran
UV	ultra-violet
UV/Vis	ultra-violet/visible
V-501	4,4'-azobis(4-cyanovaleric acid)
VA-044	2,2'-azobis[2-(2-imidazolin-2-yl)propane]dihydrochloride
XPS	X-ray photoelectron spectroscopy

CD-Complexed RAFT Agents (Appendix to Chapter 3)

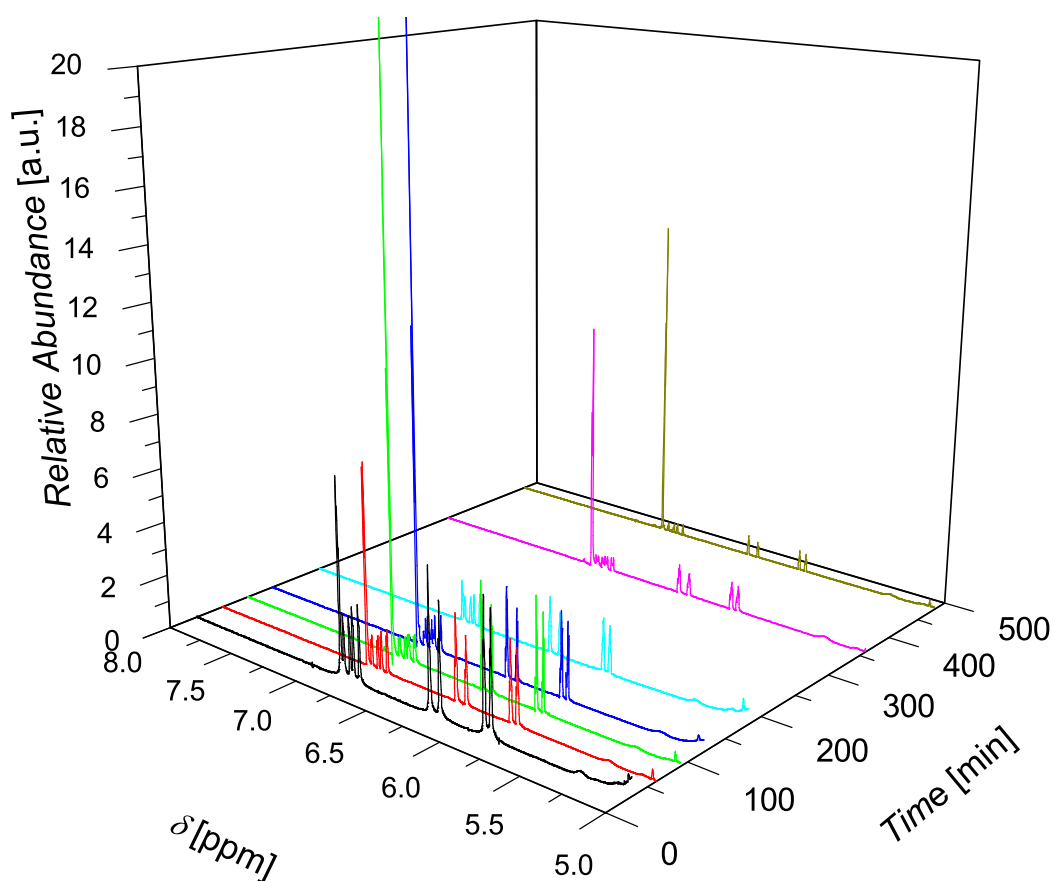


Figure A.1: 3D plot of the vinyl region of the kinetic $^1\text{H-NMR}$ -data for the polymerization of DMAAm at 25 °C with DMAAm/1/I: 298/1/0.2.

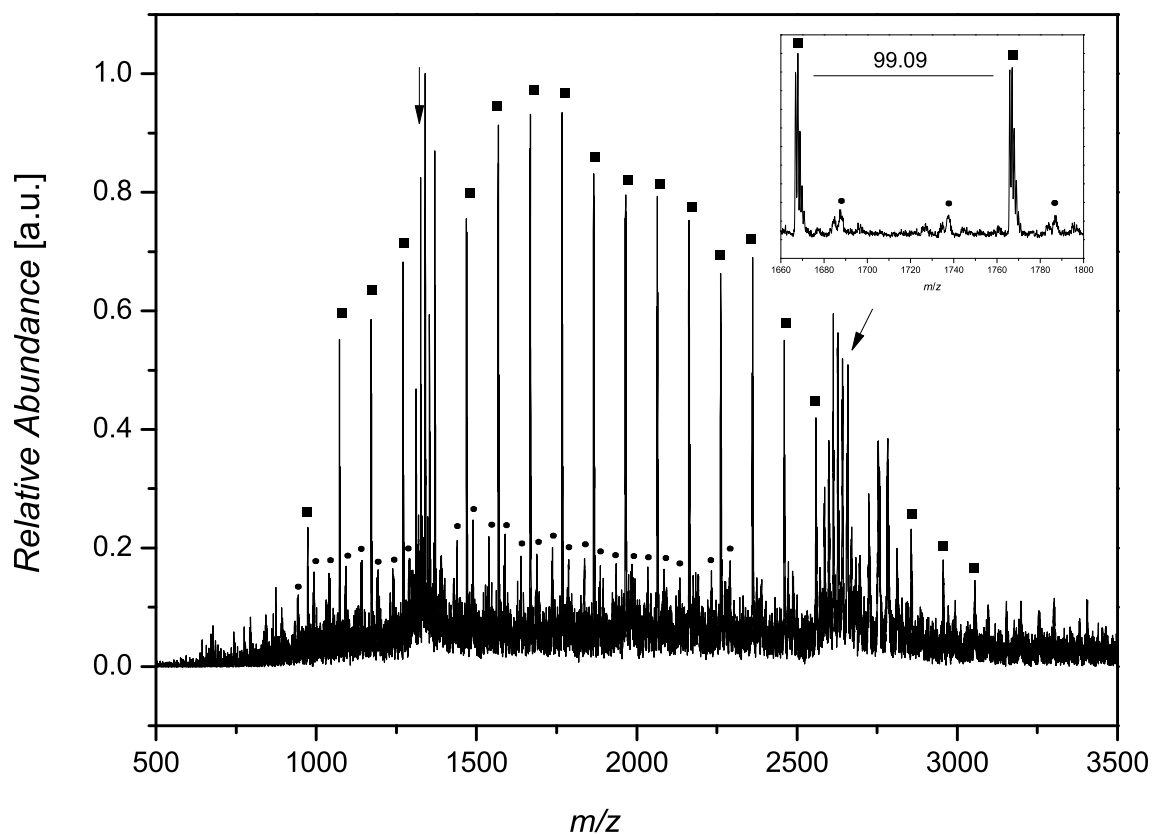


Figure A.2: ESI-MS-spectrum of PDMAAm ($M_{nSEC} = 3000 \text{ g}\cdot\text{mol}^{-1}$, $D_m = 1.18$) polymerized with **1** (the arrow marks residual Me- β -CD).

Table A.1: Theoretical and experimental m/z of PDMAAm polymerized with **1**.

Species	m/z_{theo}	m/z_{exp}	$\Delta m/z$
■ $[2+(\text{DMAAm})_{13}+\text{Na}]^+$	1666.97	1666.82	0.15
● $[2+(\text{DMAAm})_{30}+2\text{Na}]^{2+}$	1687.57	1687.27	0.30

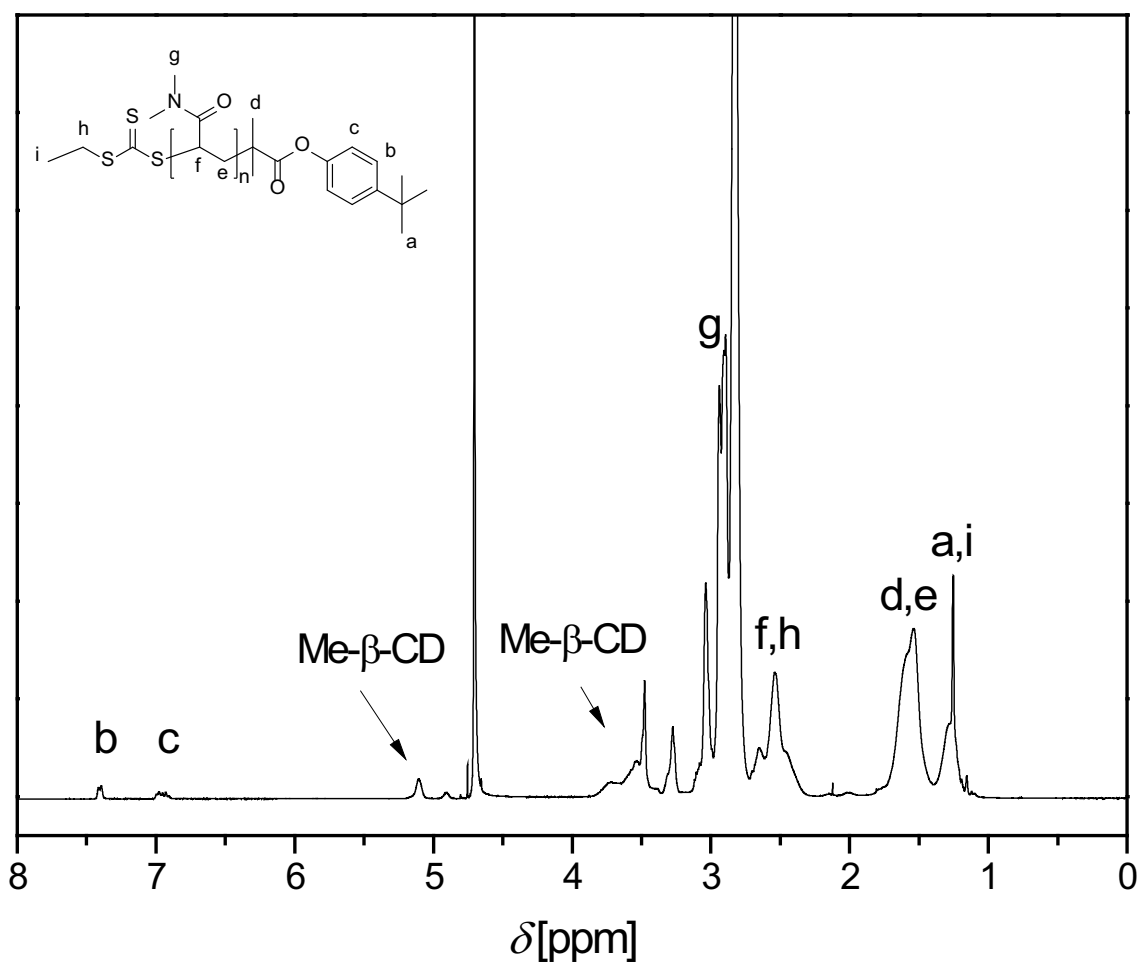


Figure A.3: $^1\text{H-NMR}$ spectrum (400 MHz, D_2O) of PDMAAm polymerized with 1 ($M_{\text{nSEC}} = 10000 \text{ g}\cdot\text{mol}^{-1}$, $D_{\text{m}} = 1.17$).

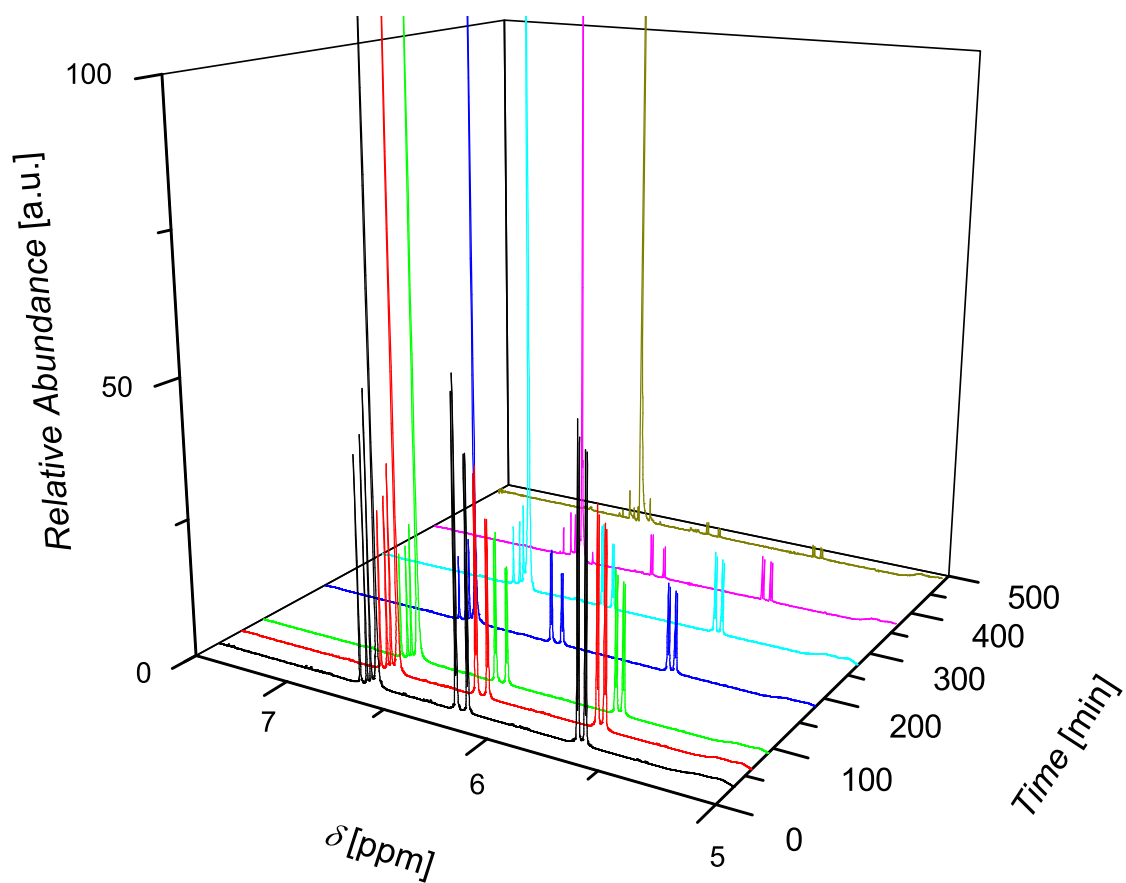


Figure A.4: 3D plot of the vinyl region of the kinetic $^1\text{H-NMR}$ -data for the polymerization of DEAAm at 25 °C with DEAAm/1/I: 242/1/0.2.

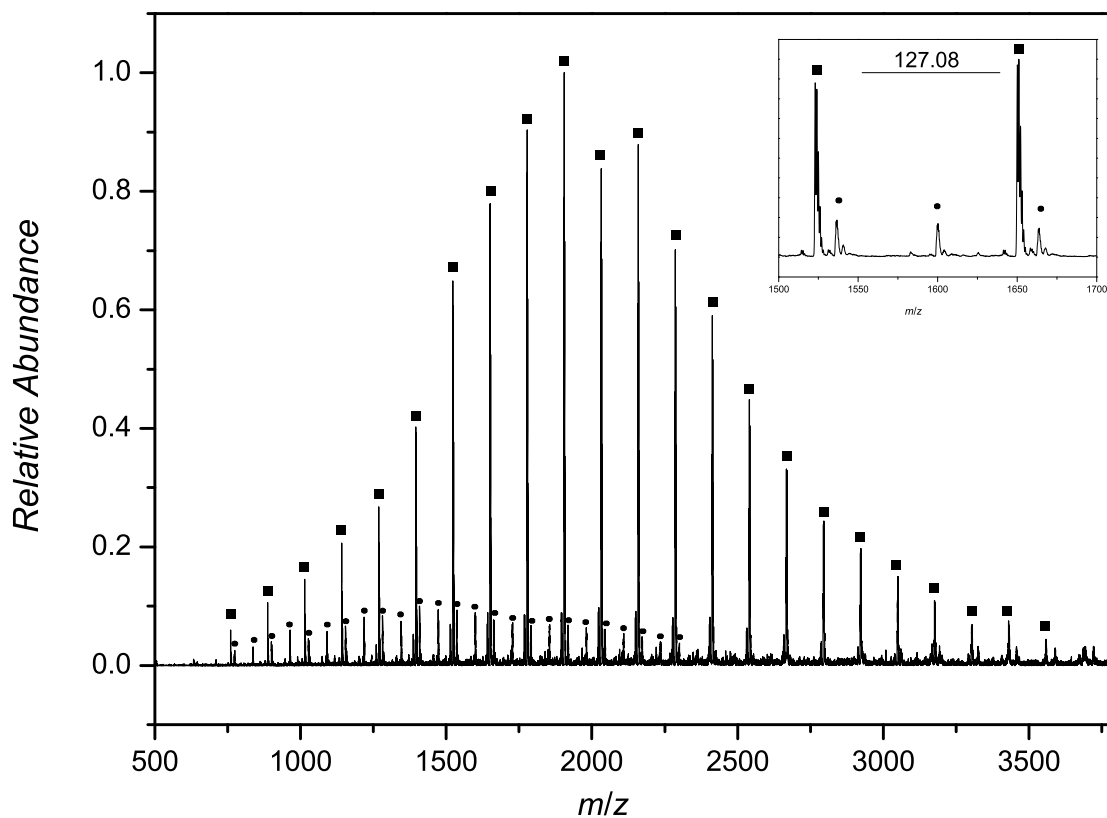


Figure A.5: ESI-MS-spectrum of PDEAAm ($M_{nSEC} = 4000 \text{ g}\cdot\text{mol}^{-1}$, $D_m = 1.15$) polymerized with **1**.

Table A.2: Theoretical and experimental m/z of PDEAAm polymerized with **1**.

Species	m/z_{theo}	m/z_{exp}	$\Delta m/z$
■ $[1+(\text{DEAAm})_9+\text{Na}]^+$	1522.98	1523.00	0.02
● $[1+(\text{DEAAm})_{22}+2\text{Na}]^{2+}$	1599.75	1600.25	0.50

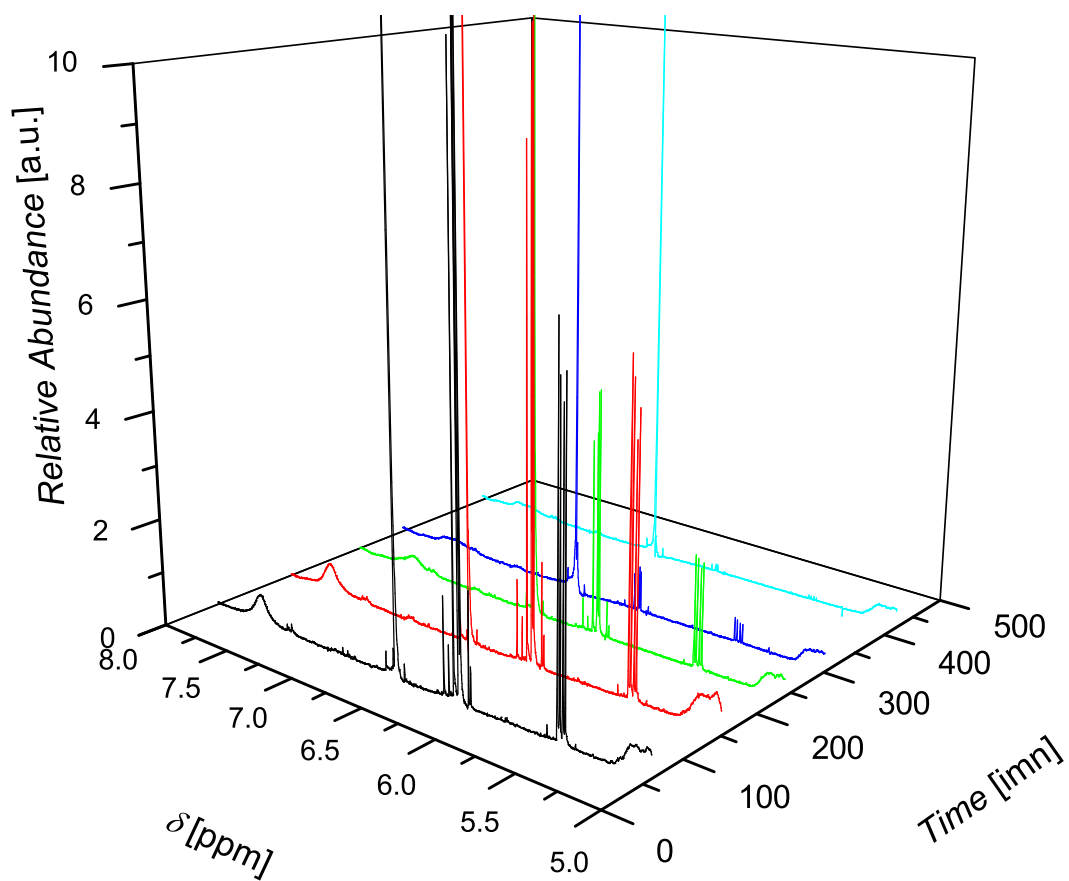


Figure A.7: 3D plot of the vinyl region of the kinetic $^1\text{H-NMR}$ -data for the polymerization of NIPAAm at 25 °C with NIPAAm/1/I: 48/1/0.2.

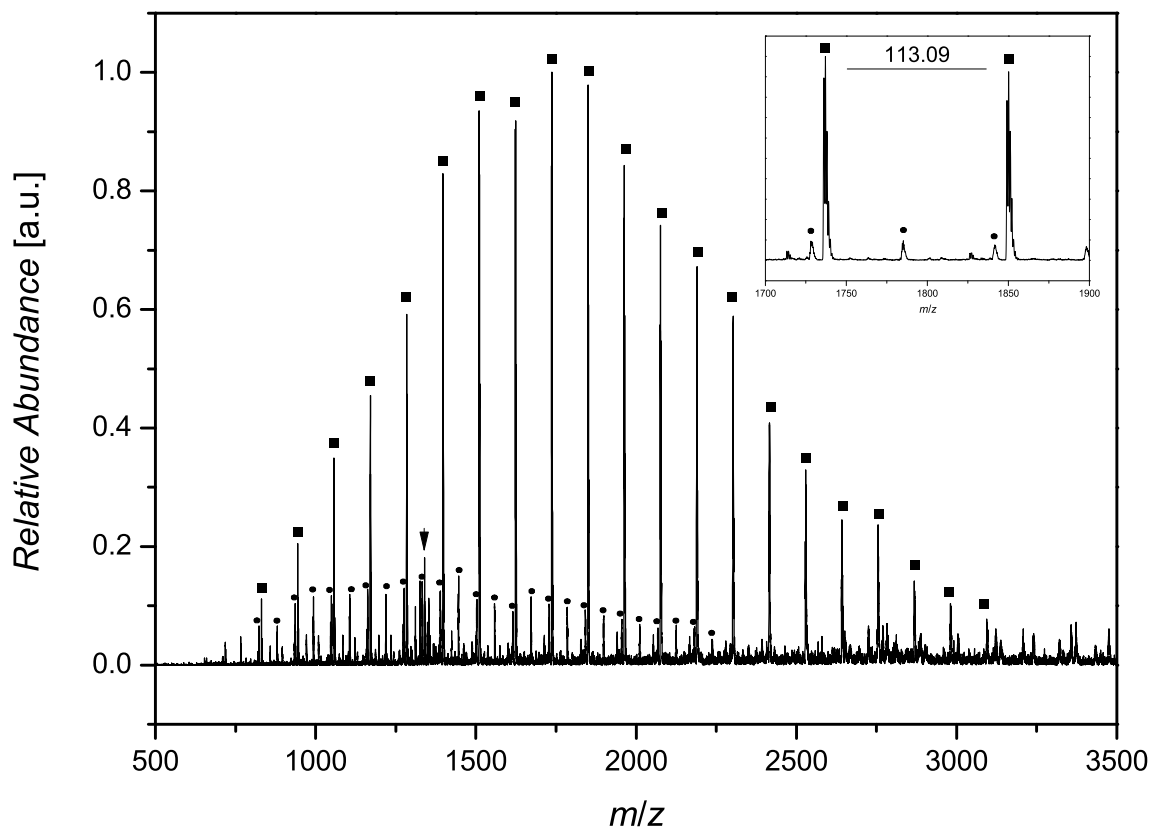


Figure A.8: ESI-MS-spectrum of PNIPAAm ($M_{nSEC} = 4000 \text{ g}\cdot\text{mol}^{-1}$, $D_m = 1.15$) polymerized with **1**.

Table A.3: Theoretical and experimental m/z of PNIPAAm polymerized with **1**.

Species	m/z_{theo}	m/z_{exp}	$\Delta m/z$
■ $[1+(\text{NIPAAm})_{12}+\text{Na}]^+$	1736.09	1736.18	0.09
● $[1+(\text{NIPAAm})_{27}+2\text{Na}]^{2+}$	1728.18	1728.09	0.09

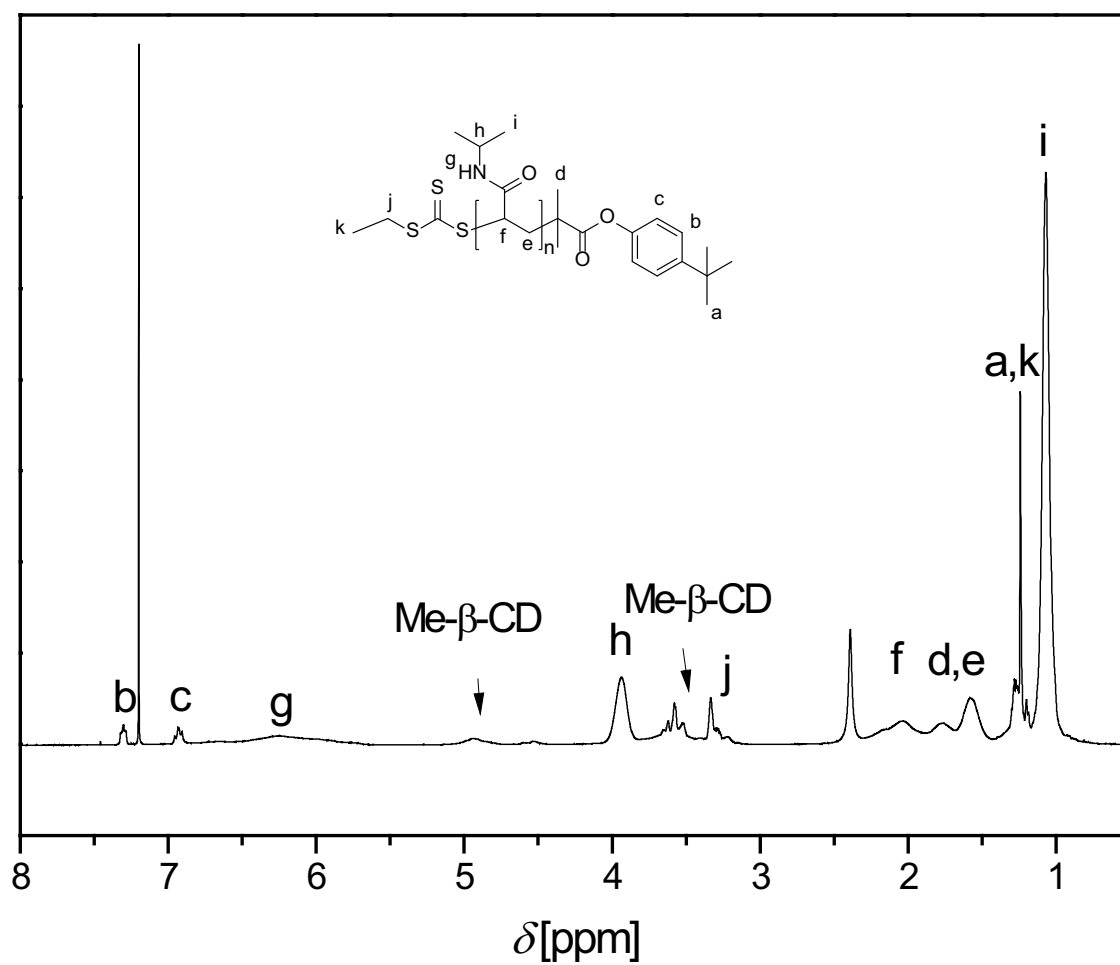


Figure A.9: $^1\text{H-NMR}$ spectrum (400 MHz, CDCl_3) of PNIPAAm polymerized with 1 ($M_{\text{nSEC}} = 4000 \text{ g}\cdot\text{mol}^{-1}$, $D_m = 1.15$).

APPENDIX **B**

Supramolecular ABA Triblock Copolymers (Appendix to Chapter 4)

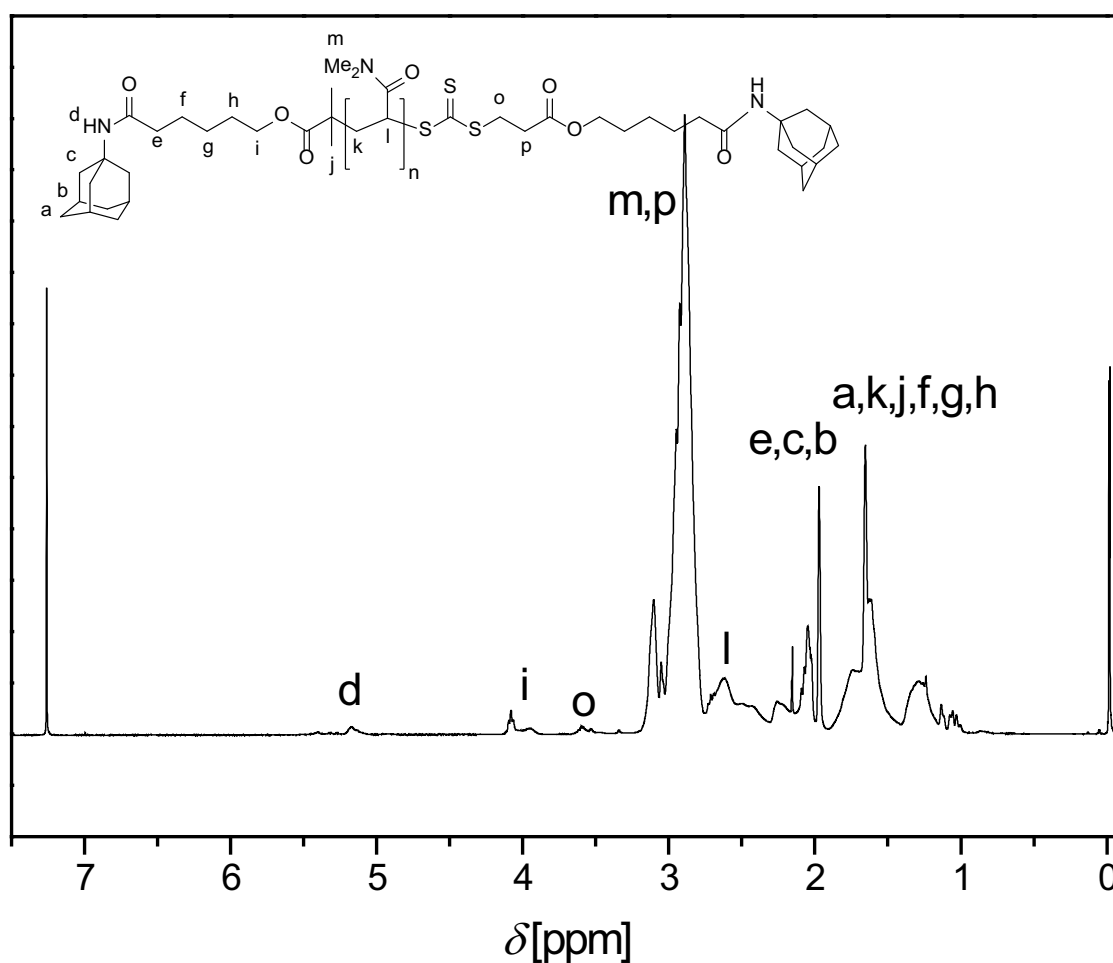


Figure B.1: $^1\text{H-NMR}$ spectrum (400 MHz, CDCl_3) of doubly adamantyl-functionalized PDMAAm ($M_{n\text{SEC}} = 6400 \text{ g}\cdot\text{mol}^{-1}$, $D_m = 1.06$) polymerized with **5** at 25 °C.

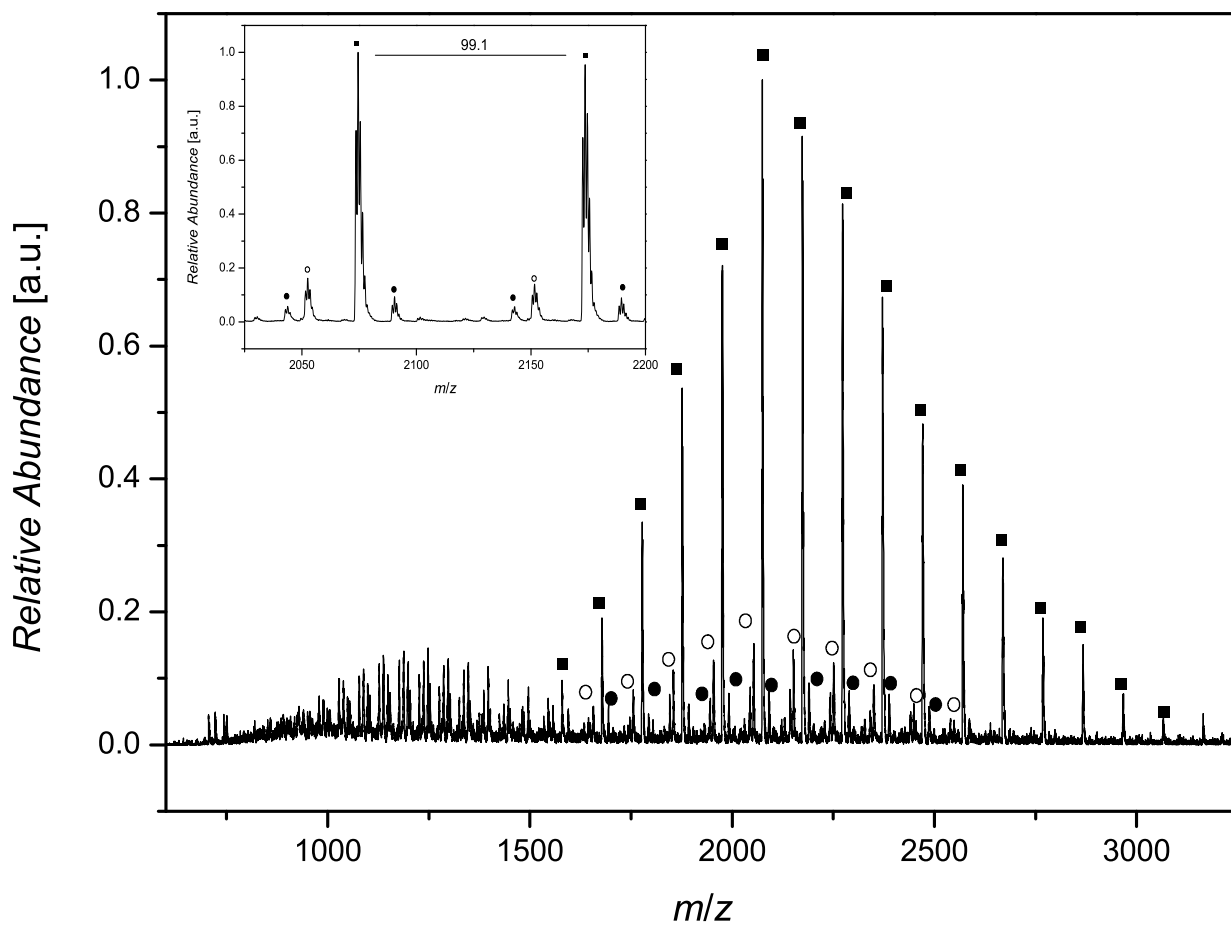


Figure B.2: ESI-MS spectrum of doubly adamantyl-functionalized PDMAAm ($M_{nSEC} = 3300 \text{ g}\cdot\text{mol}^{-1}$, $D_m = 1.06$) polymerized with 5.

Table B.1: Theoretical and experimental m/z of PDMAAm polymerized with 5.

Species	m/z_{theo}	m/z_{exp}	$\Delta m/z$
■ $[5+(\text{DMAAm})_{13}+\text{Na}]^+$	2074.26	2074.45	0.19
○ $[5+(\text{DMAAm})_{14}+\text{H}]^+$	2151.35	2151.45	0.10
● $[5+(\text{DMAAm})_{34}+2\text{Na}]^{2+}$	2089.34	2090.18	0.84

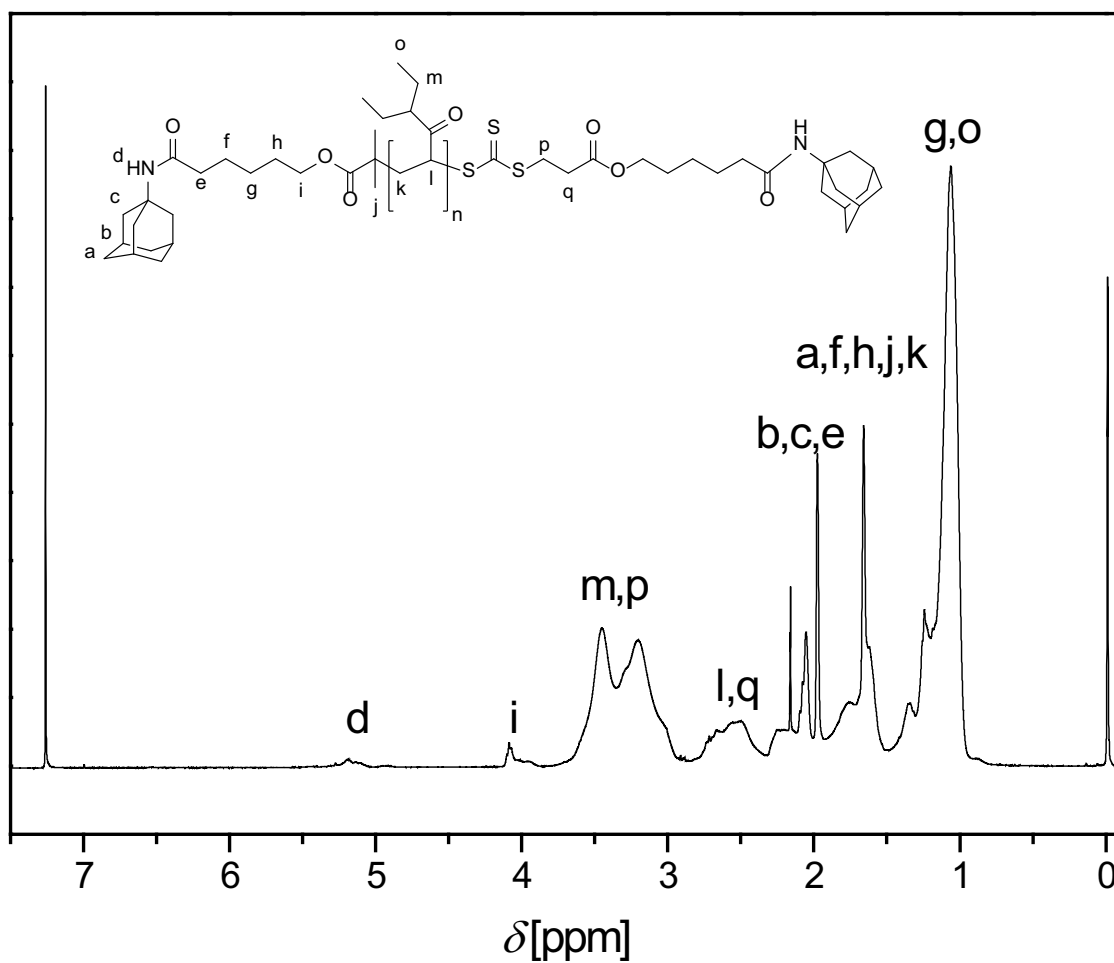


Figure B.3: ¹H-NMR spectrum (400 MHz, CDCl₃) of doubly adamantyl-functionalized PDEAAm ($M_{nSEC} = 5100 \text{ g}\cdot\text{mol}^{-1}$, $D_m = 1.05$) polymerized with 5 at 25 °C.

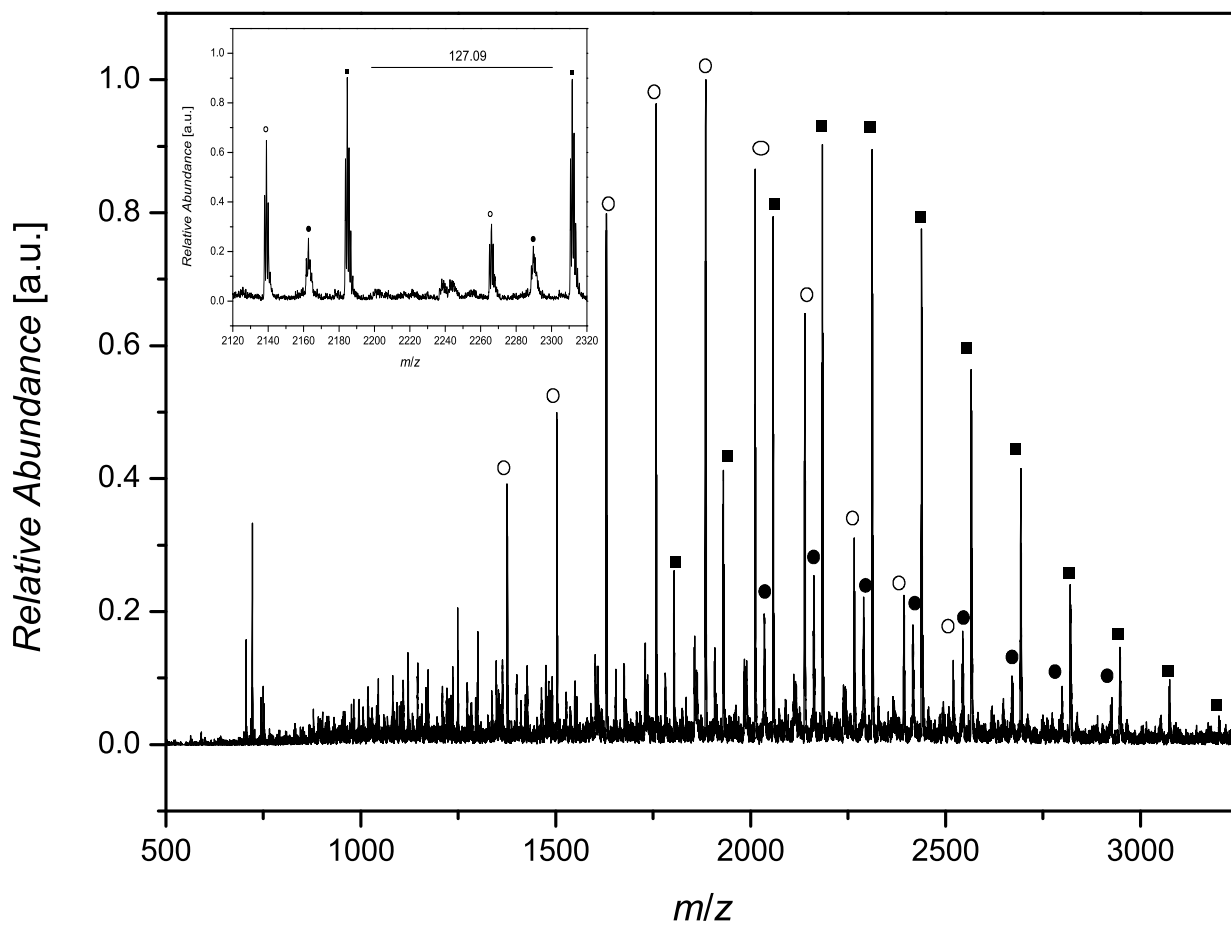


Figure B.4: ESI-MS spectrum of doubly adamantyl-functionalized PDEAAm ($M_{nSEC} = 1800 \text{ g}\cdot\text{mol}^{-1}$, $D_m = 1.06$) polymerized with 5.

Table B.2: Theoretical and experimental m/z of PDEAAm polymerized with 5.

Species	m/z_{theo}	m/z_{exp}	$\Delta m/z$
■ $[5+(\text{DEAAm})_{11}+\text{Na}]^+$	2074.26	2074.45	0.19
○ $[5+(\text{DEAAm})_{10}\text{-C}_{20}\text{H}_{30}\text{NO}_3\text{S}_3+\text{Na}]^+$	2151.35	2151.45	0.10
● $[5+(\text{DEAAm})_{11}+\text{H}]^+$	2089.34	2090.18	0.84

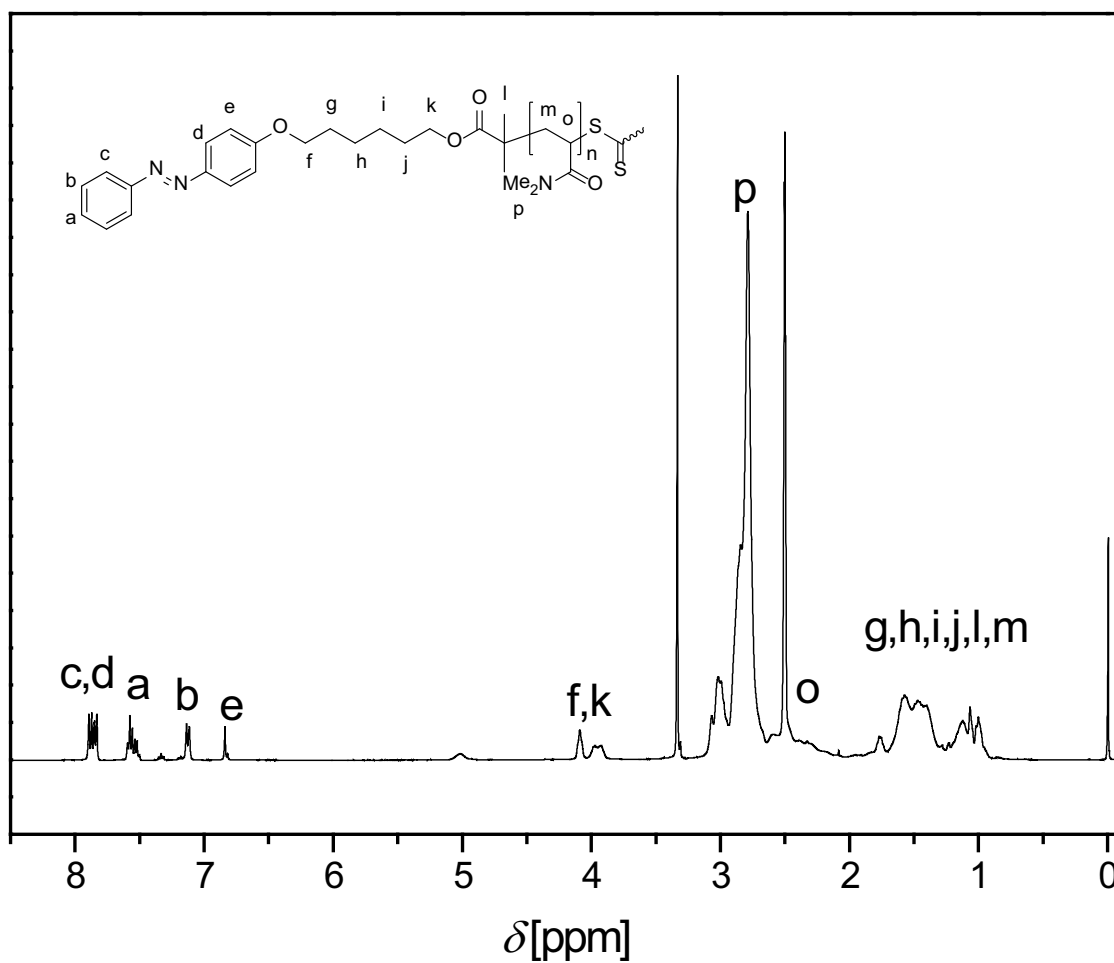


Figure B.5: $^1\text{H-NMR}$ spectrum (400 MHz, DMSO-D_6) of doubly azobenzene-functionalized PDMAAm ($M_{n\text{SEC}} = 5400 \text{ g}\cdot\text{mol}^{-1}$, $D_m = 1.10$) polymerized with **6** at 25°C .

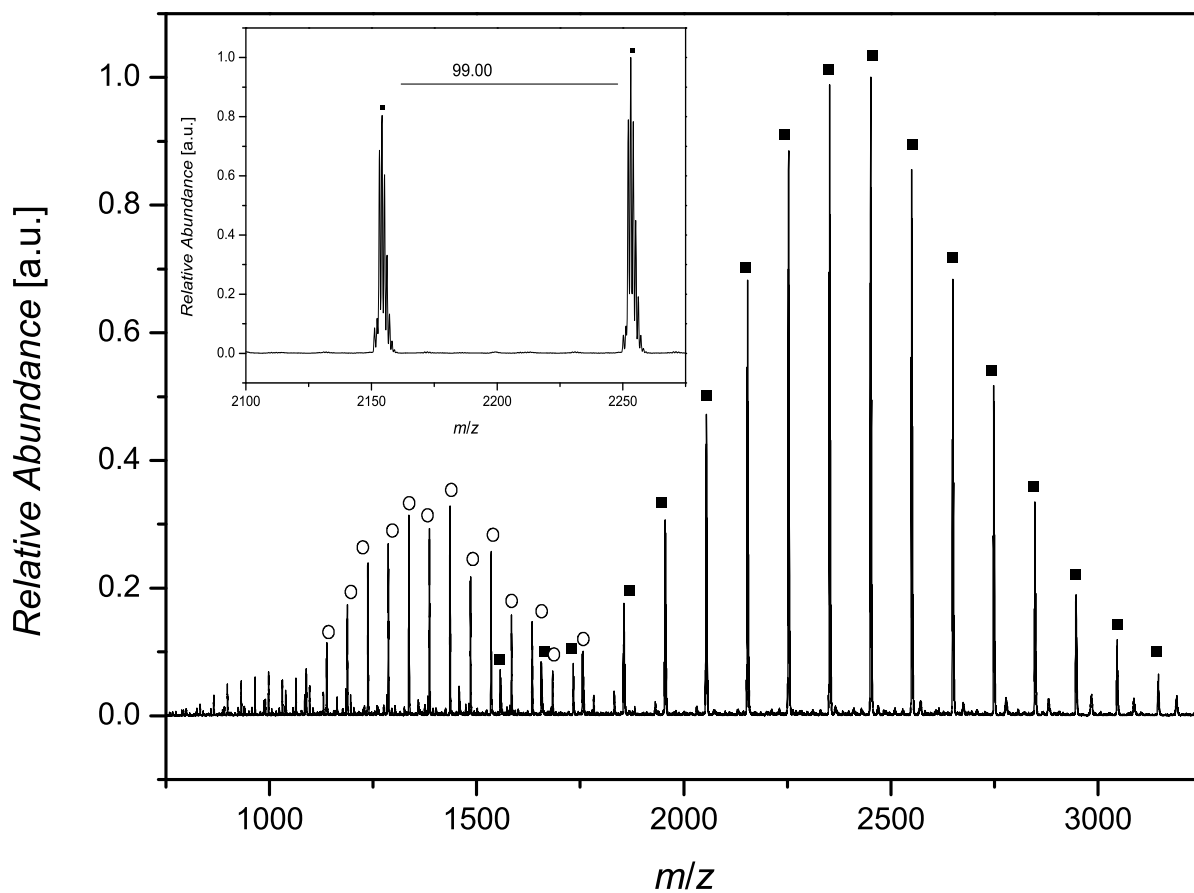


Figure B.6: ESI-MS spectrum of doubly azobenzene-functionalized PDMAAm ($M_{nSEC} = 4000 \text{ g}\cdot\text{mol}^{-1}$, $D_m = 1.06$) polymerized with **6**.

Table B.3: Theoretical and experimental m/z of PDMAAm polymerized with **6**.

Species	m/z_{theo}	m/z_{exp}	$\Delta m/z$
■ $[6+(\text{DMAAm})_{15}+\text{Na}]^+$	2352.34	2352.27	0.07
○ $[6+(\text{DMAAm})_{20}+2\text{Na}]^{2+}$	1435.34	1435.82	0.48

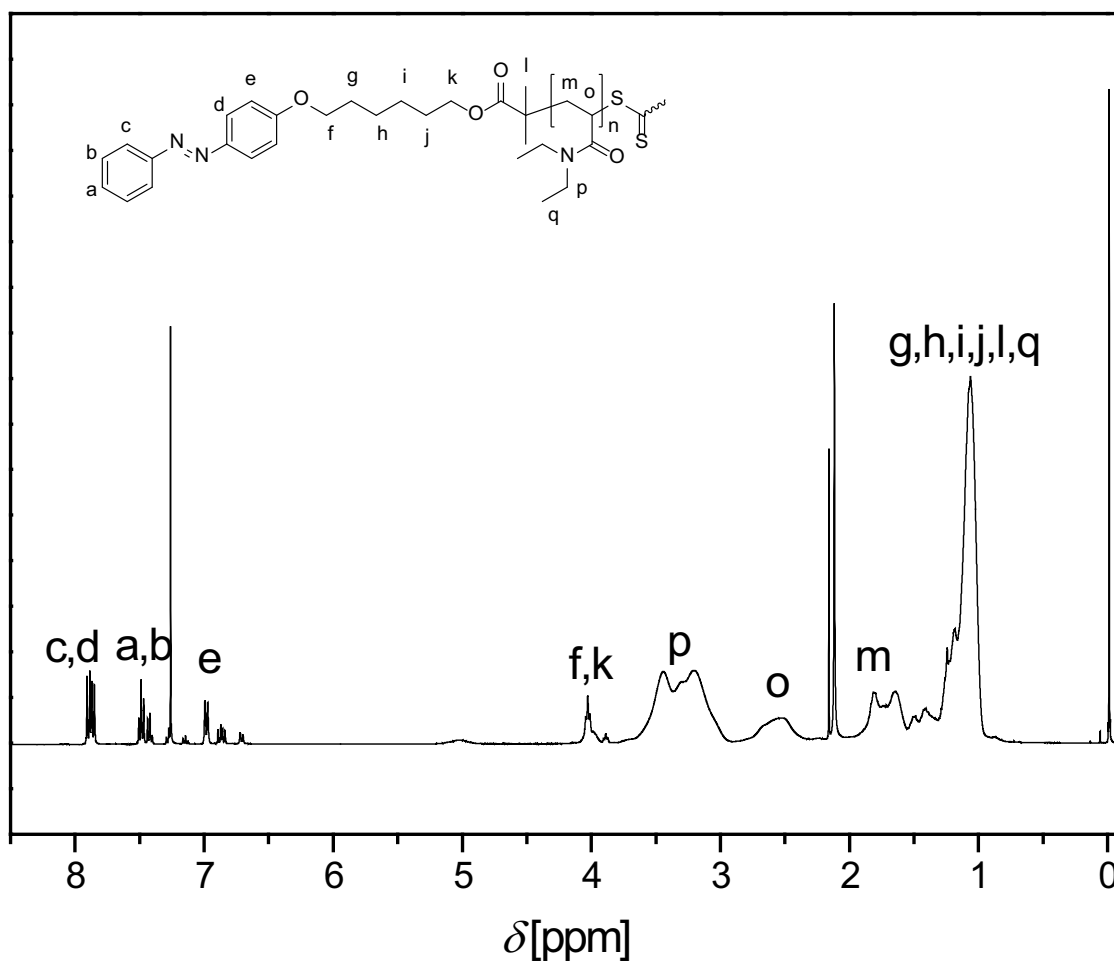


Figure B.7: ^1H -NMR spectrum (400 MHz, CDCl_3) of doubly azobenzene-functionalized PDEAAm ($M_{\text{nSEC}} = 4000 \text{ g}\cdot\text{mol}^{-1}$, $D_{\text{m}} = 1.10$) polymerized with 6 at 25°C .

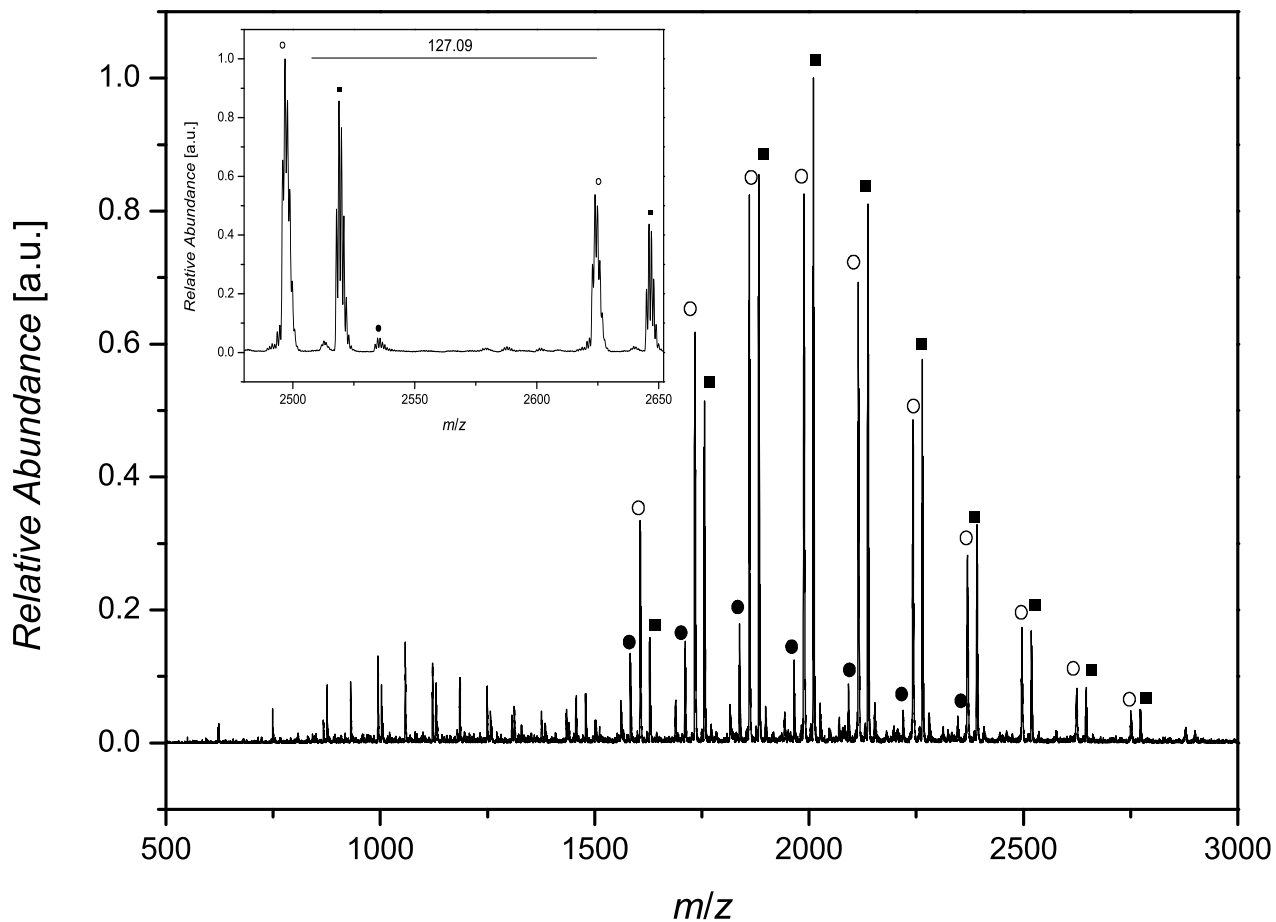


Figure B.8: ESI-MS spectrum of doubly azobenzene-functionalized PDEAAm ($M_{nSEC} = 1900 \text{ g}\cdot\text{mol}^{-1}$, $D_m = 1.05$) polymerized with **6**.

Table B.4: Theoretical and experimental m/z of PDEAAm polymerized with **6**.

Species	m/z_{theo}	m/z_{exp}	$\Delta m/z$
■ $[6+(\text{DEAAm})_{13}+\text{Na}]^+$	2518.6100	2518.55	0.06
○ $[6+(\text{DEAAm})_{13}+\text{H}]^+$	2496.6820	2496.45	0.23
● $[6+(\text{DEAAm})_8-\text{C}_{18}\text{H}_{21}\text{N}_2\text{O}_2+\text{Na}]^+$	1584.9477	1584.09	0.86

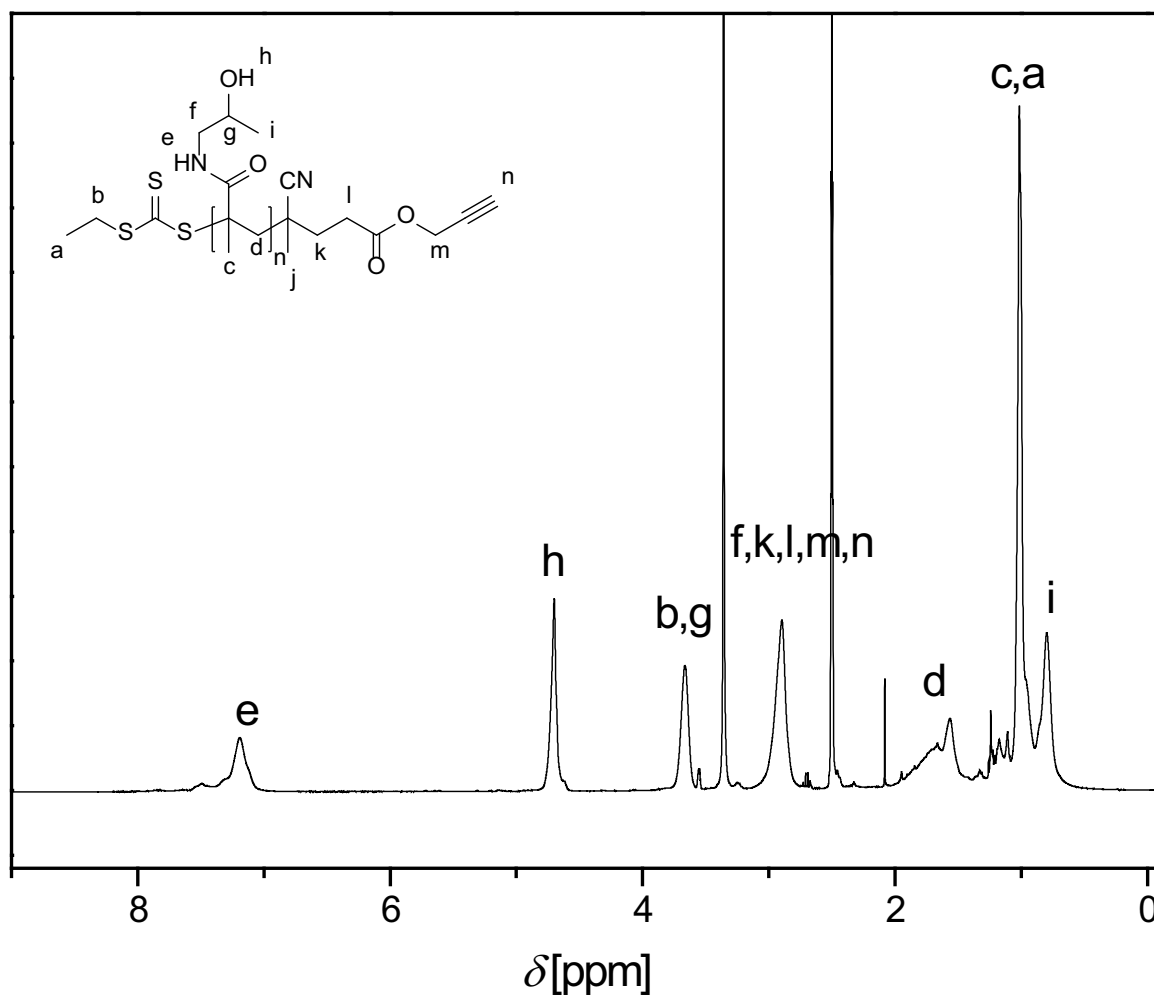


Figure B.9: ¹H-NMR spectrum (400 MHz, DMSO-D₆) of an alkyne-functionalized PHPMA ($M_{nSEC} = 4300 \text{ g}\cdot\text{mol}^{-1}$, $D_m = 1.15$) polymerized with 7 at 25 °C.

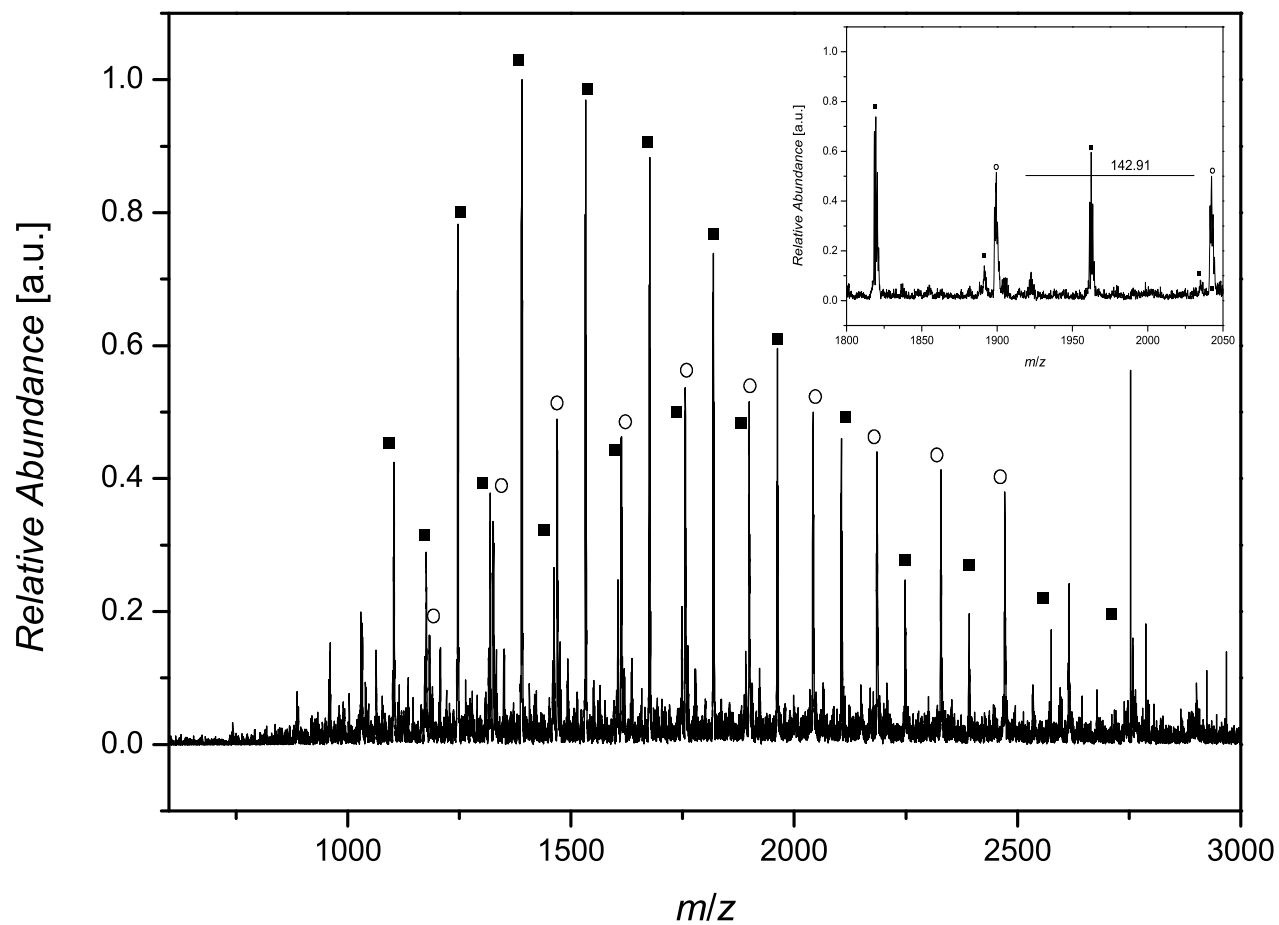


Figure B.10: ESI-MS spectrum of an alkyne-functionalized PHPMA ($M_{nSEC} = 3900 \text{ g}\cdot\text{mol}^{-1}$, $D_m = 1.17$) polymerized with 7.

Table B.5: Theoretical and experimental m/z of PHPMA polymerized with 7.

Species	m/z_{theo}	m/z_{exp}	$\Delta m/z$
■ $[7+(\text{HPMA})_{17}+2\text{Na}]^{2+}$	1390.31	1390.18	0.13
○ $[7+(\text{HPMA})_{10}+\text{Na}]^+$	1754.96	1755.27	0.31

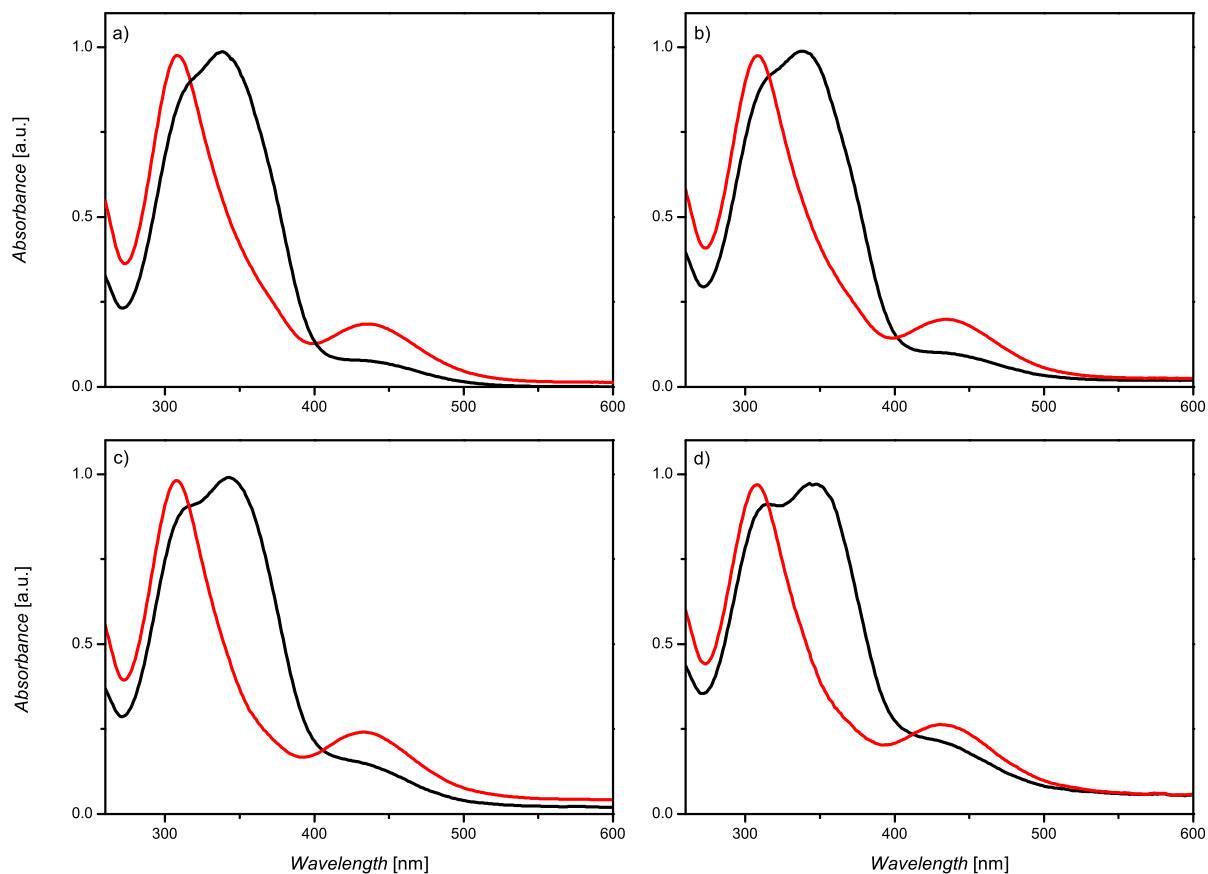


Figure B.11: Overlay of the UV spectra before irradiation (black curve) and after irradiation at 350 nm for 30 min (red curve) at 25 °C: a) PDMAAm₄₆AzO₂; b) PDMAAm₄₆AzO₂-*b*-(PHPMA₂₆-β-CD)₂; c) PDMAAm₁₀₃AzO₂; d) PDMAAm₁₀₃AzO₂-*b*-(PHPMA₂₆-β-CD)₂.

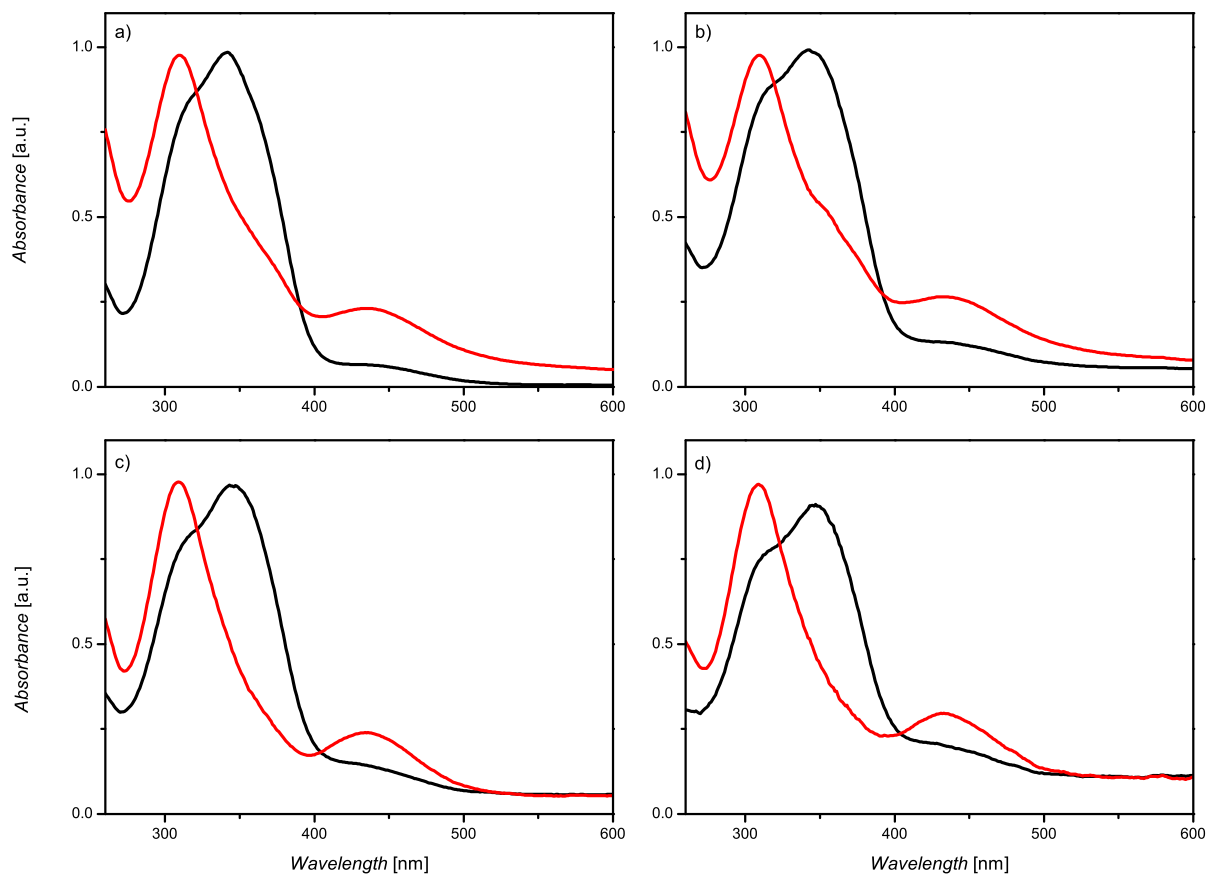


Figure B.12: Overlay of the UV spectra before irradiation (black curve) and after irradiation at 350 nm for 30 min (red curve) at 10 °C: a) PDEAAm₃₆Azo₂; b) PDEAAm₃₆Azo₂-*b*-(PHPMA₂₈-β-CD)₂; c) PDEAAm₈₀Azo₂; d) PDEAAm₈₀Azo₂-*b*-(PHPMA₂₈-β-CD)₂.

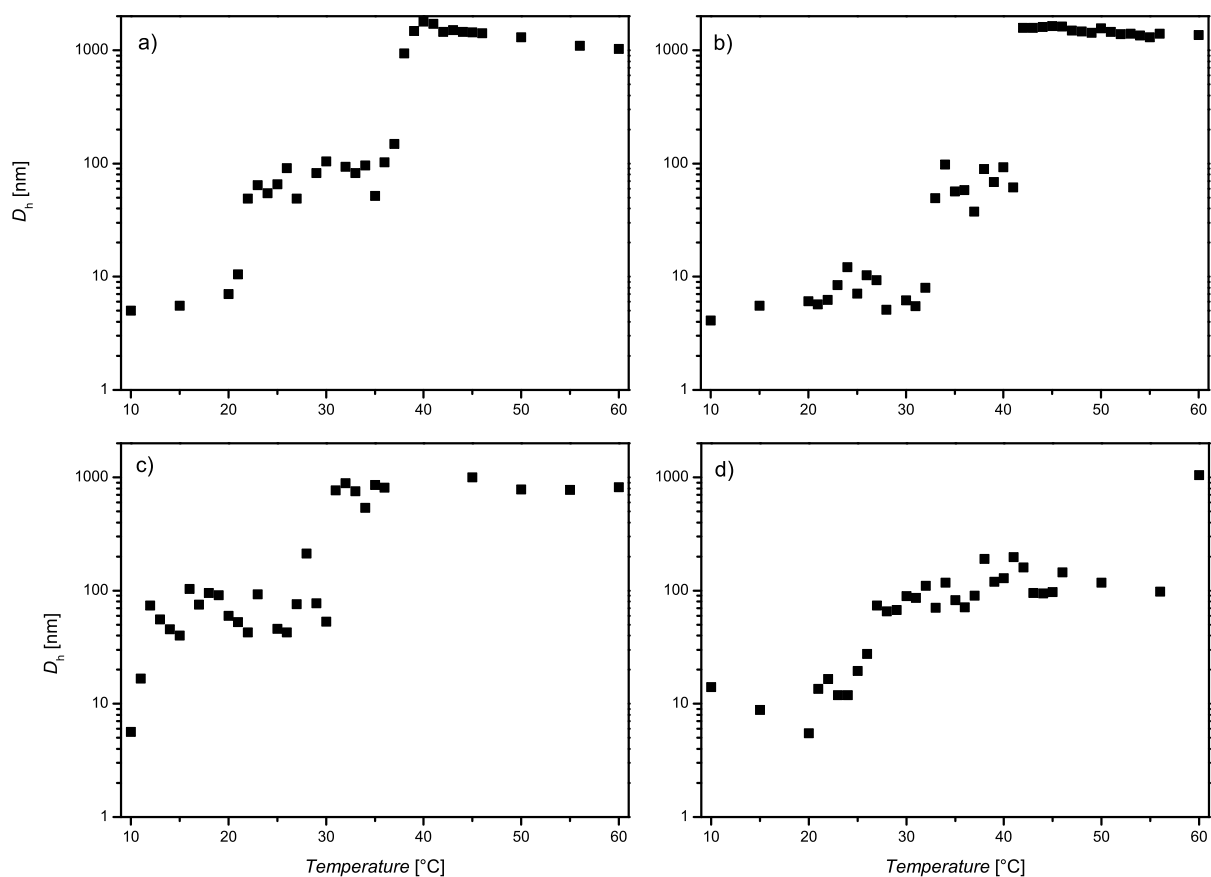


Figure B.13: a) Temperature sequenced DLS measurement of PDEAAm₄₅Ad₂-*b*-(PHPMA₂₈-β-CD)₂ at a heating rate of 0.2 °C·min⁻¹ and a concentration of 1 mg·mL⁻¹; b) temperature sequenced DLS measurement of PDEAAm₈₉Ad₂-*b*-(PHPMA₂₈-β-CD)₂ at a heating rate of 0.2 °C·min⁻¹ and a concentration of 1 mg·mL⁻¹; c) temperature sequenced DLS measurement of PDEAAm₃₆Azo₂-*b*-(PHPMA₂₈-β-CD)₂ at a heating rate of 0.2 °C·min⁻¹ and a concentration of 1 mg·mL⁻¹; d) temperature sequenced DLS measurement of PDEAAm₈₀Azo₂-*b*-(PHPMA₂₈-β-CD)₂ at a heating rate of 0.2 °C·min⁻¹ and a concentration of 1 mg·mL⁻¹.

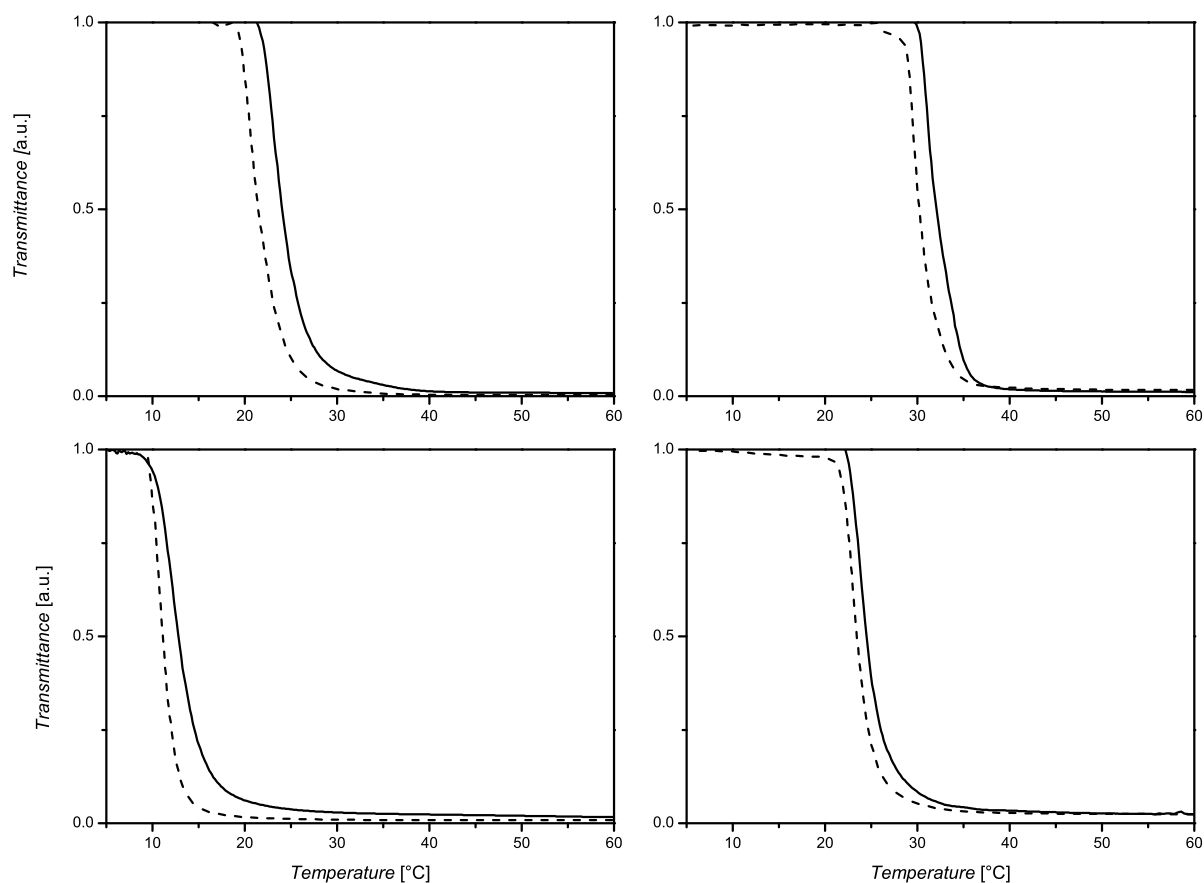


Figure B.14: Turbidity measurements (cooling ramp) with a heating/cooling rate of $0.32\text{ }^{\circ}\text{C}\cdot\text{min}^{-1}$ and at a concentration of $1\text{ mg}\cdot\text{mL}^{-1}$ for a) PDEAAm₄₅Ad₂ (dashed line) and the supramolecular triblock copolymer PDEAAm₄₅Ad₂-*b*-(PHPMA₂₈-β-CD)₂ (solid line); b) PDEAAm₈₉Ad₂ (dashed line) and the supramolecular triblock copolymer PDEAAm₈₉Ad₂-*b*-(PHPMA₂₈-β-CD)₂ (solid line); c) PDEAAm₃₆Azo₂ (dashed line) and the supramolecular triblock copolymer PDEAAm₃₆Azo₂-*b*-(PHPMA₂₈-β-CD)₂ (solid line); d) PDEAAm₈₀Azo₂ (dashed line) and the supramolecular triblock copolymer PDEAAm₈₀Azo₂-*b*-(PHPMA₂₈-β-CD)₂ (solid line).

Supramolecular Three Armed Star
Polymers (Appendix to Chapter 5)

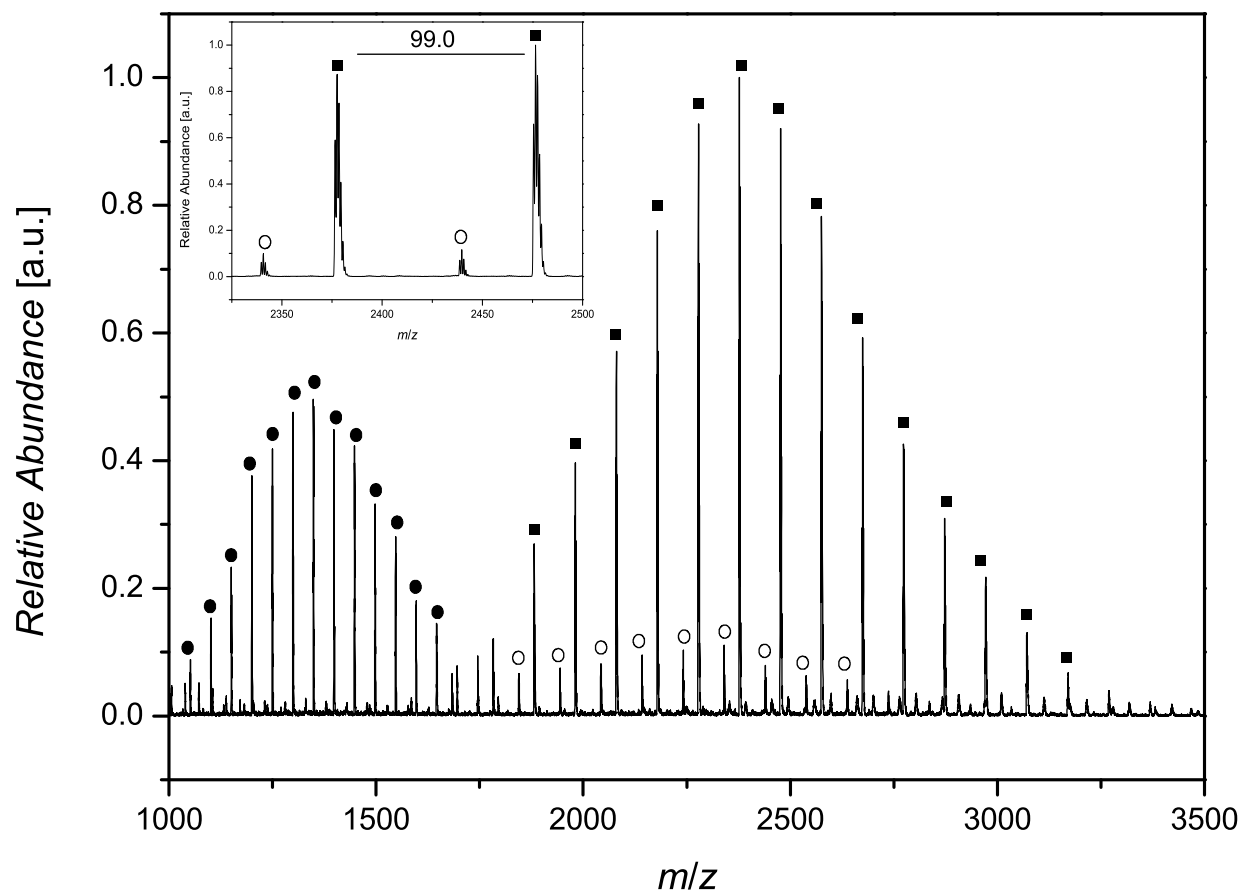


Figure C.1: ESI-MS-spectrum of an adamantyl-functionalized PDMAAm ($M_{nSEC} = 3900 \text{ g}\cdot\text{mol}^{-1}$, $D_m = 1.07$) polymerized with **10**.

Table C.1: Theoretical and experimental m/z of PDMAAm polymerized with **10**.

Species	m/z_{theo}	m/z_{exp}	$\Delta m/z$
■ $[\mathbf{10}+(\text{DMAAm})_{20}+\text{Na}]^+$	2476.56	2476.55	0.01
● $[\mathbf{10}+(\text{DMAAm})_{23}+2\text{Na}]^{2+}$	1348.84	1348.82	0.02
○ $[\mathbf{10}+(\text{DMAAm})_{25}\text{-Adamantyl}+\text{Na}]^+$	2440.516	2439.82	0.69

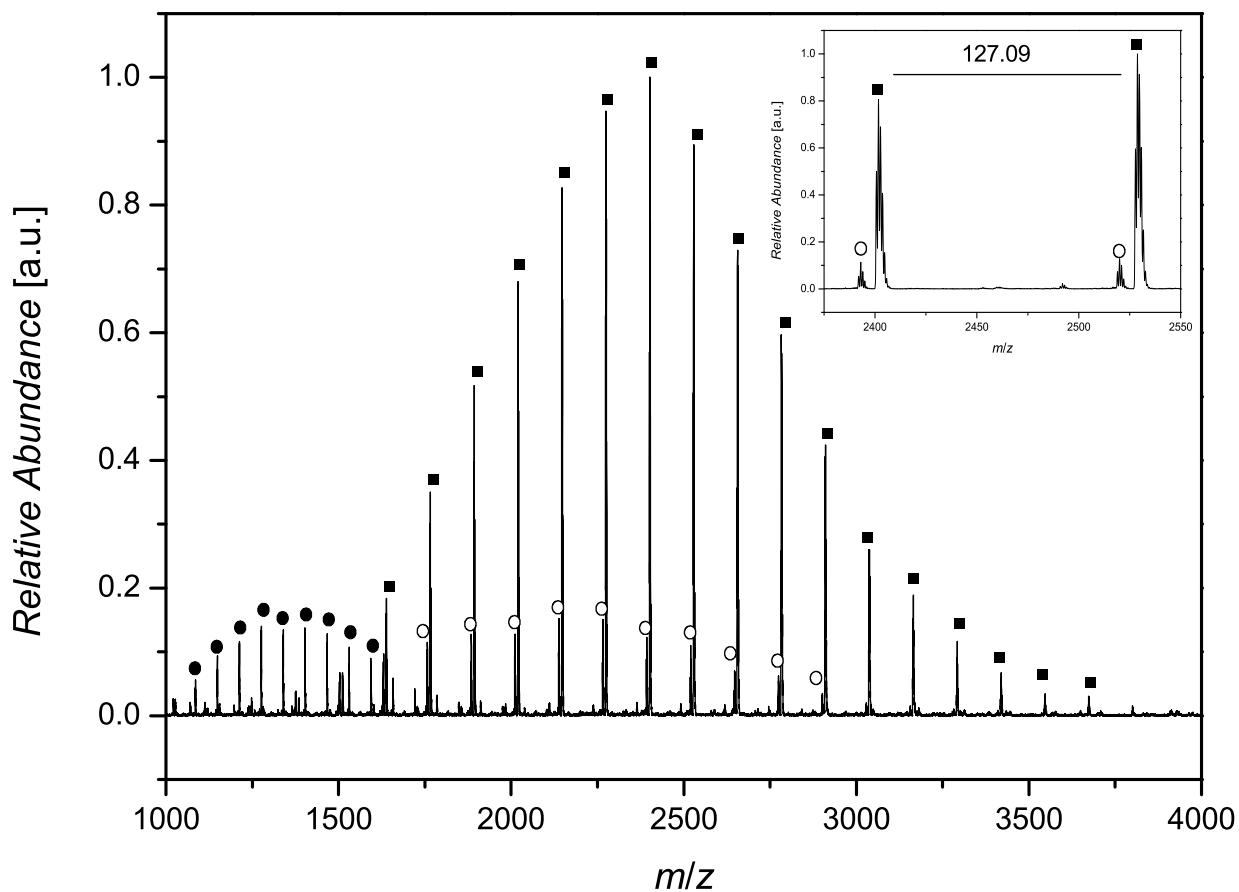


Figure C.2: ESI-MS-spectrum of an adamantyl-functionalized PDEAAm ($M_{nSEC} = 2700 \text{ g}\cdot\text{mol}^{-1}$, $D_m = 1.08$) polymerized with **10**.

Table C.2: Theoretical and experimental m/z of PDEAAm polymerized with **10**.

Species	m/z_{theo}	m/z_{exp}	$\Delta m/z$
■ $[\mathbf{10}+(\text{DEAAm})_{16}+\text{Na}]^+$	2528.78	2528.82	0.04
● $[\mathbf{10}+(\text{DEAAm})_{17}+2\text{Na}]^{2+}$	1339.44	1339.45	0.01
○ $[\mathbf{10}+(\text{DEAAm})_{17}\text{-Adamantyl}+\text{Na}]^+$	2520.76	2500.00	0.76

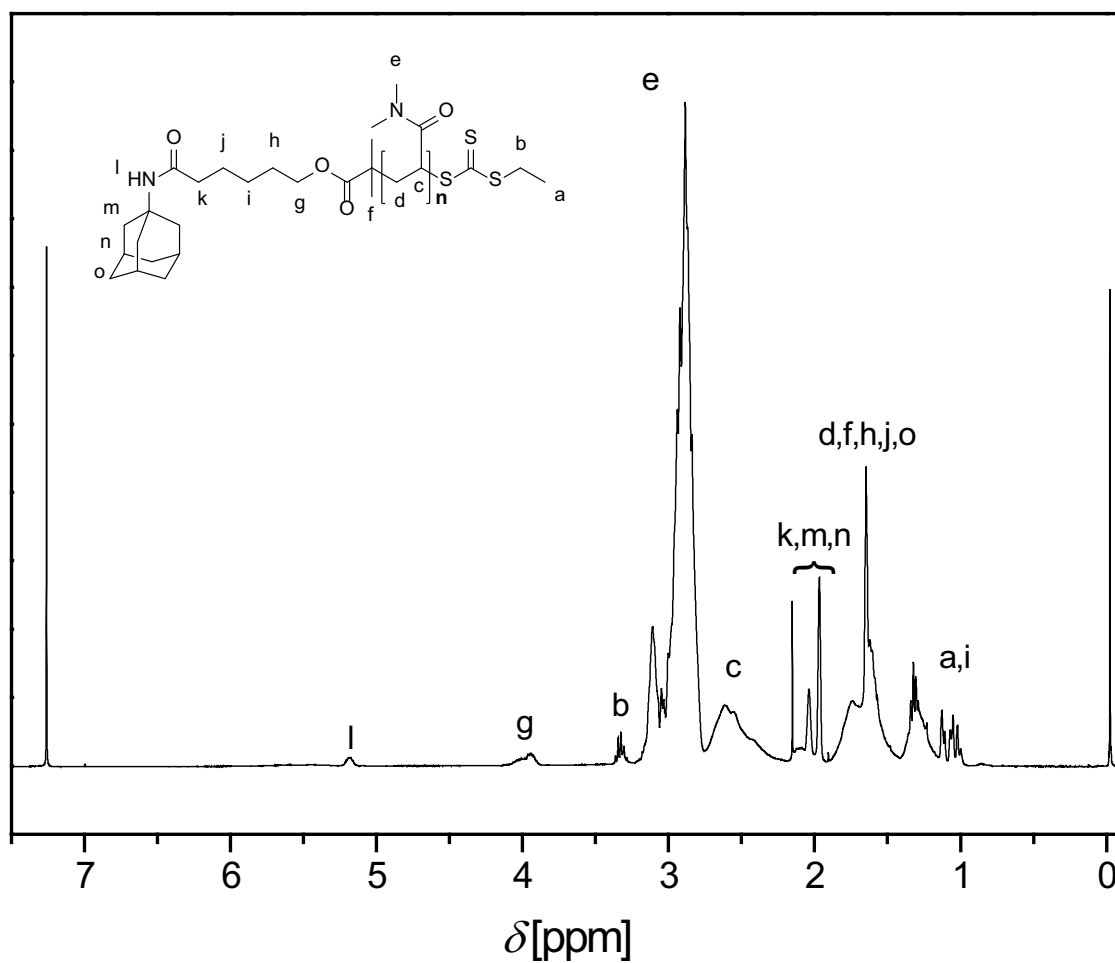


Figure C.3: ¹H-NMR spectrum (400 MHz, CDCl₃) of an adamantyl-functionalized PDMAAm ($M_{nSEC} = 3900 \text{ g}\cdot\text{mol}^{-1}$, $D_m = 1.07$) at 25 °C polymerized with **10**.

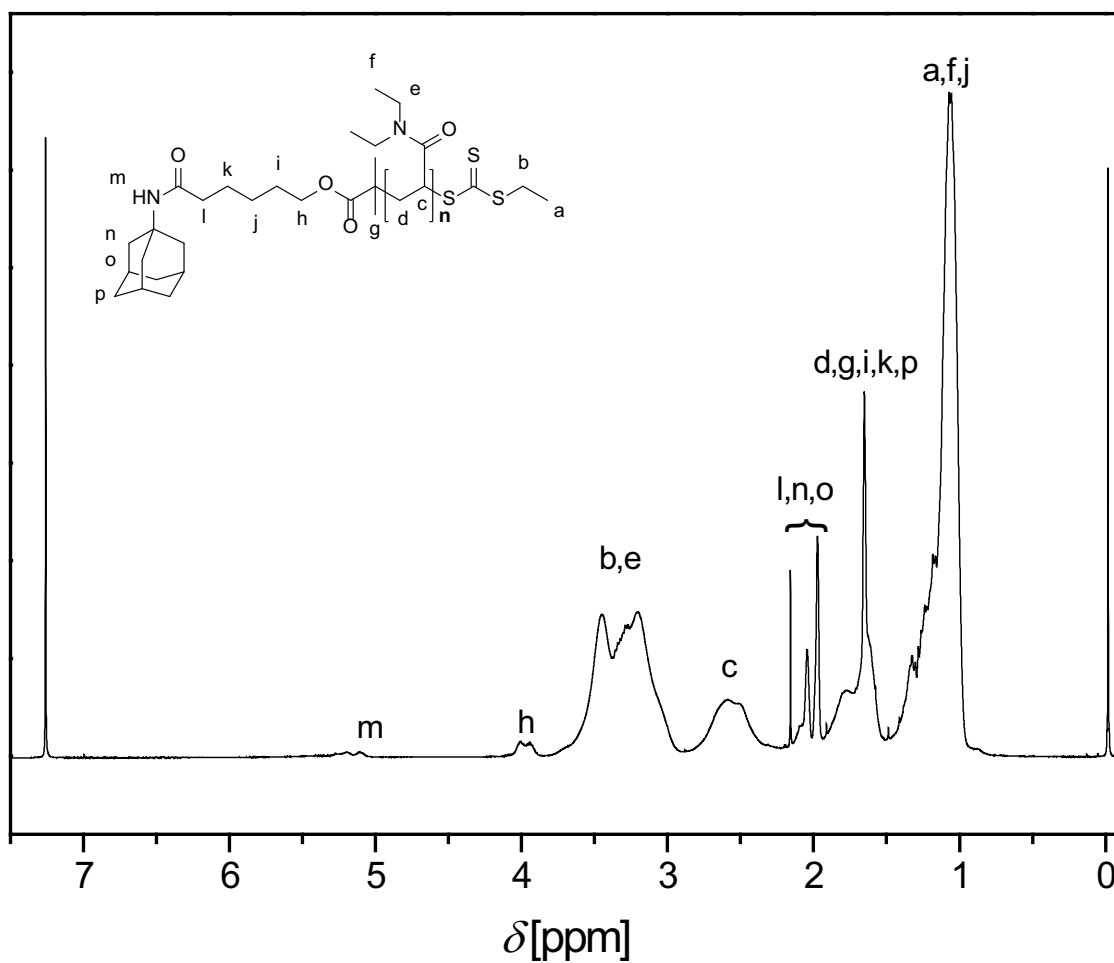


Figure C.4: $^1\text{H-NMR}$ spectrum (400 MHz, CDCl_3) of an adamantyl-functionalized PDEAAm ($M_{n\text{SEC}} = 2700 \text{ g}\cdot\text{mol}^{-1}$, $D_m = 1.08$) at 25°C polymerized with **10**.

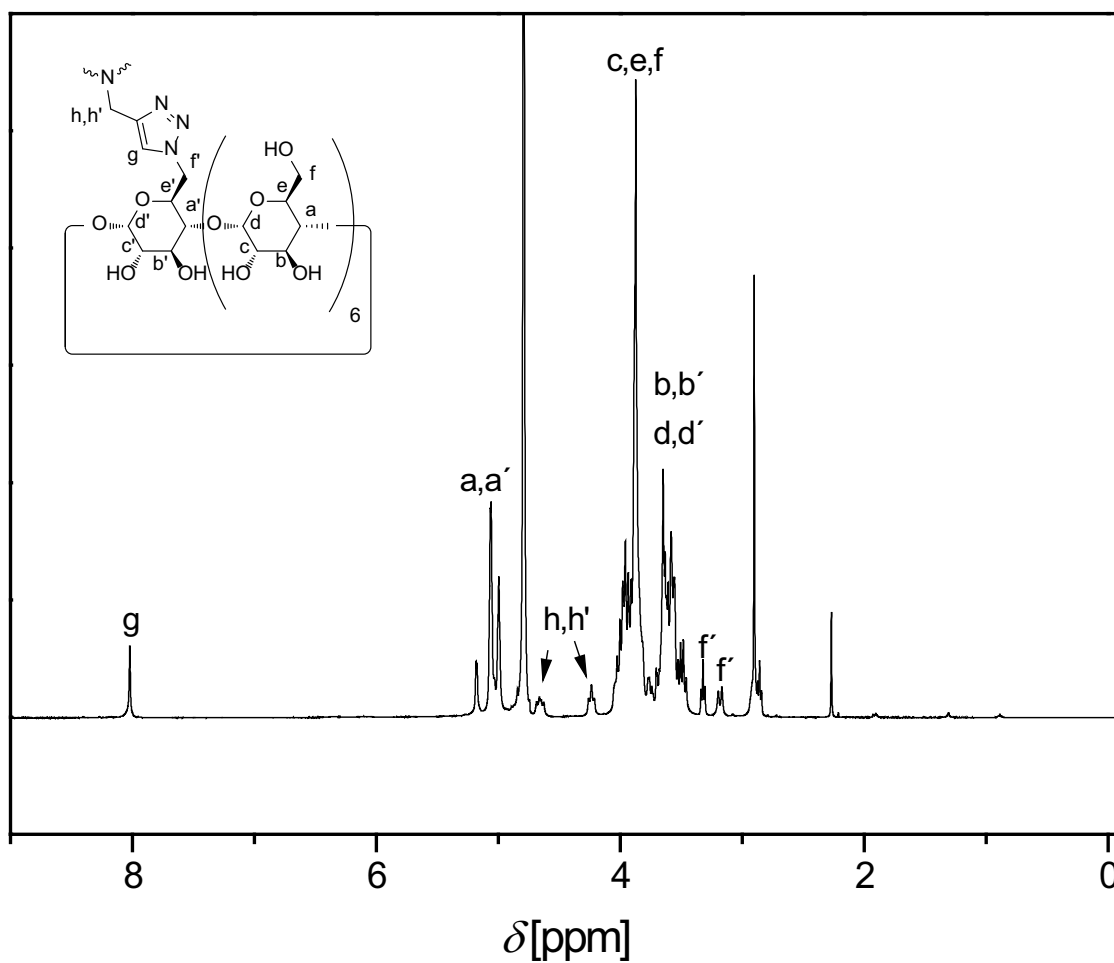


Figure C.5: $^1\text{H-NMR}$ spectrum of the three-pronged $\beta\text{-CD}$ core ($\beta\text{-CD}_3$) recorded in D_2O at 25°C .

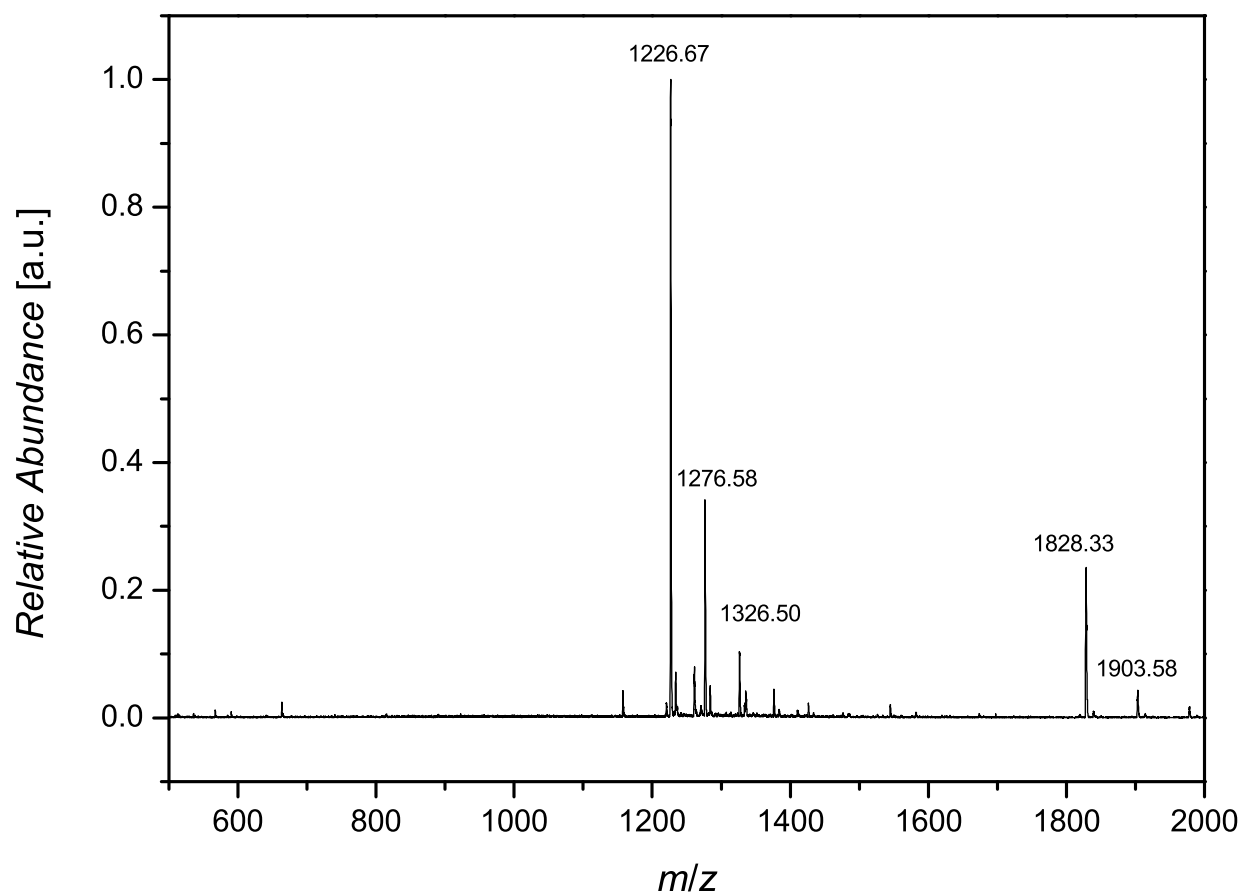


Figure C.6: ESI-MS-spectrum of the three-pronged β -CD core (β -CD₃) (ionized with NaI).

Table C.3: Theoretical and experimental m/z of β -CD₃ (ionized with NaI).

Species	m/z _{theo}	m/z _{exp}	Δ m/z
$[\beta\text{-CD}_3+2\text{Na}]^{2+}$	1828.09	1828.33	0.24
$[\beta\text{-CD}_3+\text{I}^-+3\text{Na}]^{2+}$	1903.04	1903.58	0.54
$[\beta\text{-CD}_3+3\text{Na}]^{3+}$	1226.396	1226.67	0.28
$[\beta\text{-CD}_3+\text{I}^-+4\text{Na}]^{3+}$	1276.66	1276.58	0.22
$[\beta\text{-CD}_3+2\text{I}^-+5\text{Na}]^{3+}$	1326.32	1326.50	0.18

ABA Miktoarm Star Polymers
(Appendix to Chapter 6)

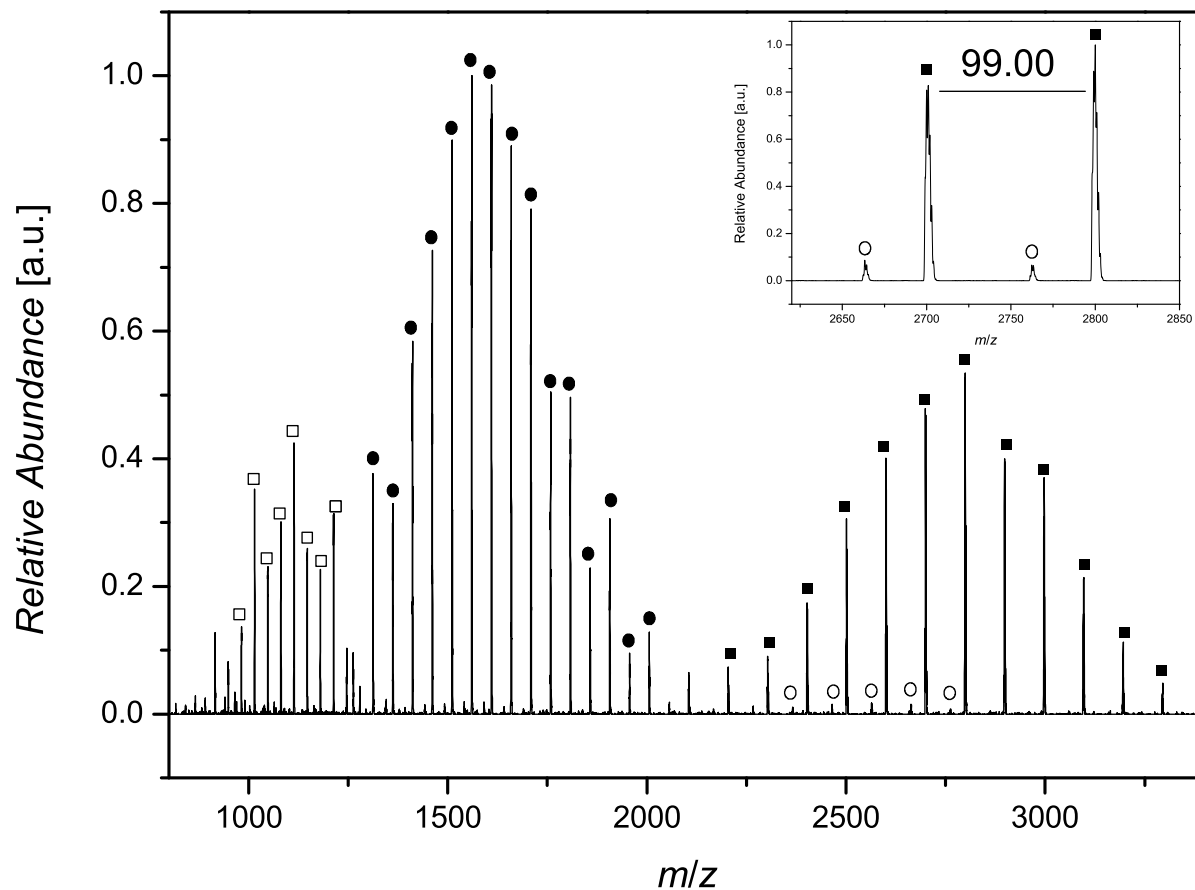


Figure D.1: ESI-MS-spectrum of a mid-chain adamantyl-functionalized PDMAAm ($M_{nSEC} = 4000 \text{ g}\cdot\text{mol}^{-1}$, $D_m = 1.09$) polymerized with **11**.

Table D.1: Theoretical and experimental m/z of PDMAAm polymerized with **11**.

Species	m/z_{theo}	m/z_{exp}	$\Delta m/z$
■ $[\mathbf{11}+(\text{DMAAm})_{20}+\text{Na}]^+$	2798.59	2799.09	0.50
● $[\mathbf{11}+(\text{DMAAm})_{21}+2\text{Na}]^{2+}$	1559.39	1559.73	0.34
○ $[\mathbf{11}+(\text{DMAAm})_{25}+3\text{Na}]^{3+}$	1113.30	1113.91	0.61
□ $[\mathbf{11}+(\text{DMAAm})_{20}\text{-Adamantyl}+\text{Na}]^+$	2663.47	2663.27	0.20

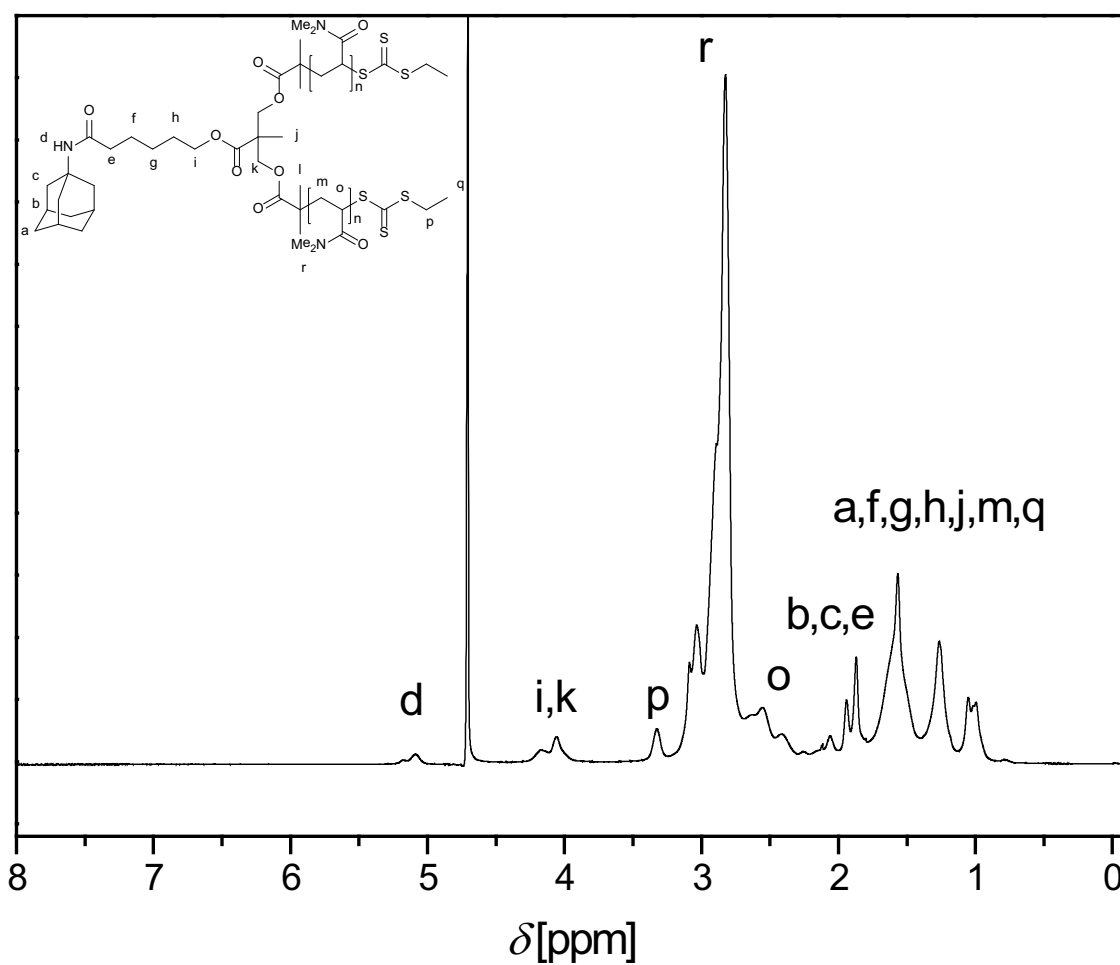


Figure D.2: ¹H-NMR spectrum (400 MHz, D₂O) of a mid-chain adamantyl-functionalized PDMAAm polymerized with **11** ($M_{nSEC} = 4000 \text{ g}\cdot\text{mol}^{-1}$, $D_m = 1.09$) at 25 °C.

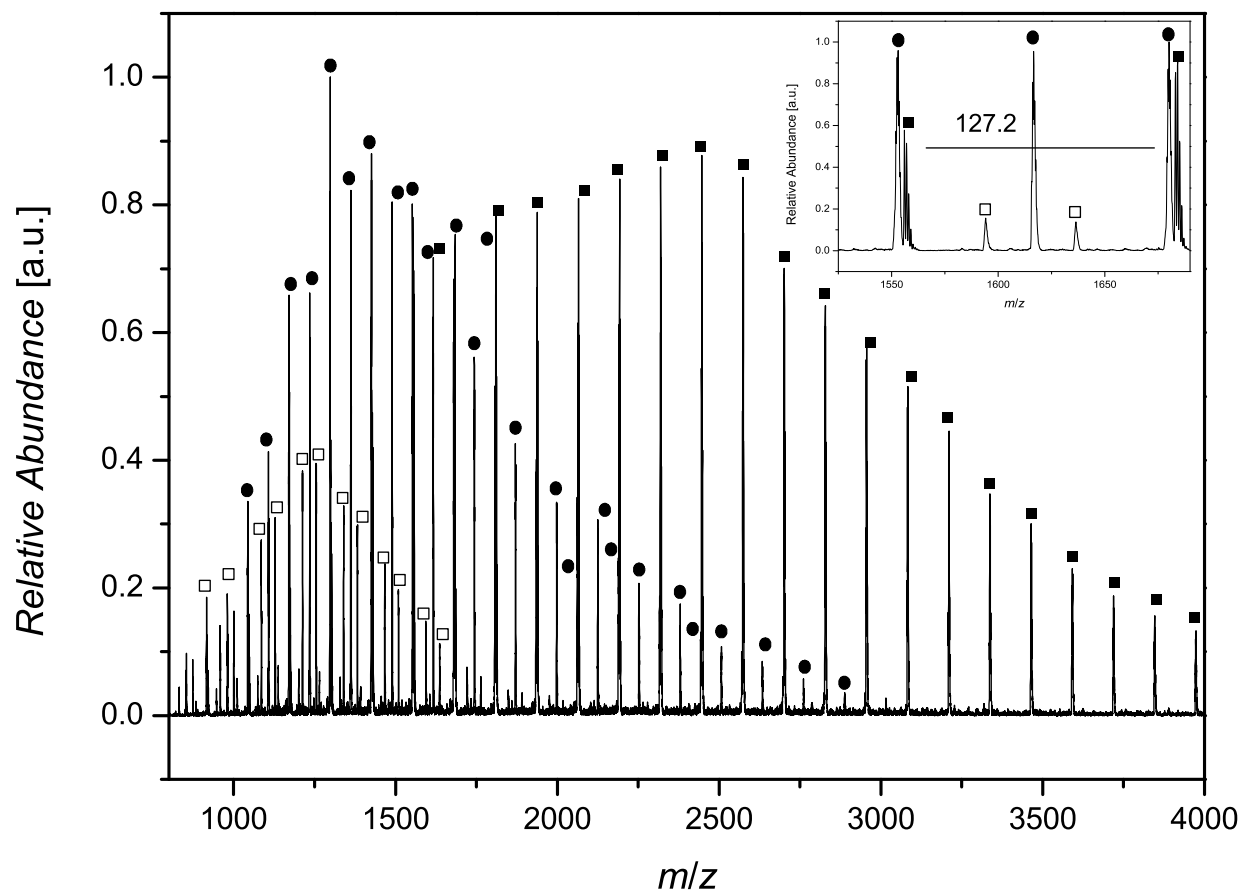


Figure D.3: ESI-MS-spectrum of the alkyne-functionalized PDEAAm ($M_{nSEC} = 2400 \text{ g}\cdot\text{mol}^{-1}$, $D_m = 1.14$) polymerized with **12**.

Table D.2: Theoretical and experimental m/z of PDEAAm polymerized with **12**.

Species	m/z_{theo}	m/z_{exp}	$\Delta m/z$
■ $[\mathbf{12}+(\text{DEAAm})_{11}+\text{Na}]^+$	1683.10	1683.18	0.08
● $[\mathbf{12}+(\text{DEAAm})_{22}+2\text{Na}]^{2+}$	1552.60	1552.55	0.05
□ $[\mathbf{12}+(\text{DEAAm})_{35}\text{-Adamantyl}+3\text{Na}]^{3+}$	1593.83	1594.09	0.26

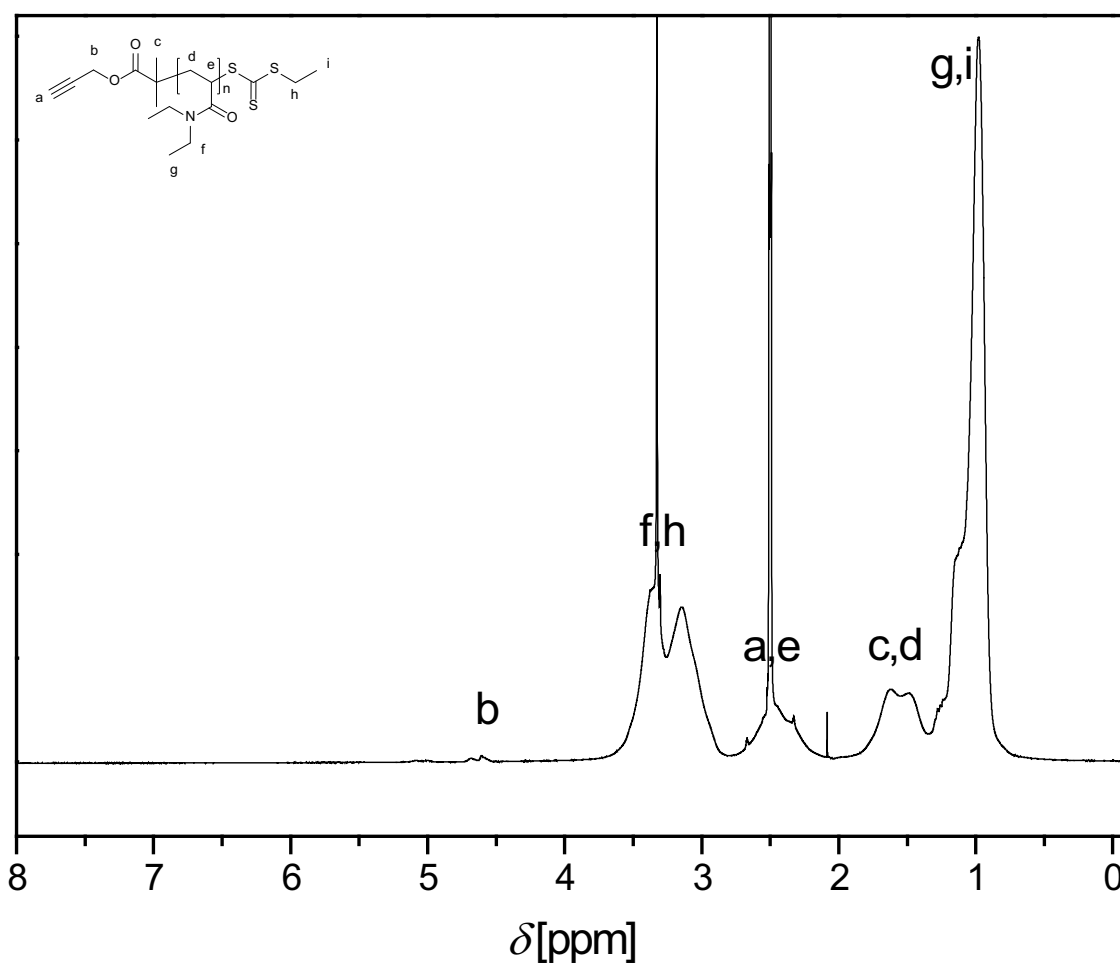


Figure D.4: $^1\text{H-NMR}$ spectrum (400 MHz, DMSO-D_6) of the alkyne-functionalized PDEAAm polymerized with **12** ($M_{\text{nSEC}} = 6800 \text{ g}\cdot\text{mol}^{-1}$, $D_{\text{m}} = 1.13$) at 25°C .

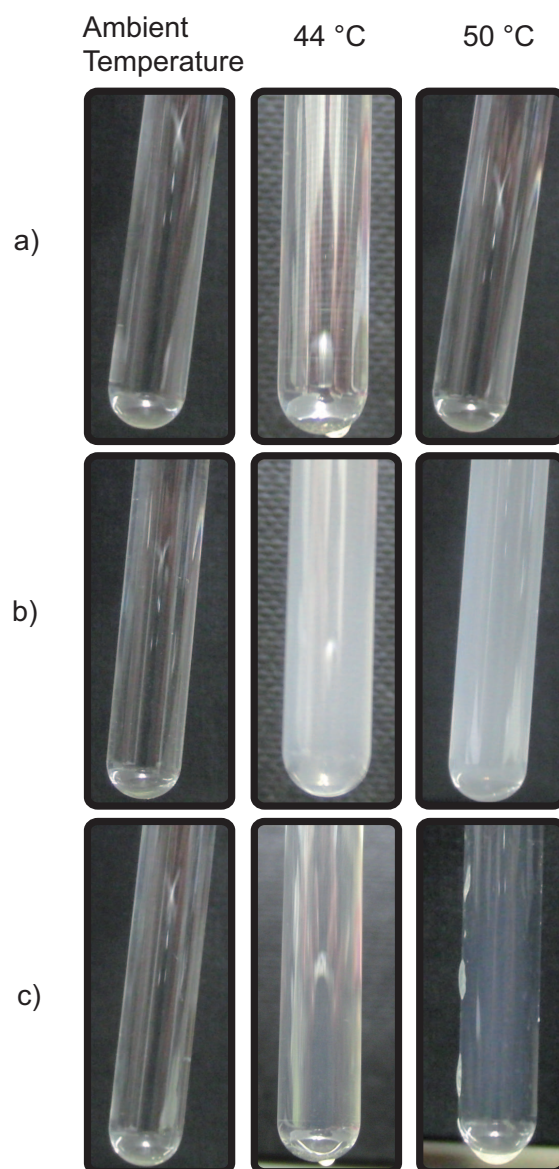


Figure D.5: Pictures of the polymer solutions at different temperatures at a concentration of $1 \text{ mg} \cdot \text{mL}^{-1}$. a) Mid-chain adamantyl-functionalized PDMAAm₁₅₅-Ad, b) β -CD-functionalized PDEAAm₅₇- β -CD and c) the supramolecular miktoarm star polymer.

Modulation of the Thermoresponsivity of PDEAAm via CD Addition (Appendix to Chapter 7)

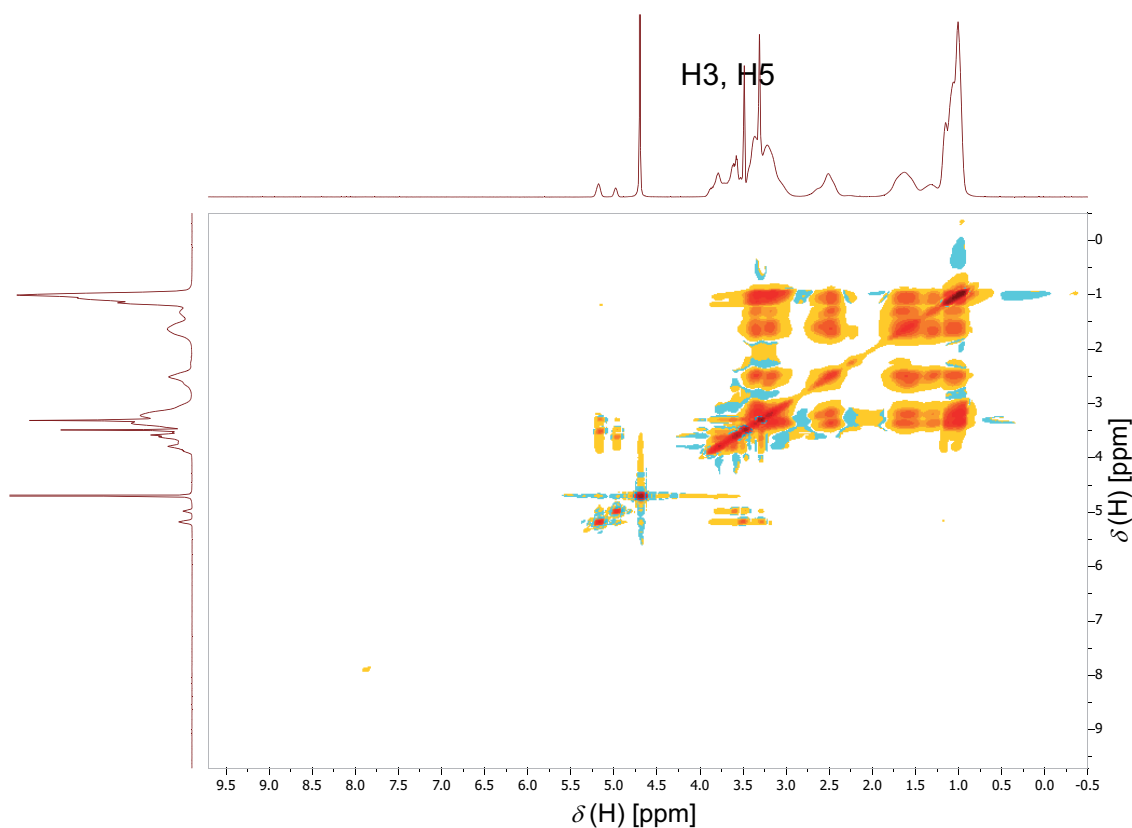


Figure E.1: NOESY spectrum in D_2O at 25 °C of a mixture of carboxylic acid functionalized PDEAAm ($M_n = 6600 \text{ g}\cdot\text{mol}^{-1}$) and 2 eq. of Me- β -CD.

Table E.1: SEC-data of the utilized polymers (polymerized with **EMP** in DMF at 60 °C for 24 h with AIBN as initiator) and the corresponding T_c s before and after addition of Me- β -CD.^a

DEAAm/CTA/I	Conv.	$M_{n\text{theo}}$ [g·mol ⁻¹]	$M_{n\text{SEC}}$ [g·mol ⁻¹]	D_m	T_c [°C]	$T_{c\text{Me-}\beta\text{-CD}}$ [°C]
17/1/0.2	quant.	2400	1600	1.08	32.3/31.2	39.5/39.4
34/1/0.2	99%	4500	3500	1.07	41.1/39.9	40.9/41.0
48/1/0.2	97%	6100	5000	1.10	39.9/38.1	38.8/37.4
65/1/0.2	98%	8300	6600	1.09	37.4/35.5	41.6/40.1
82/1/0.2	98%	10400	7200	1.10	37.5/35.8	40.0/38.4
160/1/0.2	90%	18500	10800	1.18	37.7/35.6	37.7/36.7

a: first T_c from the heating ramp / second T_c from the cooling ramp

Table E.2: SEC-data of the utilized polymers (polymerized with **1** in DMF at 60 °C for 24 h with AIBN as initiator) and the corresponding T_c s before and after addition of Me- β -CD.^a

DEAAm/CTA/I	Conv.	$M_{n\text{theo}}$ [g·mol ⁻¹]	$M_{n\text{SEC}}$ [g·mol ⁻¹]	D_m	T_c [°C]	$T_{c\text{Me-}\beta\text{-CD}}$ [°C]
16/1/0.2	99%	2400	1800	1.06	< 4	22.9/37.3
33/1/0.2	99%	4500	3800	1.08	26.5/25.9	32.9/38.1
49/1/0.2	99%	6600	5300	1.07	28.4/27.7	32.6/31.7
65/1/0.2	99%	8600	6500	1.09	30.3/28.3	33.5/32.0
79/1/0.2	99%	10400	7700	1.1	31.6/30.1	34.2/32.8
159/1/0.2	99%	20600	11200	1.2	33.0/31.5	34.5/32.6

a: first T_c from the heating ramp / second T_c from the cooling ramp

Table E.3: SEC-data of the utilized polymers (polymerized with **17** in DMF at 60 °C for 24 h with AIBN as initiator) and the corresponding T_c s before and after addition of Me- β -CD.^a

DEAAm/CTA/I	Conv.	$M_{n\text{theo}}$ [g·mol ⁻¹]	$M_{n\text{SEC}}$ [g·mol ⁻¹]	D_m	T_c [°C]	$T_{c\text{Me-}\beta\text{-CD}}$ [°C]
16/1/0.2	98%	2400	1800	1.18	< 4	33.5/38.9
31/1/0.2	99%	4300	3000	1.19	< 4	35.6/38.7
42/1/0.2	99%	5700	3700	1.21	7.7/12.7	35.3/35.2
64/1/0.2	99%	8500	4400	1.28	26.1/24.2	38.0/36.8
81/1/0.2	99%	10600	5600	1.28	26.8/26.8	36.1/34.4
155/1/0.2	99%	19900	7400	1.28	30.7/28.2	36.7/34.9

a: first T_c from the heating ramp / second T_c from the cooling ramp

Table E.4: SEC-data of the utilized polymers (polymerized with **10** in DMF at 60 °C for 24 h with AIBN as initiator) and the corresponding T_c s before and after addition of Me- β -CD.^a

DEAAm/CTA/I	Conv.	$M_{n\text{theo}}$ [g·mol ⁻¹]	$M_{n\text{SEC}}$ [g·mol ⁻¹]	D_m	T_c [°C]	$T_{c\text{Me-}\beta\text{-CD}}$ [°C]
33/1/0.2	98%	4600	3200	1.07	27.3/27.8	33.4/33.3
59/1/0.2	99%	7900	4900	1.11	29.8/31.7	35.1/34.1
157/1/0.2	99%	20200	8300	1.21	33.7/31.7	35.6/34.2

a: first T_c from the heating ramp / second T_c from the cooling ramp

Table E.5: SEC-data of the utilized polymers (polymerized with **5** in DMF at 60 °C for 24 h with AIBN as initiator) and the corresponding T_c s before and after addition of Me- β -CD.^a

DEAAm/CTA/I	Conv.	$M_{n\text{theo}}$ [g·mol ⁻¹]	$M_{n\text{SEC}}$ [g·mol ⁻¹]	D_m	T_c [°C]	$T_{c\text{Me-}\beta\text{-CD}}$ [°C]
34/1/0.2	99%	5000	5100	1.05	< 4	27.8/28.3
65/1/0.2	99%	8900	7700	1.10	< 4	33.9/32.2
154/1/0.2	99%	20100	12700	1.24	33.0/31.5	36.1/35.2

a: first T_c from the heating ramp / second T_c from the cooling ramp

Table E.6: SEC-data of the utilized polymers (polymerized with **19** in DMF at 60 °C for 24 h with AIBN as initiator) and the corresponding T_c s before and after addition of Me- β -CD.^a

DEAAm/CTA/I	Conv.	$M_{n\text{theo}}$ [g·mol ⁻¹]	$M_{n\text{SEC}}$ [g·mol ⁻¹]	D_m	T_c [°C]	$T_{c\text{Me-}\beta\text{-CD}}$ [°C]
32/1/0.2	92%	4200	3600	1.09	15.1/16.0	17.4/15.7
65/1/0.2	92%	8100	5000	1.13	25.3/24.0	25.9/24.0
158/1/0.2	97%	20000	7700	1.23	29.0/27.0	30.2/30.7

a: first T_c from the heating ramp / second T_c from the cooling ramp

Table E.7: SEC-data of the utilized polymers (polymerized with **6** in DMF at 60 °C for 24 h with AIBN as initiator) and the corresponding T_c s before and after addition of Me- β -CD.^a

DEAAm/CTA/I	Conv.	$M_{n\text{theo}}$ [g·mol ⁻¹]	$M_{n\text{SEC}}$ [g·mol ⁻¹]	D_m	T_c [°C]	$T_{c\text{Me-}\beta\text{-CD}}$ [°C]
32/1/0.2	81%	4100	4000	1.1	< 4	< 4
66/1/0.2	78%	7400	5300	1.19	15.6/17.3	14.8/ -
160/1/0.2	89%	18800	11500	1.33	25.5/30.2	25.1/29.3

a: first T_c from the heating ramp / second T_c from the cooling ramp

Table E.8: SEC-data of the utilized polymers (polymerized with **19** in DMF at 60 °C for 24 h with AIBN as initiator) and the corresponding T_c s before and after addition of α -CD.^a

DEAAm/CTA/I	Conv.	$M_{n\text{theo}}$ [g·mol ⁻¹]	$M_{n\text{SEC}}$ [g·mol ⁻¹]	\bar{D}_m	T_c [°C]	$T_{c\alpha\text{-CD}}$ [°C]
32/1/0.2	92%	4200	3600	1.09	15.1/16.0	15.1/13.9
65/1/0.2	92%	8100	5000	1.13	25.3/24.0	24.7/23.8
158/1/0.2	97%	20000	7700	1.23	29.0/27.0	28.7/27.7

a: first T_c from the heating ramp / second T_c from the cooling ramp

Table E.9: SEC-data of the utilized polymers (polymerized with **6** in DMF at 60 °C for 24 h with AIBN as initiator) and the corresponding T_c s before and after addition of α -CD.^a

DEAAm/CTA/I	Conv.	$M_{n\text{theo}}$ [g·mol ⁻¹]	$M_{n\text{SEC}}$ [g·mol ⁻¹]	\bar{D}_m	T_c [°C]	$T_{c\alpha\text{-CD}}$ [°C]
32/1/0.2	81%	4100	4000	1.1	< 4	< 4
66/1/0.2	78%	7400	5300	1.19	15.6/17.3	13.7/16.8
160/1/0.2	89%	18800	11500	1.33	25.5/30.2	24.8/23.8

a: first T_c from the heating ramp / second T_c from the cooling ramp

Table E.10: T_c s in dependence of the Me- β -CD equivalents for a sample polymer polymerized with **1** or EMP.^a

equiv. CD/ polymer	1: $M_{n\text{SEC}} = 3800$ g·mol ⁻¹ $T_{c\text{Me-}\beta\text{-CD}}$ [°C]	1: $M_{n\text{SEC}} = 6500$ g·mol ⁻¹ $T_{c\text{Me-}\beta\text{-CD}}$ [°C]	EMP: $M_{n\text{SEC}} = 3500$ g·mol ⁻¹ $T_{c\text{Me-}\beta\text{-CD}}$ [°C]
0.5	28.5/29.6	30.5/28.8	38.9/40.0
1.0	32.5/37.3	31.8/31.0	39.5/38.9
1.5	30.7/33.0	33.1/33.1	40.1/39.8
2.0	32.9/38.1	33.5/32.0	40.9/41.0
3.0	34.4/36.5	33.4/32.1	41.6/41.4
5.0	36.6/36.5	34.9/34.6	40.9/40.2

a: first T_c from the heating ramp / second T_c from the cooling ramp

Table E.11: T_c s of polymers polymerized with **1** or **17** after addition of 16 eq. 1-adamantylamine hydrochloride.^a

polymer	T_c [°C]	$T_{c\text{Me-}\beta\text{-CD}}$ [°C]	$T_{c\text{Me-}\beta\text{-CD Ad}}$ [°C]
1: $M_{n\text{SEC}} = 3800$ g·mol ⁻¹	26.5/25.9	32.9/38.1	27.9/-
17: $M_{n\text{SEC}} = 5600$ g·mol ⁻¹	26.8/26.8	36.1/34.4	30.9/-

a: first T_c from the heating ramp / second T_c from the cooling ramp

Table E.12: T_c s after enzymatic treatment of polymers polymerized with **17** or **EMP** and complexed with β -CD.^a

polymer	$T_{c\text{Me-}\beta\text{-CD Enzyme}}$ [°C]	$T_{c\text{Me-}\beta\text{-CD}}$ [°C]	T_c [°C]
1: $M_{n\text{SEC}} = 4400 \text{ g}\cdot\text{mol}^{-1}$	26.5/24.9	30.4/28.9	26.1/24.2
EMP: $M_{n\text{SEC}} = 5000 \text{ g}\cdot\text{mol}^{-1}$	40.8/39.0	40.6/39.6	39.9/38.1

a: first T_c from the heating ramp / second T_c from the cooling ramp

Curriculum Vitae

Date of Birth: January the 2nd, 1984
Place of Birth: Hanau, Germany
Nationality: German

Education

06/2010 - 07/2013 **Doctoral Studies in Chemistry**
Under the supervision of Prof. Dr. Christopher Barner-Kowollik
Karlsruhe Institute of Technology, Germany
Topic: "Novel Macromolecular Architectures via Combination of Cyclodextrin Host/Guest Complexation and RAFT Polymerization"

09/2009 **Diploma in Chemistry: Diplom Ingenieur**
Diploma thesis under supervision of Prof. M. Rehahn: "Synthese endfunktionalisierter Poly(*N*-Vinylcarbazole) durch kontrollierte radikalische Polymerisation"
Technical University Darmstadt, Germany

10/2004 - 09/2009 **Studies of Chemistry**
Technical University Darmstadt, Germany

08/1994 - 06/2003 **High School Certificate (Abitur)**
Grimmelshausen Gymnasium Gelnhausen, Germany

Professional Experience

- 06/2010 - 09/2013 **Institut für Technische Chemie und Polymer Chemie**
Karlsruhe Institute of Technology, Karlsruhe, Germany
Scientific Co-worker
- 01/2010 - 03/2010 **Fraunhofer Institute for Applied Polymer Science**
in the group of Dr. habil. J.-F. Lutz
Potsdam/Golm, Germany
Complementary Scientist
- 10/2009 - 12/2009 **Fraunhofer Institute for Applied Polymer Science**
in the group of Dr. habil. J.-F. Lutz
Potsdam/Golm, Germany
Internship
- 08/2004 **Degussa**
Industriepark Wolfgang, Germany
Internship
- 10/2003 - 07/2004 **Community Service**
Kath. Kirchengemeinde St. Peter, Behindertenwerk
Main-Kinzig
Care for the elderly and disabled

Publications and Conference Contributions

Peer Reviewed Publications

1. Defined Poly[styrene-*block*-(ferrocenylmethyl methacrylate)] Diblock Copolymers via Living Anionic Polymerization
Gallei, M.; Schmidt, B. V. K. J.; Klein, R.; Rehahn, M. *Macromol. Rapid Commun.* **2009**, *30* (13), 1463-1469.
2. Controlled folding of synthetic polymer chains through the formation of positionable covalent bridges
Schmidt, B. V. K. J.; Fechler, N.; Falkenhagen, J.; Lutz, J.-F. *Nat. Chem.* **2011**, *3* (3), 234-238.
3. Tailored Polymer Microstructures Prepared by Atom Transfer Radical Copolymerization of Styrene and N-substituted Maleimides
Lutz, J.-F.; Schmidt, B. V. K. J.; Pfeifer, S. *Macromol. Rapid Commun.* **2011**, *32* (2), 127-135.
4. Low Temperature Aqueous Living/Controlled (RAFT) Polymerization of Carboxybetaine Methacrylamide up to High Molecular Weights
Rodriguez-Emmenegger, C.; Schmidt, B. V. K. J.; Sedláková, Z.; Šubr, V.; Bologna Alles, A.; Brynda, E.; Barner-Kowollik, C. *Macromol. Rapid Commun.* **2011**, *32*, 958-965.

The with * marked publications or conference contributions were accomplished in the course of this thesis

5. *Cyclodextrin-Complexed RAFT Agents for the Ambient Temperature Aqueous Living/Controlled Radical Polymerization of Acrylamido-Monomers
Schmidt, B. V. K. J.; Hetzer, M.; Ritter, H.; Barner-Kowollik, C. *Macromolecules* **2011**, *44* (18), 7220-7232.
6. *Miktoarm Star Polymers via Cyclodextrin-Driven Supramolecular Self-Assembly
Schmidt, B. V. K. J.; Hetzer, M.; Ritter, H.; Barner-Kowollik, C. *Polym. Chem.* **2012**, *3*, 3064-3067.
7. *Supramolecular Three-Armed Star Polymers via Cyclodextrin Host/Guest Self-Assembly
Schmidt, B. V. K. J.; Rudolph, T.; Hetzer, M.; Ritter, H.; Schacher, F. H.; Barner-Kowollik, C. *Polym. Chem.* **2012**, *3*, 3139-3154.
8. Limitations of Cyclodextrin Mediated Amphiphilic Block Copolymer Formation
Hetzer, M.; Schmidt, B. V. K. J.; Barner-Kowollik, C.; Ritter, H. *J. Polym. Sci. A: Polym. Chem.* **2013**, *51* (11), 2504-2517.
9. *UV-Light and Temperature Supramolecular ABA Triblock Copolymers via Reversible Cyclodextrin Complexation
Schmidt, B. V. K. J.; Hetzer, M.; Ritter, H.; Barner-Kowollik, C. *Macromolecules* **2013**, *46* (3), 1054-1065.
10. Photochemical Generation of Light Responsive Surfaces
Blasco, E.; Piñol, M.; Oriol, L.; Schmidt, B. V. K. J.; Welle, A.; Trouillet, V.; Barner-Kowollik, C. *Adv. Funct. Mater.* **2013**, *23* (32), 4011-4019.
11. *Complex Macromolecular Architecture Design via Cyclodextrin Host/Guest Complexes
Schmidt, B. V. K. J.; Hetzer, M.; Ritter, H.; Barner-Kowollik, C. *Prog. Polym. Sci.* **2013**, *accepted*.
12. Dual Thermo- and Photo-Responsive Micelles Based on Miktoarm Star Polymers
Blasco, E.; Schmidt, B. V. K. J.; Barner-Kowollik, C.; Piñol, M.; Oriol, L. *Polym. Chem.* **2013**, *4*, 4506-4514.
13. *Modulation of the Thermo-responsive Behavior of Poly(*N,N*-diethylacrylamide) via Cyclodextrin Host/Guest Interactions
Schmidt, B. V. K. J.; Hetzer, M.; Ritter, H.; Barner-Kowollik, C. *Macromol. Rapid Commun.* **2013**, *34* (16), 1306-1311..

14. Visual Recognition of Supramolecular Graft Polymer Formation via Phenolphthalein-Cyclodextrin Association
Hetzler, M.; Fleischmann, C.; Schmidt, B. V. K. J.; Barner-Kowollik, C.; Ritter, H.
Polymer **2013**, *54* (19), 5141-5147.

15. Supramolecular Polymer Networks of Precision Tailored Building Blocks
Hetzler, M.; Schmidt, B. V. K. J.; Barner-Kowollik, C.; Ritter, H. **2013**, submitted.

Non-peer Reviewed Publications

1. Defined Poly(Styrene-*b*-Ferrocenylmethyl methacrylate) Diblock Copolymers via Living Anionic Polymerization
Gallei, M.; Schmidt, B. V. K. J.; Klein, R.; Rehahn, M. *Polym. Preprints* **2009**, *50*(2), 456-457.

Conference Contributions (the presenter is underlined)

1. Novel poly(carboxybetaine methacrylamides) Synthesized via Living/Controlled Aqueous RAFT Polymerization
Rodriguez-Emmenegger, C.; Schmidt, B. V. K. J.; Sedláková, Z.; Šubr, V.; Bologna Alles, A.; Brynda, E.; Barner-Kowollik, C.
European Polymer Congress, Granada **2011**.
2. * Cyclodextrin-Complexed RAFT Agents for the Ambient Temperature Aqueous Living/Controlled Radical Polymerization of Acrylamido-Monomers
Schmidt, B. V. K. J.; Hetzer, M.; Ritter, H.; Barner-Kowollik, C.
Bayreuth Polymer Symposium, Bayreuth **2011**.
3. * Miktoarm Starpolymers via Cyclodextrin-Driven Supramolecular Self-Assembly
Schmidt, B. V. K. J., Hetzer, M.; Ritter, H.; Barner-Kowollik, C.
Macrogroup UK International Conference on Polymer Synthesis & UKPCF International Conference on Polymer Colloids, Warwick **2012**.
4. * Supramolecular Three-Armed Star Polymers via Cyclodextrin Host/Guest Self-Assembly
Schmidt, B. V. K. J.; Rudolph, T.; Hetzer, M.; Ritter, H.; Schacher, F. H.; Barner-Kowollik, C.
Smart Polymers: Biennial Meeting of the GDCh-Division of Macromolecular Chemistry, Mainz **2012**.
5. Photochemical Generation of Light Responsive Surfaces
Blasco, E.; Schmidt, B. V. K. J.; Welle, A.; Bruns, M.; Barner-Kowollik, C.; Piñol, M.; Oriol, L.
5^a Jornada de Jóvenes Investigadores en Aragón, Zaragoza **2012**.
6. Limitations of Cyclodextrin Mediated Amphiphilic Block Copolymer Formation
Hetzer, M.; Schmidt, B. V. K. J.; Barner-Kowollik, C.; Ritter, H.
Belgian-German (Macro)Molecular Meeting: Advanced Materials by Modular Strategies: From Synthesis to Industrial Applications, Houffalize **2012**.

Acknowledgements

First, and foremost, I am indebted to Prof. Christopher Barner-Kowollik for offering me the opportunity to undergo my doctoral studies under his supervision. I am thankful for his trust in my abilities, his enthusiasm for my project, the discussions that pushed the projects forward and his support throughout my doctoral studies.

Furthermore I would like to thank Prof. Helmut Ritter and Dipl. WiChem. Martin Hetzer for the support and fruitful discussions in our collaborative project.

I am thankful for the great cooperation with Prof. Felix Schacher and Dipl. Chem. Tobias Rudolph. It was a pleasure to work with you. Furthermore I thank Prof. Mathias Rehahn and Dr. Markus Gallei for a great collaboration as well. Especially Markus has to be mentioned, as he had a significant impact on my lab-skills and on my development as a scientist.

Thanks go to Eva Blasco and Dr. Cesar Rodriguez-Emmenegger for fruitful collaborations during their stay in our group as visitor. I would also like to thank Dipl. Chem. Tanja Claus, Dipl. Chem. Doris Abt and B. Sc. Janin Offenloch whom I supervised in their advanced lab course, diploma thesis or bachelor thesis respectively. It was a pleasure to work with you, to teach you and to follow how you develop into good scientists.

Many thanks go to all present and former members of the *macroarc* research team. It was a pleasure to work and laugh with you. Furthermore I thank the AC crew for the nice atmosphere and company, especially Dr. Anna-Marie Zorn, Dr. Dominik Voll, Dipl. Chem. Johannes Willenbacher and Peter Gerstel. Additional thanks go to Dipl. Chem. Christiane Lang, Dr. Dominik Voll, Dipl. Chem. Johannes Willenbacher and

Dipl. Chem. Michael Kaupp for proof reading of this thesis.

Many thanks to Gabriele Herrmann and Evelyn Stüring for the support in administrative matters, as well as Dr. Maria Schneider and Peter Gerstel for ordering every item that was used in the course of this thesis. Furthermore I would like to thank Dr. Maria Schneider for the great teamwork in the supervision of the SEC instruments and I am thankful to Pia Lang and Tanja Ohmer for performing NMR measurements at the institute of organic chemistry.

Special thanks go to Anna-Marie Zorn, Astrid Hirschbiel, Azize Ünal, Cesar Rodriguez-Emmenegger, Christiane Lang, Christoph Dürr, Dominik Voll, Doris Abt, Jan Müller, Johannes Willenbacher, Kim Öhlenschläger and Pieter Derboven for their friendship during my time in Karlsruhe. I appreciate your support and care for me. I will never forget you and hope to see you again.

I thank my chemistry teacher Hubert Giar for infecting me with his enthusiasm for science, and chemistry in particular. Furthermore I thank Peter Gerstel for supporting me in scientific matters as well as the more important things in life. If I only had half of the spirit of you two I would be a great man.

Thanks go out to my friends, especially (in chronological order) Youssef Afkir, Martin Krauß, Jan Paul Marschollek, Ali Hartwig, Jan-Eric Teves and Tobi Rudi. I am very proud to call you my friends.

Ich danke Anna-Elisabeth Kreuder für ihre Unterstützung. Sie hat einen maßgeblichen Anteil am Erfolg dieser Arbeit. Auch wenn Dinge enden, bleibt doch immer etwas zurück und es ist mehr als diese Arbeit.

Zu guter letzt möchte ich mich bei meinen Eltern und meiner Schwester für die Unterstützung auf meinem bisherigen Lebensweg danken.

Ich erkläre hiermit, dass ich die vorliegende Doktorarbeit im Rahmen der Betreuung durch Prof. Dr. Christopher Barner-Kowollik, selbständig verfasst und keine anderen als die angegebenen Quellen und Hilfsmittel verwendet habe. Hiermit erkläre ich, dass ich mich derzeit in keinem laufenden Promotionsverfahren befinde, und auch keine vorausgegangenen Promotionsversuche unternommen habe.

Karlsruhe, den 19.07.2013

I don't mind your thinking slowly; I mind your publishing faster than you think.
Wolfgang Ernst Pauli